

NOAA Technical Memorandum ERL PMEL-21

PHYSICAL ENVIRONMENT OF THE EASTERN BERING SEA  
MARCH 1979

S. A. Salo  
C. H. Pease  
R. W. Lindsay

Pacific Marine Environmental Laboratory  
Seattle, Washington  
May 1980



**UNITED STATES  
DEPARTMENT OF COMMERCE  
Philip M. Klutznick, Secretary**

**NATIONAL OCEANIC AND  
ATMOSPHERIC ADMINISTRATION  
Richard A. Frank, Administrator**

**Environmental Research  
Laboratories  
Wilmot N. Hess, Director**

## NOTICE

The Environmental Research Laboratories do not approve, recommend, or endorse any proprietary product or proprietary material mentioned in this publication. No reference shall be made to the Environmental Research Laboratories or to this publication furnished by the Environmental Research Laboratories in any advertising or sales promotion which would indicate or imply that the Environmental Research Laboratories approve, recommend, or endorse any proprietary product or proprietary material mentioned herein, or which has as its purpose an intent to cause directly or indirectly the advertised product to be used or purchased because of this Environmental Research Laboratories publication.

## CONTENTS

Abstract	1
1. INTRODUCTION	1
2. OCEANOGRAPHY AND METEOROLOGY AT THE ICE EDGE	2
2.1 Data	2
2.2 Discussion	3
2.3 Conclusion	6
3. BOUNDARY LAYER OBSERVATIONS NEAR THE ICE EDGE	6
3.1 Measurements	6
3.2 Case A	7
3.3 Case B	8
3.4 Surface Heat Fluxes	9
3.5 Conclusion	10
4. ACKNOWLEDGEMENTS	10
5. REFERENCES	11
APPENDIX A: Salinity, Temperature, and Density Profiles, CTD Casts 1-41.	57
APPENDIX B: Surface Air Isotherms at 00Z and 12Z, from the WSFO Surface Analyses. Temperatures are degrees Kelvin.	98
APPENDIX C: Surface Winds derived from the WSFO Surface Analyses.	109

## LIST OF TABLES

		<u>Page</u>
Table 1.	CTD Operations Summary.	13
Table 2.	Airsonde Soundings	15

## LIST OF FIGURES

Figure 1.	Cruise region in the Bering Sea, March 1979.	16
Figure 2a.	Ship's cruise track. Positions at times in GMT and Julian Day are marked.	17
Figure 2b.	Ship's cruise track. Positions at times in GMT and Julian Day are marked.	18
Figure 3.	Aerial reconnaissance of the position of the ice edge on March 2 and March 8, 1979.	19
Figure 4.	Locations of CTD stations.	20
Figure 5.	Locations of airsonde launches.	21
Figure 6.	Location of CTD transects.	22
Figure 7a.	CTD transect showing a surface lens of meltwater. Numbers on the horizontal axis are CTD stations. Isotherms, isohalines and isopleths are labeled.	23
Figure 7b.	CTD transect showing a surface lens of meltwater. Numbers on the horizontal axis are CTD stations. Isotherms, isohalines and isopleths are labeled.	24
Figure 7c.	CTD transect showing a surface lens of meltwater. Numbers on the horizontal axis are CTD stations. Isotherms, isohalines and isopleths are labeled.	25
Figure 8a.	CTD transect taken at the beginning of the cruise, showing a front. This is the only time during the cruise such a feature was seen.	26
Figure 8b.	CTD transect taken at the beginning of the cruise, showing a front. This is the only time during the cruise such a feature was seen.	27

	<u>Page</u>
Figure 8c. CTD transect taken at the beginning of the cruise, showing a front. This is the only time during the cruise such a feature was seen.	28
Figure 9a. Dynamic depth anomaly at 35 m, in dynamic centimeters.	29
Figure 9b. Dynamic depth anomaly at 35 m, in dynamic centimeters.	30
Figure 10a. Air temperature and pressure. Dry bulb temperature.	31
Figure 10b. Air temperature and pressure. Thermistor temperature.	32
Figure 10c. Air temperature and pressure. Surface pressure.	33
Figure 11. Sea surface isotherms.	34
Figure 12. Sea surface isohalines.	35
Figure 13. True wind magnitude and direction calculated from relative wind magnitude and direction data. Direction is the vector direction rather than the meteorological convention's direction.	36
Figure 14a. Calculated surface wind compared to winds measured at the ship and three surface stations.	37
Figure 14b. Calculated surface wind compared to winds measured at the ship and three surface stations.	38
Figure 14c. Calculated surface wind compared to winds measured at the ship and three surface stations.	39
Figure 14d. Calculated surface wind compared to winds measured at the ship and three surface stations.	40
Figure 15. Map of the Bering Sea and the locations of cases A and B.	41
Figure 16a. Potential temperature for all soundings. The zero point on the abscissa is different for each sounding.	42
Figure 16b. Potential temperature for all soundings. The zero point on the abscissa is different for each sounding.	43
Figure 16c. Potential temperature for all soundings. The zero point on the abscissa is different for each sounding.	44

	<u>Page</u>
Figure 16d. Potential temperature for all soundings. The zero point on the abscissa is different for each sounding.	45
Figure 17. Potential temperature for Case A, one origin.	46
Figure 18. Surface pressure and 850-mb maps for Case A, 00Z 5 March 1979.	47
Figure 19. Upper air soundings from the National Weather Service, 00Z 5 March. The dots indicate the 850-mb level.	48
Figure 20. Map of the locations of soundings used in Case A.	49
Figure 21. Cross section of potential temperature for Case A.	50
Figure 22. Surface pressure and 850-mb maps for Case B, 00Z 15 March 1979.	51
Figure 23. Upper air soundings from the National Weather Service, 00Z 15 March. The dots indicate the 850-mb level.	52
Figure 24. Cross section of potential temperature for Case B.	53
Figure 25. Map of the locations of the soundings for Case B with wind and temperature observations plotted at the time of each launch and similar observations from the aircraft at 100 m, 350 m, and 680 m.	54
Figure 26. Integrated difference in heat content between the first and last soundings for Case A.	55
Figure 27. Integrated difference in heat content between the first and last soundings for Case B.	56

Physical Environment of the Eastern Bering Sea  
March 1979\*

by

S. A. Salo, C. H. Pease, and R. W. Lindsay

Pacific Marine Environmental Laboratory  
3711 - 15th Ave. NE, Seattle, WA 98105

ABSTRACT. This report includes two analyses of data collected by the NOAA ship Surveyor in the southeastern Bering Sea during March, 1979. The first section presents CTD's and data on sea surface temperature and salinity and on surface winds and air temperature. The data indicate that ice was advected south to the ice edge by northerly winds, and that net melting occurred at the ice edge. The second section describes two cases when cold continental air moved from the ice over the water at the edge. An estimate is made of the resulting surface heat flux.

## 1. INTRODUCTION

During the first two weeks of March 1979, the NOAA ship SURVEYOR (frontispiece) collected data along the ice edge in the southeastern Bering Sea. The region of the cruise and the ship's cruise track are shown in Figures 1 and 2. The ice edge was at approximately  $58^{\circ}$  to  $60^{\circ}$  latitude,  $3^{\circ}$  of latitude north of the shelf break in water less than 100 m deep. The position of the ice as surveyed by joint NOAA-Navy ice reconnaissance overflights on March 2 and March 8 is shown in Figure 3.

This paper presents all the field data and two preliminary interpretations of the data set; a discussion of the manifestations of melting ice at the ice edge; and a report on the atmospheric boundary layer thermal structure near the ice edge during two outbreaks of cold air.

\*Contribution No. 467 from the NOAA/ERL Pacific Marine Environmental Laboratory.

## 2. OCEANOGRAPHY AND METEOROLOGY AT THE ICE EDGE

### 2.1 Data

Forty-one CTD casts and twenty-three airsondes were taken at locations shown in Figures 4 and 5; Table 1 summarizes information about the CTD casts. Individual CTD casts in Table 2, casts 1-41, were plotted using PMEL graphics program R2D2 (Pearson et al., 1979). Isotherms, isohalines, and isopycnals were drawn by hand for the vertical sections of Figures 7 and 8, at locations shown on Figure 6. Dynamic depth anomaly at 35 m, the greatest common depth, was calculated using R2D2 and plotted in Figure 9.

CTD's were taken with a model 9040 conductivity/temperature/depth sensor manufactured by Plessey Environmental Systems. The standard deviation of error for the CTD when calibrated in January 1979 was: conductivity, 0.017 m-Siemans/cm; temperature, 0.006°C; pressure, 0.73 PSI.

The atmosphere sounding system used was that of the Atmospheric Instrumentation Research Co. It consists of 100-g helium inflated balloons, an expendable aerodynamically shaped instrument package (the "airsonde"), a receiving antenna, a receiver and data processing unit, and a cassette tape recorder for data logging. The instrument package transmits pressure and wet and dry bulb temperatures. No information on wind was obtained. The data rate is one frame (time, dry bulb temperature, wet bulb temperature, and pressure) every 6 sec. The ascent rate is about  $2.5 \text{ ms}^{-1}$ ; there are about 15 m between samples. The precision in the wet and dry bulb temperatures is  $\pm 0.5^\circ\text{C}$  and in the pressure it is  $\pm 3 \text{ mb}$ .

During the first 2 days at the ice edge, sea surface temperature was measured every half hour as a bucket temperature with a thermometer calibrated to  $\pm 0.1^\circ\text{C}$ . Dry bulb air temperature readings were made throughout the cruise. The salinity of bucket samples taken every 2 hr was determined using a Guildline 8400 salinometer precise to  $\pm 0.001 \text{ ppt}$ . Air temperature and pressure during the cruise are plotted on Figure 10. Figures 11 and 12 exhibit sea surface isotherms and isohalines.



Relative wind magnitude and direction were continuously monitored with a Bendix 120 wind velocity and direction transmitter accurate to  $\pm 0.1\%$  for velocity and  $\pm 3^\circ$  for direction. Relative wind data were digitized over 10-min intervals. The ship's course recorder chart was digitized over the same time intervals, and the ship's velocity was approximated from positions logged every 15-30 min. The true wind magnitude and direction shown in Figure 13 were calculated from this information.

Surface analyses for the Bering Sea region at 00Z and 12Z of March 1-March 31 were obtained from the National Weather Service Forecast Office in Anchorage and digitized for temperature and pressure. The isotherms thus derived are in Appendix A. The surface winds shown in Appendix B were computed from the pressure field by rotating the calculated gradient wind  $20^\circ$  toward lower pressure and decreasing its magnitude by 20% using METLIB (Overland et al., 1980), a software package for meteorological fields. In regions with little bias due to topography, calculated winds agree well with observed winds. In Figure 14 observed and calculated winds at St. Paul and the ship agree in magnitude, but the angle of rotation of calculated wind is slightly too large. This error may be due in part to the fact that the wind vector at St. Paul is the average of three readings, and the ship's wind vectors are derived from 6-hr averages of data digitized over 10-min intervals, while the calculated winds are derived from the instantaneous pressure field.

## 2.2 Discussion

Winds over the eastern Bering Sea were generally from the northeast during March 1979. This is in accord with usual winter wind patterns (Brower et al., 1977).

Under the influence of persistent northerly winds, ice formed in the shallow northern regions of the Bering Sea would be consistently advected southward (Muench and Ahlnäs, 1976), ultimately reaching the edge. Southward motion of the ice edge itself over most of the region can be seen in Figure 4. A comparison of CTD descriptions in Table 2 with positions in Figure 5 also illustrates motion of the ice edge.

For example, CTD casts 7 and 38, roughly 40 km apart, were both taken in the zone of decaying ice at the edge on March 3 and 13, respectively.

As the ice advected south, it was subject to increased air temperatures (Appendix B). Air temperature at the ice edge was typically  $-10^{\circ}$  to  $+5^{\circ}\text{C}$ .

Water at the ice edge had a salinity of about 32 ppt (Fig. 14). Thus its freezing point would be about  $-1.75^{\circ}\text{C}$ . Virtually no sea surface temperatures this cold were measured; the ice edge was not an ice-forming region. Since the salinity of the ice is about 15 ppt, its melting point is about  $-0.8^{\circ}\text{C}$ . It can be seen in both Appendix A and Figure 11 that water warmer than  $-0.8^{\circ}\text{C}$  was common at the ice edge.

Ice at the edge was melting, as shown most readily by the CTD's. CTD's from ice-free areas south of the ice edge illustrated well-mixed water (for example Appendix A, Numbers 5, 11). CTD's from within or at the ice edge generally exhibited a surface layer, 15 to 25 m deep, of relatively cold and fresh meltwater (see Appendix A, Numbers 33, 39-41). The change from well-mixed to two-layer water occurred across a transition zone over which short ice advances and consequent melting had apparently occurred.

Figure 7 presents a cross section of an ice edge surface lens of meltwater; the position of this vertical section is shown in Figure 6. The CTD section in Figure 8 illustrates the presence of a front near the ice edge; CTD casts 1-5 used for this section were taken during the coldest air temperatures seen on the cruise, on the only day grease ice formation was observed. They are also the shallowest CTD casts made; this transect therefore represents an anomaly to the more representative transect of Figure 7.

Due to melting at the advancing ice edge, the colder isotherms and fresher isohalines were moved to the south during the 2 weeks of the cruise, although the isolines further from the ice edge were relatively stationary. In Figures 11 and 12, the  $-1.0^{\circ}\text{C}$  and 31.8 ppt isolines moved about 40 km to the south in the 13 days which elapsed between the first and final readings near the eastern end of the cruise track.

The dynamic topography shown in Figure 9 indicates a current to the northwest along the ice edge. This agrees with the currents obtained by Charnell, Schumacher, Coachman, and Kinder (1979). The density distribution near the ice edge is changing faster than geostrophic currents could adjust, due to ice movement and melting. However, the dynamic method offers an order-of-magnitude calculation for currents near the ice edge. The CTD transect shown in Figure 7 suggests a narrow current of 1-2 cm sec<sup>-1</sup> and the transect in Figure 8 a current with a maximum velocity of about 6 cm sec<sup>-1</sup> at the front. Thus, currents at the ice edge are transporting water parallel to the edge and it is unlikely that they would cause the isoline motion seen in Figures 11 and 12.

An estimate was made of the amount of ice which had melted to create the temperature profile of the lens in Figure 7, using:

$$m_i = \frac{C_p \Delta T_w m_w}{L}$$

where  $C_p$  is the specific heat,  $\Delta T_w$  is the change in water temperature,  $L$  is the latent heat of freezing and  $m_i$  and  $m_w$  are the masses of ice and water per unit area, respectively.

This formula was used to estimate the heat removed from 'cores' of water of unit surface area for every kilometer along the transect. The heat removed from each core was assumed to be a centered average of the heat per area about the core. It was assumed that the temperature was originally +0.1°C, (see CTD cast 39, Appendix A), and that density was constant at 1.03 g cm<sup>3</sup>.  $C_p$  was set at 0.94 cal g<sup>-1</sup>deg<sup>-1</sup> (The Oceans, 1942). It was assumed in the equation that all the heat extracted was used to melt ice, that the ice was already at the melting point, and that the salinity of the ice was 15 ppt so that the latent heat was 16 cal g<sup>-1</sup> (Neumann and Pierson, 1966).

This calculation indicates that enough heat was extracted from the lens to melt a 60-km strip of ice averaging 50 cm thick. Lower initial water temperature or salinity of the ice gives lower values, as would the inclusion of cooling of the lens due to off-ice winds. Martin and Kauffman (1979), who took cores along transects into the ice pack, found that the pack was generally 30 cm thick except in the outer couple of kilometers,

where rafting increased thickness to more than 1 m. Thus the 50-cm estimate for ice thickness may be too large, which would lead to an underestimate of lateral ice melting of almost one-third.

Further discussion of marginal ice zone physics during March 1979 can be found in Pease (1980), McNutt (1980), Bauer and Martin (1980), and Squire and Moore (1980).

### 2.3 Conclusion

Data taken along the ice edge in the southeastern Bering Sea in March 1979 are consonant with the advance of the ice edge due to northerly winds, but retarded and limited by the melting of ice due to advection to warmer water. Ice formation at the edge was only observed on one occasion, during the coldest air temperatures and in the shallowest water of the cruise in the lee of Nunivak Island.

## 3. BOUNDARY LAYER OBSERVATIONS NEAR THE ICE EDGE

### 3.1 Measurements

At many times during the cruise there were cold air outbreaks in which continental air passed from the ice to the water with a consequent large increase in surface heat flux. Because of other demands on the ship's time, only two cases were documented: Case A on March 5 and Case B on March 15. Case B also benefitted from simultaneous overflights by the NASA C-130 aircraft. The location of Case A and B is shown in Figure 15.

A total of 23 airsonde flights were made. They are summarized in Table 2. The potential temperature for each sounding is plotted to 2000 m in Figure 16. In all of the soundings we see a mixed layer capped by a sharp inversion at 400 to 1000 meters. We noted a warming and deepening of the mixed layer and a cooling of the inversion layer as observations were taken at increasing distances from the ice edge. This is shown clearly in Figure 17 where potential temperature is plotted for the four soundings of Case A. Note that the superadiabatic layer near the surface may be amplified by thermal contamination from the ship's stack. The warming of the mixed layer was clearly a result of heat flux from the warm ocean, while cooling of the inversion layer can

be attributed to entrainment of cold air from the underlying mixed layer. This entrainment produced a net downward heat flux, adding to the warming of the mixed layer and cooling the inversion layer. The inversion was further cooled by radiation from the cloud layer that developed soon after the air passed over the water, a product of the greatly increased moisture flux.

An additional mechanism that may contribute to the deepening of the mixed layer is found in the increased stress due to buoyant mixing. This increased stress slows the air in the mixed layer and creates a low level convergence that results in a positive vertical velocity at the inversion. With potential temperature conserved the adiabats rise, as in Figures 21 and 25.

### 3.2 Case A

At the time of Case A, ~ 0300Z 5 March, there was a small low pressure system about 180 km southeast of the ship (see the surface and 850 mb analyses, Figure 18, and the National Weather Service soundings for four nearby stations, Figure 19). The geostrophic flow was from the east, with most of Alaska dominated by this zonal flow. The wind at the ship was 9 to 13  $\text{ms}^{-1}$  at 020° to 040°. As shown in Figure 20 the ship steamed downwind 70 km to the southwest and four balloons were launched at 1-hr intervals (0243Z to 0634Z, 5 March). A cross section of the potential temperature of the four soundings is presented in Figure 21, in which we see the warming and deepening of the mixed layer as a function of distance from the ice. Note also the rising of the -4 and -6°C adiabats indicating the cooling of the inversion. The interpretation of this figure is limited by two major difficulties. The first is the nonsynoptic nature of the observations. The 850-mb maps (1100 m) indicate a 6°C warming from 00Z to 12Z 5 March and a shifting of the 7 to 10  $\text{ms}^{-1}$  winds from 030° to 090° as the low to the south developed. Second, the distance the air travels over the water may be different than the distance the ship traveled since ice was last observed, due to the irregular nature of the ice edge. Nevertheless the warming and deepening of the boundary layer and the cooling of the inversion are clear.

### 3.3 Case B

Case B was characterized by a weak and nearly stationary low pressure center 250 n mi south of the ship with an occluded front to its southwest (see the surface and 850-mb analyses, Fig. 22, and the upper air soundings, Fig. 23.) The geostrophic wind was from the northeast at the ship's position and there was a very weak flow off of the Alaskan land mass. The 850-mb maps (1300 m) indicate a shift in the wind from  $045^{\circ}/3 \text{ ms}^{-1}$  at 12Z 15 March to  $330^{\circ}/3 \text{ ms}^{-1}$  at 12Z 15 March. The temperature was steady to within  $1^{\circ}\text{C}$ .

Again we see a warming and deepening of the mixed layer as the ship steamed to the south. Figure 24 is a cross section of potential temperature as the ship made a 180-km transit south from the ice edge. Figure 25 is a map of the ice edge with the winds and temperatures measured by the bridge plotted for the time of each airsonde launch, and wind and temperature observations by the NASA C-130 aircraft plotted on three legs at 100 m, 350 m, and 680 m.

The airplane data indicate the same general shape to the profile but the temperatures are up to  $5^{\circ}\text{C}$  warmer than those measured by the airsonde. The airsonde data are supported by two independent sources: the temperature measured by the airsonde before launch matched that of the bridge to within  $0.5^{\circ}\text{C}$ , and the temperature of the wet bulb while it froze rose to  $-0.6^{\circ}\text{C}$  (for pure water it should have been  $0^{\circ}\text{C}$ ), indicating that the temperature circuit was functioning reasonably well. The variance of the temperature as measured by the airplane was substantially larger at the 650-m level than at lower levels. This level was near the height of the maximum temperature as indicated by the airsonde sounding. Large temperature fluctuations would be expected in this region as the airplane passed in and out of plumes of cold air from below or warm air from above. These fluctuations are further evidence of active entrainment near the inversion.

Also evident in the airplane data plotted in Figure 25 is a slight counterclockwise backing of the wind with height. Ekman turning of the wind normally veers in a clockwise sense and the backing is indicative of cold air advection. (The thermal wind component normal to the ship's

track for Case A was  $12 \text{ ms}^{-1} \text{ km}^{-1}$  from a mean horizontal temperature gradient of  $0.03^\circ\text{C km}^{-1}$ .) For Case B it was  $18 \text{ ms}^{-1} \text{ km}^{-1}$  from a gradient of  $0.05^\circ\text{C km}^{-1}$ .

There were high level altostratus and cirrus moving into the area from the south and a well developed layer of stratocumulus clouds within a few kilometers south of the ice edge. This layer of saturated air was observed in the airsonde surroundings, but unfortunately the thickness of the cloud layer could not be determined because the wet bulb wick was in the process of freezing for most of the soundings during this critical time.

### 3.4 Surface Heat Fluxes

A very rough estimate of the surface heat flux may be obtained by the bulk aerodynamic method in which the wind speed at 10 m,  $U_{10}$ , and the air sea temperature difference,  $\Delta T$ , are used to find the surface heat flux:

$$F_H = \rho c_p U_{10} \Delta T C_h ,$$

where  $C_h$  is the bulk heat transfer coefficient (approximately  $1.2 \times 10^{-3}$ , Kraus, 1972),  $c_p$  ( $1004 \text{ J deg}^{-1}\text{kg}^{-1}$ ) is the heat capacity and  $\rho$  ( $\cong 1.3 \text{ kg m}^{-3}$ ) is the density of the air. For Case A ( $U_{10} = 10 \text{ ms}^{-1}$ ,  $\Delta T = 10^\circ\text{C}$ ) the heat flux is about  $120 \text{ Wm}^{-2}$  and for Case B ( $U_{10} = 5 \text{ ms}^{-1}$ ,  $\Delta T = 5^\circ\text{C}$ ) it is about  $30 \text{ Wm}^{-2}$ .

We can also find the difference in heat content between two columns of air of depth  $Z$  by integrating the expression

$$\Delta H(Z) = c_p \int_0^Z \rho (T_2 - T_1) dz , \quad (1)$$

in which  $T_1$  and  $T_2$  are the temperatures of the two air columns. The heat flux into the air column can then be approximated from

$$F_H = \frac{U\Delta H}{d} , \quad (2)$$

where  $U$  is the mean wind speed in the air column and  $d$  is the distance between the soundings. We must assume steady state conditions and that the second sounding is directly downwind from the first.

If no heat were transferred through the inversion ( $Z=h$ ) the air above would remain unchanged from the first sounding to the second.  $\Delta H$  would then be constant for  $z>h$  and would represent the total heat flux

from the surface into the mixed layer. Equation (1) is plotted for Cases A and B in Figures 26 and 27. In Case A we see that this constant is about  $1.5 \times 10^6 \text{ Jm}^{-2}$  at  $Z=1000 \text{ m}$ , and using (2) we obtain  $210 \text{ Wm}^{-2}$  for the heat flux into the column (vs  $120 \text{ Wm}^{-2}$  from the bulk aerodynamic method). For Case B we find no hint of a constant  $\Delta H$ ; the fact that  $\Delta H$  is negative above 800 m could reflect a bias in one of the temperature sensors or a violation of the assumptions of steady state, downwind profiles.

This method of calculating heat fluxes places extreme requirements on the accuracy of the temperature profiles, for with a precision of  $0.5^\circ\text{C}$  the expected error in the heat flux calculated with  $Z=1000 \text{ m}$ ,  $d=50 \text{ km}$ , and  $U=10 \text{ ms}^{-1}$  is  $140 \text{ Wm}^{-2}$ . The expected error for a precision of  $0.5^\circ\text{C}$  is plotted for each case in Figures 26 and 27. Clearly the error is very large and quickly overwhelms the value of  $\Delta H$  as we integrate upward. If we could be certain that at some high level the temperatures of the two profiles were the same, any bias in the temperature sensors could be adjusted for, and the expected error would be much smaller. Unfortunately, the nonsynoptic nature of the observations precluded any such certainty.

### 3.5 Conclusion

There are many questions that remain about the air modification that occurs at the ice edge. Of most interest is the nature of the three-dimensional wind field near the ice edge that reflects different values of the surface stress and heat flux at the up- and downwind sides. It would also be very useful to accurately determine the heat and moisture fluxes as a function of distance from the ice edge. Accurate field observations could be used to verify the results obtained with various air modification models or to substantiate working assumptions of ocean or ice circulation models. This study represents a first and somewhat cloudy look at an intriguing phenomena.

### 4. ACKNOWLEDGEMENTS

This study was financed in part by the Marine Services Project of the Marine Meteorological Studies Group at Pacific Marine Environmental



Laboratory and in part by the Bureau of Land Management through inter-agency agreement with the National Oceanic and Atmospheric Administration under a multiyear program, responding to needs of petroleum development of the Alaskan continental shelf, managed by the Outer Continental Shelf Environmental Assessment Program (OCSEAP) Office. The cruise time on the NOAA ship SURVEYOR was requested by the late Robert Charnell of PMEL and was arranged by the OCSEAP Juneau Project Office. Seelye Martin of the Department of Oceanography at the University of Washington acted as chief scientist on the cruise. The shipboard measurements were carried out with the help of the survey technicians and other crew members of the SURVEYOR under the command of Captain James G. Grunwell.

The National Weather Service Forecast Office in Anchorage supplied the surface analyses, and the National Climate Center in Nashville supplied the NWS soundings. Bruce Webster, ice forecaster at WSFO in Fairbanks, contributed ice and pressure analyses. Francis Parmenter of NESS in Anchorage provided NOAA and TIROS satellite images. Lt. (jg.) Daniel V. Munger and AGC William B. Damico flew the Navy ice reconnaissance for the NOAA-Navy Joint Ice Center under the leadership of Commander James C. Langemo.

James D. Schumacher, James E. Overland, and R. Michael Reynolds gave advice and direction on the physics. Sally A. Schoenberg did much of the digitizing and Linda Green generated many of the computer plots. Peter Lanore helped with the wind analysis. Joy I. Golly and Gini May prepared the drafted figures and James Anderson and Claudia J. Smith did virtually all the photography. Lai K. Lu typed the original manuscript and the PMEL Word Processing Center prepared the final draft.

## 5. REFERENCES

- Bauer, J., and S. Martin (1980): Field observations of the Bering Sea ice edge properties during March 1979. Monthly Wea. Rev. (in press).
- Brower, W. A., Jr., H. F. Diaz, A. S. Prechtel, H. W. Searby, and J. L. Wise (1977): Climatic Atlas of the Outer Continental Shelf Waters and Coastal Regions of Alaska, Vol. II, Bering Sea. Arctic Environmental Information and Data Center, University of Alaska, Anchorage, Alaska National Climatic Center - Environmental Data Service, Asheville, North Carolina, National Oceanic and Atmospheric Administration, 443 pp.

- Charnell, R. L., J. D. Schumacher, L. K. Coachman, and T. H. Kinder: (1979) Bristol Bay Oceanographic Processes 4th Annual Report. 30 March 1979. Environmental Assessment of the Alaskan Continental Shelf, Vol. VII Transport, Outer Continental Shelf Environmental Assessment Program, Boulder, Colorado, October, 1979, p 309-317.
- Kraus, E. B. (1972): Atmosphere-Ocean Interaction, Clarendon Press Oxford, 275 pp.
- Martin, S., and P. Kauffman (1979): Data Report on the Ice Cores Taken during the March 1979 Bering Sea Ice Edge Field Cruise on the NOAA Ship SURVEYOR (Sept. 14, 1979), University of Washington, Department of Oceanography, Special Report, Number 89, 69 pp.
- McNutt, S. L. (1980): Remote Sensing analysis of the ice regime in the Eastern Bering Sea. Monthly Wea. Rev. (in press).
- Muench, R. D., and K. Ahnläs (1976): Ice Movement and Distribution in the Bering Sea from March to June 1974. J. Geophys. Res., 81(24): 4467-4476.
- Neumann, G., and W. J. Pierson Jr. (1966): Principles of Physical Oceanography. Prentice-Hall, Inc., Englewood Cliffs, N.J. p 41-48.
- Overland, J. E., R. A. Brown, and C. D. Mobley (1980): METLIB-A Program Library for Calculating and Plotting Marine Boundary Layer Wind Fields, PMEL-NOAA Technical Memorandum, PMEL CONTRIBUTION NO. 441
- Pearson, C. A., G. A. Krancus, and R. L. Charnell (1979): R2D2: An interactive graphics program for rapid retrieval and display of oceanographic data. Second Working Conference on Oceanographic Data Systems Proceedings, 1978, Woods Hole Oceanographic Institution, September 26-28, 1978, 318-329.
- Pease, C. H. (1980): Eastern Bering Sea ice processes. Monthly Wea. Rev. (in press).
- Squire, V. A., and S. C. Moore (1980): Direct measurement of the attenuation of ocean waves by pack ice. Nature, 283(5745):365-368.
- Sverdrup, H. U., M. W. Johnson and R. H. Fleming (1942): The Oceans: Their Physics, Chemistry, and General Biology. Prentice Hall, Englewood Cliffs, N.J. p 61-65.

TABLE 1. CTD OPERATIONS SUMMARY

Cast #	LATITUDE(N)	LONGITUDE(W)	ICE CONDITIONS	DEPTH(M)	DAY	TIME
1	58° 26.8'	165° 57.0'	Loose pancakes and grease ice	40.9	062	0009
2	58° 21.7'	165° 58.9'	Same	37.5	062	0652
3	58° 16.9'	165° 59.2'	Same	38.4	062	0909
4	58° 14.3'	165° 59.6'	Adjacent Edge of Loose Cakes	41.4	062	1035
5	58° 11.2'	166° 00.2'	Clear of Ice Open Water	43.6	062	1152
6	58° 15.0'	167° 18.8'	Condensed Pancakes	55.8	063	2246
7	58° 13.8'	167° 21.3'	Adjacent Edge of Condensed Cakes	56.7	064	0013
8	58° 11.9'	167° 21.0'	Near-By Lead Open Water	57.0	064	0213
9	57° 41.4'	168° 00.8'	Clear of Ice Open Water	63.1	064	0614
10	58° 13.8'	167° 44.0'	Adjacent Ice Edge	55.3	065	0511
11	58° 13.6'	167° 49.8'	Clear of Ice Open Water	56.2	065	0554
12	58° 29.8'	167° 56.1'	Adjacent Ice Edge Moving North	50.6	066	0406
13	58° 45.9'	168° 45.1'	8 NM into Loose Pack Ice	47.3	066	1636
14	58° 45.1'	168° 47.8'	Inside Ice Pack, Floes Compacting	49.6	067	0403
15	58° 38.7'	169° 05.2'	Clear of Ice Open Water	58.5	067	0805
16	59° 02.2'	170° 01.2'	Adjacent Ice Edge, Cakes Rotting	63.5	067	1635
17	58° 58.1'	170° 12.0'	Slightly Away From Ice Edge	66.6	068	0340
18	58° 57.2'	170° 45.6'	Same	67.2	068	0804
19	59° 22.2'	170° 59.2'	Adjacent Rotting Pack Ice Edge	67.2	068	1635

(TABLE 1 Contin.)

Cast #	LATITUDE(N)	LONGITUDE(W)	ICE CONDITIONS	DEPTH(M)	DAY	TIME
20	59° 16.6'	171° 04.5'	Same	69.5	069	0212
21	59° 11.2'	172° 22.0'	Same	83.6	069	0807
22	59° 37.1'	172° 40.0'	Adjacent Rotting Pack Ice Edge	82.7	069	1625
23	59° 30.8'	172° 36.4'		83.4	069	2129
24	59° 22.8'	172° 19.7'		81.8	070	0000
25	59° 17.7'	172° 02.4'		78.1	070	0136
26	59° 13.2'	171° 45.3'	Decaying Cakes and Rubble	77.0	070	0316
27	59° 07.9'	171° 28.5'		75.7	070	0440
28	59° 02.4'	171° 10.8'		72.0	070	0614
29	58° 58.4'	170° 57.6'		69.5	070	0736
30	58° 53.7'	170° 40.8'		69.8	070	0928
31	58° 49.2'	170° 23.3'		68.0	070	1117
32	58° 44.2'	170° 07.2'	Decaying Ice, Rubble Field	65.9	070	1316
33	58° 56.5'	170° 06.8'	Adjacent Ice Edge, Rotting Floes	63.4	070	1639
34	58° 53.8'	170° 13.9'	Rubble Field, CTD Hung Up	65.4	071	0439
35	58° 52.6'	170° 17.9'	Decaying Rubble	67.1	071	0822
36	58° 46.9'	170° 25.3'	Adjacent Ice Edge, Rotting Floes	70.2	071	1636
37	57° 58.5'	168° 21.1'	Clear of Ice, Open Water	67.1	072	0438
38	57° 45.2'	167° 37.7'	Open Water in Lead, Compact Floes	61.0	072	0812
39	58° 01.6'	166° 14.9'	Same	54.9	073	0436
40	58° 00.5'	166° 14.7'	Same	54.0	073	0809
41	58° 00.2'	166° 14.4'	Same	56.4	073	1632

< indicate gaps of more than 12 hours

TABLE 2 AIRSONDE SOUNDINGS

No.	Date (Mar., 1979)	Time (GMT)	Lat. (N)	Long. (W)	Air Temp (°C)	Wind Speed (m/sec)	Wind Direc- tion (True)	Max ht. (m)	Comments
1	2	2000	58°28.6'	165°56.1'	-10.5	6	025	-	Bad Antenna connection
2	3	0223	58°25.0'	165°59.0'	-11.2	10	015	4039	20 km into the ice
3	3	1230	58°11.2'	166°01.5'	- 9.5	8	027	5329	10 km into the ice
4	3	2118	58°21.5'	166°08.8'	-12.0	10	010	4761	6/8 ice coverage
5	3	2302	58°16.4'	166°16.2'	-12.1	13	006	5130	isolated ice bands
6	3	0147	57°59.8'	166°47.1'	-10.0	14	010	-	bad airsonde
7	4	0406	57°40.2'	167°25.8'	-10.0	14	020	4749	90 km S.W. of ice edge
8	5	0243	58°11.2'	167°21.9'	- 9.5	13	025	3402	4 km S.W. of ice edge, Case A
9	5	0345	58°01.6'	167°33.1'	-10.9	9	042	4646	20 km S.W. of ice edge, Case A
10	5	0453	57°49.9'	167°47.9'	-11.0	12	040	5009	50 km S.W. of ice edge, Case A
11	5	0634	57°41.7'	168°01.9'	- 5.5	12	035	4062	70 km S.W. of ice edge, Case A
12	10	2049	59°32.2'	172°36.0'	- 2.0	10	010	5390	in ice bands
13	12	0425	58°53.7'	170°13.2'	- 2.5	9	020	5378	near ice edge
14	13	2105	58°03.4'	166°11.0'	- 6.0	5	335	5407	near ice edge
15	14	2022	57°58.8'	166°16.0'	- 5.5	8	055	4449	near ice edge
16	14	2248	57°58.5'	166°16.6'	- 3.9	7	050	5063	near ice edge, NASA overflight Case B
17	14	2337	57°55.3'	166°19.5'	- 3.0	5	025	4605	6 km S. of ice edge, Case B
18	15	0020	57°51.6'	166°20.8'	- 5.0	5	006	2400	13 km S. of ice edge, Case B
19	15	0055	57°46.9'	166°21.6'	- 4.5	5	033	539	22 km S. of ice edge, (burst)
20	15	0118	57°42.2'	166°19.4'	- 3.5	5	029	4736	30 km S. of ice edge, Case B
21	15	0216	57°29.4'	166°14.1'	- 2.1	7	019	4874	53 km S. of ice edge, Case B
22	15	0334	57°12.2'	166°07.4'	- 1.6	5	005	5503	87 km S. of ice edge, Case B
23	15	0435	56°58.6'	166°02.9'	- 1.6	5	005	5564	111 km S. of ice edge, Case B

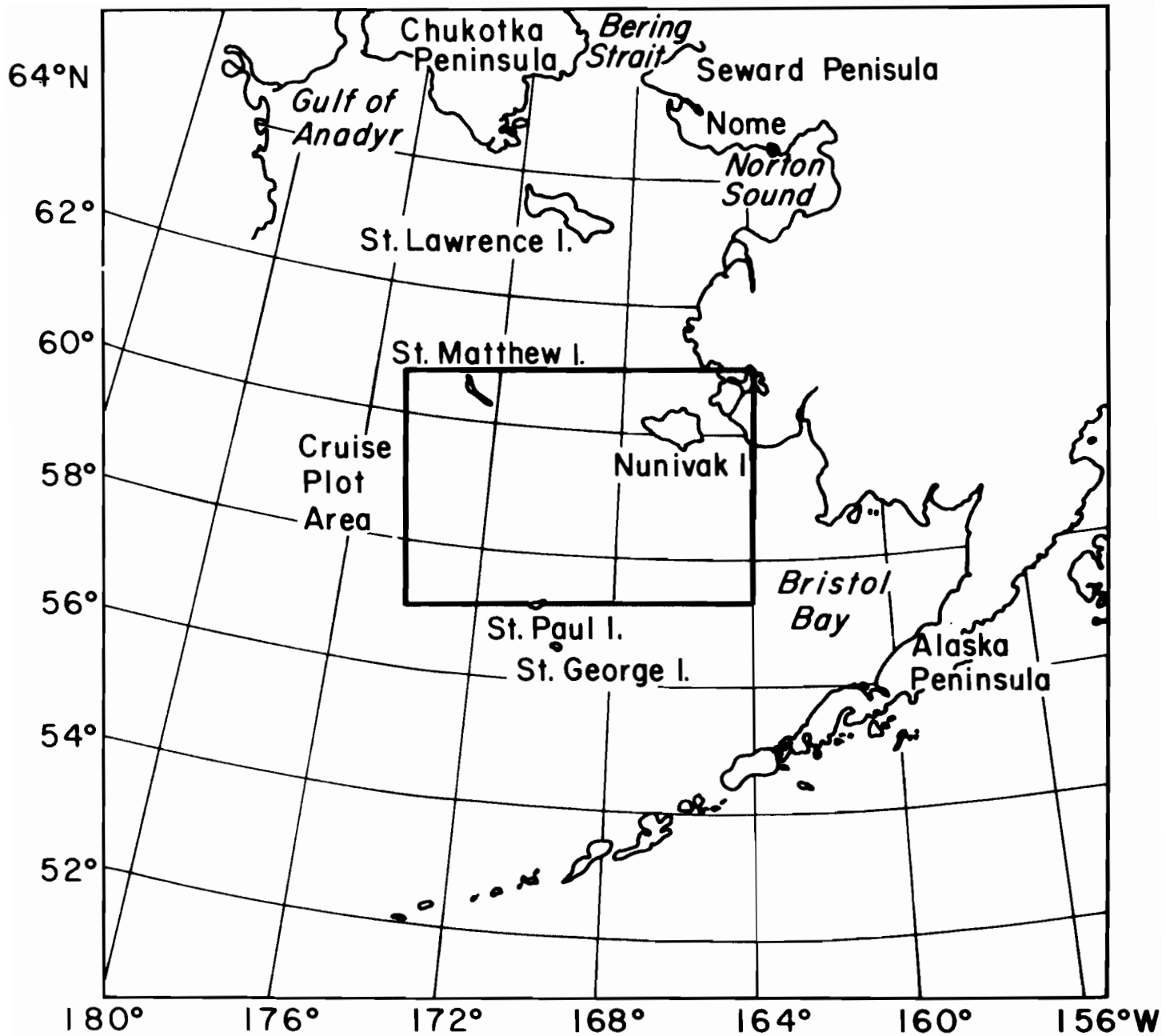


Figure 1. Cruise region in the Bering Sea, March 1979.

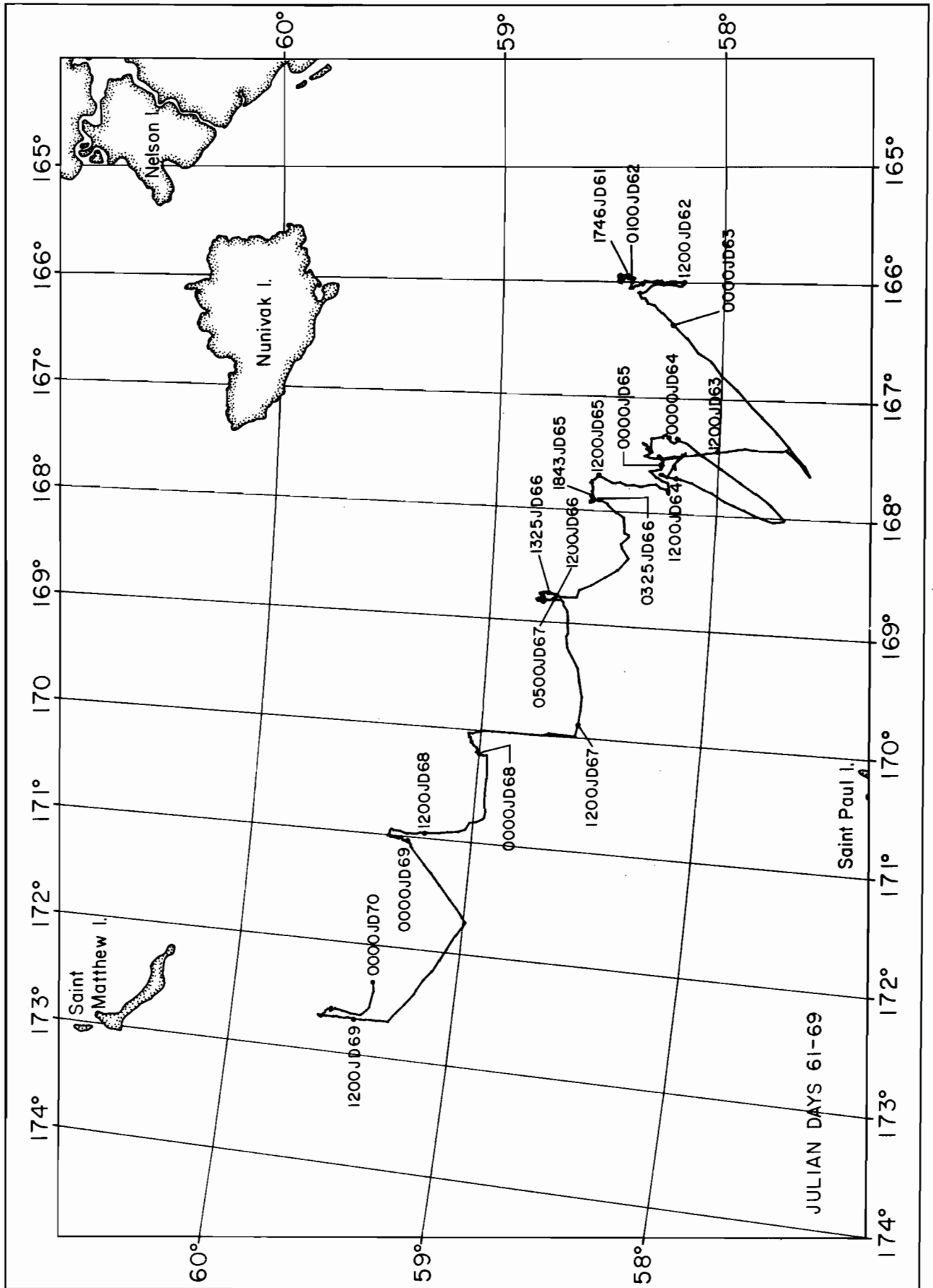


Figure 2a. Ship's cruise track. Positions at times in GMT and Julian Day are marked.

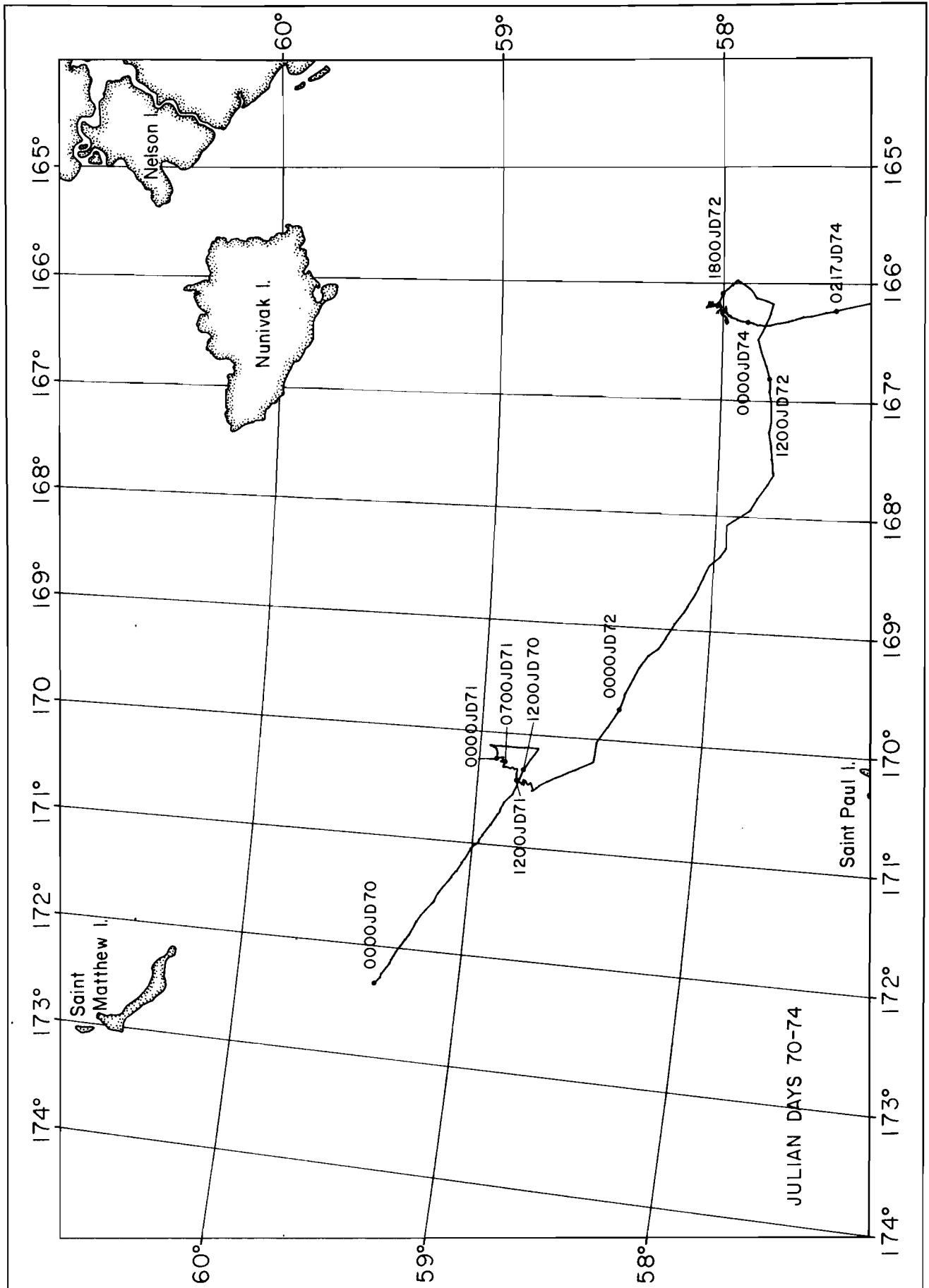


Figure 2b. Ship's cruise track. Positions at times in GMT and Julian Day are marked.



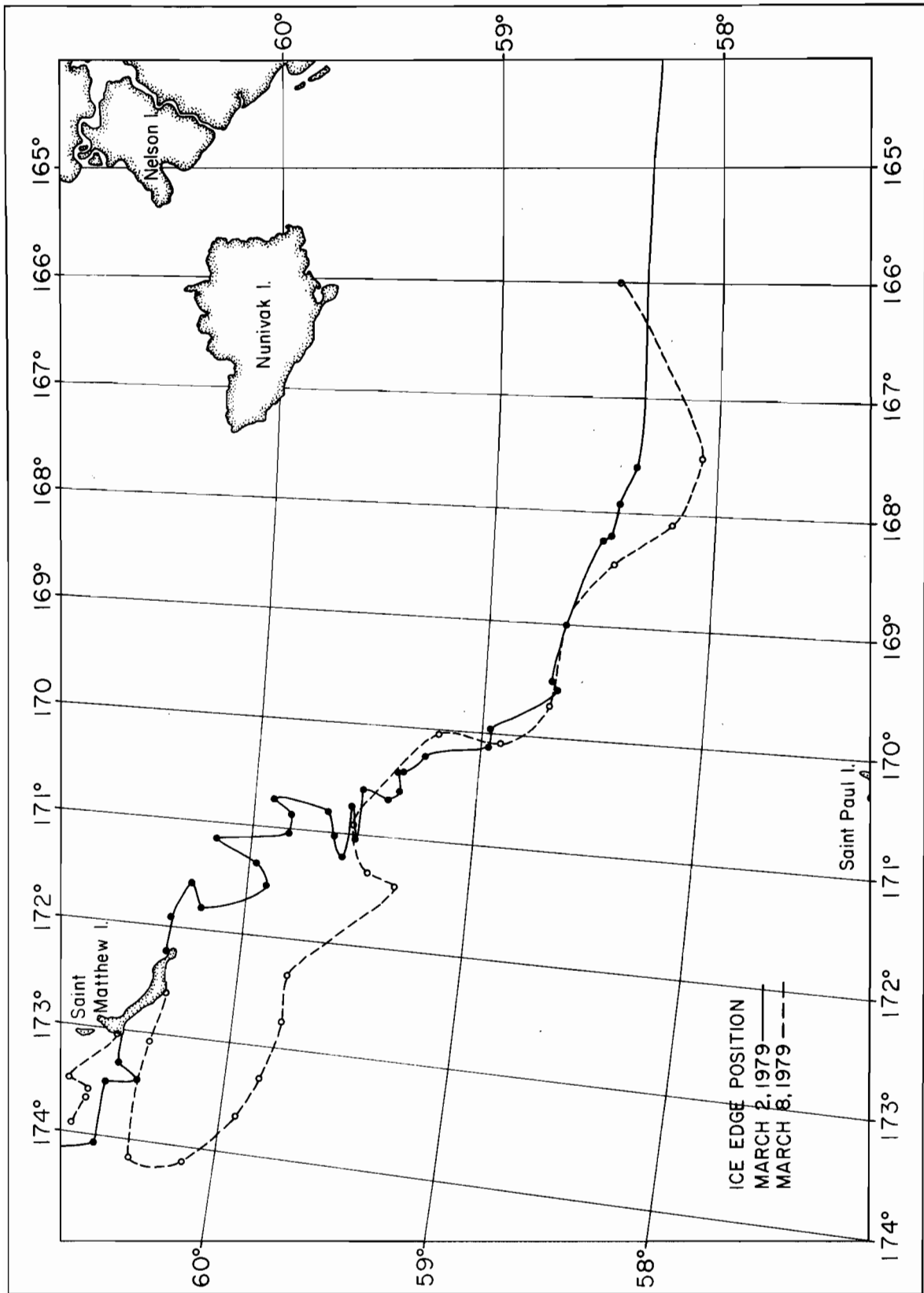


Figure 3. Aerial reconnaissance of the position of the ice edge on March 2 and March 8, 1979.

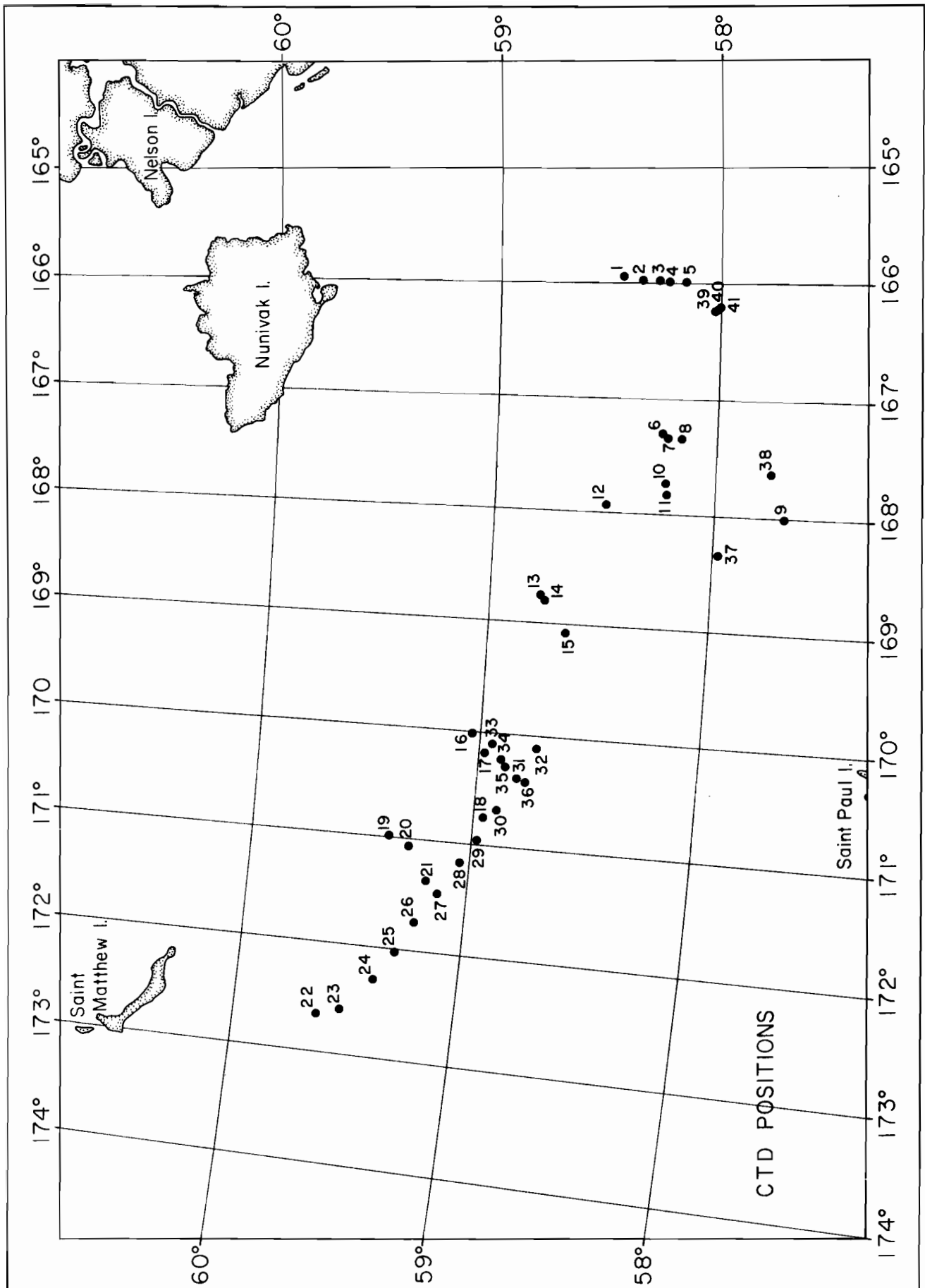


Figure 4. Locations of CTD stations.

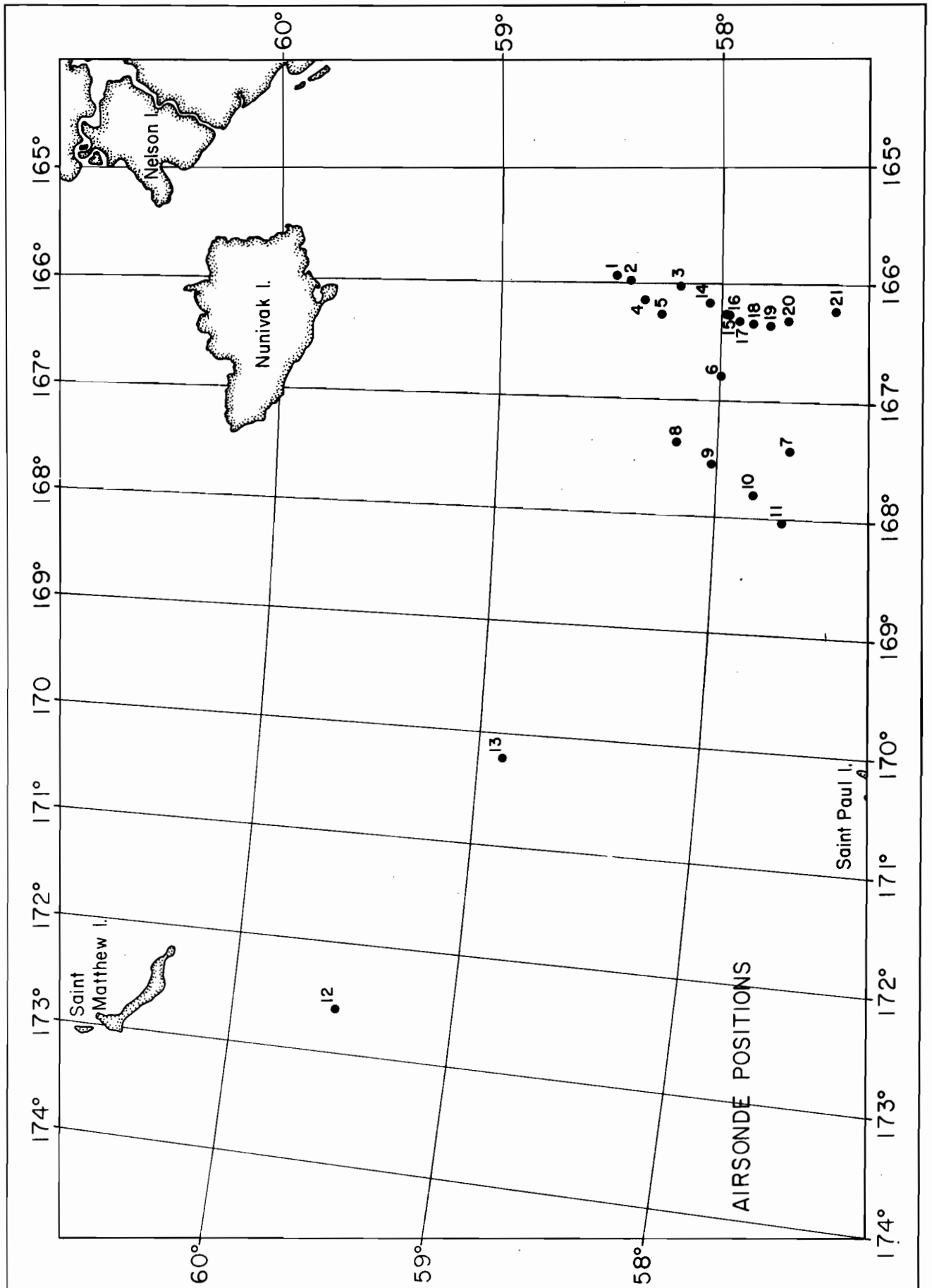


Figure 5. Locations of airsonde launches.

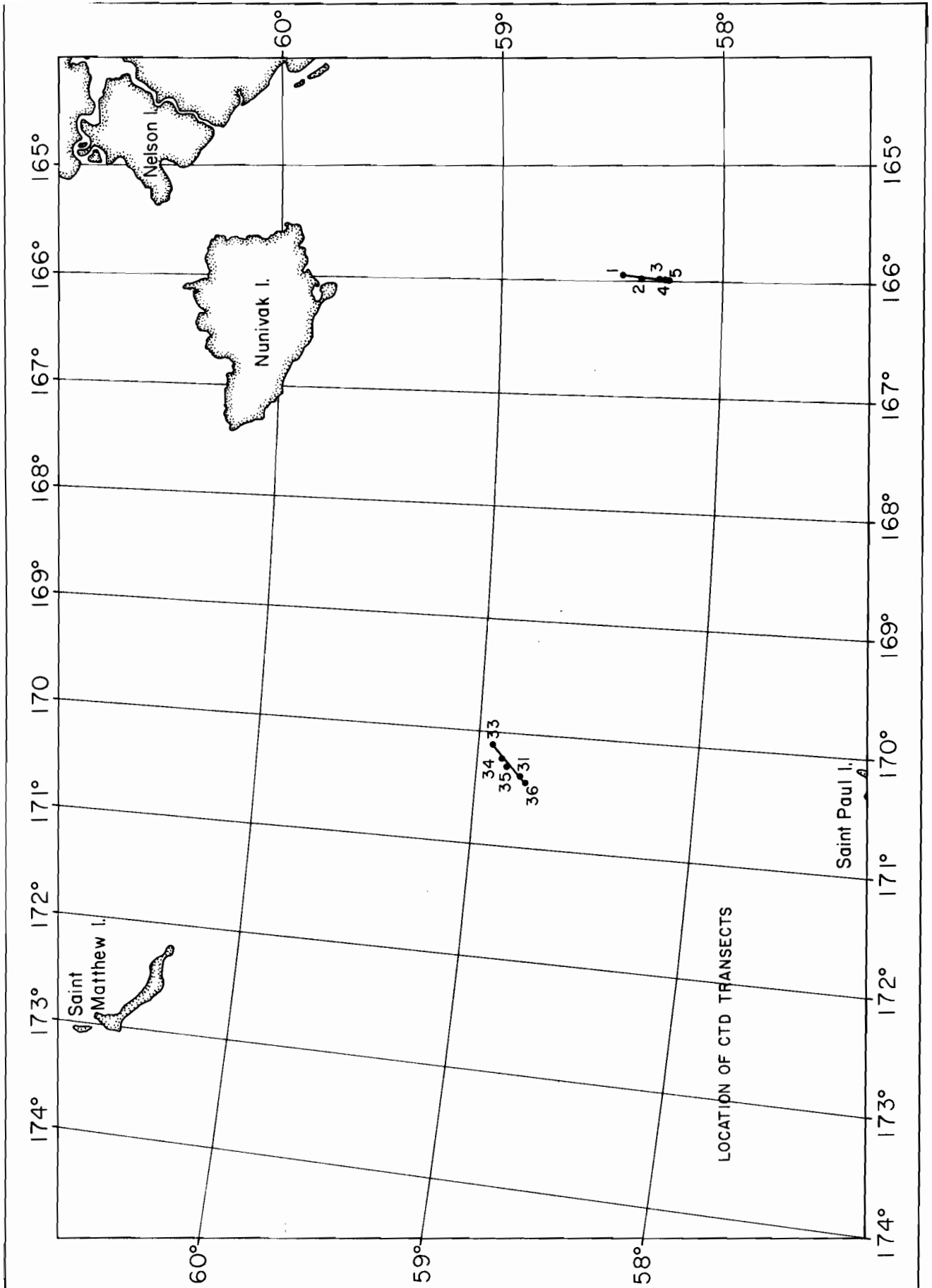


Figure 6. Location of CTD transects.

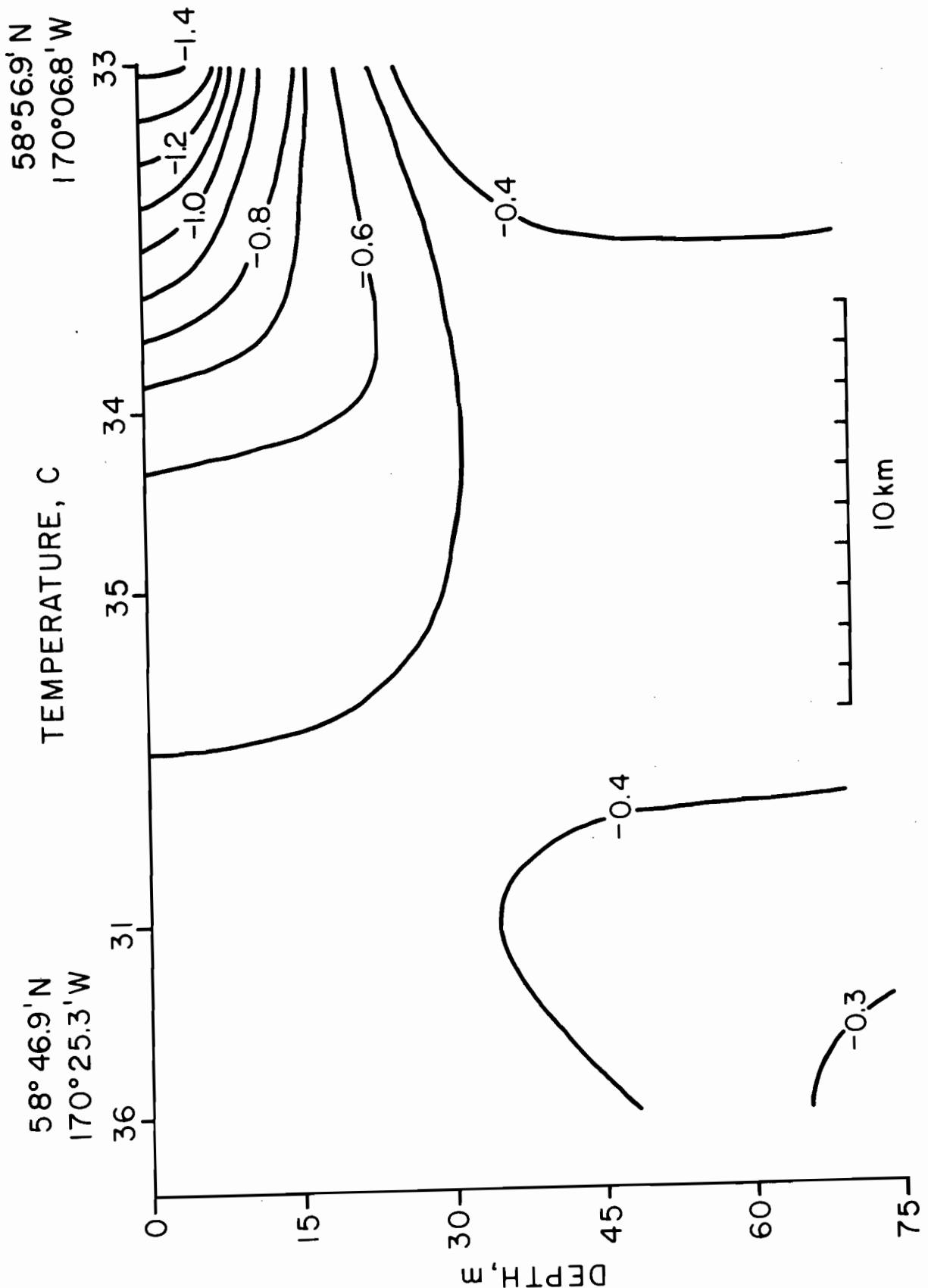


Figure 7a. CTD transect showing a surface lens of meltwater. Numbers on the horizontal axis are CTD stations. Isotherms, isohalines and isopleths are labeled.

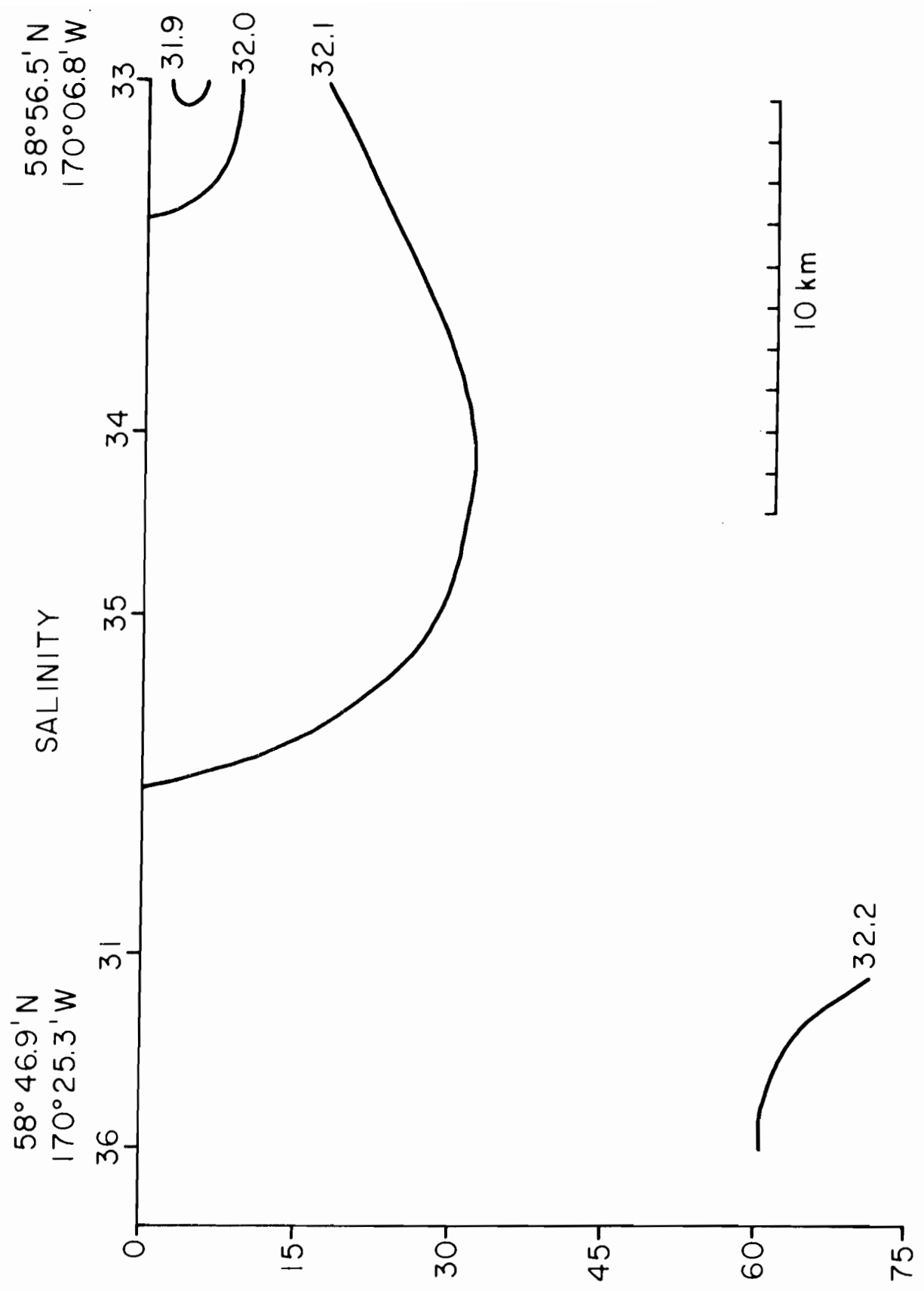


Figure 7b. CTD transect showing a surface lens of meltwater. Numbers on the horizontal axis are CTD stations. Isotherms, isohalines and isopleths are labeled.

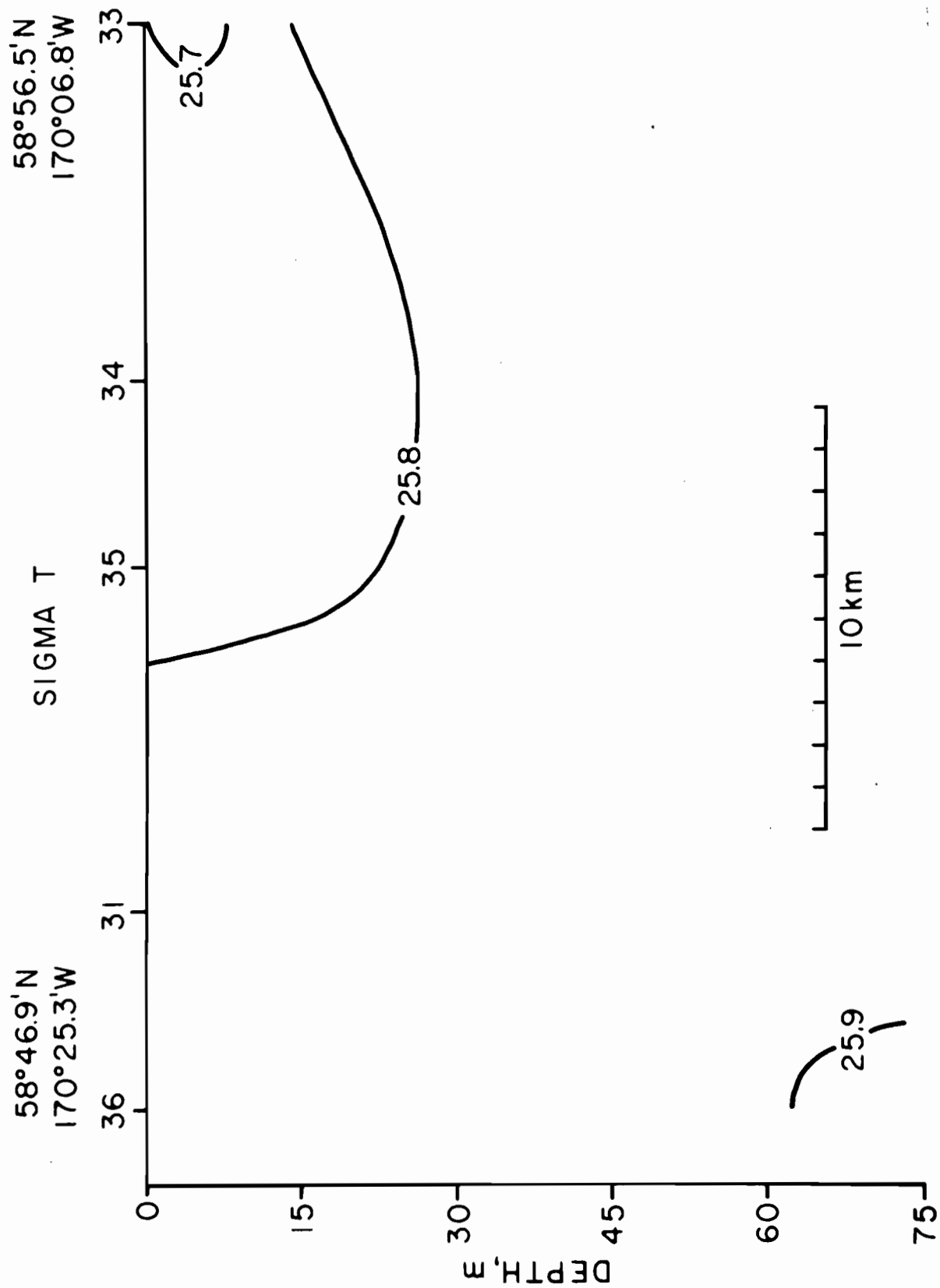


Figure 7c. CTD transect showing a surface lens of meltwater. Numbers on the horizontal axis are CTD stations. Isotherms, isohalines and isopleths are labeled.

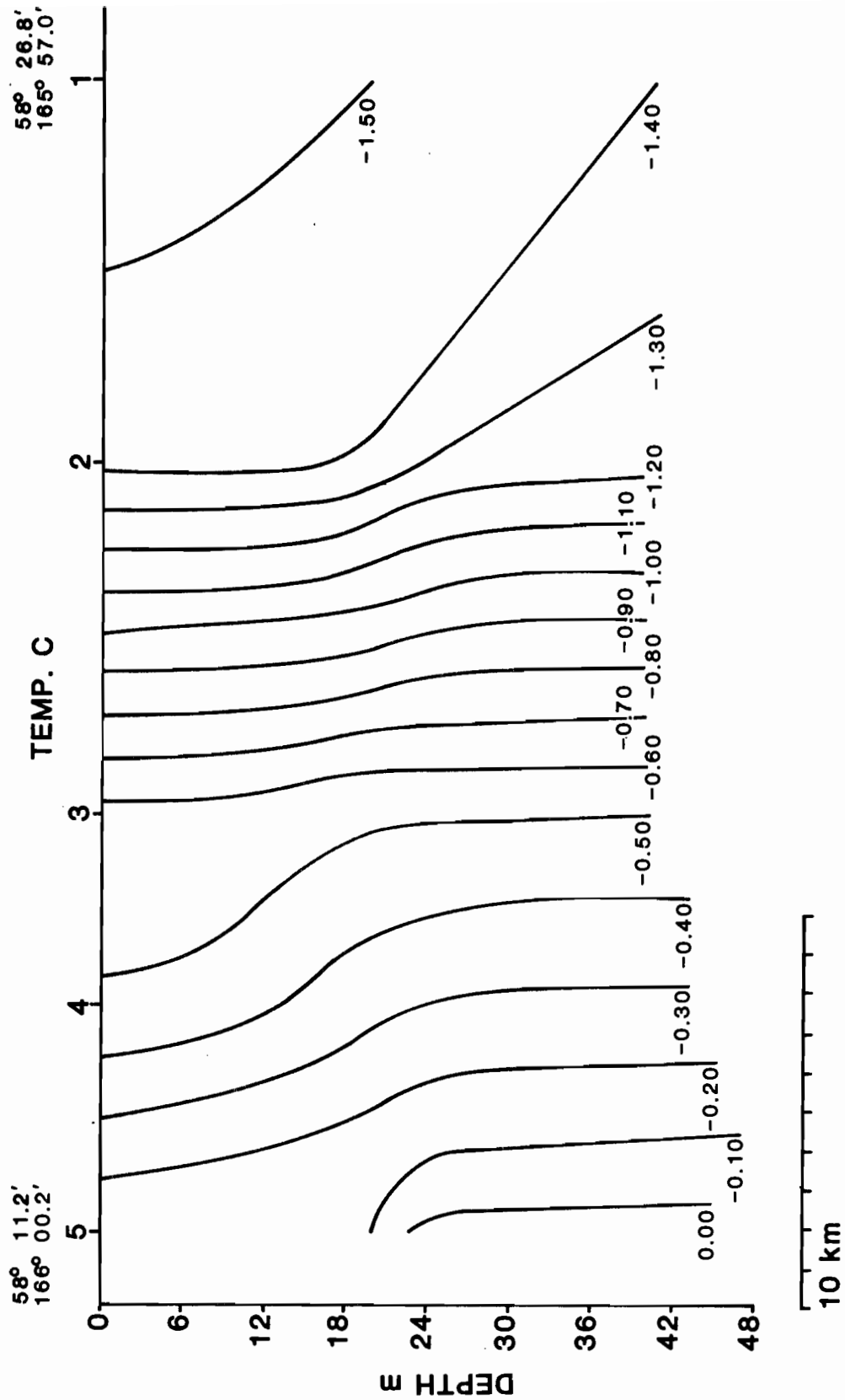


Figure 8a. CTD transect taken at the beginning of the cruise, showing a front. This is the only time during the cruise such a feature was seen.



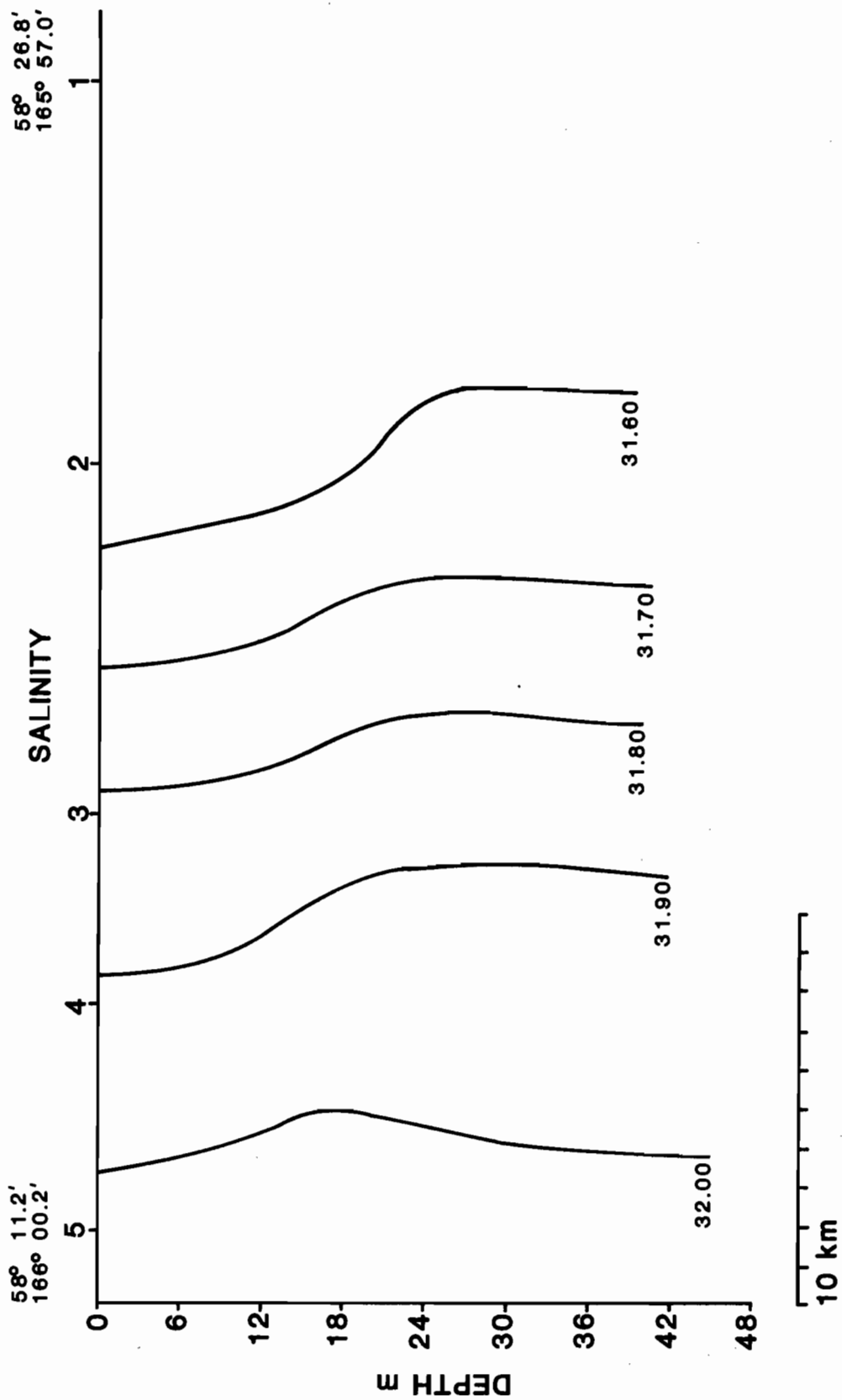


Figure 8b. CTD transect taken at the beginning of the cruise, showing a front. This is the only time during the cruise such a feature was seen.

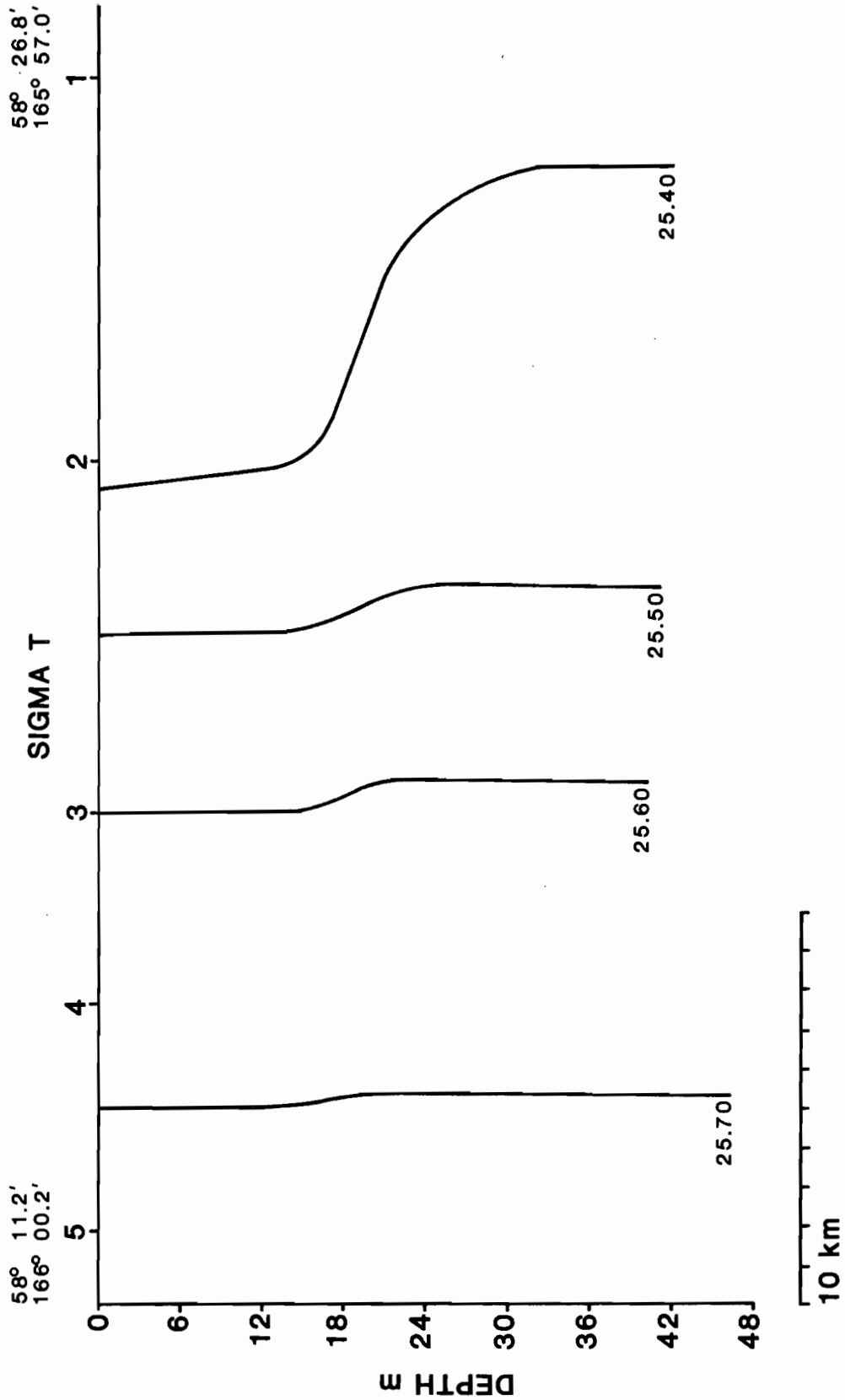


Figure 8c. CTD transect taken at the beginning of the cruise, showing a front. This is the only time during the cruise such a feature was seen.

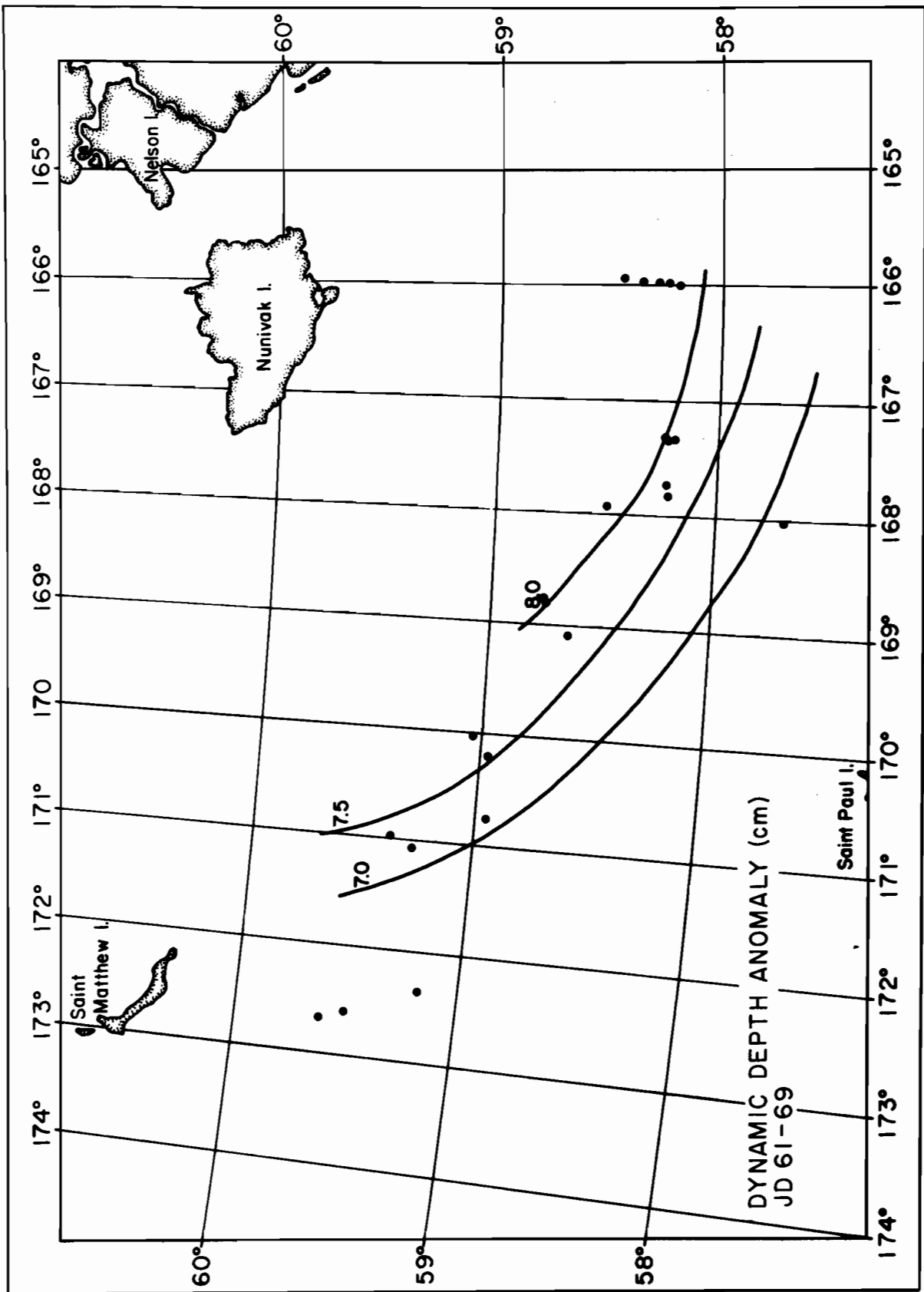


Figure 9a. Dynamic depth anomaly at 35 m, in dynamic centimeters.

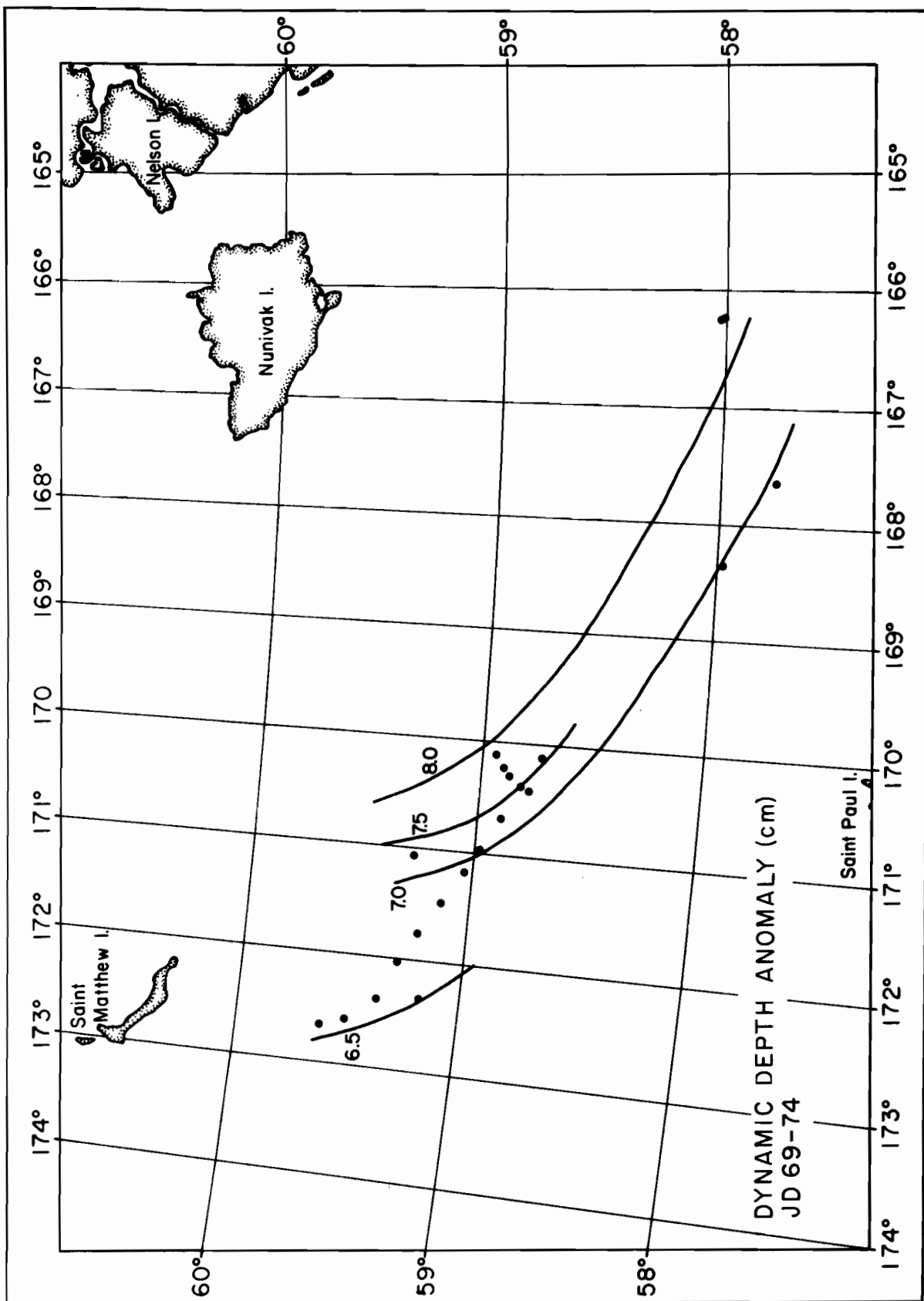


Figure 9b. Dynamic depth anomaly at 35 m, in dynamic centimeters.

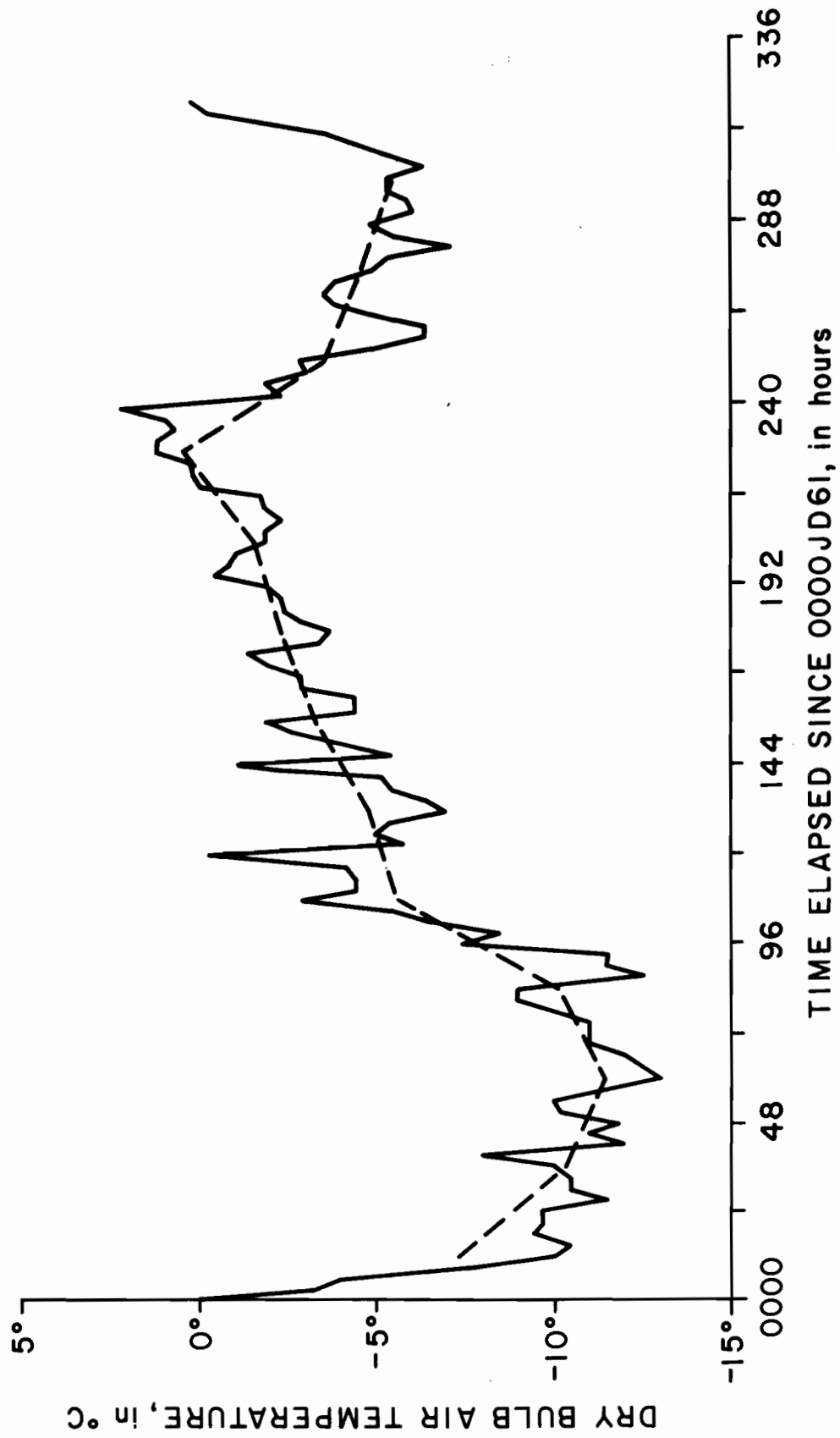


Figure 10a. Air temperature and pressure. Dry bulb temperature.

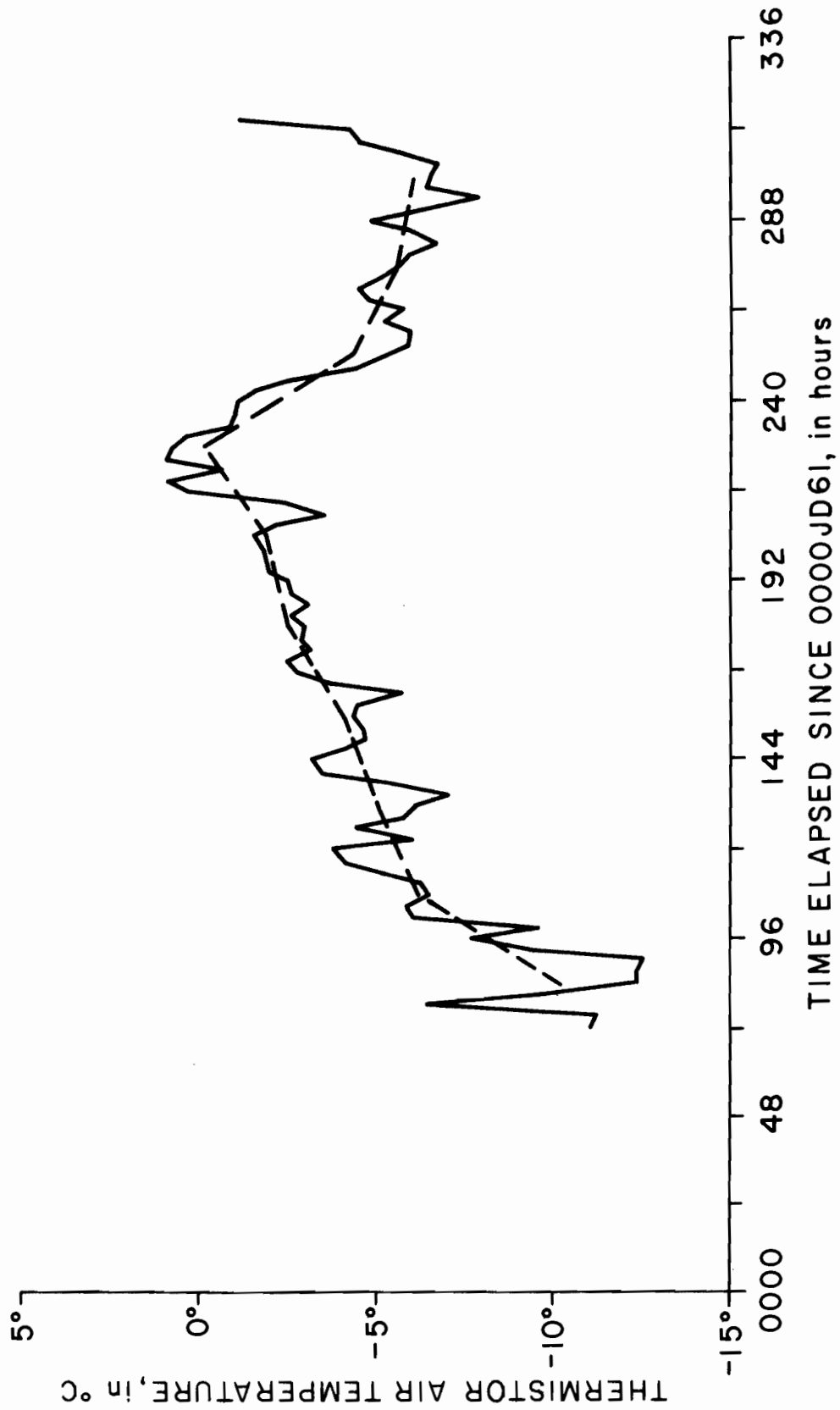


Figure 10b. Air temperature and pressure. Thermistor temperature.

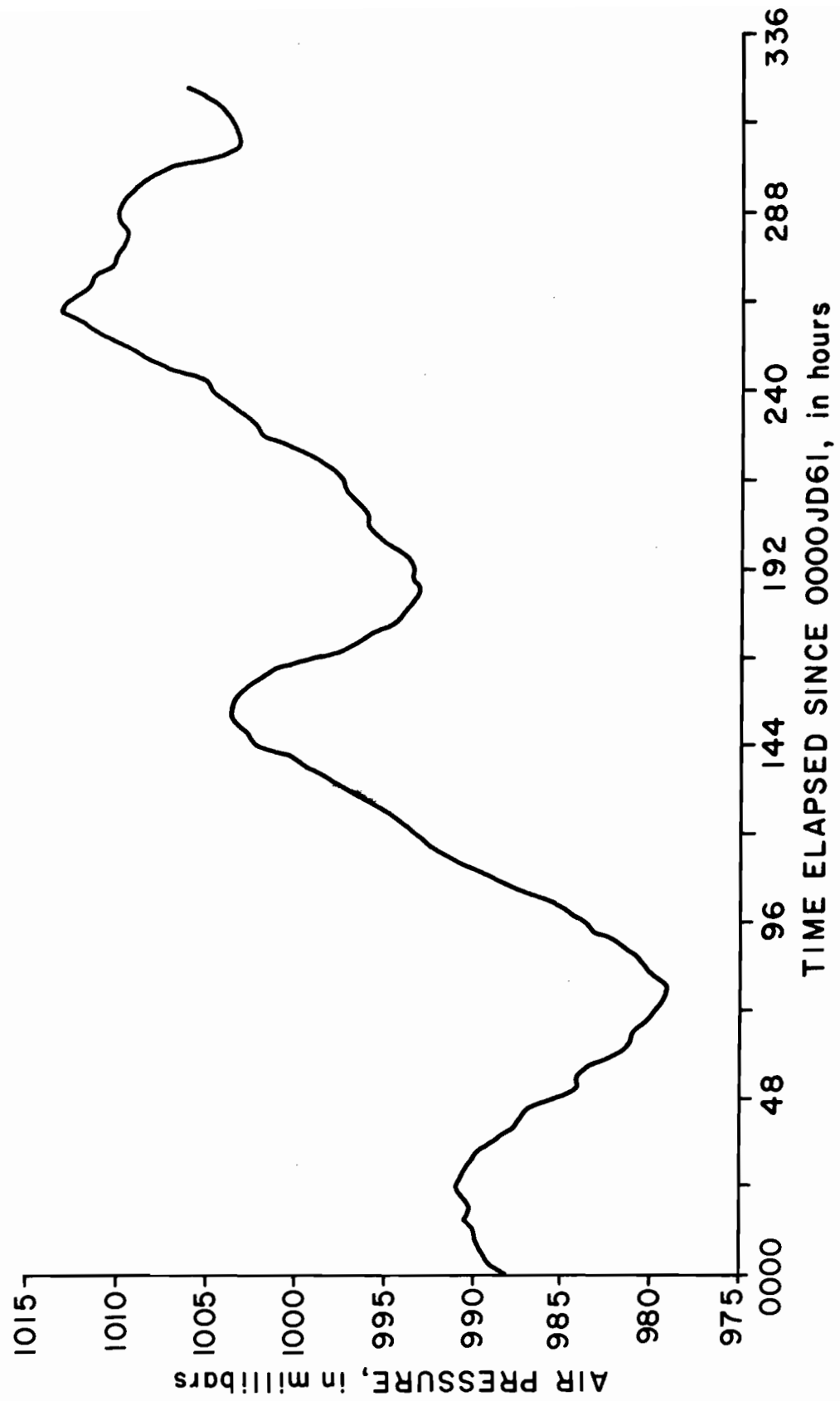


Figure 10c. Air temperature and pressure. Surface pressure.

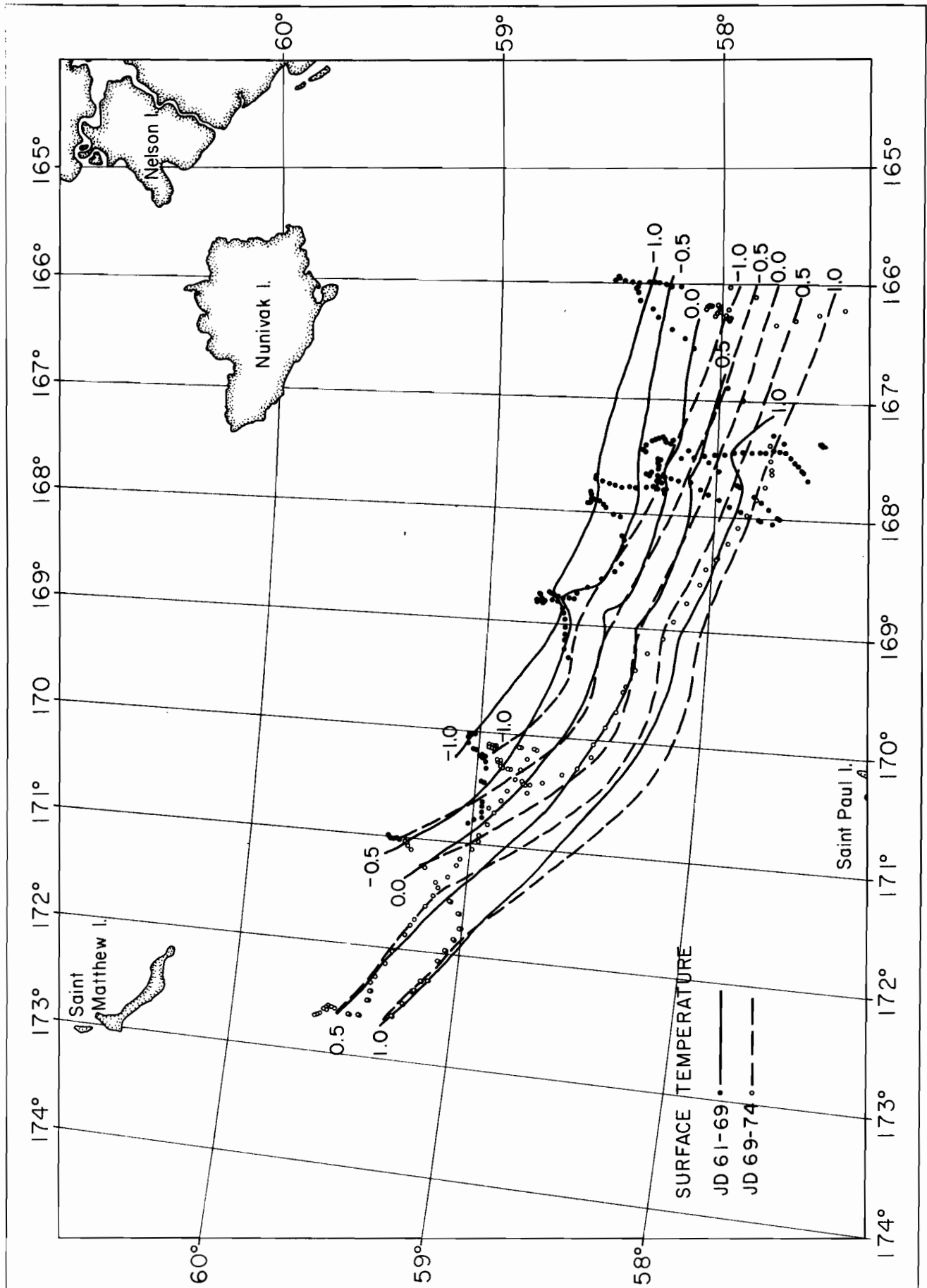


Figure 11. Sea surface isotherms.



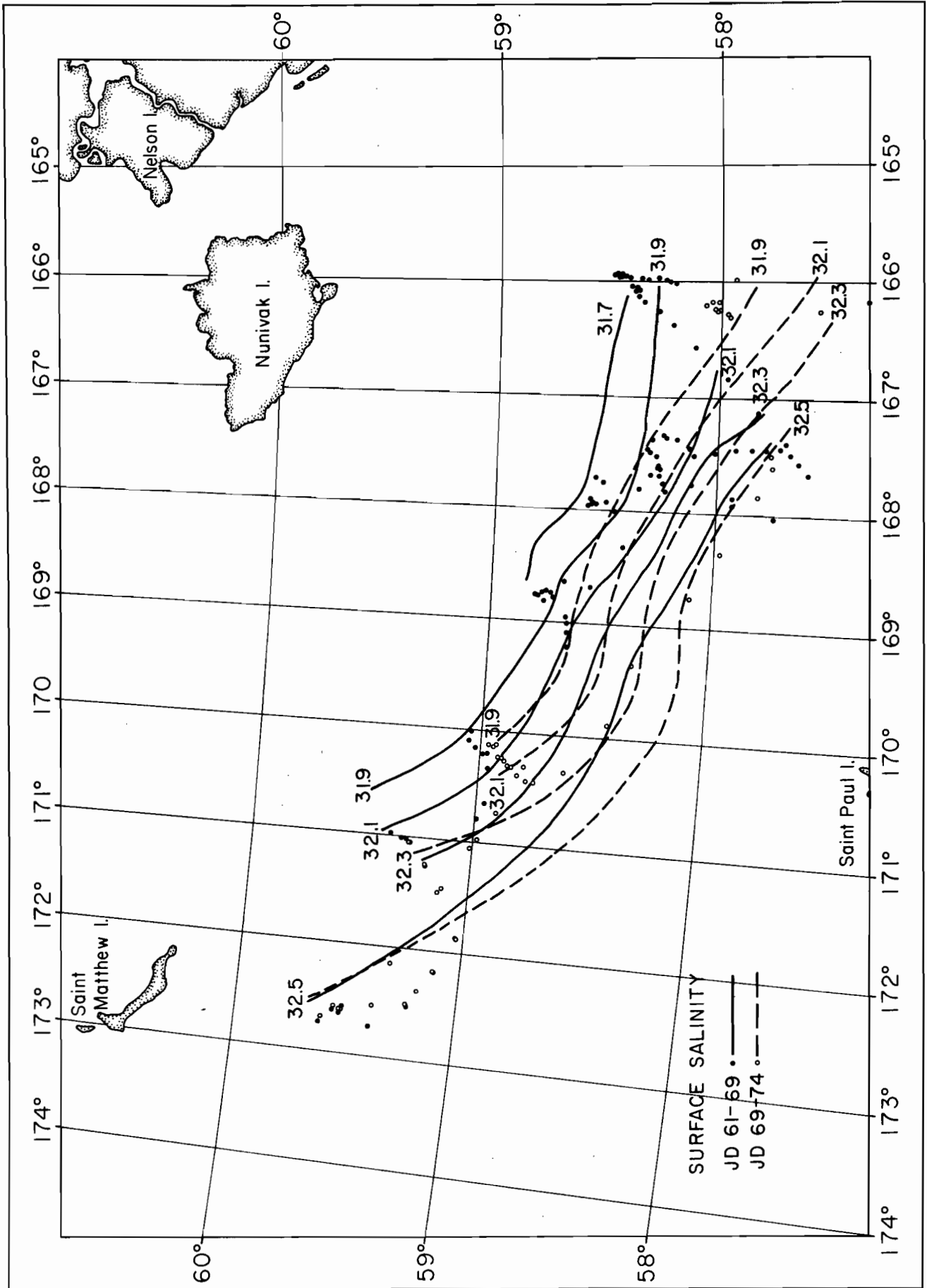


Figure 12. Sea surface isohalines.

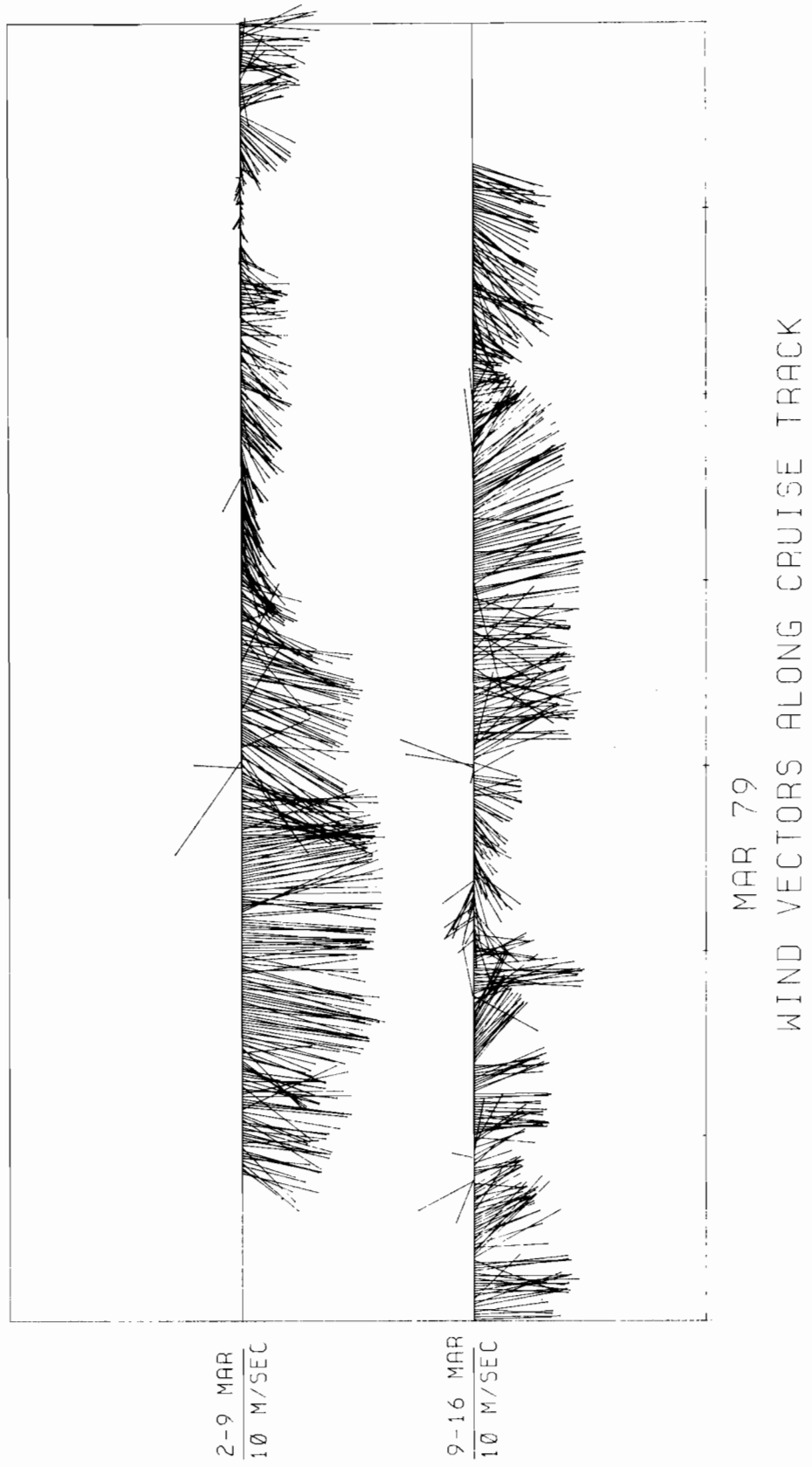


Figure 13. True wind magnitude and direction calculated from relative wind magnitude and direction data. Direction is the vector direction rather than the meteorological convention's direction.

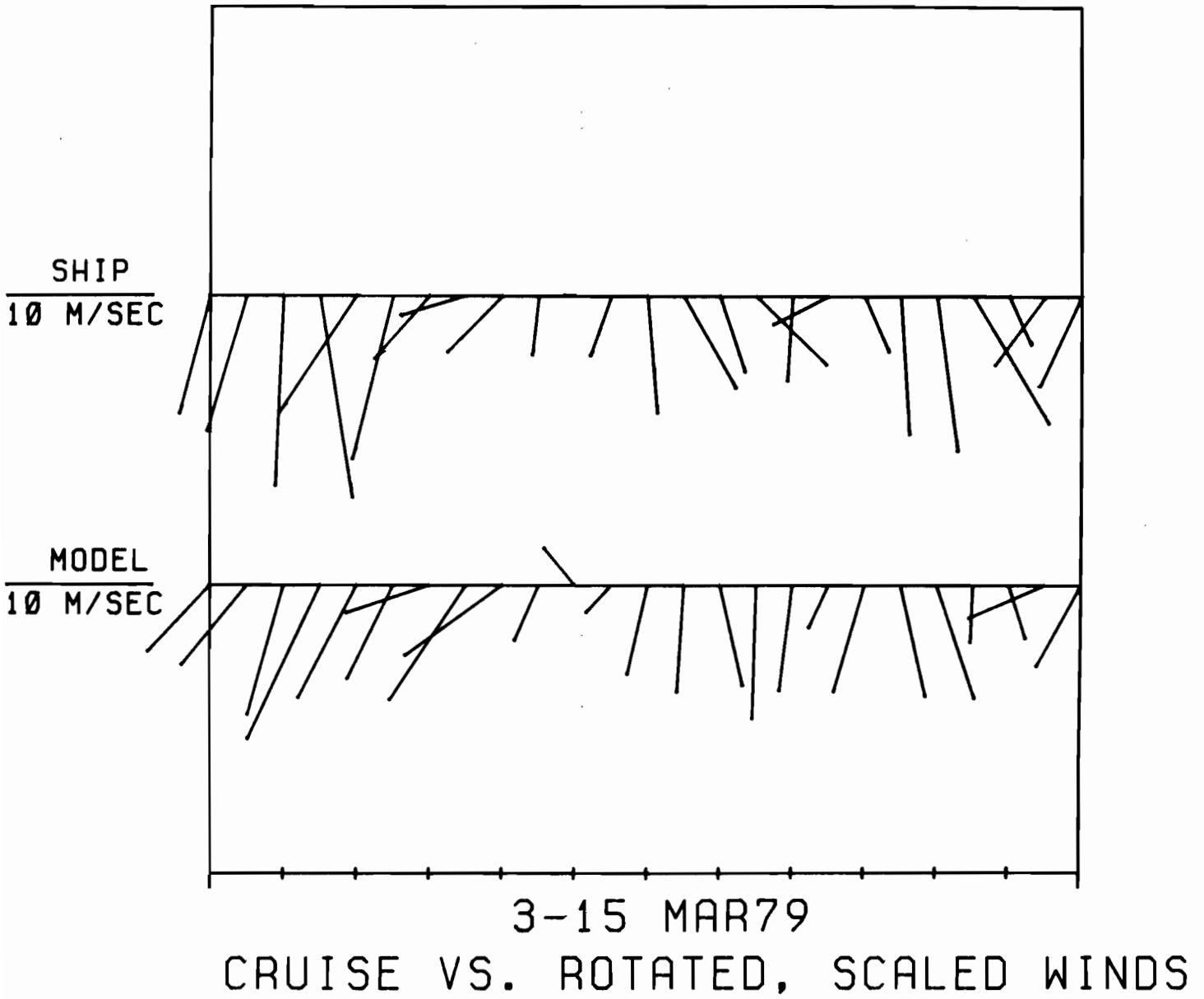


Figure 14a. Calculated surface wind compared to winds measured at the ship and three surface stations.

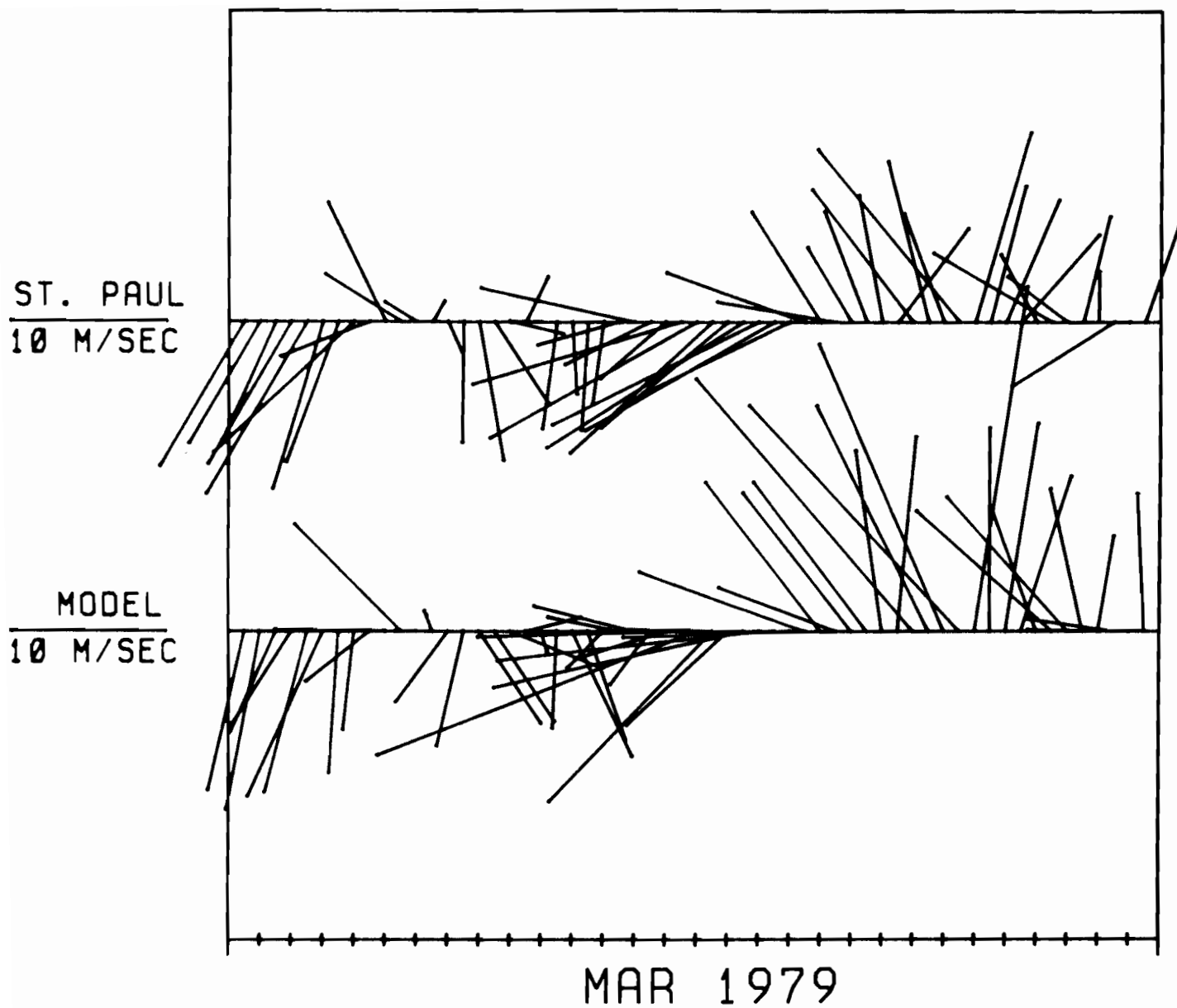


Figure 14b. Calculated surface wind compared to winds measured at the ship and three surface stations.

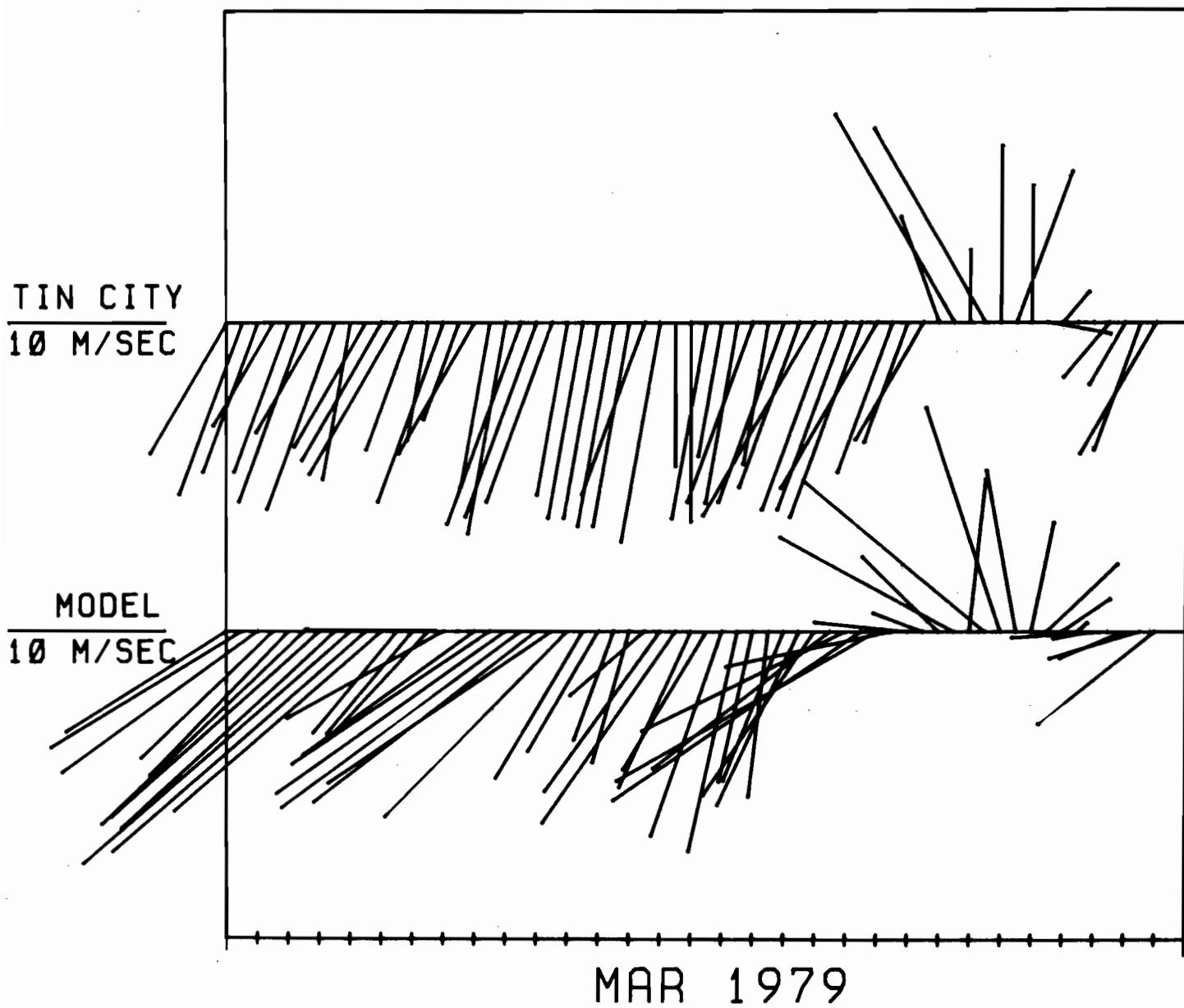


Figure 14c. Calculated surface wind compared to winds measured at the ship and three surface stations.

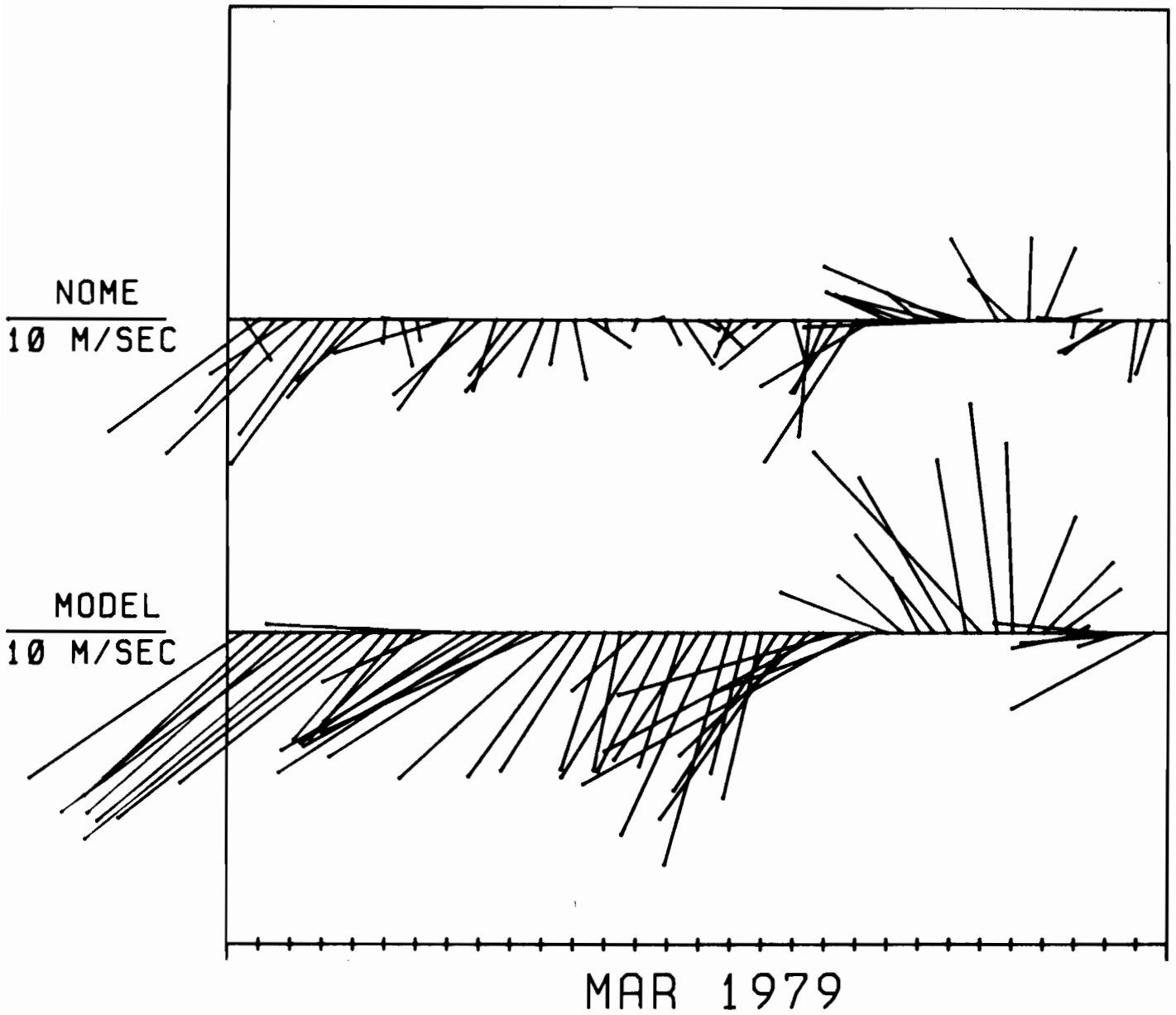


Figure 14d. Calculated surface wind compared to winds measured at the ship and three surface stations.

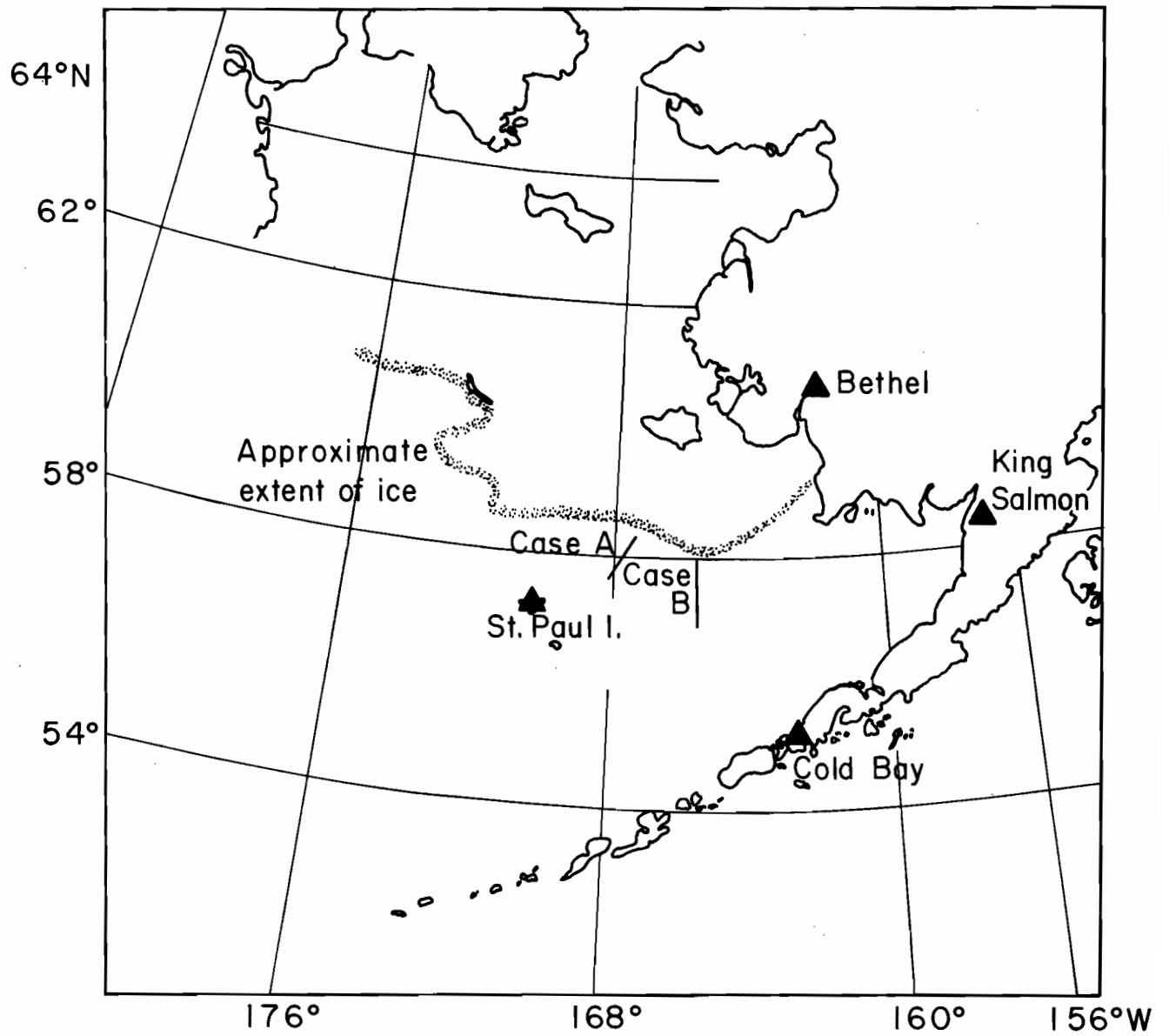


Figure 15. Map of the Bering Sea and the locations of cases A and B.

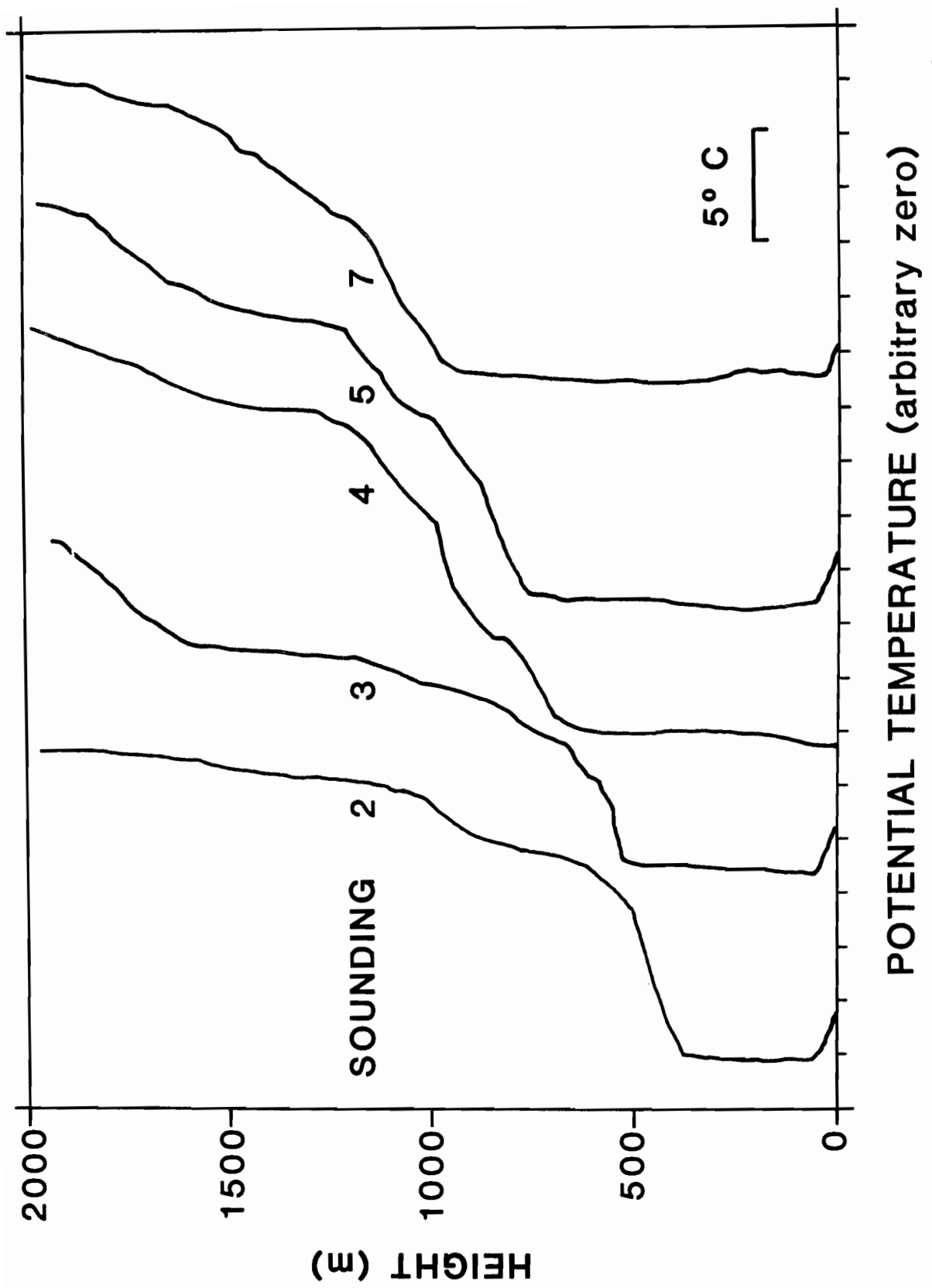


Figure 16a. Potential temperature for all soundings. The zero point on the abscissa is different for each sounding.



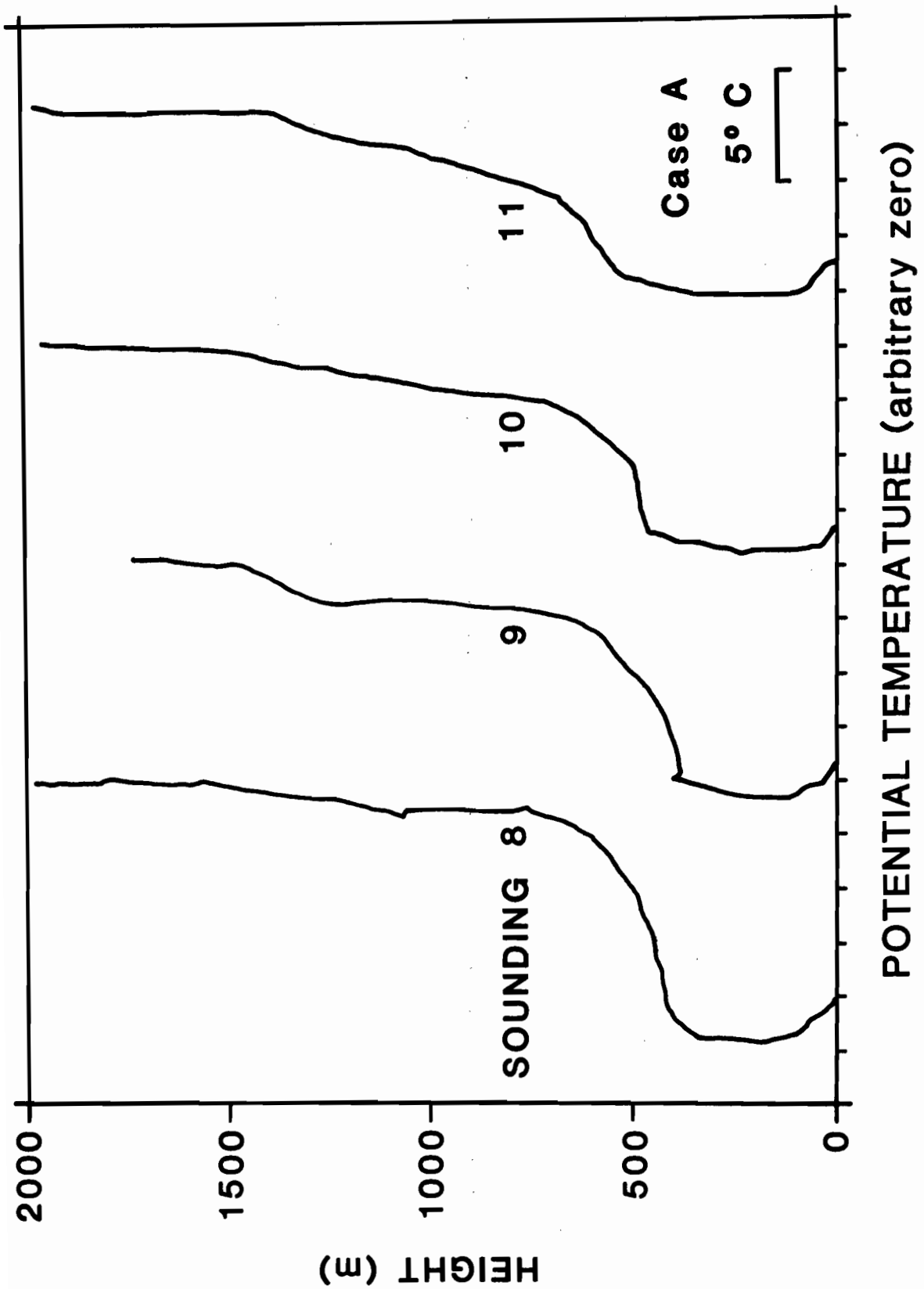


Figure 16b. Potential temperature for all soundings. The zero point on the abscissa is different for each sounding.

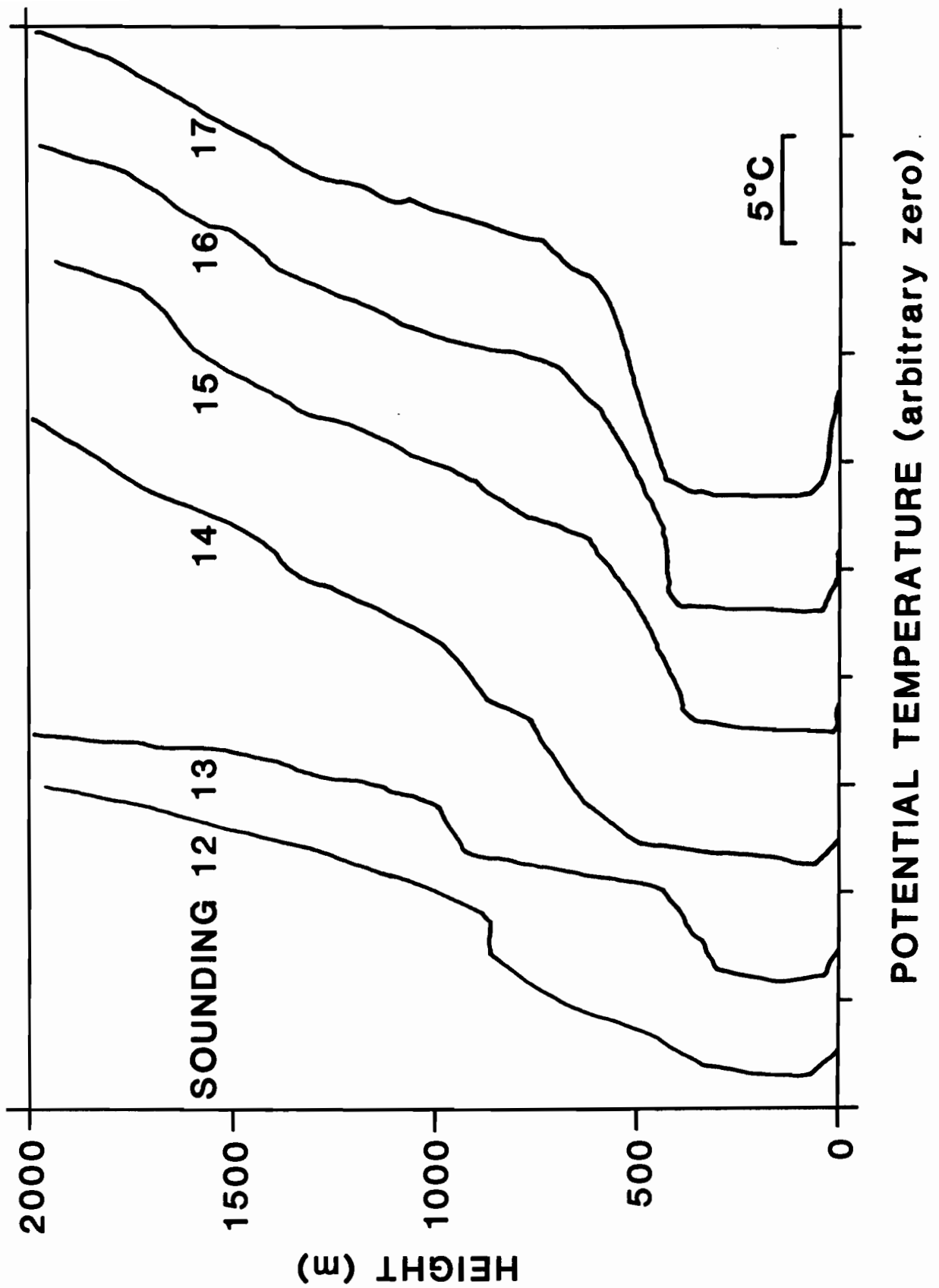


Figure 16c. Potential temperature for all soundings. The zero point on the abscissa is different for each sounding.

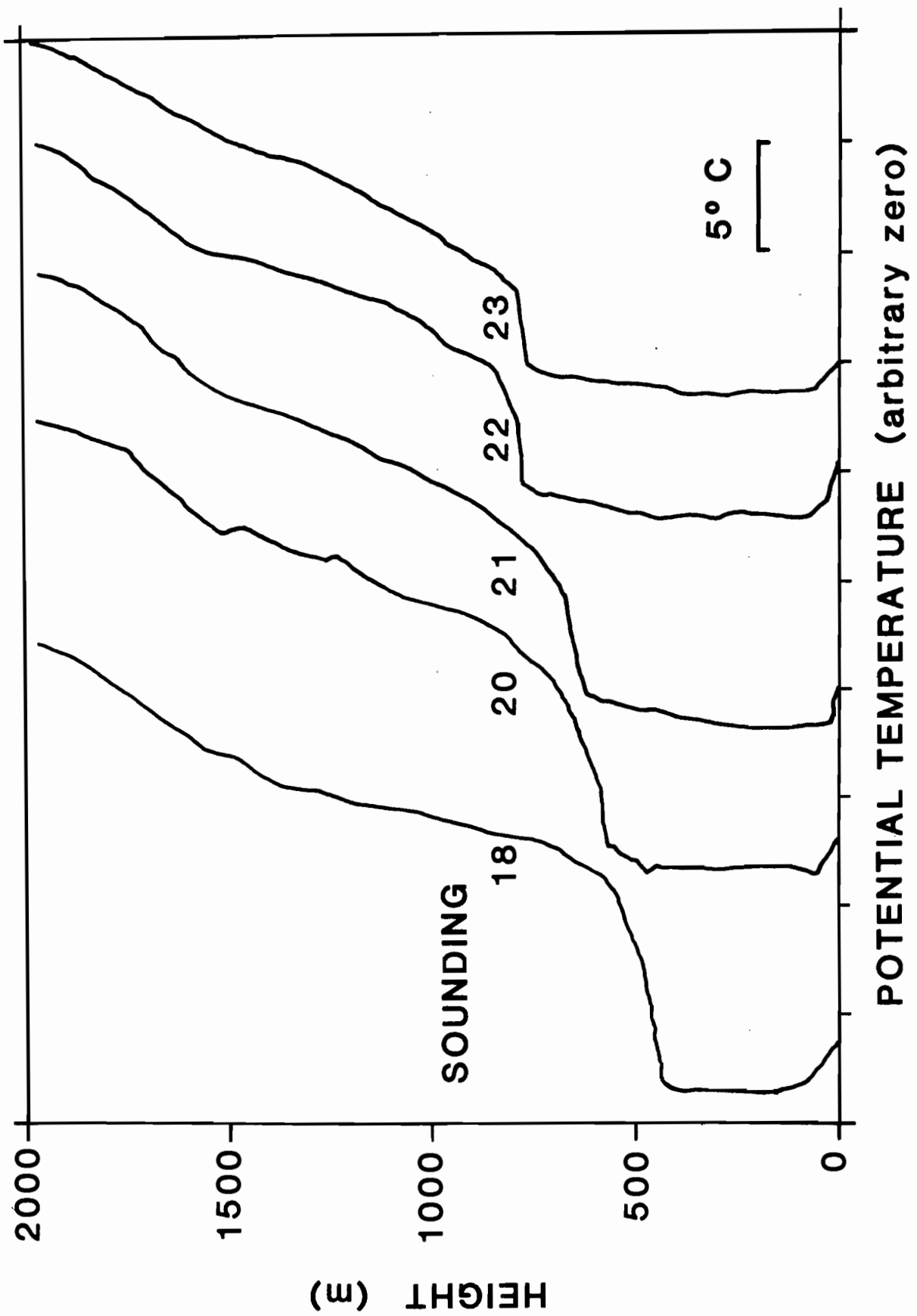


Figure 16d. Potential temperature for all soundings. The zero point on the abscissa is different for each sounding.

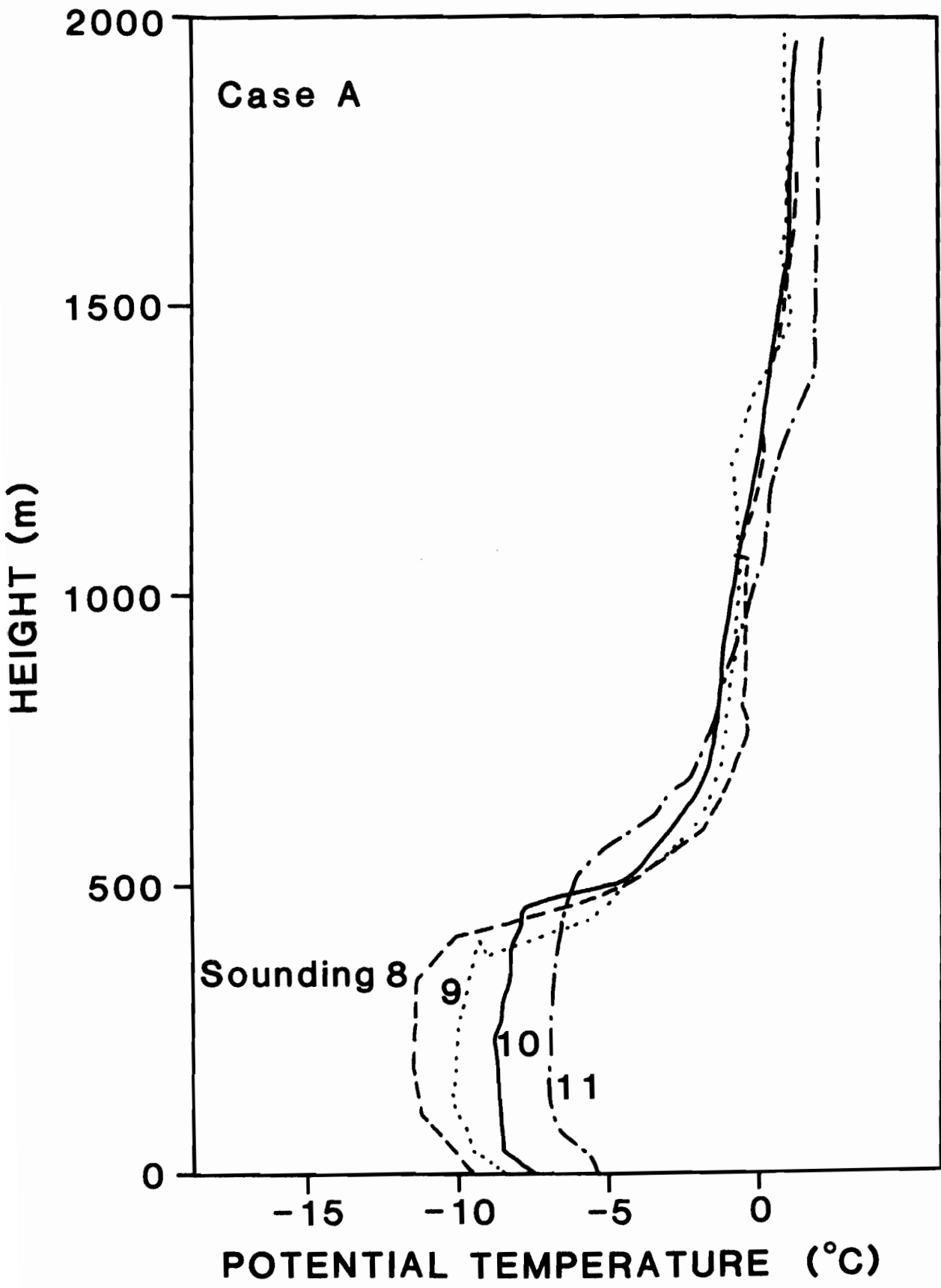


Figure 17. Potential temperature for Case A, one origin.

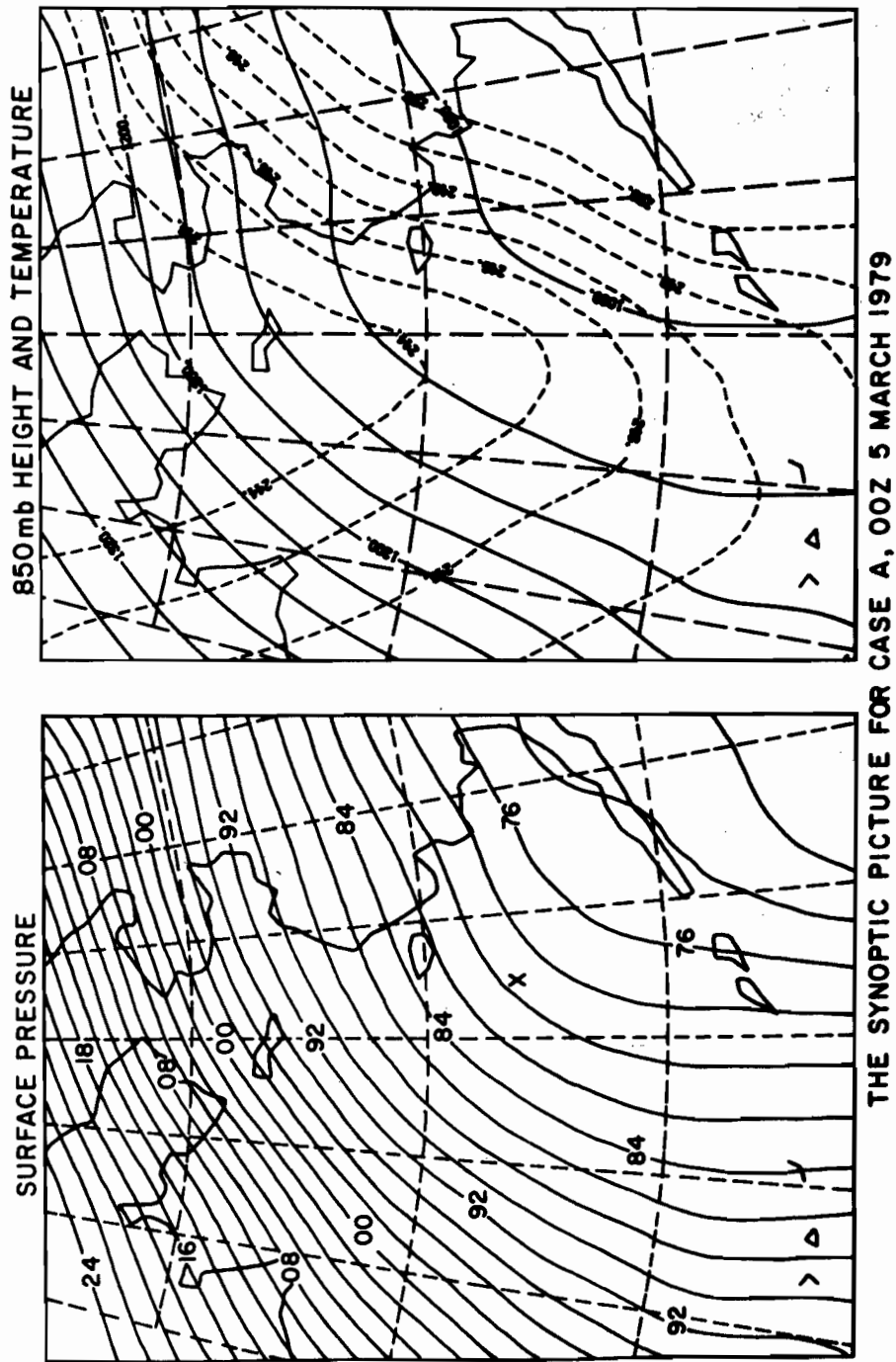


Figure 18. Surface pressure and 850-mb maps for Case A, 00Z 5 March 1979.

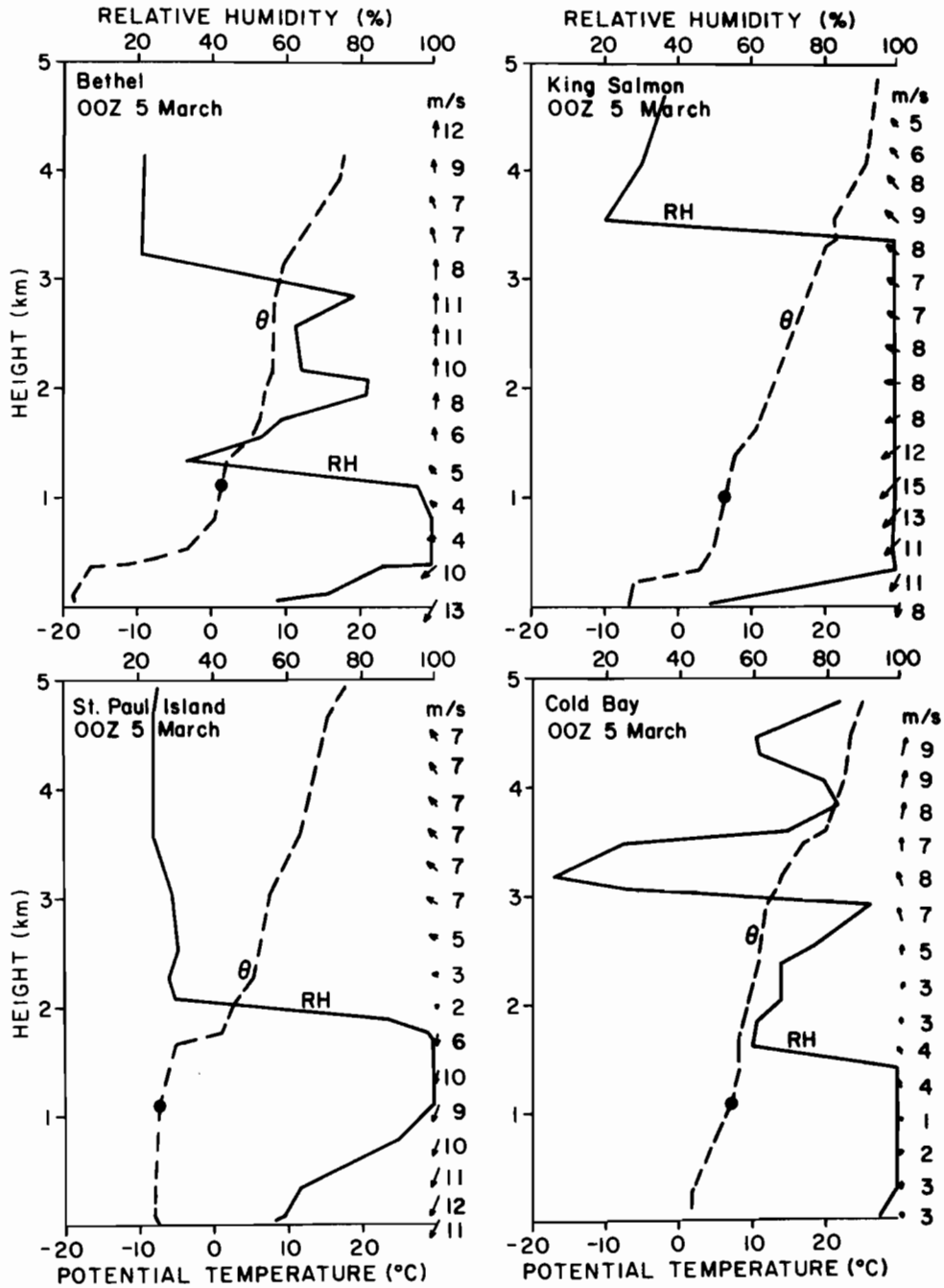


Figure 19. Upper air soundings from the National Weather Service, 00Z 5 March. The dots indicate the 850-mb level.

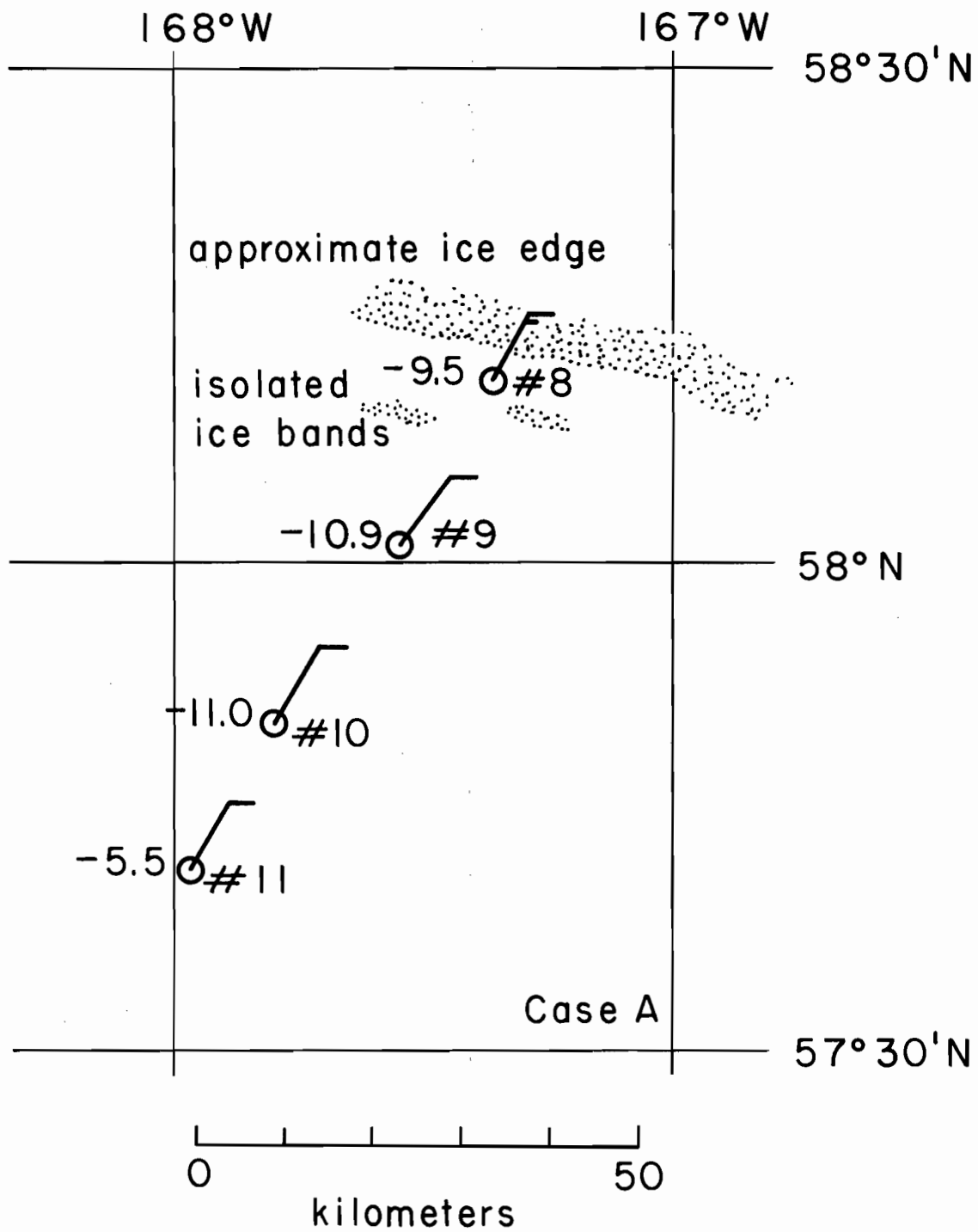


Figure 20. Map of the locations of soundings used in Case A.

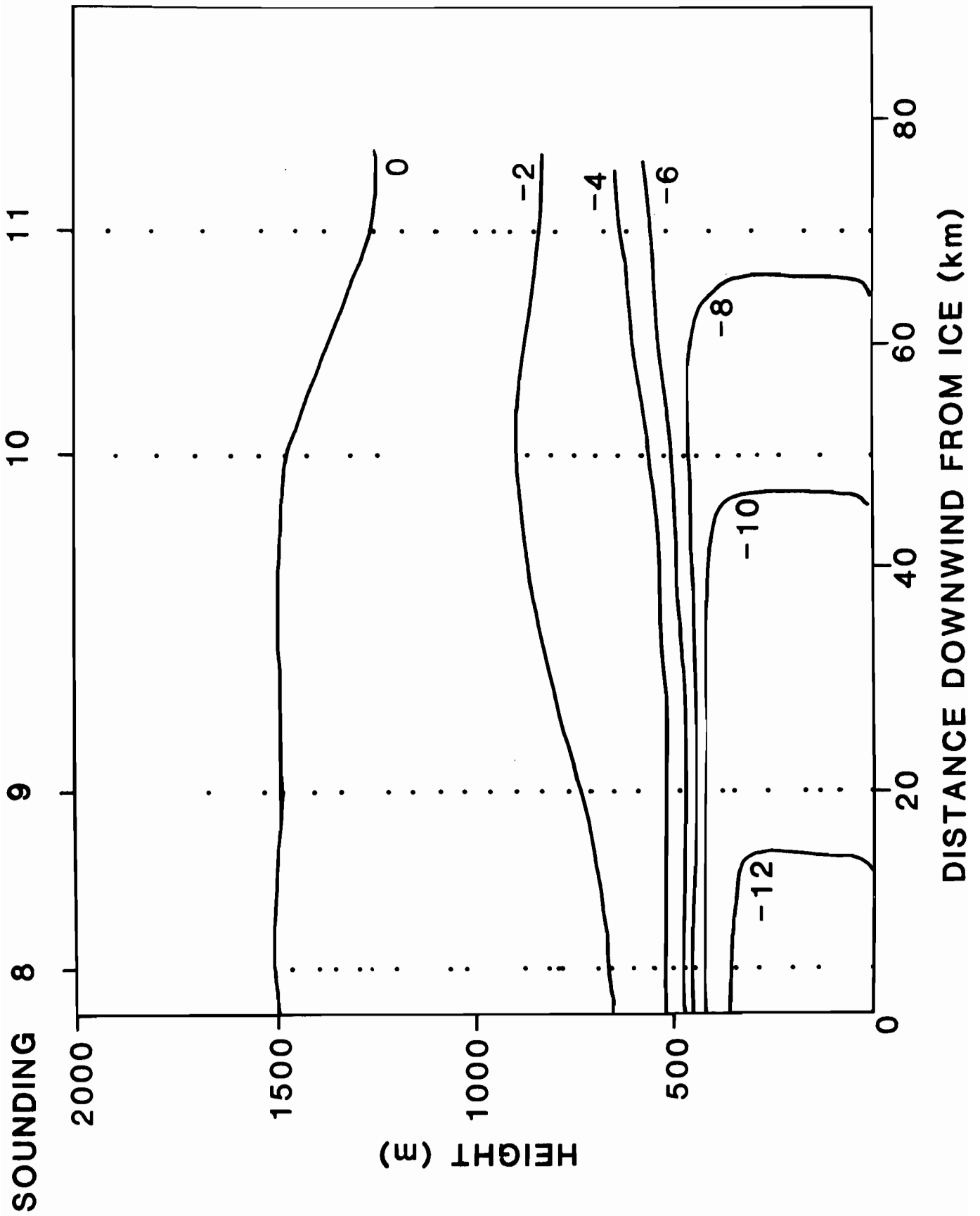
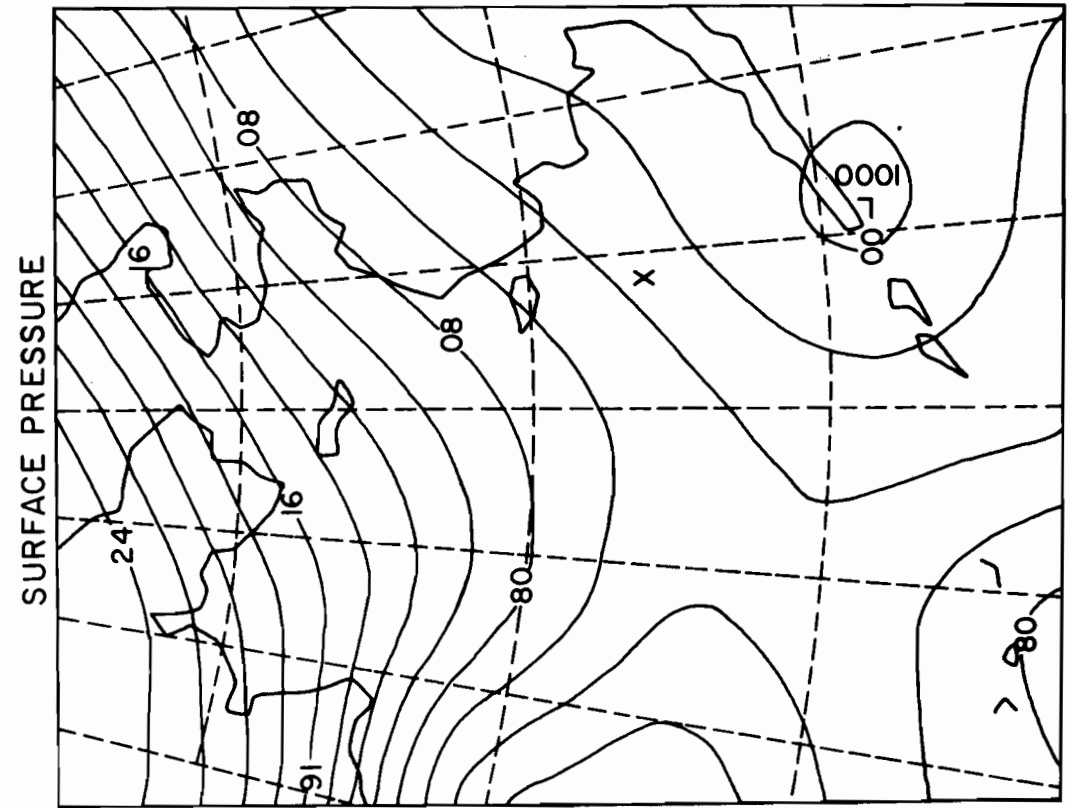
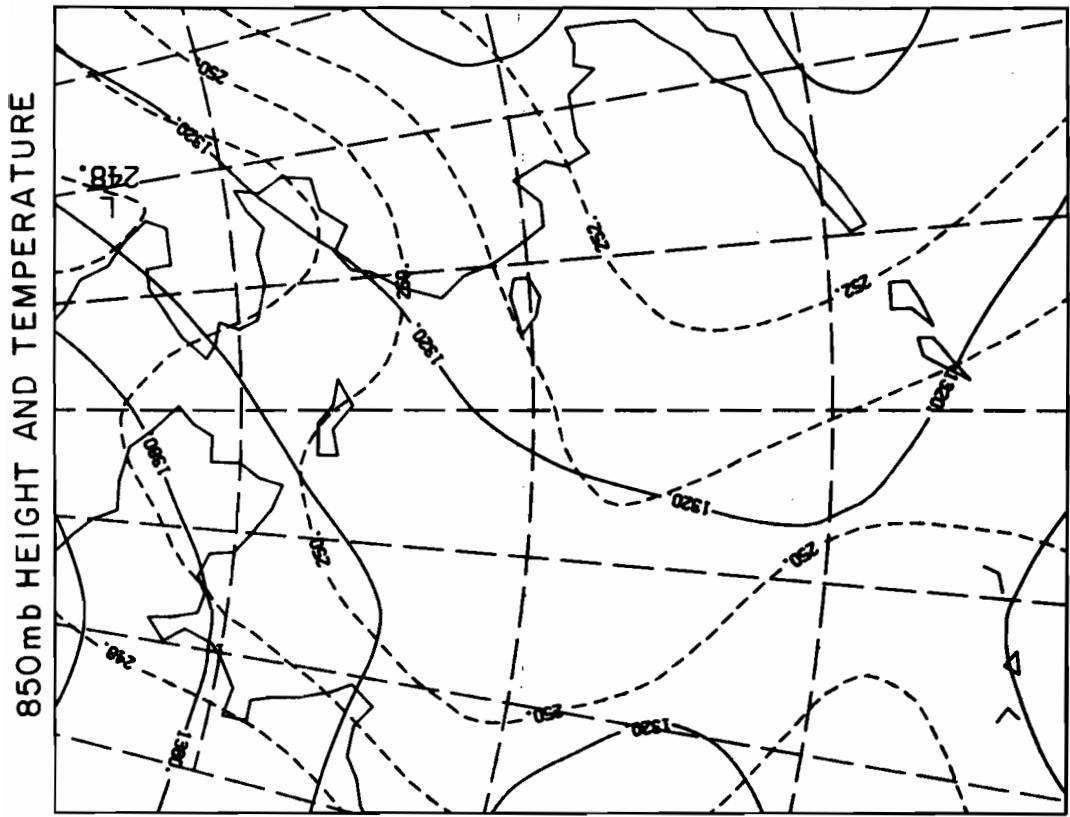


Figure 21. Cross section of potential temperature for Case A.





THE SYNOPTIC PICTURE FOR CASE B, 00Z 15 MARCH 1979

Figure 22. Surface pressure and 850-mb maps for Case B, 00Z 15 March 1979.

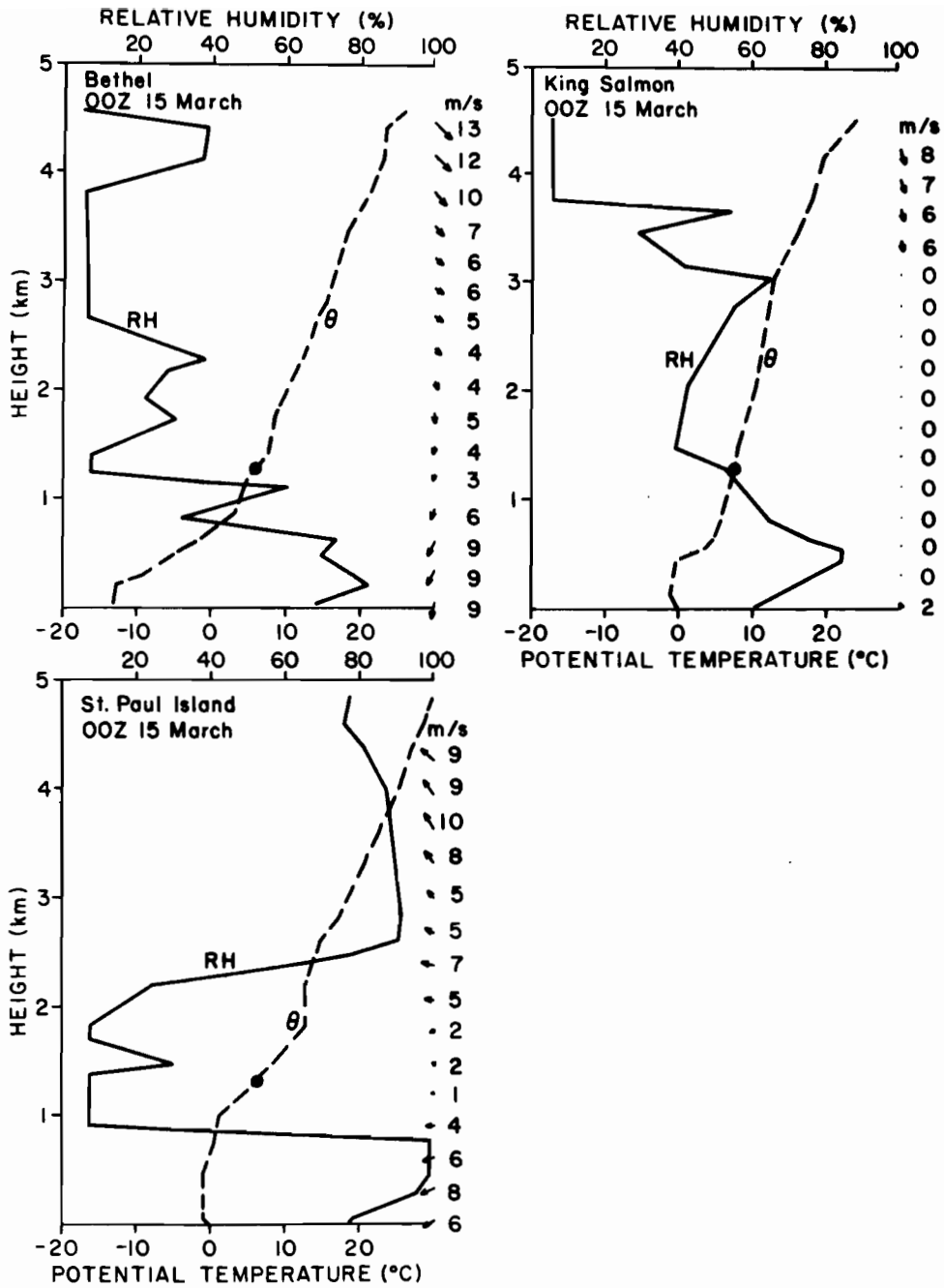


Figure 23. Upper air soundings from the National Weather Service, 00Z 15 March. The dots indicate the 850-mb level.

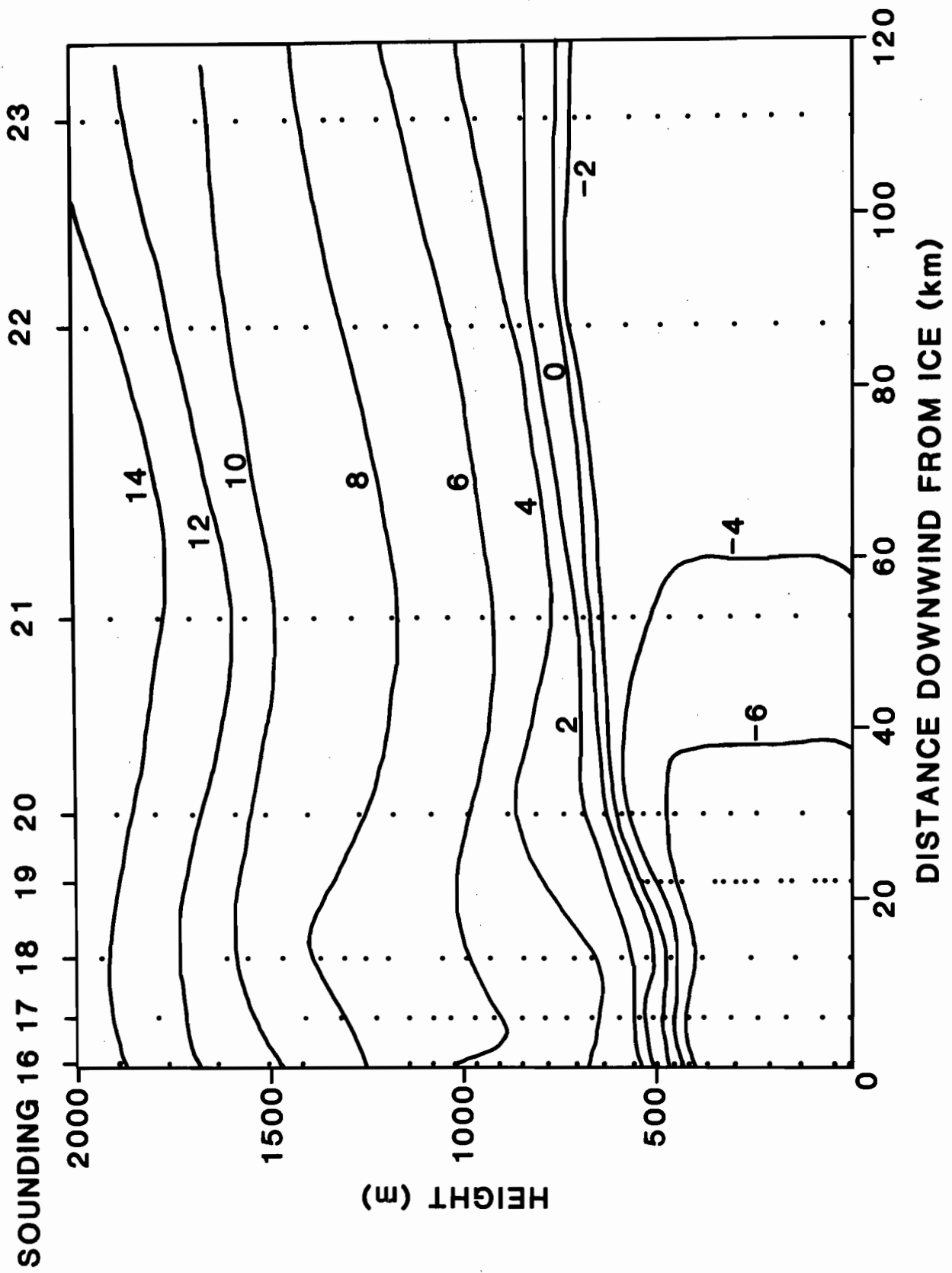


Figure 24. Cross section of potential temperature for Case B.

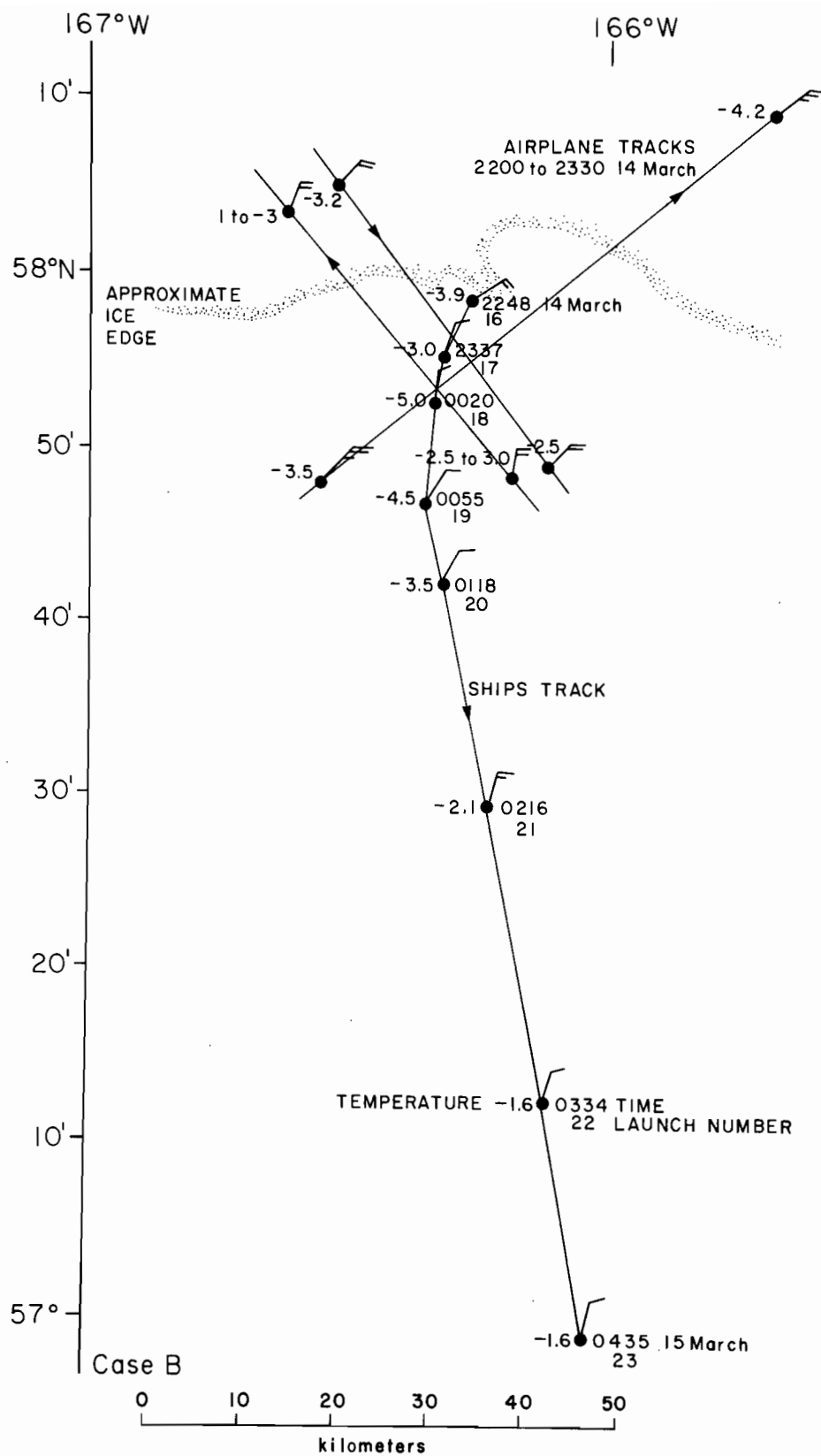


Figure 25. Map of the locations of the soundings for Case B with wind and temperature observations plotted at the time of each launch and similar observations from the aircraft at 100 m, 350 m, and 680 m.

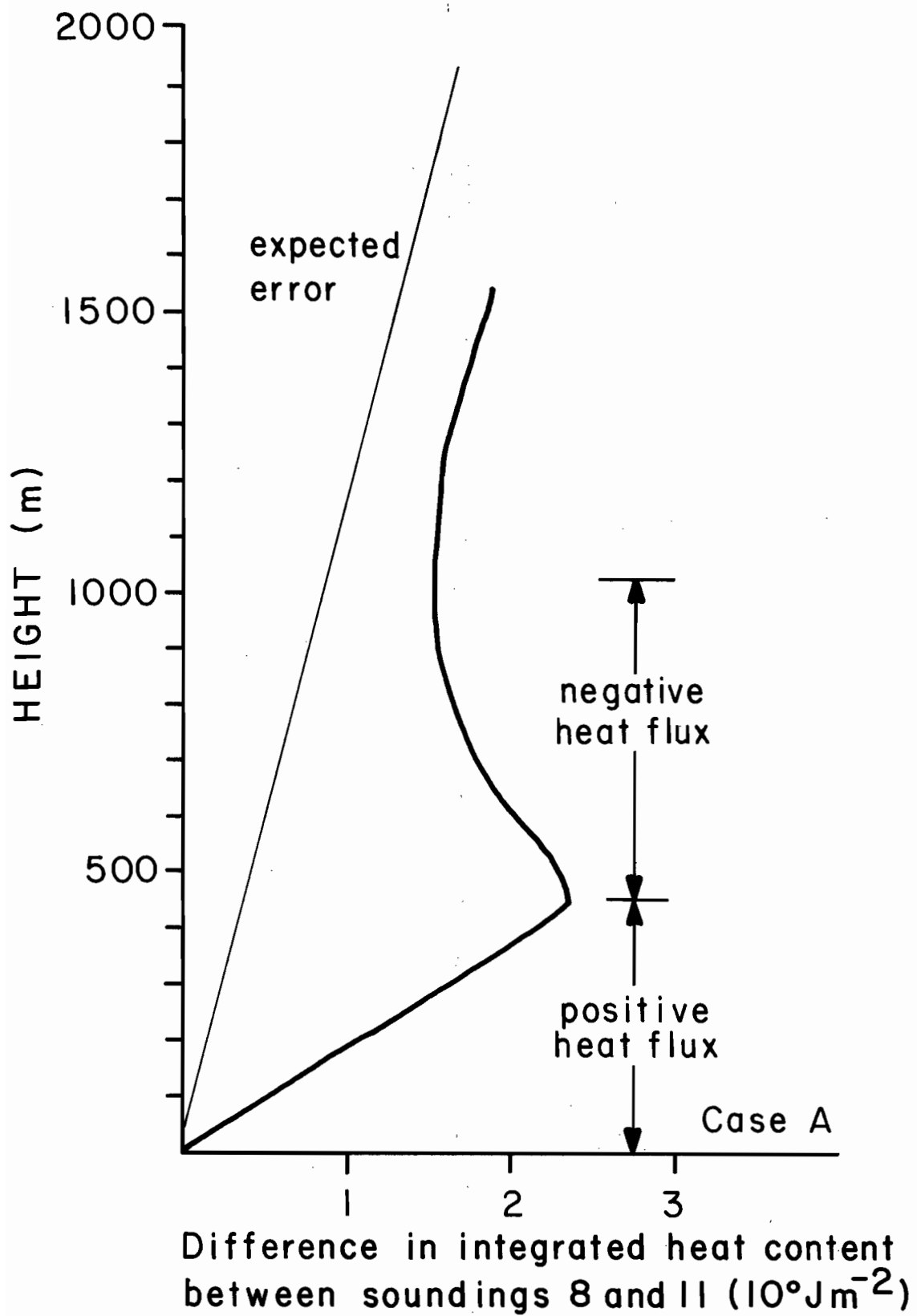


Figure 26. Integrated difference in heat content between the first and last soundings for Case A.

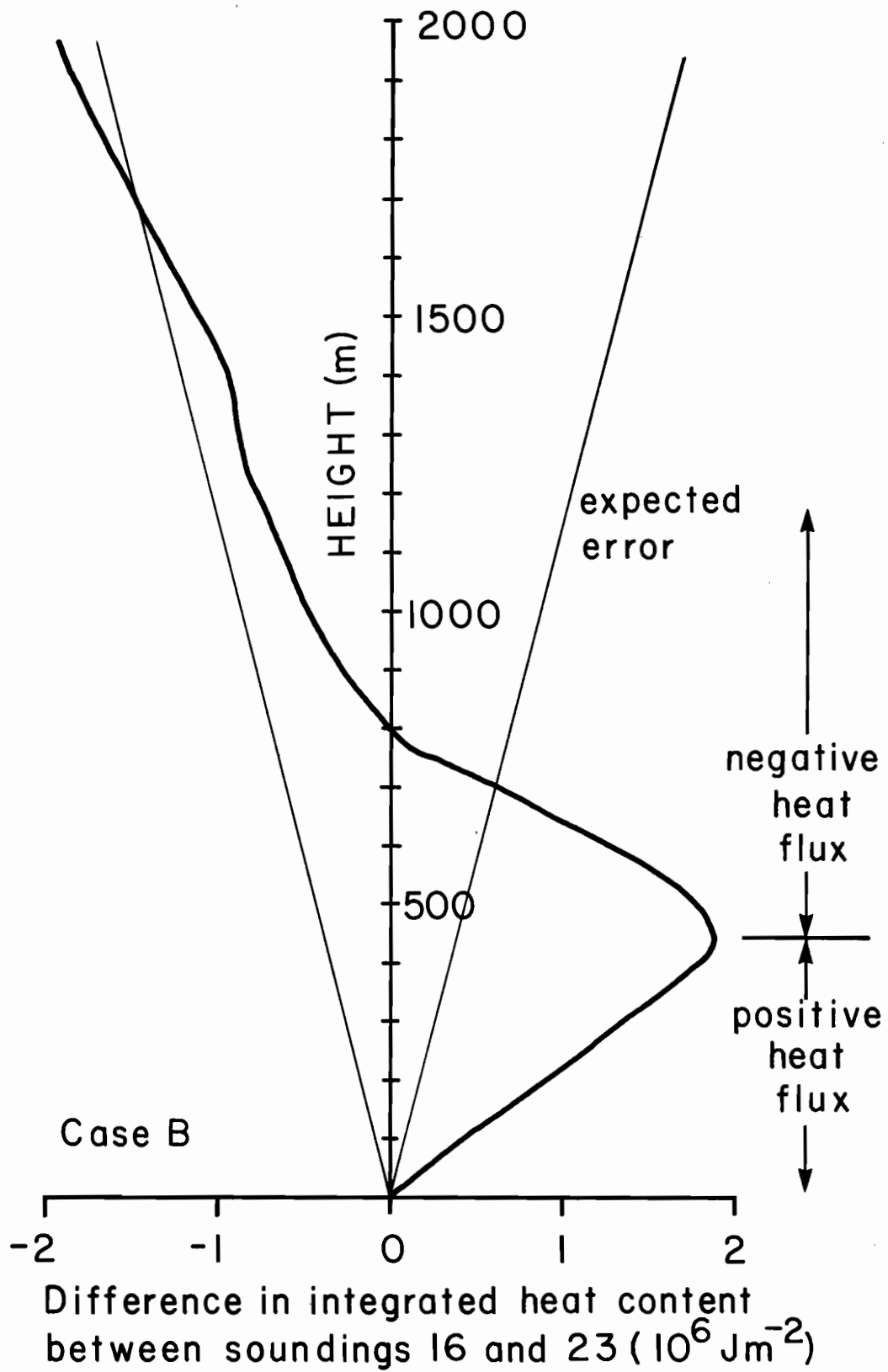
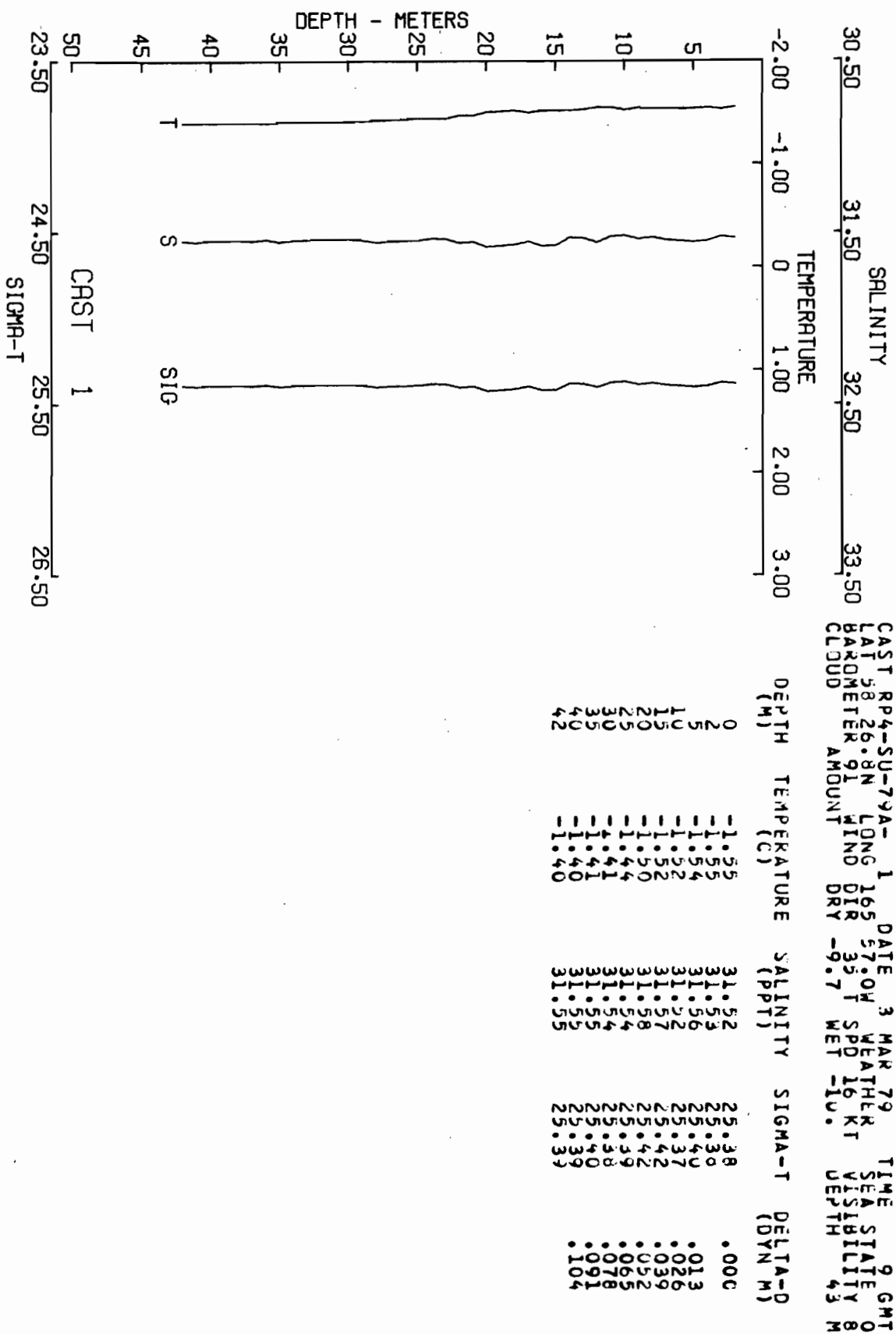
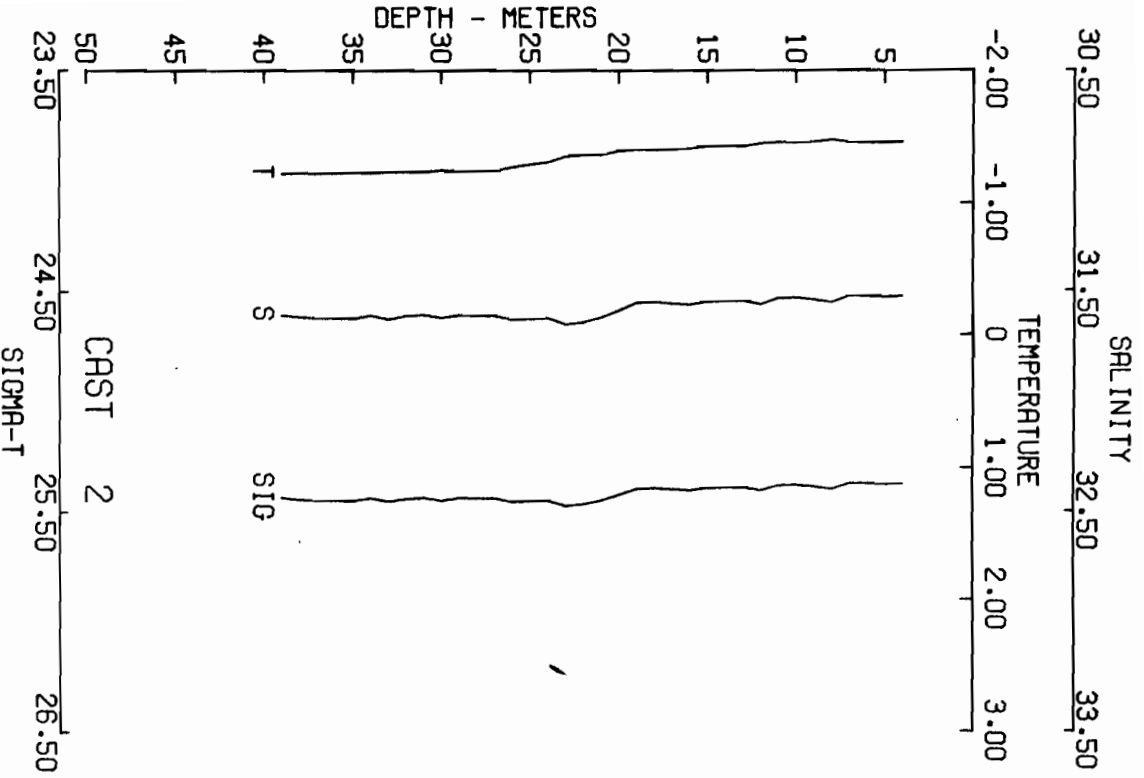


Figure 27. Integrated difference in heat content between the first and last soundings for Case B.

APPENDIX A: SALINITY, TEMPERATURE, AND DENSITY PROFILES, CTD CASTS 1-41.

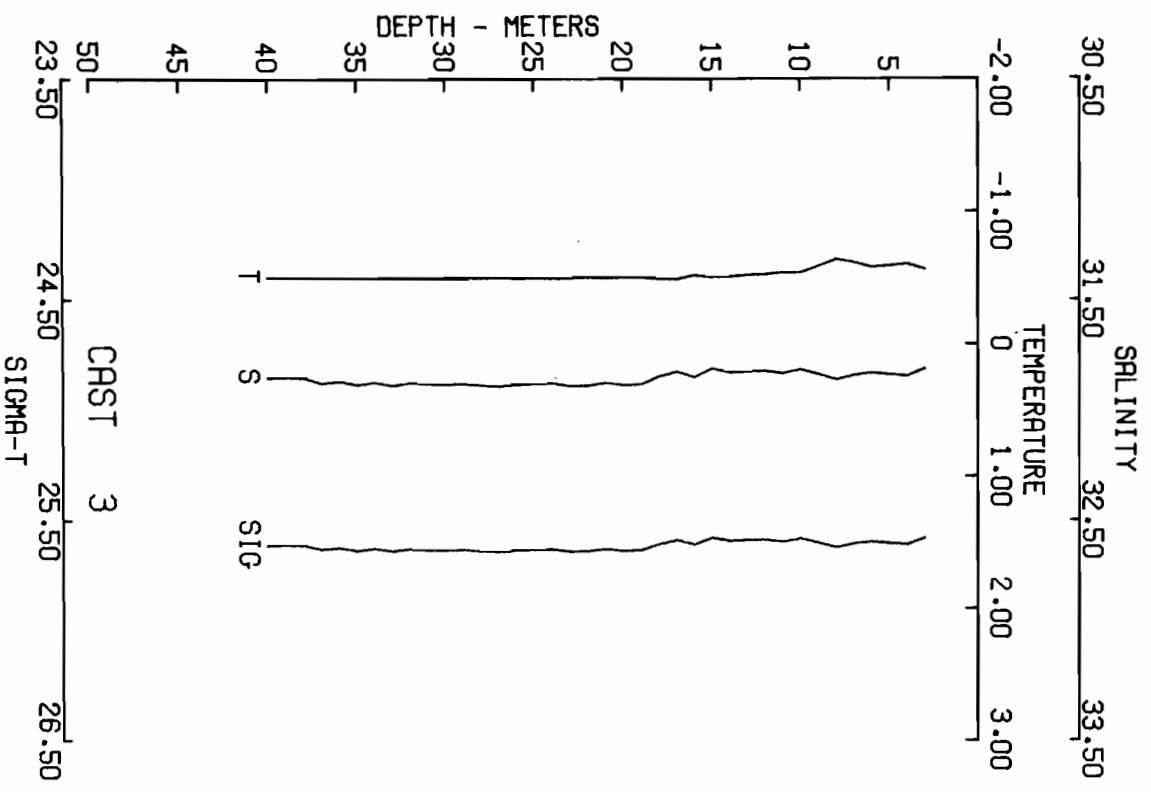




CAST RP4-SU-79A-2 DATE 3 MAR 79 TIME 652 GMT  
 LAT 58 21.7N LONG 165 58.9W WEATHER KT SEA STATE 0  
 BAROMETER 90 WIND DIR -11.0 SPD 17 VISIBILITY 40 M  
 CLOUD AMOUNT DRY -11.0 WET -12 DEPTH 7

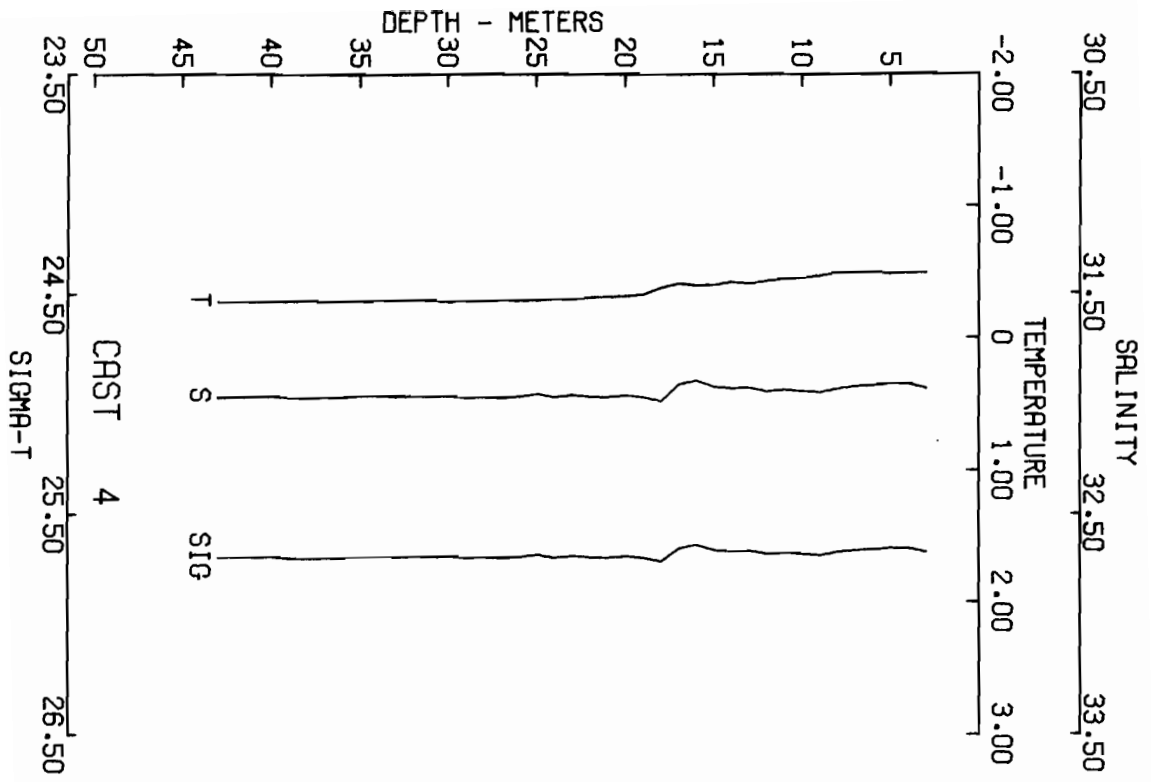
DEPTH (M)	TEMPERATURE (C)	SALINITY (PPT)	SIGMA-T	DELTA-D (GVN M)
0	-1.045	31.023	25.038	.000
4	-1.045	31.023	25.037	.013
5	-1.044	31.053	25.038	.026
10	-1.044	31.055	25.039	.039
15	-1.043	31.029	25.042	.052
20	-1.028	31.063	25.045	.065
25	-1.024	31.062	25.045	.077
30	-1.023	31.062	25.044	.090
35	-1.022	31.061	25.044	
39	-1.022	31.061	25.044	





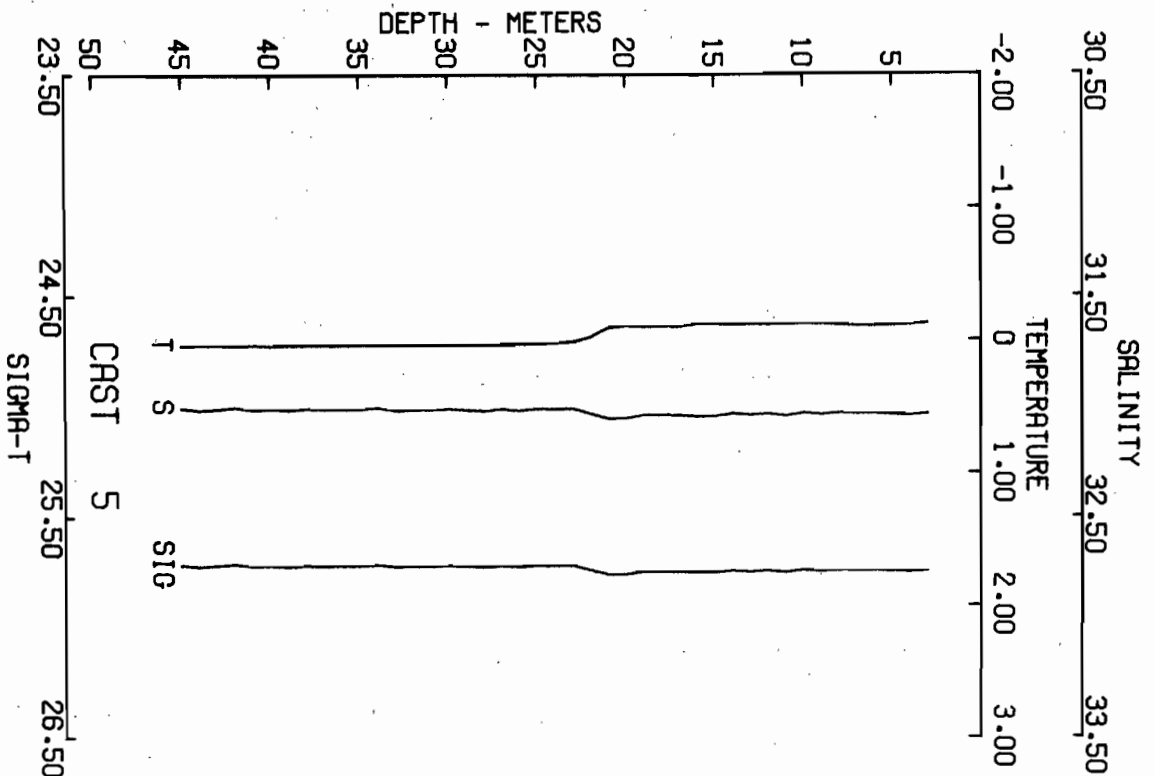
CAST RPT4-SU-79A-3 DATE 3 MAR 79 TIME 909 GMT  
 LAT 59 16.9N LONG 165 59.2W WEATHER SEA STATE 0  
 BAROMETER AMOUNT WIND DIR 40 T SPD 13.1 VISIBILITY 8  
 CLOUD DRY -11. MET -11. DEPTH 42 M

DEPTH (M)	TEMPERATURE (C)	SALINITY (PPT)	SIGMA-T	DELTA-D (DYN M)
0	-.25	31.81	25.58	.000
3	-.27	31.81	25.58	.012
5	-.60	31.84	25.58	.024
10	-.54	31.81	25.58	.036
15	-.21	31.88	25.63	.046
20	-.50	31.88	25.63	.060
25	-.50	31.88	25.64	.072
30	-.50	31.88	25.64	.083
35	-.50	31.88	25.61	.098
40	-.50	31.88	25.61	.098



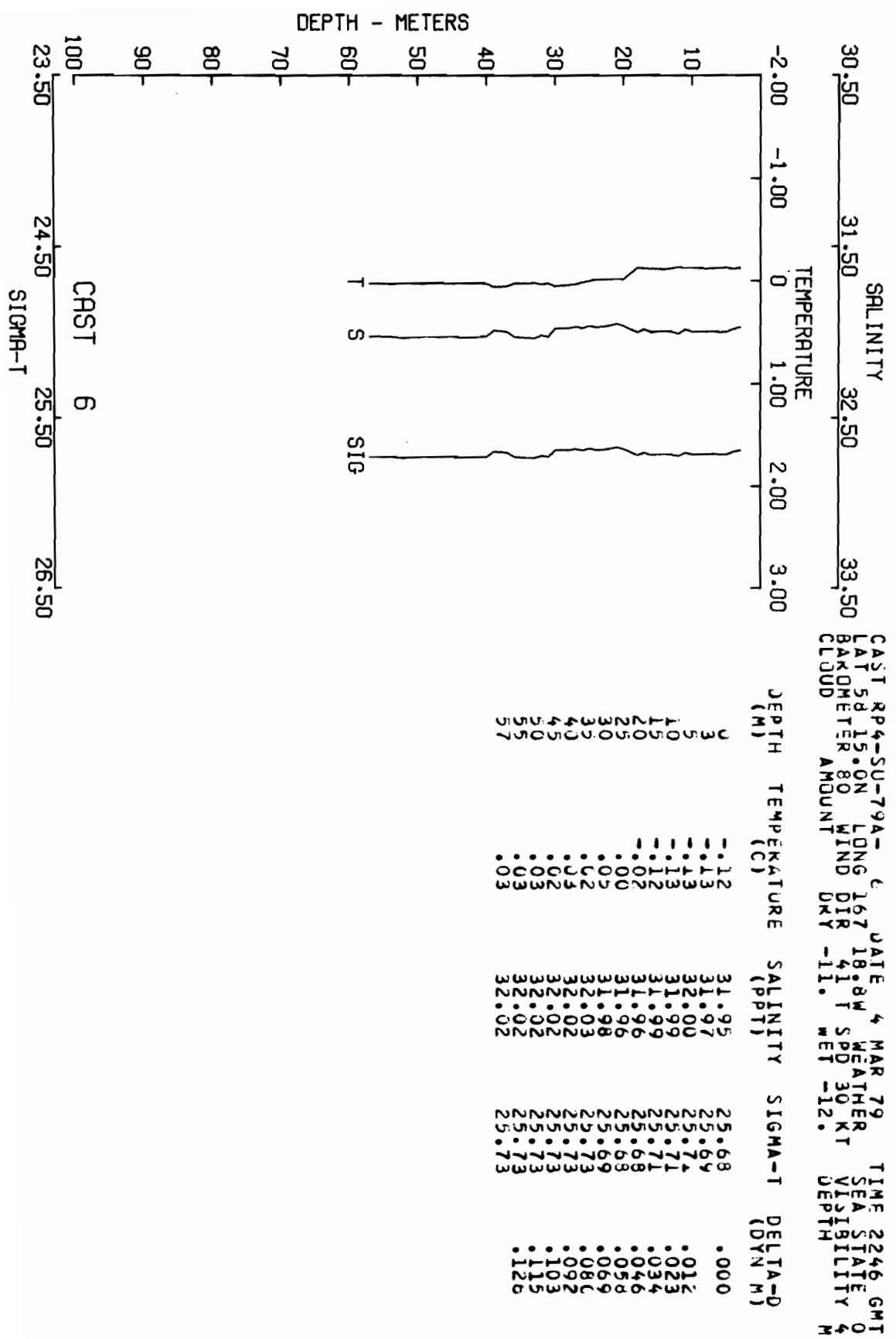
CAST R4-SU-79A-4  
 LAT 58 14.3N LONG 165 59.0W DATE 3 MAR 79 TIME 1035 GMT  
 BAROMETER 89 WIND DIR 38 T SPD 10 KT WEATHER SEA STATE 0  
 CLOUD AMOUNT -10.0 WET -11. VISIBILITY 45 M

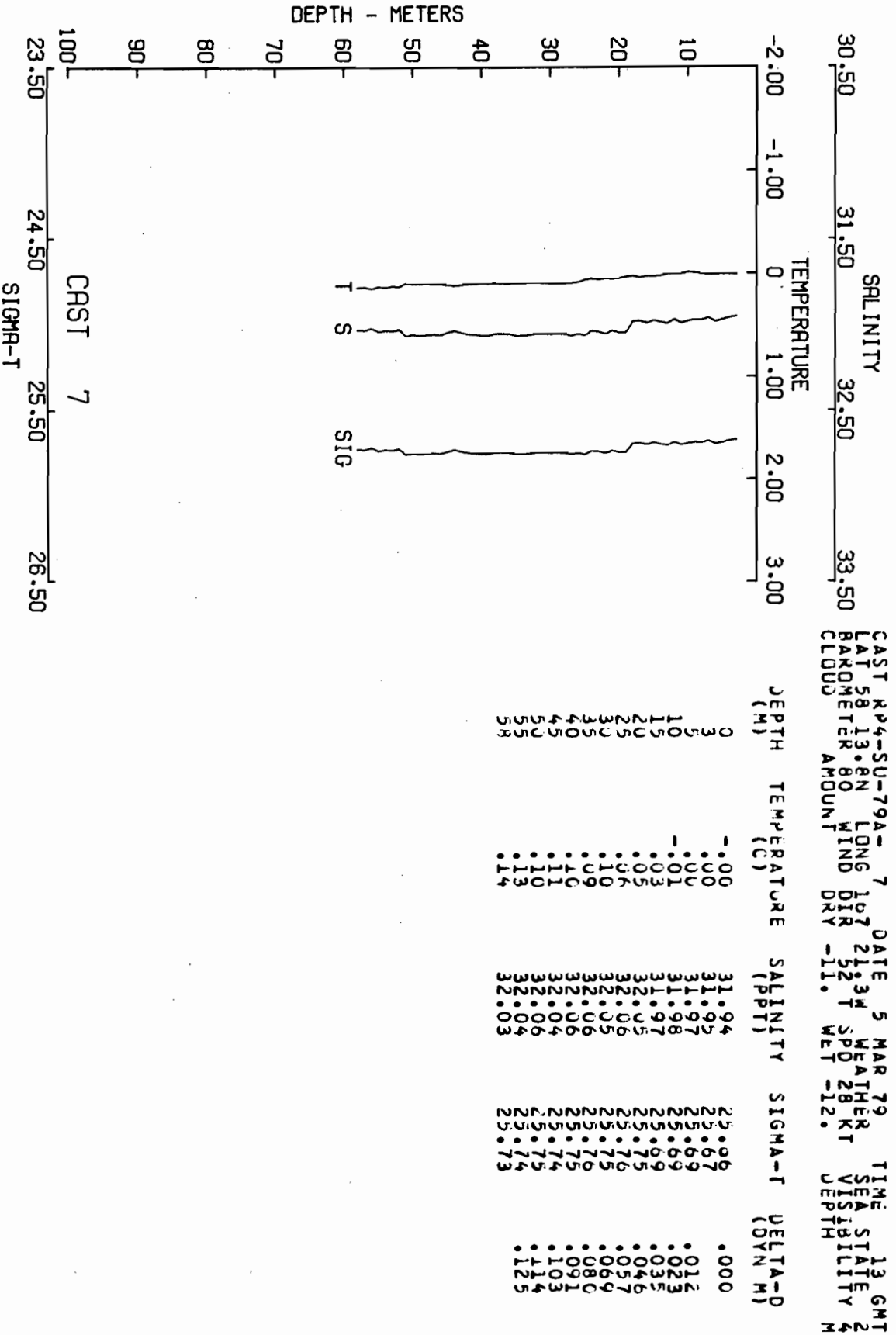
DEPTH (M)	TEMPERATURE (C)	SALINITY (PPT)	SIGMA-T	DELTA-D (DYN M)
0	1.49	31.92	25.67	.000
3	1.49	31.93	25.67	.000
5	1.44	31.91	25.65	.012
10	1.45	31.94	25.68	.023
15	1.40	31.92	25.66	.047
20	1.31	31.96	25.63	.058
25	1.29	31.95	25.68	.070
30	1.28	31.96	25.69	.081
35	1.28	31.96	25.69	.081
40	1.28	31.96	25.69	.081
45	1.28	31.96	25.69	.081
50	1.28	31.97	25.69	.093

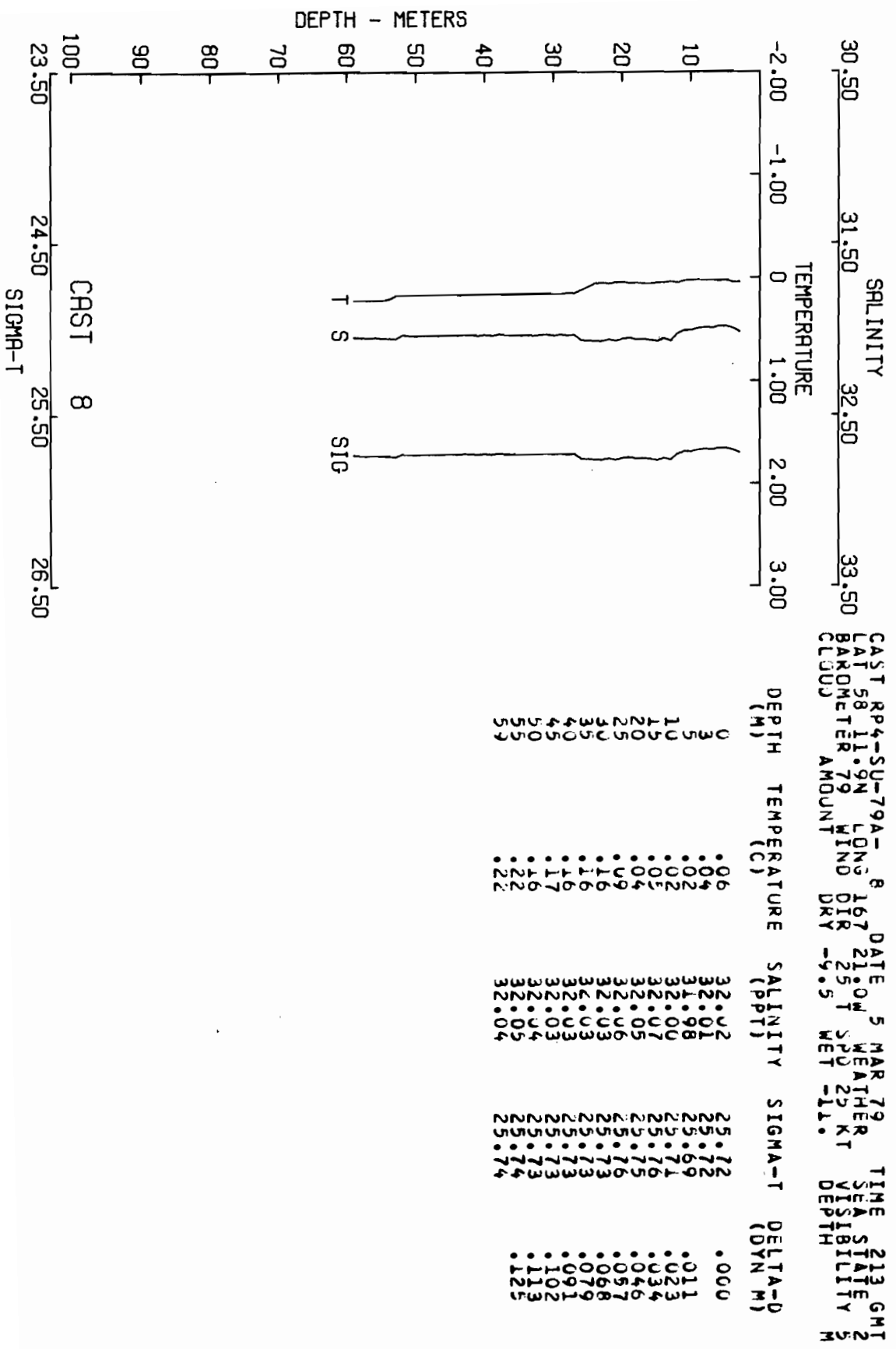


30.50 SALINITY 31.50 32.50 33.50  
 CAST RP4-SU-79A-5 DATE 3 MAR 79 TIME 1152 GMT  
 LAT 58 11.2N LONG 00.2W WEATHER KT SEA STATE 0  
 BAROMETER 89 WIND DIR 35 T SPD 18 KT VISIBILITY 7  
 CLUD AMOUNT DRY -10. MET -11. DEPTH M

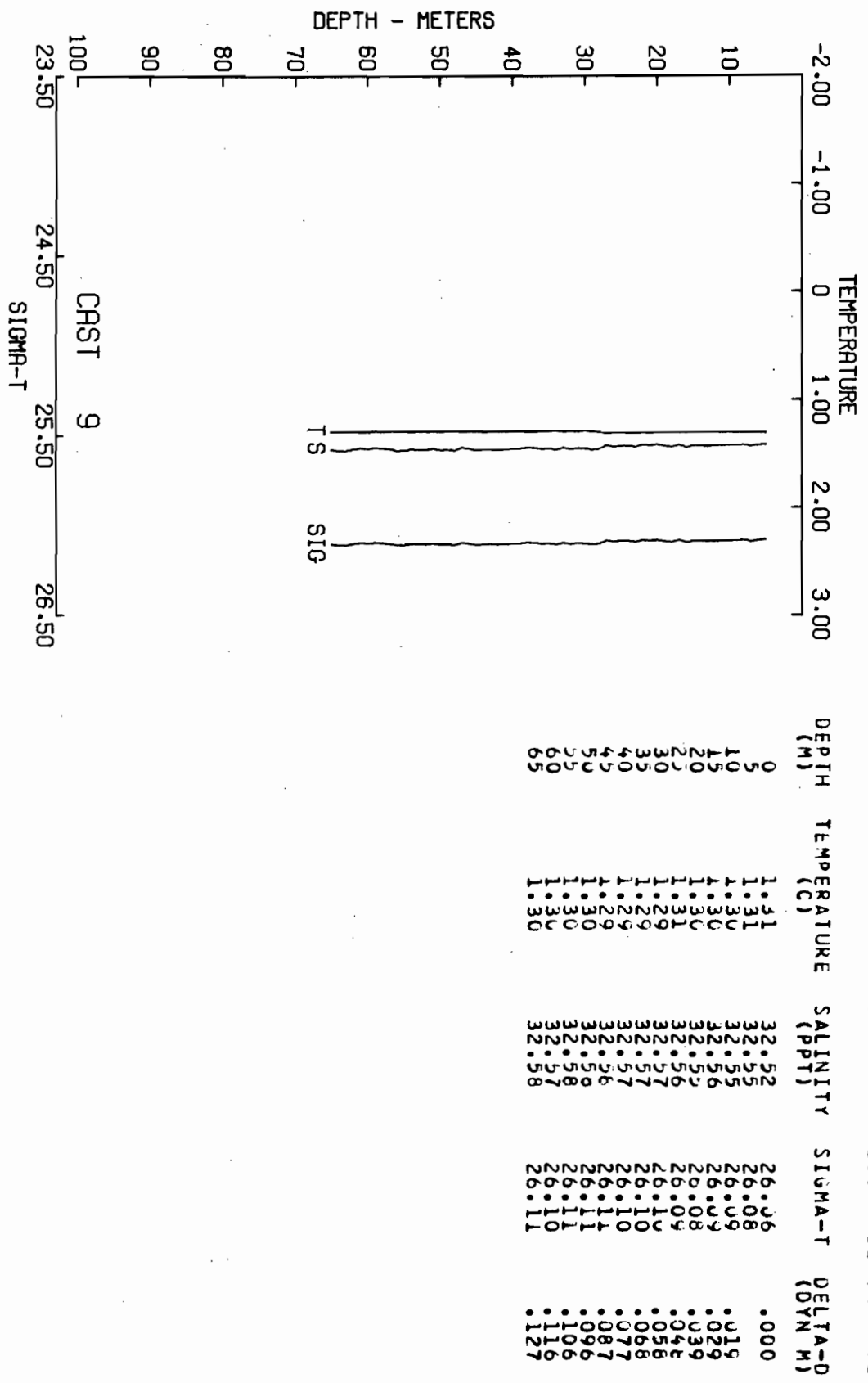
DEPTH (M)	TEMPERATURE (C)	SALINITY (PPT)	SIGMA-T (DYN M)	DELTA-T
0	-.13	32.04	25.75	.000
3	-.12	32.03	25.74	.011
5	-.11	32.04	25.74	.023
10	-.12	32.03	25.74	.034
15	-.11	32.05	25.76	.045
20	-.11	32.01	25.72	.056
25	.02	32.01	25.72	.068
30	.04	32.01	25.72	.079
35	.04	32.01	25.72	.094
40	.04	32.01	25.72	.104
45	.04	32.01	25.71	.104

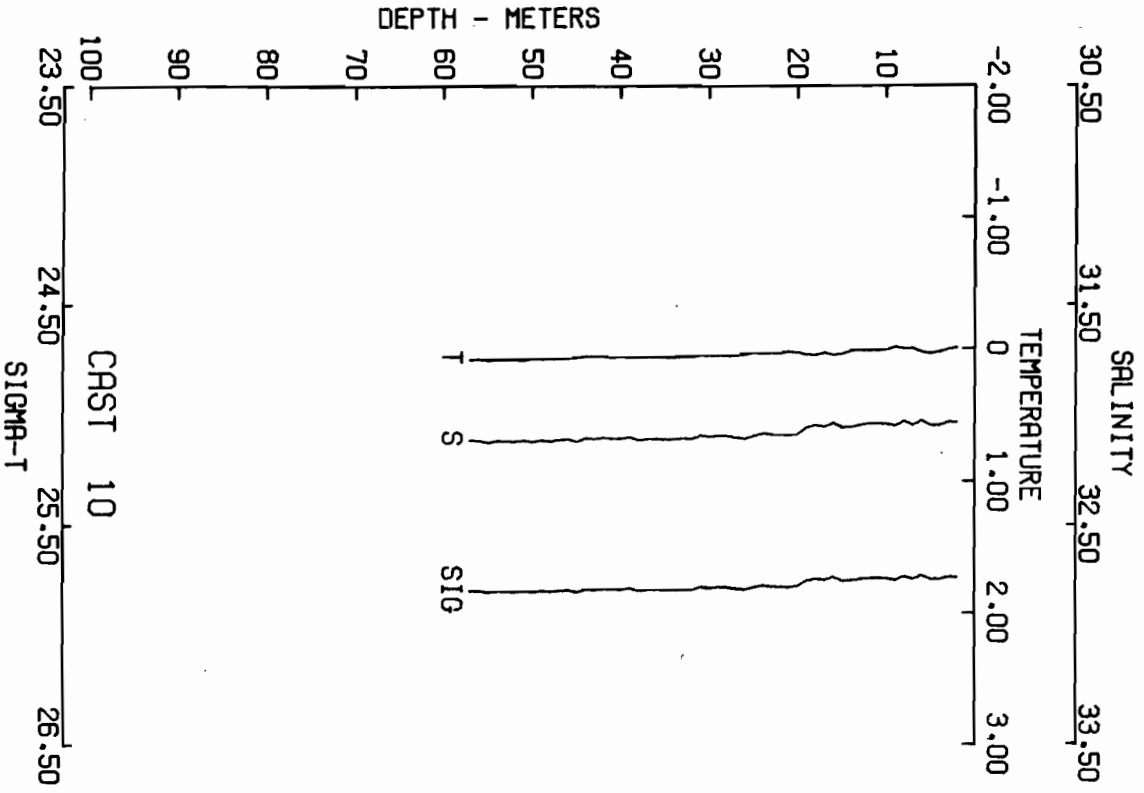






CAST RP4-SU-79A-9 DATE 5 MAR 79 TIME 614 GMT  
 LAT 27 41.4N LONG 168 00.8W WEATHER SEA STATE 3  
 BAROMETER 79 WIND DIR 40 T SPD 24 VIS 8  
 CLDUD AMOUNT DRY -10. WET -11. DEPTH 71 M

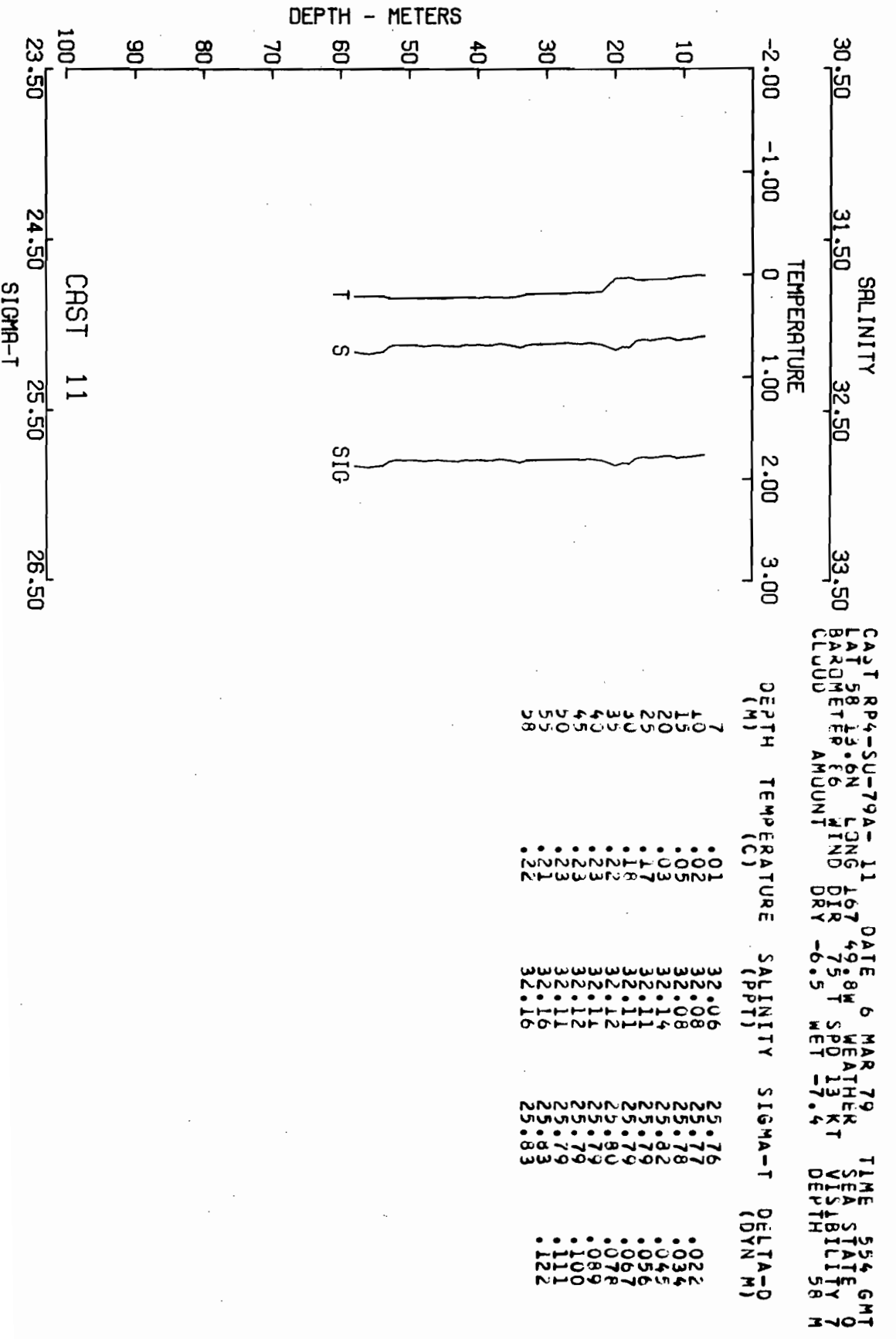


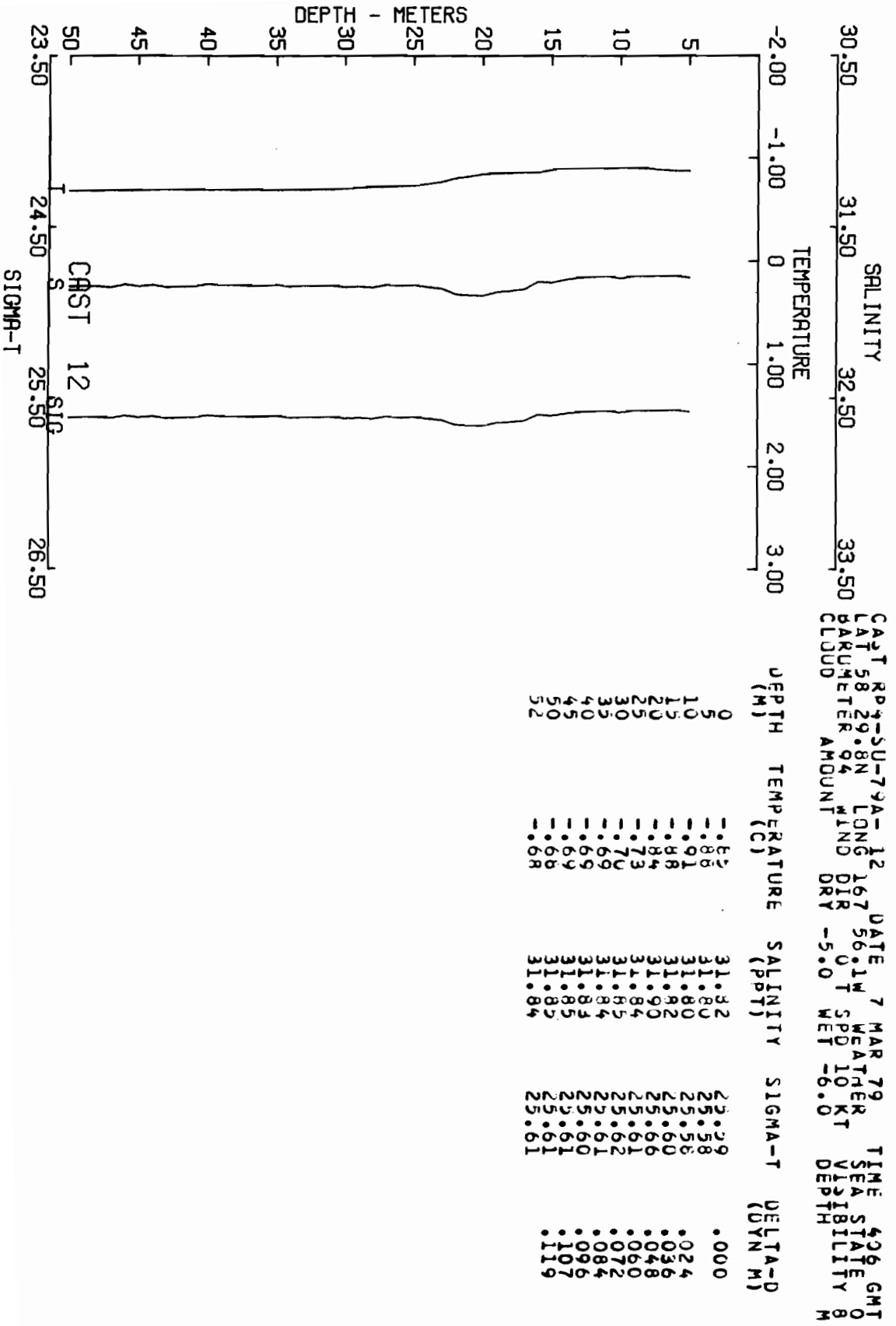


CAST R P4-20-79A-10 DATE 6 MAR 79 TIME 511 GMT  
 LAT 58.43.8N LONG 107.44.0W WEATHER SEA STATE 2  
 BAROMETER 86 WIND DIR 68 T SPU 13 K VISIBILITY 62 M  
 CLOUD DRY -7.2 WET -7.5 DEPTH 62 M

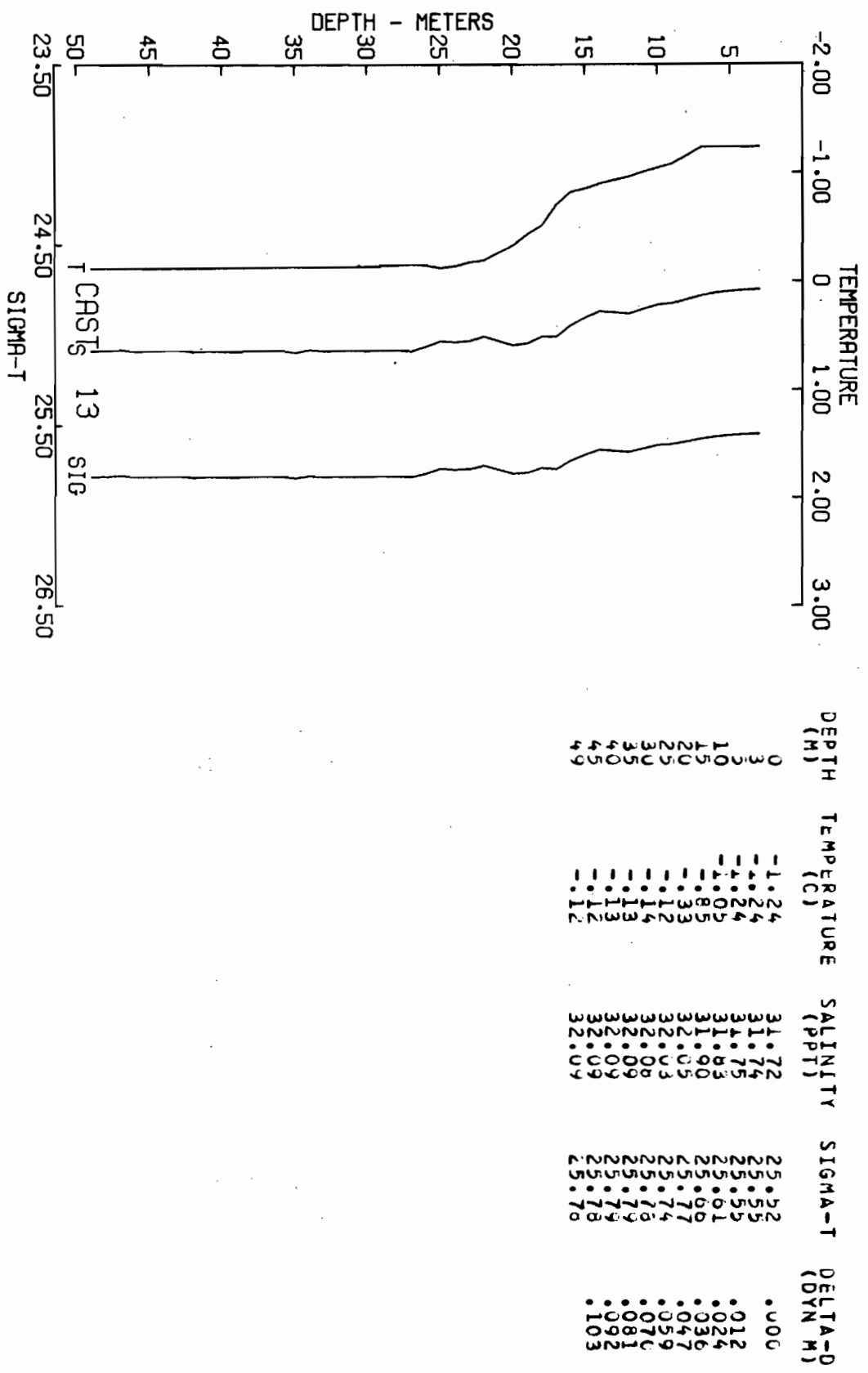
DEPTH (M)	TEMPERATURE (C)	SALINITY (PPT)	SIGMA-T (DYN M)	DELTA-D
0	.00	32.03	25.74	.000
2.5	.01	32.03	25.74	.011
5	.04	32.05	25.75	.023
10	.01	32.04	25.74	.034
15	.03	32.06	25.75	.045
20	.03	32.08	25.78	.056
25	.05	32.09	25.78	.067
30	.05	32.10	25.79	.078
35	.06	32.11	25.79	.089
40	.07	32.11	25.80	.101
45	.08	32.12	25.80	.112
50	.08	32.12	25.81	.123
55	.09	32.11	25.80	.123
57	.08	32.11	25.80	.123

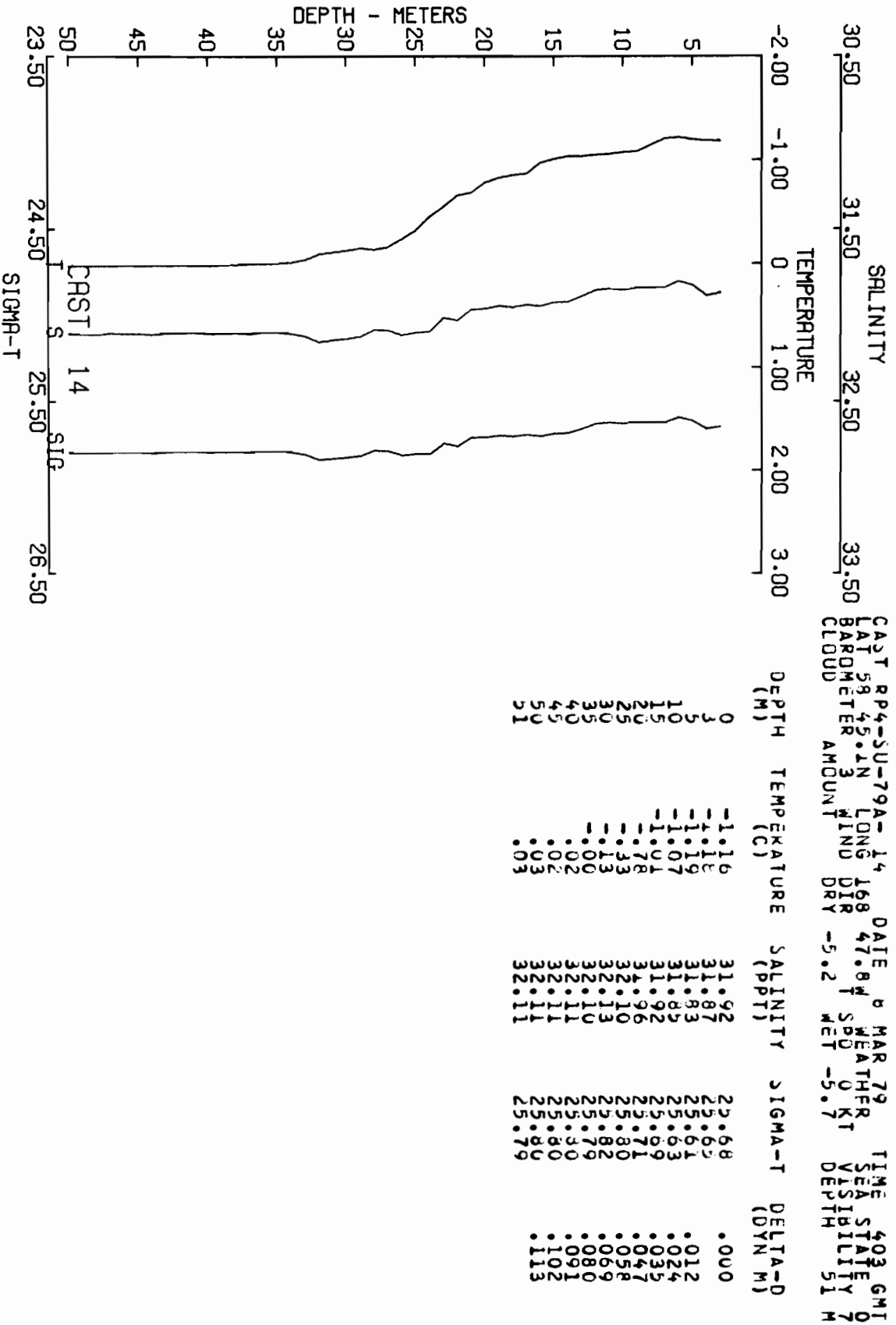


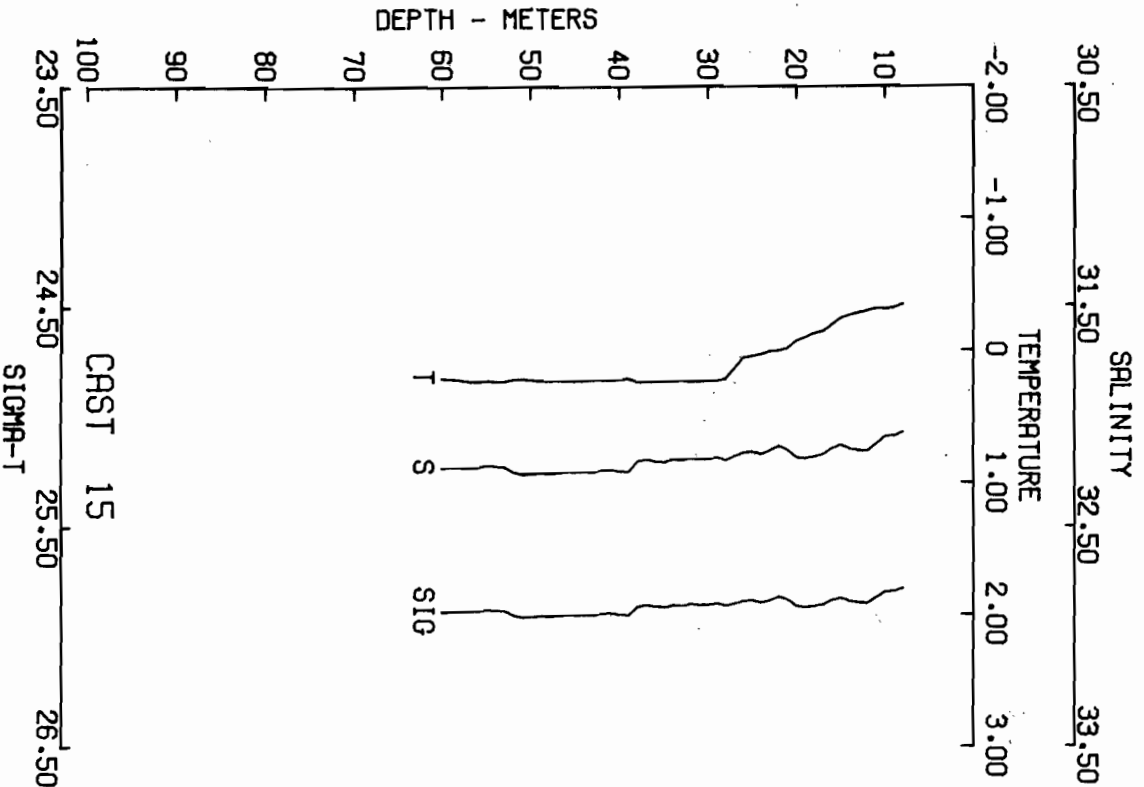




30.50 SALINITY 31.50 32.50 33.50  
 30.50 31.50 32.50 33.50  
 CAST RP4-SU-79A-13 DATE 7 MAR 79 TIME 1636 GMT  
 LAT 58 45.9N LONG 168 42.1W WEATHER SEA STATE  
 BAROMETER 99 WIND DIR 50 T SPD 8 KT VISIBILITY 49 M  
 CLOUD AMOUNT DRY -7.0 WET -7.5 DEPTH



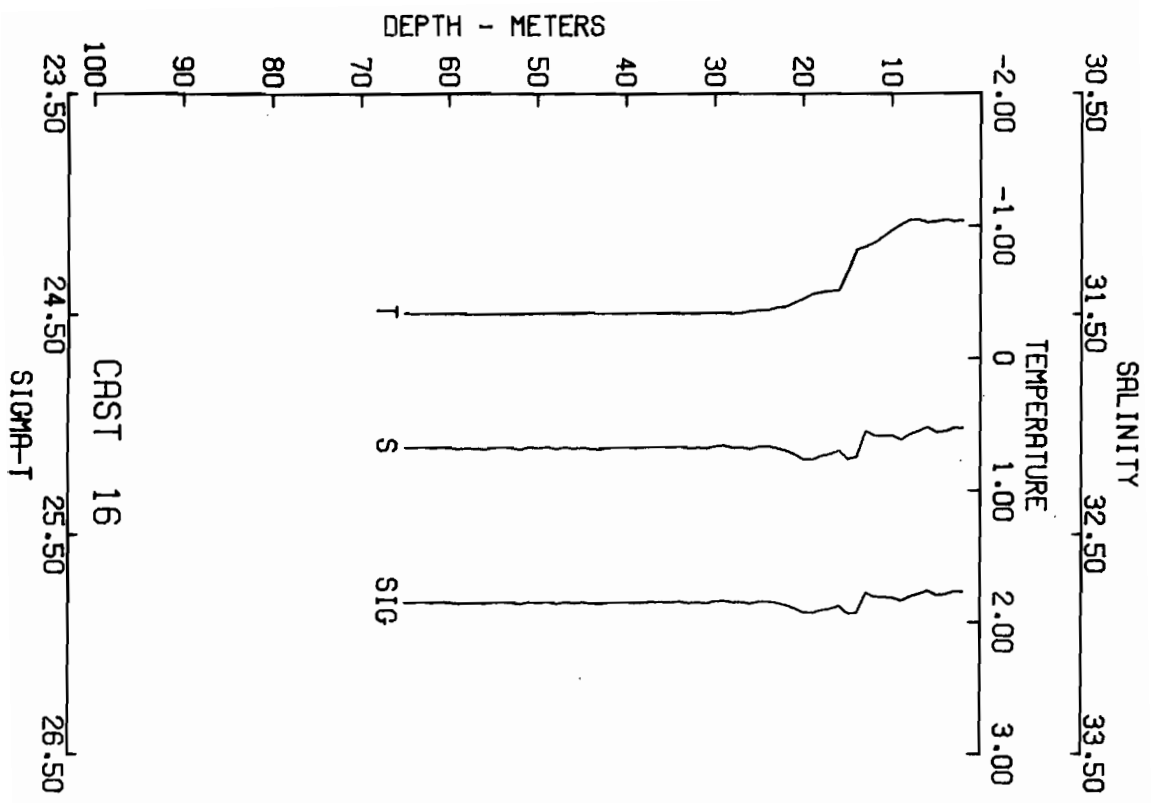




30.50 31.50 32.50 33.50  
 SALINITY  
 TEMPERATURE  
 -2.00 -1.00 0 1.00 2.00 3.00

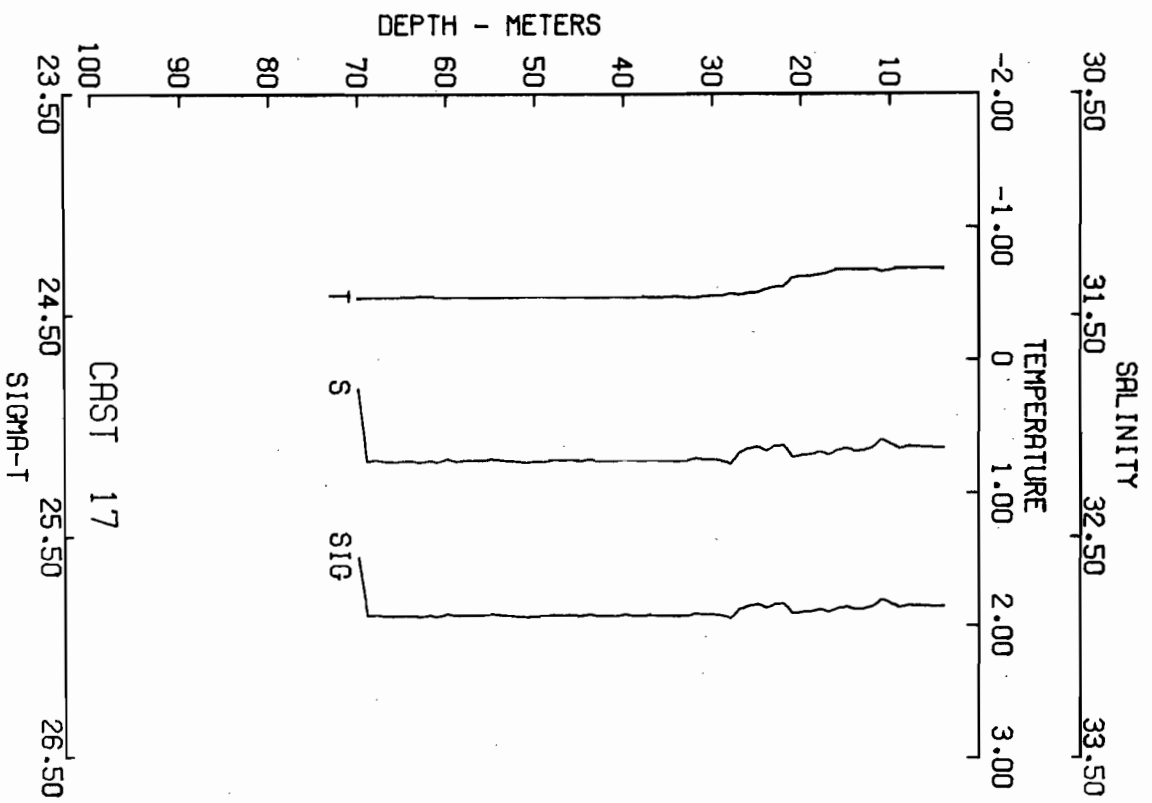
CAST RP4--SU-79A--15 DATE 6 MAR 79 TIME 805 GMT  
 LAT 38.7N LONG 169 05.2W WEATHER RT SEA STATE 0  
 BAROMETER 4 WIND DIR 80 T SPD 3 KT VISIBILITY 6  
 CLOUD AMOUNT DRY -3.1 WET -4.0 DEPTH

DEPTH (M)	TEMPERATURE (C)	SALINITY (PPT)	SIGMA-T	DELTA-D (DYN M)
0	0.31	32.09	25.78	0.22
10	0.25	32.13	25.83	0.33
20	0.25	32.18	25.86	0.44
25	0.27	32.18	25.84	0.55
30	0.23	32.19	25.85	0.65
35	0.23	32.20	25.86	0.76
40	0.22	32.22	25.90	0.87
45	0.22	32.22	25.91	1.08
50	0.22	32.22	25.88	1.19
55	0.21	32.23	25.89	1.31
60	0.21	32.23	25.89	1.31



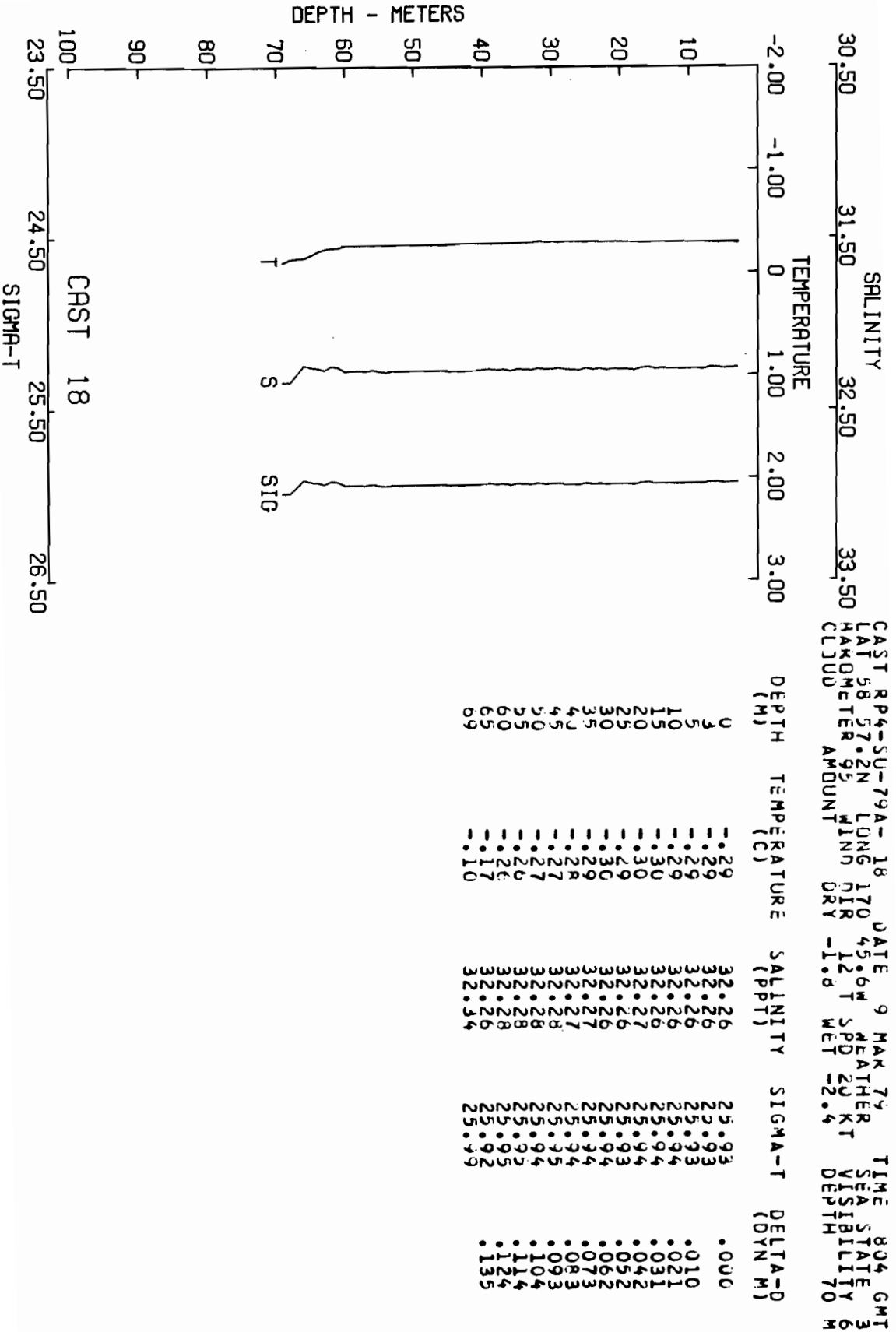
CAS1 R04-SU-79A-16 DATE 8 MAR 79 TIME 1635 GMT  
 LAT 59 02.2N LONG 01 2W WEATHER SEA STATE  
 BAROMETER AMOUNT WIND DIR 170 DIR 15 T SPD 10 KT VISIBILITY 7 M  
 CLOUD DRY -5.0 WET -5.5

DEPTH (M)	TEMPERATURE (C)	SALINITY (PPT)	SIGMA-T (DYN M)	DELTA-D
0	-1.04	32.01	25.76	.000
2	-1.04	32.03	25.77	.011
5	-1.03	32.05	25.77	.022
10	-1.03	32.05	25.79	.033
15	-1.04	32.11	25.85	.044
20	-1.37	32.10	25.85	.055
25	-1.35	32.10	25.80	.066
30	-1.35	32.10	25.81	.077
35	-1.34	32.10	25.81	.088
40	-1.34	32.11	25.81	.099
45	-1.34	32.11	25.81	.110
50	-1.34	32.11	25.81	.121
55	-1.34	32.11	25.81	.132
60	-1.34	32.11	25.81	.143

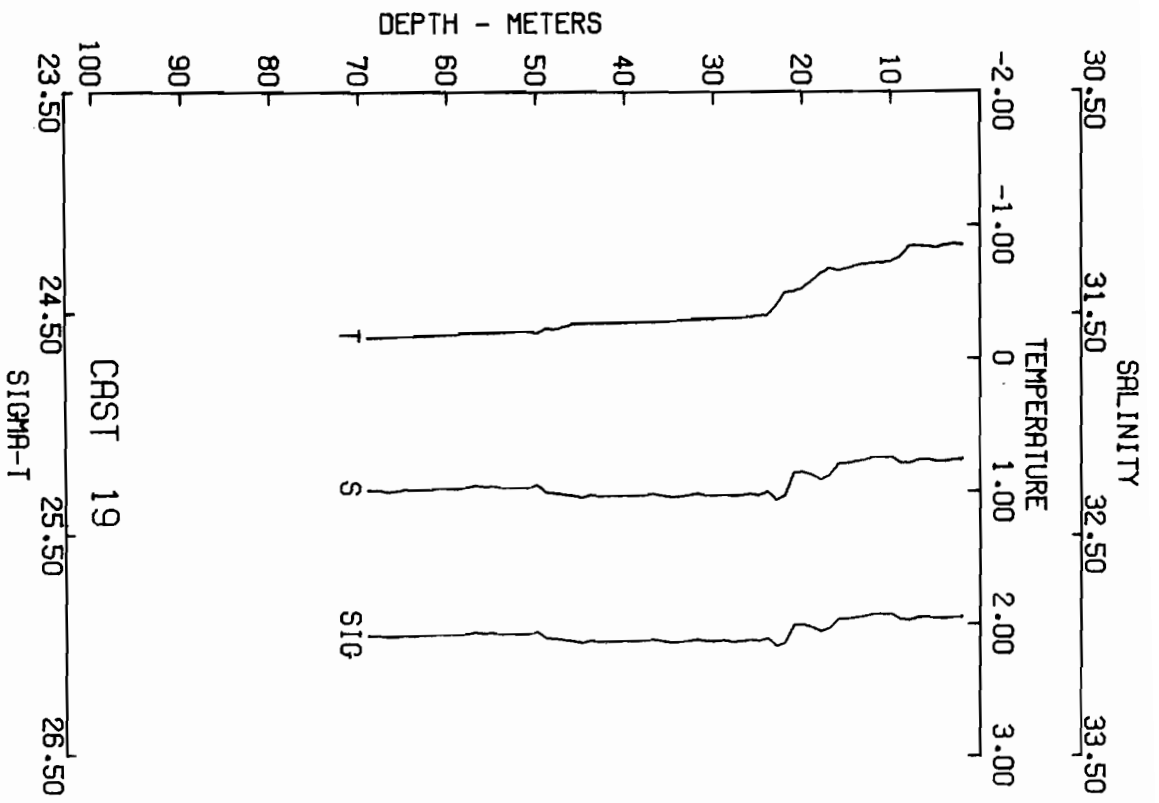


CAST KP4-SU-79A-17  
 LAT 38.28 IN LONG 120.00 WIND DIR 170 WIND DR Y -2.5 MET -3.0  
 BAROMETER AMOUNT 96 WIND DIR 170 WIND DR Y -2.5 MET -3.0  
 CLUD DATE 9 MAR 79 TIME 340 GMT  
 WEATHER SEA STATE VISIBILITY  
 MET NEPT M

DEPTH (M)	TEMPERATURE (C)	SALINITY (PPT)	SIGMA-T (DYN M)	DELTA-D (DYN M)
0	68	32.10	25.32	.000
5	69	32.10	25.81	.011
10	69	32.08	25.80	.022
15	68	32.10	25.84	.033
20	68	32.13	25.84	.044
25	63	32.09	25.80	.055
30	51	32.15	25.80	.066
35	48	32.15	25.85	.076
40	47	32.16	25.86	.087
45	47	32.16	25.86	.098
50	47	32.16	25.85	.109
55	47	32.15	25.85	.119
60	47	32.15	25.85	.130
65	47	32.15	25.86	.141
70	47	31.18	25.86	.154

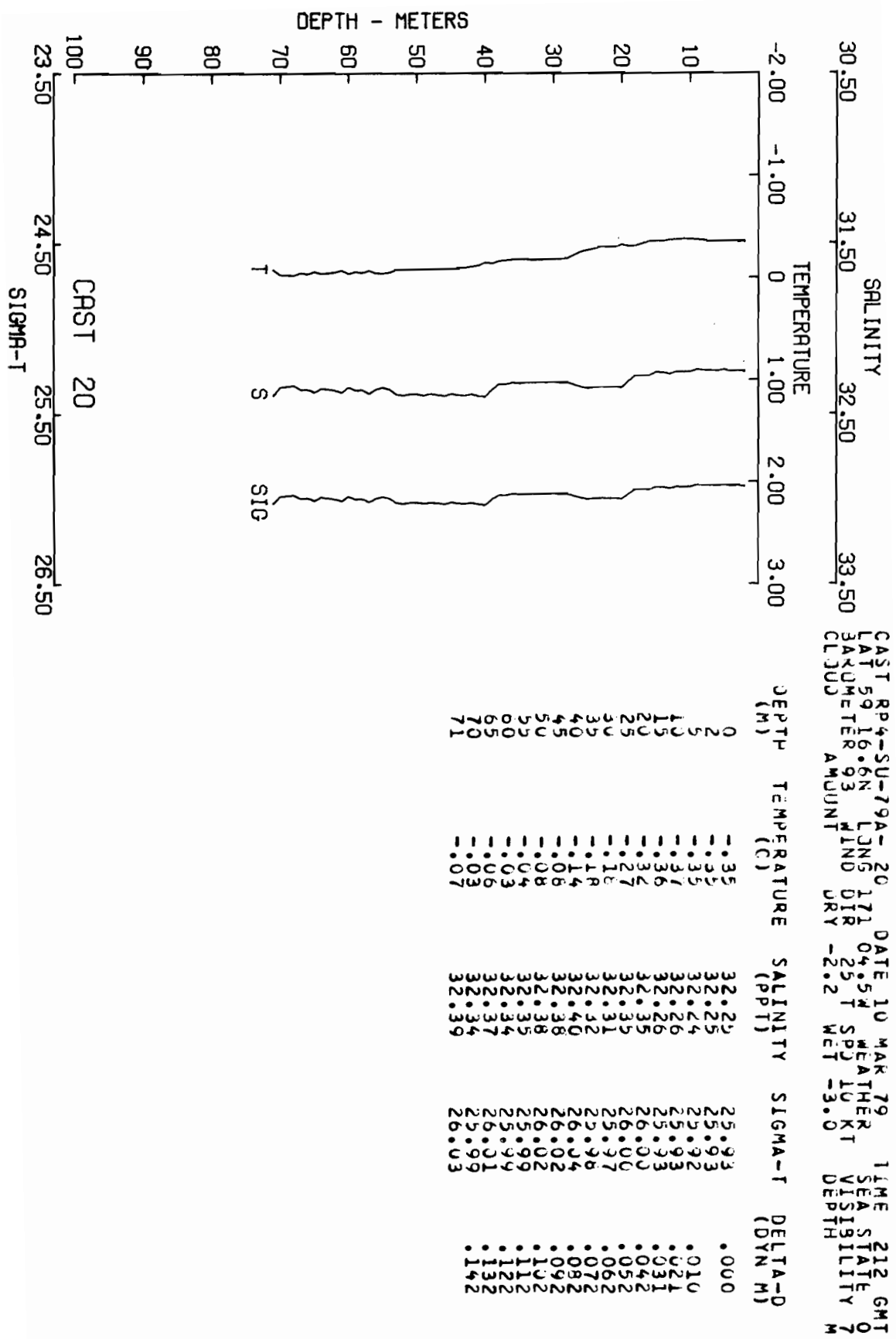


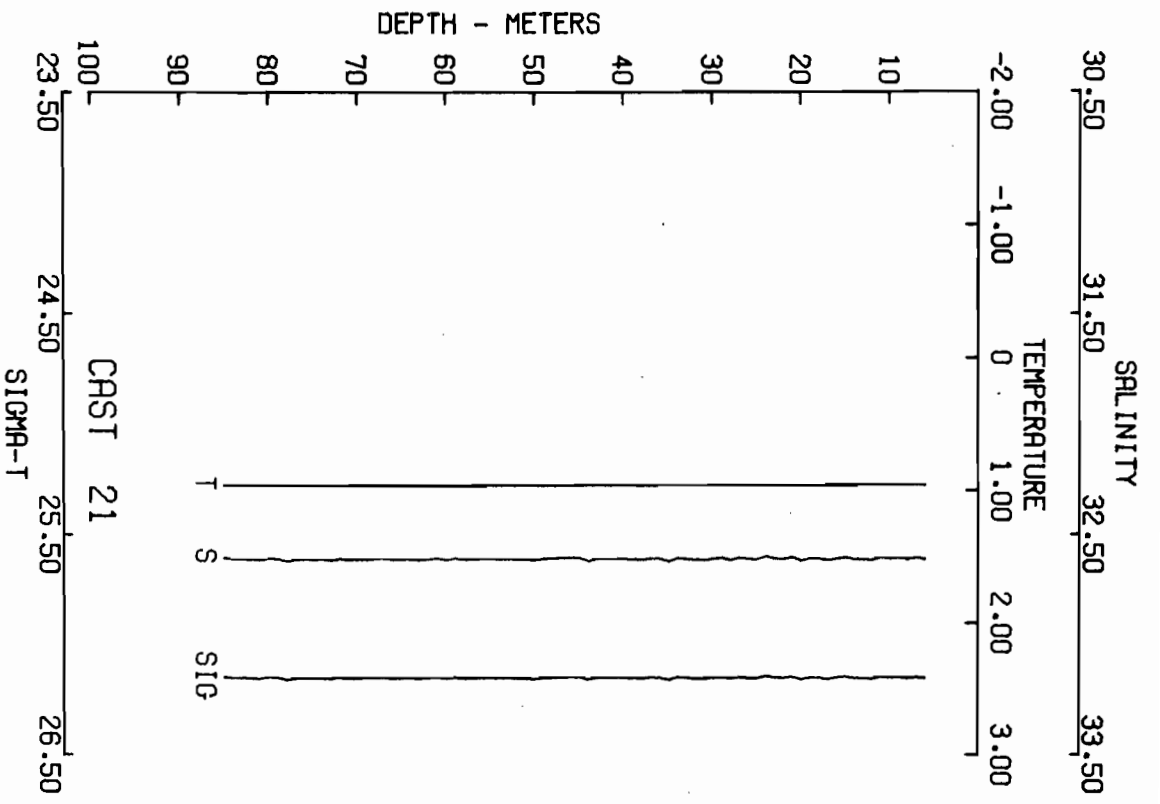




CAST RP4-SU-79A-19 DATE 9 MAR 79 TIME 1635 GMT  
 LAT 29 22.2N LONG 170 39.2W WEATHER U  
 BAROMETER 93 WIND DIR 350 T SPD 10 KT VISIBILITY 7  
 CLOUD AMOUNT DRY -4.0 WET -4.0 DEPTH 69 M

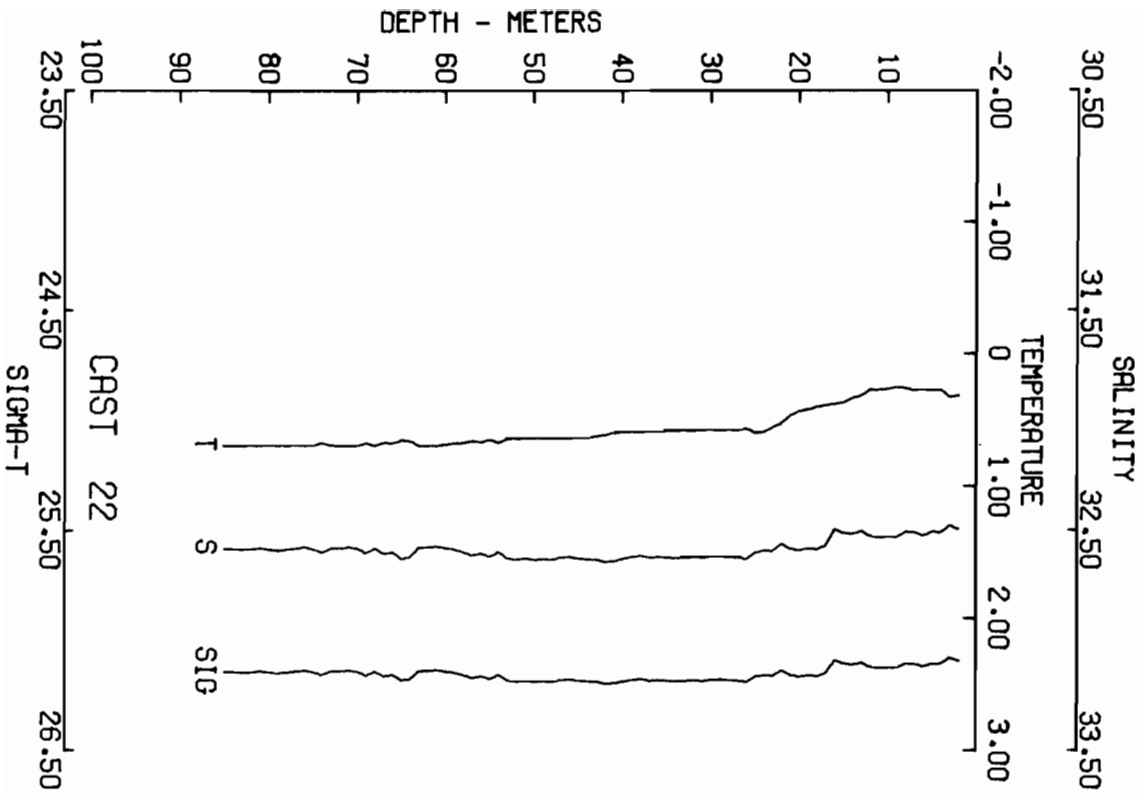
DEPTH (M)	TEMPERATURE (C)	SALINITY (DPT)	SIGMA-T	DELTA-D (DYN M)
0	1.86	32.16	25.97	.000
5	1.85	32.15	25.97	.011
10	1.73	32.15	25.98	.021
15	1.66	32.17	25.98	.032
20	1.52	32.21	25.98	.043
25	1.32	32.32	25.98	.053
30	1.30	32.32	25.98	.063
35	1.28	32.33	25.98	.073
40	1.27	32.33	25.98	.083
45	1.26	32.33	25.98	.094
50	1.19	32.27	25.97	.104
55	1.17	32.28	25.94	.114
60	1.16	32.29	25.95	.124
65	1.15	32.30	25.95	.135





CAST 21  
 LAT 54.2N LONG 172.0W DATE 10 MAR 79 TIME 0807 GMT  
 BAROMETER 95 WIND DIR 172 WEATHER KT SEA STATE 3  
 CLOUD AMOUNT DRY -1.0 SPD 17 MET -2.2 VISIBILITY 6 M

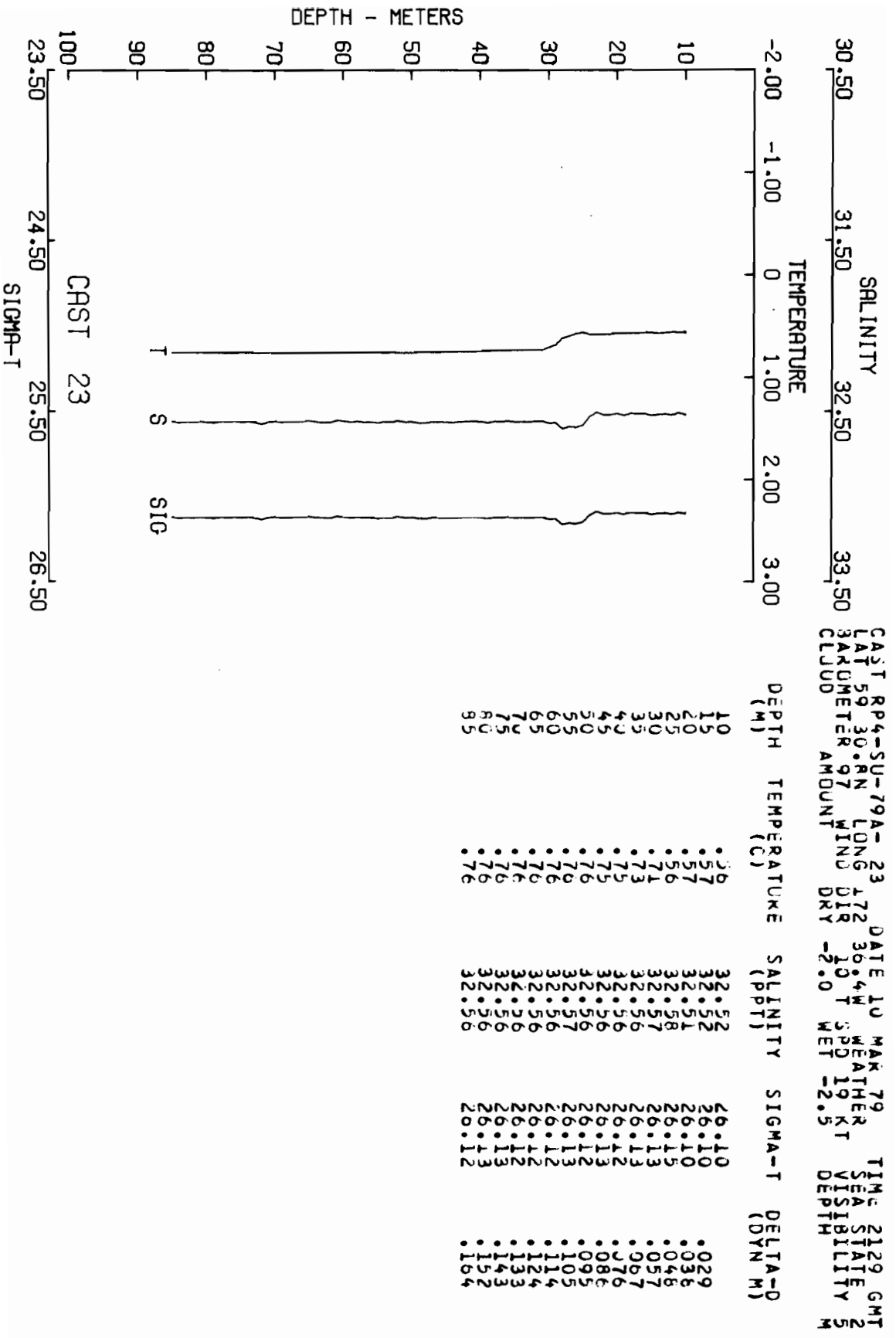
DEPTH (M)	TEMPERATURE (C)	SALINITY (PPT)	SIGMA-T (DYN M)	DELTA-D
0	96	32.64	26.17	.000
6	96	32.61	26.15	.019
10	95	32.61	26.15	.028
15	96	32.60	26.15	.037
20	96	32.62	26.15	.047
25	96	32.61	26.15	.056
30	96	32.62	26.15	.075
40	96	32.61	26.15	.084
45	96	32.61	26.15	.094
50	96	32.61	26.15	.103
55	96	32.61	26.15	.112
60	96	32.61	26.15	.122
65	96	32.61	26.15	.131
70	96	32.61	26.15	.140
75	96	32.61	26.15	.150
80	96	32.61	26.15	.161
85	96	32.61	26.15	.161



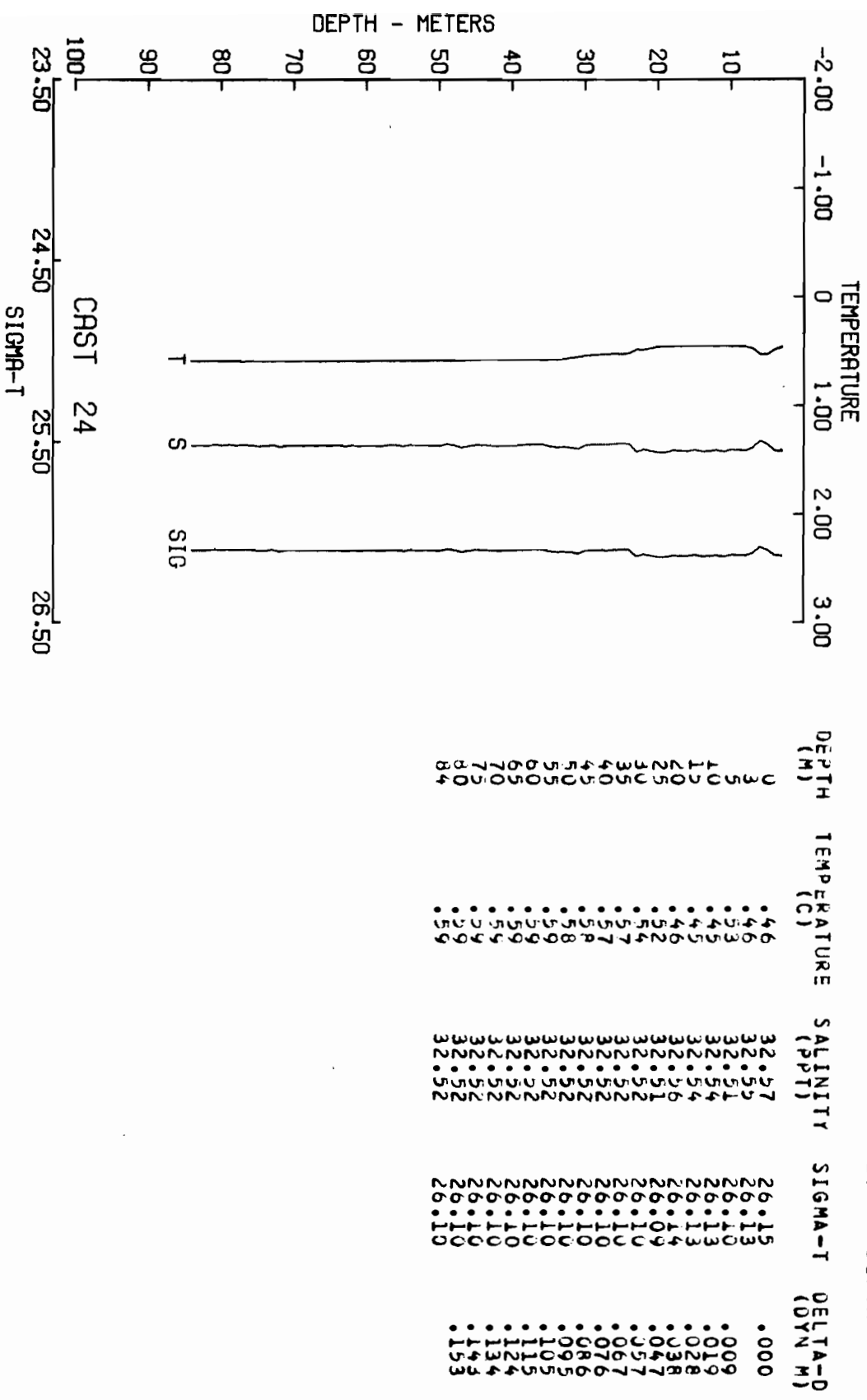
CAST 22  
SIGMA-T

CAST RP4-SU-79A-22 DATE 10 MAR 79 TIME 1625 GMT  
 LAT 29 37.1N LONG 117 40.0W WEATHER SEA STATE 0  
 BAROMETER 96 WIND DIR 15 T SPD 18 KT VISIBILITY 4  
 CLUD AMOUNT DRY -2.0 WET 18.5 DEPTH M

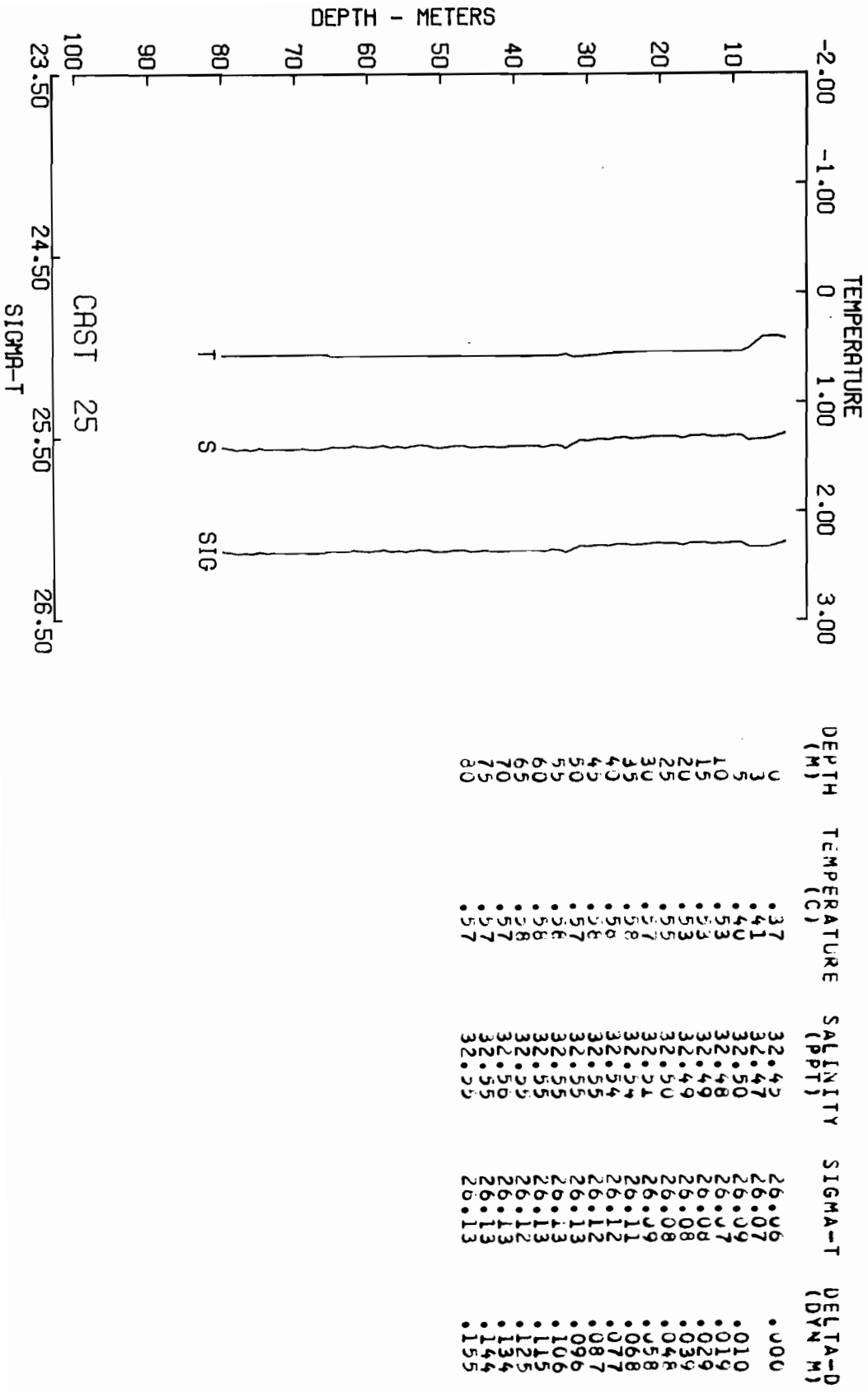
DEPTH (M)	TEMPERATURE (C)	SALINITY (PPT)	SIGMA-T (DYN M)	DELTA-D
0	.34	32.48	26.08	.000
2	.31	32.50	26.09	.010
5	.27	32.51	26.11	.019
15	.36	32.53	26.14	.029
20	.43	32.55	26.16	.038
25	.57	32.62	26.18	.057
30	.59	32.63	26.19	.066
35	.58	32.63	26.19	.075
40	.64	32.63	26.19	.084
45	.64	32.63	26.19	.093
50	.65	32.63	26.19	.103
60	.65	32.63	26.19	.112
70	.69	32.59	26.15	.131
80	.69	32.59	26.15	.149
85	.70	32.58	26.15	.161

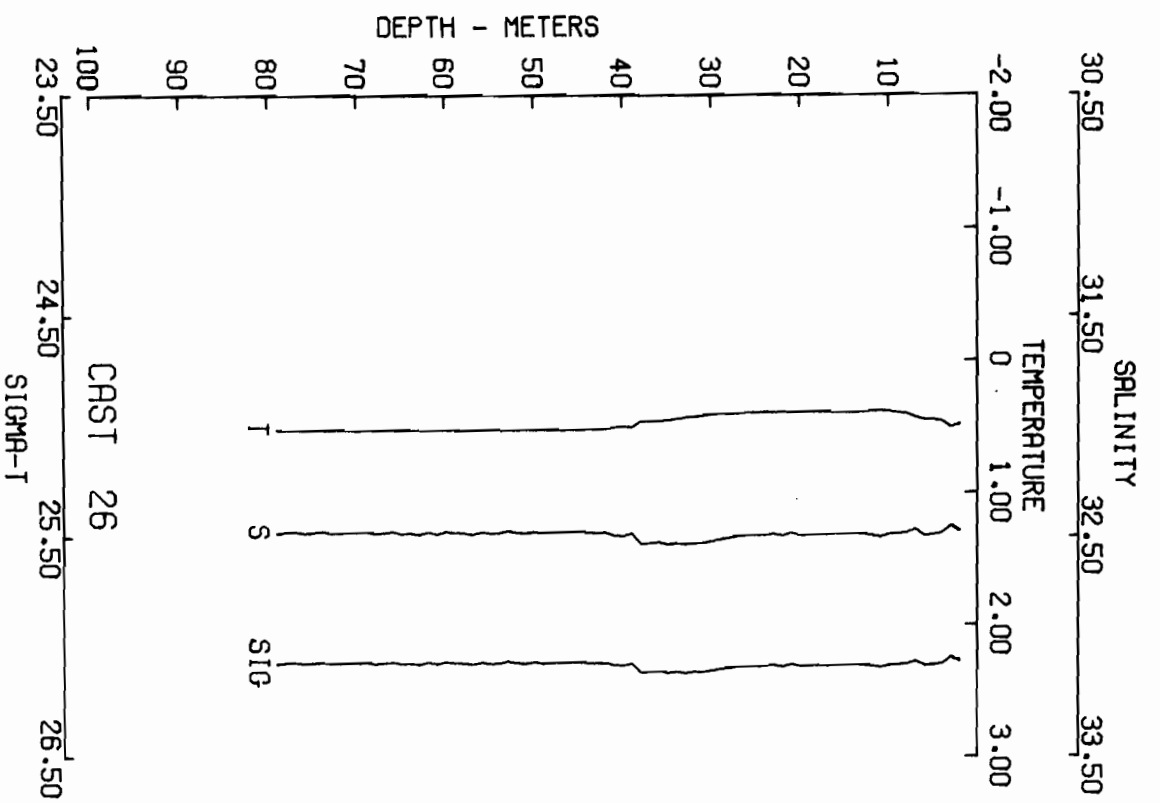


CASI RPY-SU-79A-24 DATE 11 MAR 79 TIME 0 GMT  
 LAT 29 22.8N LONG 172 19.7W WEATHER SEA STATE 2  
 BAROMETER 97 WIND DIR 10 T SPD 18 KT VIS 4  
 CLOUD AMOUNT -1.9 WET -2.6 DEPTH



CAST KP4--SU-79A-25 DATE 11 MAR 79 TIME 130 GMT  
 LAT 39 17.7N LONG 02.4W WEATHER KT SEA STATE 2  
 BAROMETER 97 WIND DIR 4 SPD 4 VISIBILITY 6  
 CLOUD AMOUNT WET -1.2 WET -2.2 DEPTH M



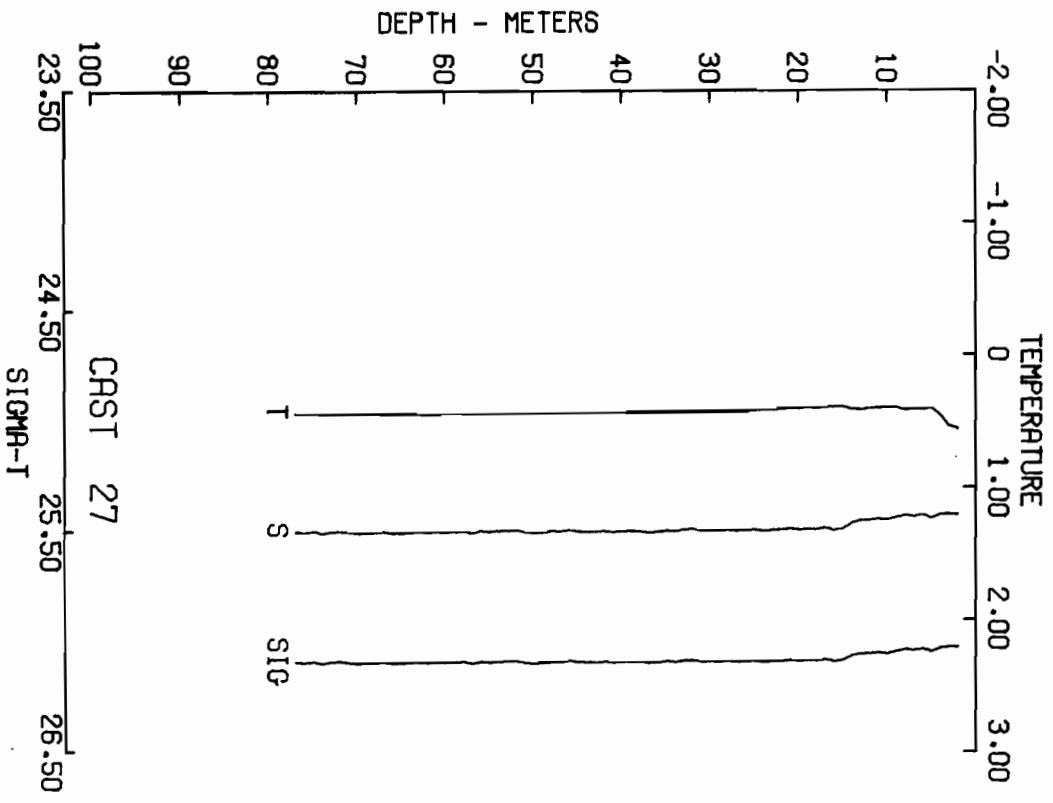


LAST RPP4-SU-79A-26 DATE 11 MAR 79 TIME 316 GMT  
 LAT 29 13.2N LONG 171 45.3W WEATHER KT SEA STATE 2  
 BAROMETER 98 WIND DIR 105 T SPD 6 K VISIBILITY 6  
 CLOUD AMOUNT DRY - WET -1.5 DEPTH

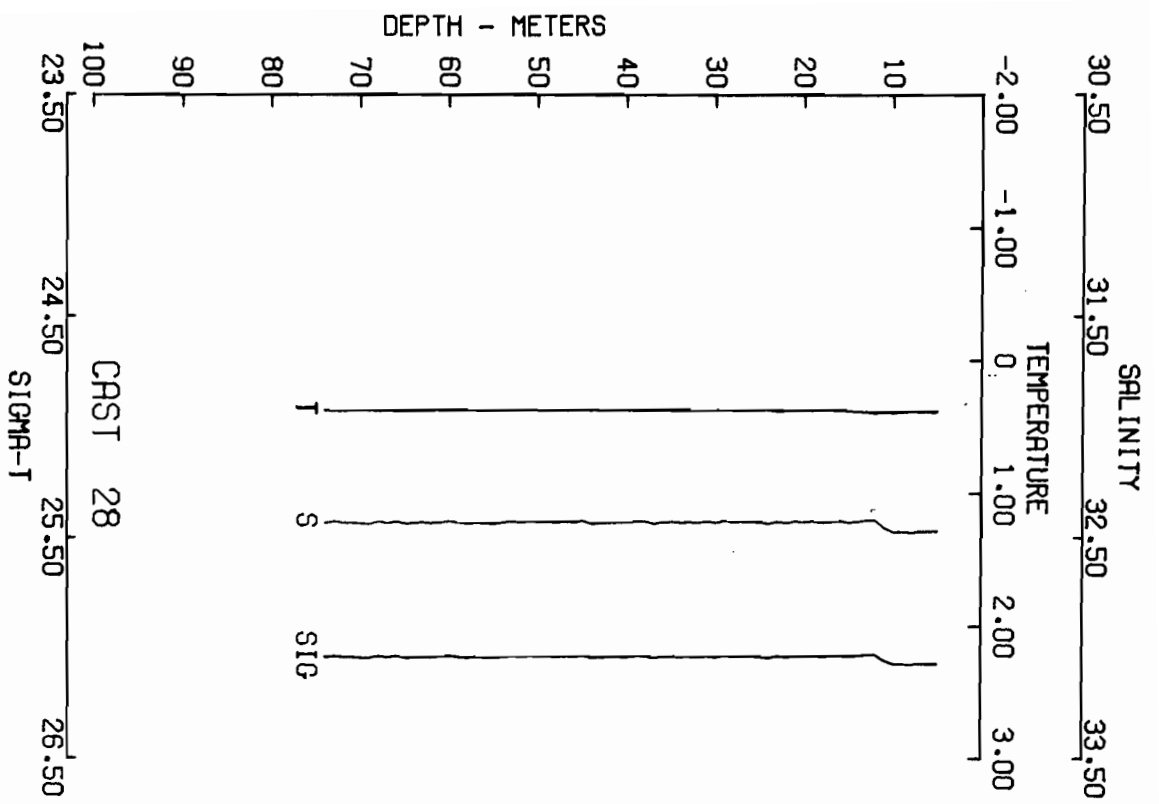
DEPTH (M)	TEMPERATURE (C)	SALINITY (PPT)	SIGMA-T	DELTA-D (DYN M)
0	5.29	32.40	26.07	.000
5	4.5	32.47	26.07	.010
10	3.9	32.49	26.09	.019
15	3.9	32.49	26.08	.029
20	3.9	32.49	26.09	.039
25	3.9	32.49	26.11	.049
30	4.4	32.52	26.11	.056
35	4.5	32.53	26.08	.068
40	5.0	32.49	26.07	.077
45	5.2	32.48	26.07	.087
50	5.2	32.48	26.07	.097
55	5.3	32.48	26.07	.106
60	5.3	32.48	26.08	.116
65	5.3	32.48	26.07	.126
70	5.3	32.48	26.07	.136
75	5.3	32.48	26.07	.145



30.50 SALINITY 32.50 33.50  
 31.50  
 32.50  
 33.50  
 CAST RP4-SU-79A-27 DATE 11 MAR 79 TIME 440 GMT  
 LAT 59.9N LONG 171.285W WEATHER SEA STATE 2  
 BAROMETER 99 WIND DIR 98 T SPD 7 VISIBILITY 6  
 CLJUD AMOUNT DRY - . . MET -1.5 DEPTH M



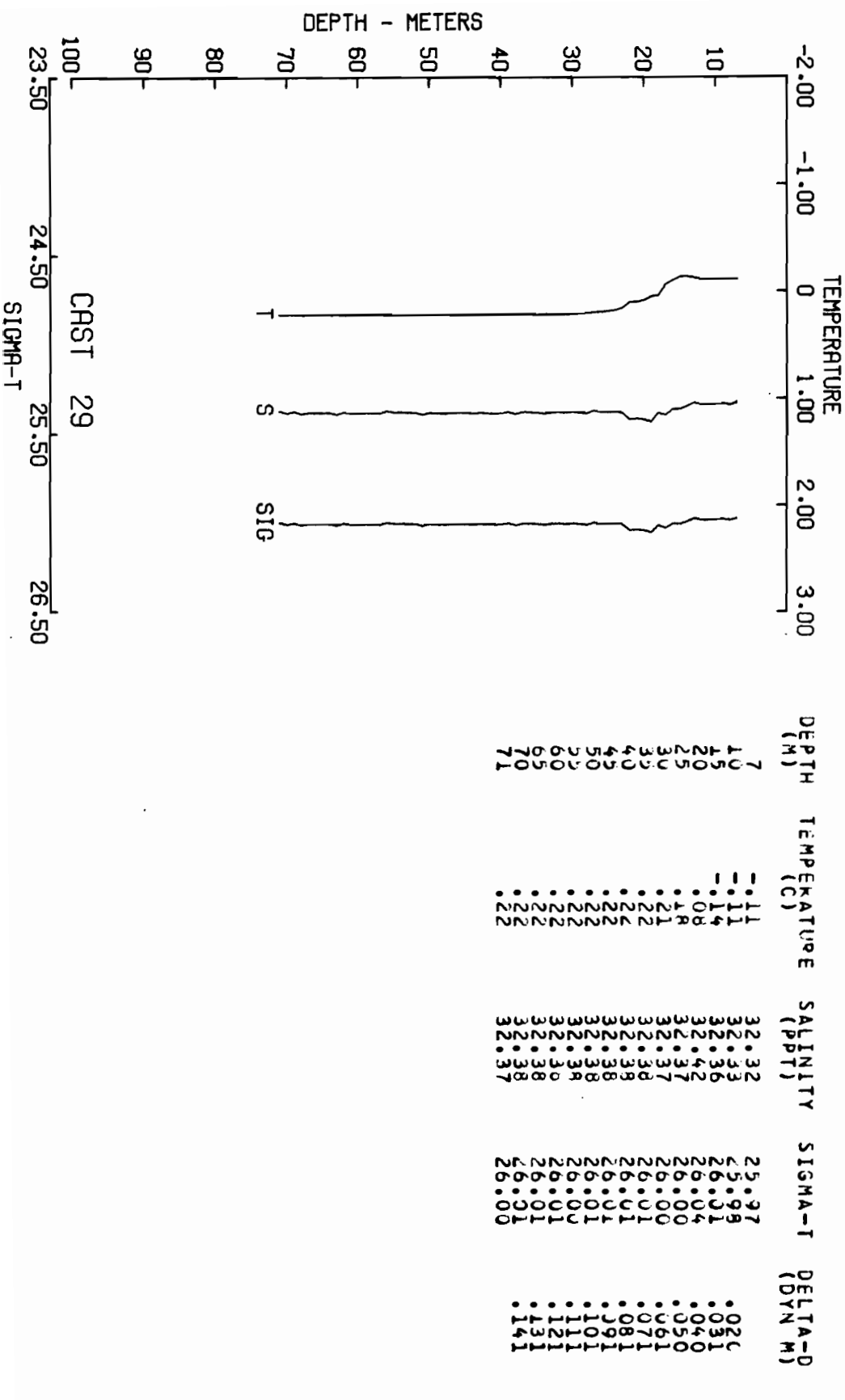
DEPTH (M)	TEMPERATURE (C)	SALINITY (PPT)	SIGMA-T	DELTA-D (DYN M)
0	1.5	32.5	26.0	0.00
2	1.4	32.5	26.0	0.00
5	1.3	32.5	26.0	0.00
10	1.2	32.5	26.0	0.00
12	1.1	32.5	26.0	0.00
20	1.0	32.5	26.0	0.00
25	0.9	32.5	26.0	0.00
30	0.8	32.5	26.0	0.00
35	0.7	32.5	26.0	0.00
40	0.6	32.5	26.0	0.00
45	0.5	32.5	26.0	0.00
50	0.4	32.5	26.0	0.00
55	0.3	32.5	26.0	0.00
60	0.2	32.5	26.0	0.00
65	0.1	32.5	26.0	0.00
70	0.0	32.5	26.0	0.00
75	-0.1	32.5	26.0	0.00
77	-0.2	32.5	26.0	0.00



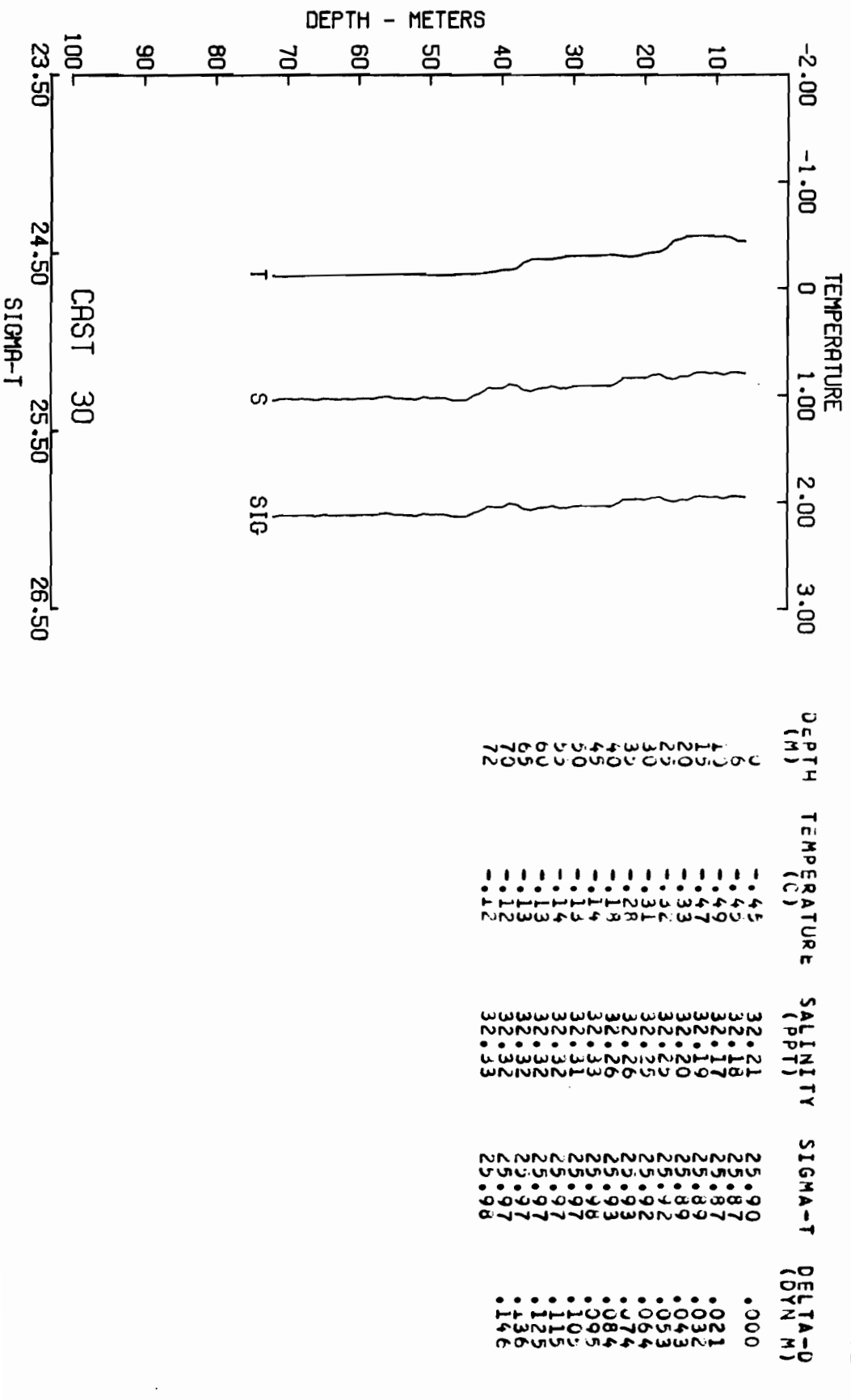
CAST KP4-SU-79A-28 DATE 11 MAR 79 TIME 614 GMT  
 LAT 52 02.4N LONG 17 10.9W SEA STATE 2  
 BAROMETER 99 WIND DIR 142 T SPD 8 KT VISIBILITY 7 M  
 CLOUD DRY WEATHER -1.4 DEPTH 74 M

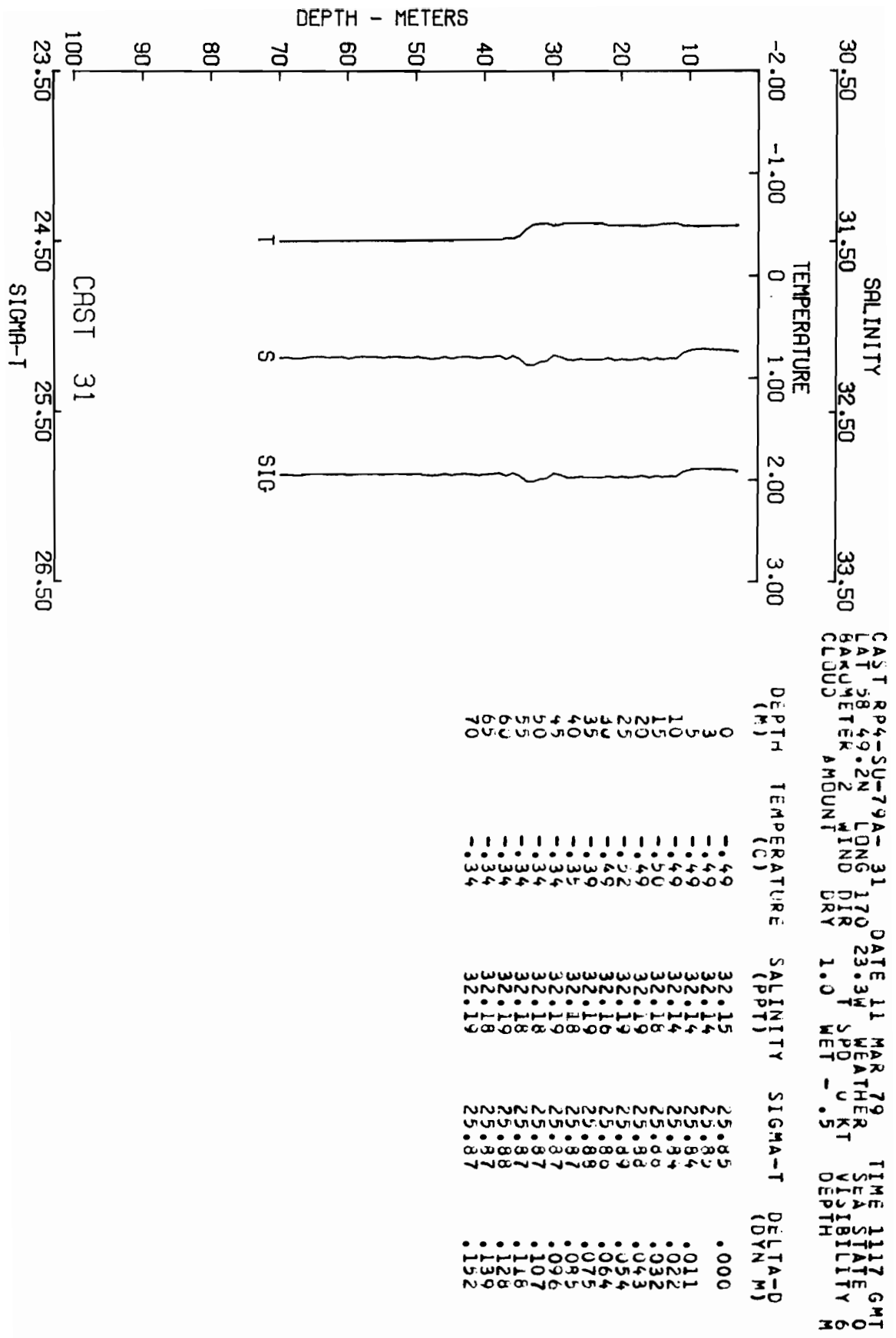
DEPTH (M)	TEMPERATURE (C)	SALINITY (PPT)	SIGMA-T (DYN M)
0	38	32.47	26.07
5	39	32.47	26.07
10	39	32.47	26.07
15	37	32.43	26.04
20	37	32.43	26.04
25	37	32.43	26.04
30	37	32.43	26.04
35	37	32.43	26.04
40	37	32.43	26.04
45	37	32.43	26.04
50	37	32.44	26.04
55	37	32.44	26.04
60	37	32.44	26.04
65	37	32.44	26.04
70	37	32.44	26.04
75	37	32.44	26.04
80	37	32.44	26.04
85	37	32.44	26.04
90	37	32.44	26.04
95	37	32.44	26.04
100	37	32.44	26.04

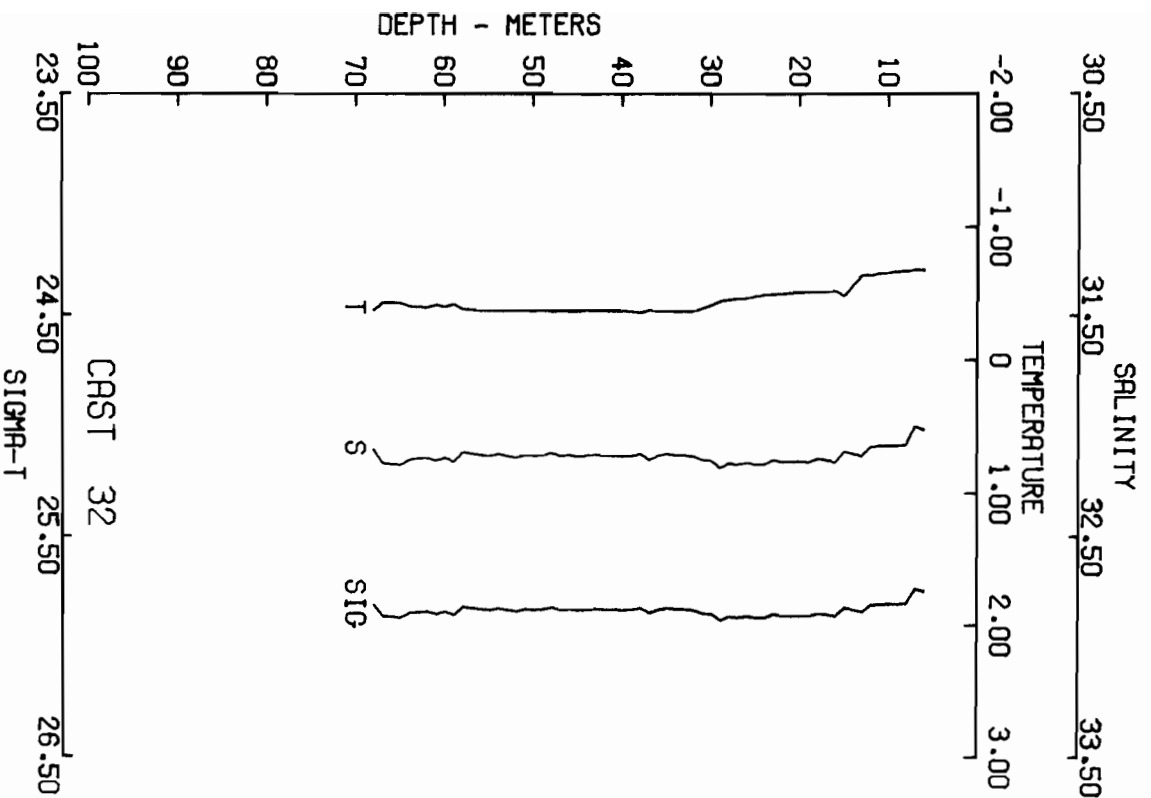
SALINITY 30.50 31.50 32.50 33.50  
 CAST RP4-SU-79A-29 DATE 11 MAR 79 TIME 736 GMT  
 LAT 58 58.4N LONG 170 57.6W WEATHER 0 VIS 18181  
 BAROMETER 0 WIND DIR 140 T SPT 8 KRT VISIBILITY 73 M  
 CLOUD 0 WET -1.4 DEPTH



30.50 31.50 32.50 33.50  
 SALINITY  
 29.23.7N 30 170 40.0 W 14.7 W 12.0  
 LAT LONG DIR WIND SPD WFT WEATHER SEA STATE VISIBILITY  
 29.00 14.7 WFT -1.0 DEPTH 72 M  
 CLDUD AMOUNT  
 DATE 11 MAR 79 TIME 928 GMT  
 BAROMETER AMOUNT  
 WIND DIR DRY  
 WFT -1.0  
 VISIBILITY 72 M



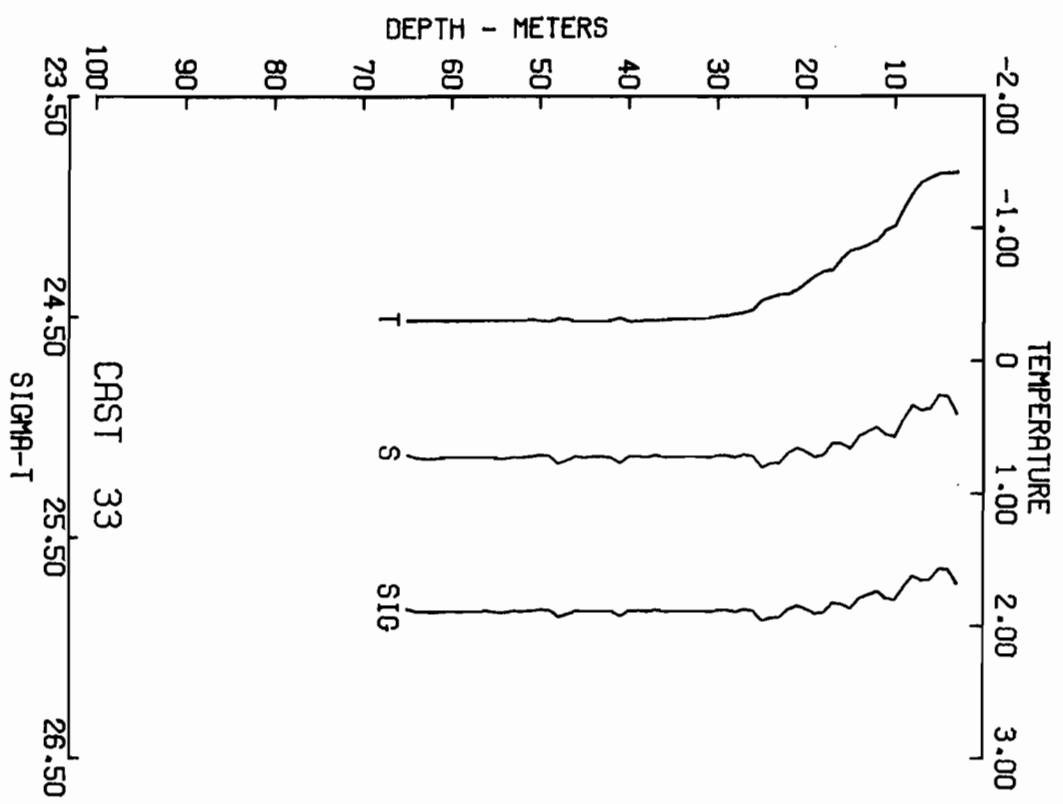




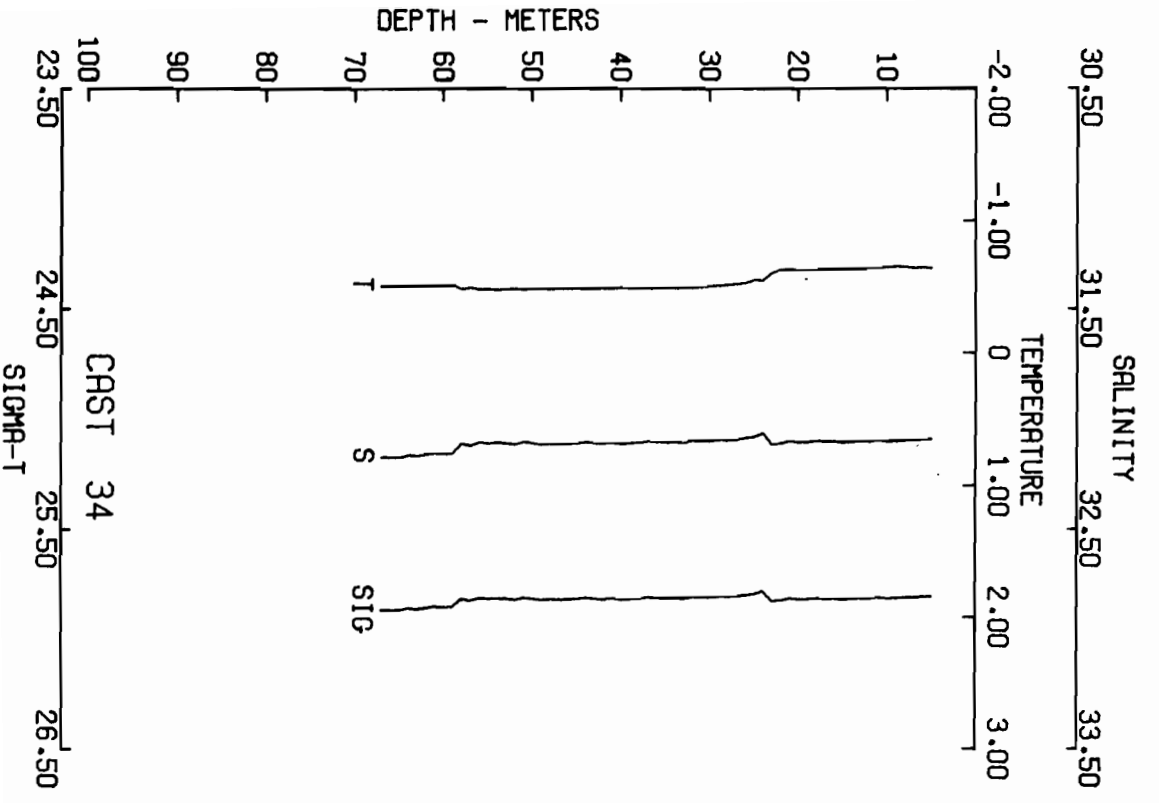
CAST R44-SU-79A-32 DATE 11 MAR 79 TIME 1316 GMT  
 LAT 58 44.2N LONG 07:2W WEATHER SEA STATE 0  
 BAROMETER 2 WIND DIR 85 U WET 8 O VISIBILITY 6  
 CLOUD DRY MET

DEPTH (M)	TEMPERATURE (C)	SALINITY (PPT)	SIGMA-T	DELTA-D (DYN M)
0	0.67	32.10	25.04	0.00
10	0.65	32.09	25.04	0.02
15	0.46	32.11	25.08	0.03
20	0.50	32.16	25.06	0.04
25	0.47	32.17	25.07	0.05
30	0.41	32.15	25.08	0.05
35	0.37	32.12	25.03	0.07
40	0.36	32.14	25.03	0.08
45	0.37	32.13	25.04	0.08
50	0.37	32.14	25.03	0.10
55	0.40	32.14	25.03	0.12
60	0.42	32.14	25.04	0.13
65	0.42	32.18	25.07	0.13
68	0.37	32.11	25.08	0.14

CAST RP4-SU-79A-33 DATE 11 MAR 79 TIME 1639 GMT  
 LAT 58 56.5N LONG 09 08 W WEATHER SEA STATE 0  
 BAROMETER 30.0 WIND DIR 70 T SPD 8 VISIBILITY 6  
 CLDUD AMOUNT 0 WET -1.3 DEPTH 0 M



DEPTH (M)	TEMPERATURE (C)	SALINITY (PPT)	SIGMA-T	DELTA-D (DYN M)
0	-1.49	31.88	25.67	.000
3	-1.42	31.94	25.71	.012
5	-1.41	31.85	25.54	.023
10	-1.02	32.04	25.78	.034
15	-.85	32.10	25.82	.045
20	-.59	32.11	25.87	.056
25	-.46	32.18	25.83	.067
30	-.34	32.13	25.83	.078
35	-.32	32.13	25.83	.089
40	-.30	32.13	25.83	.100
45	-.31	32.14	25.84	.110
50	-.31	32.14	25.84	.121
55	-.31	32.14	25.83	.132
60	-.30	32.13	25.83	.145

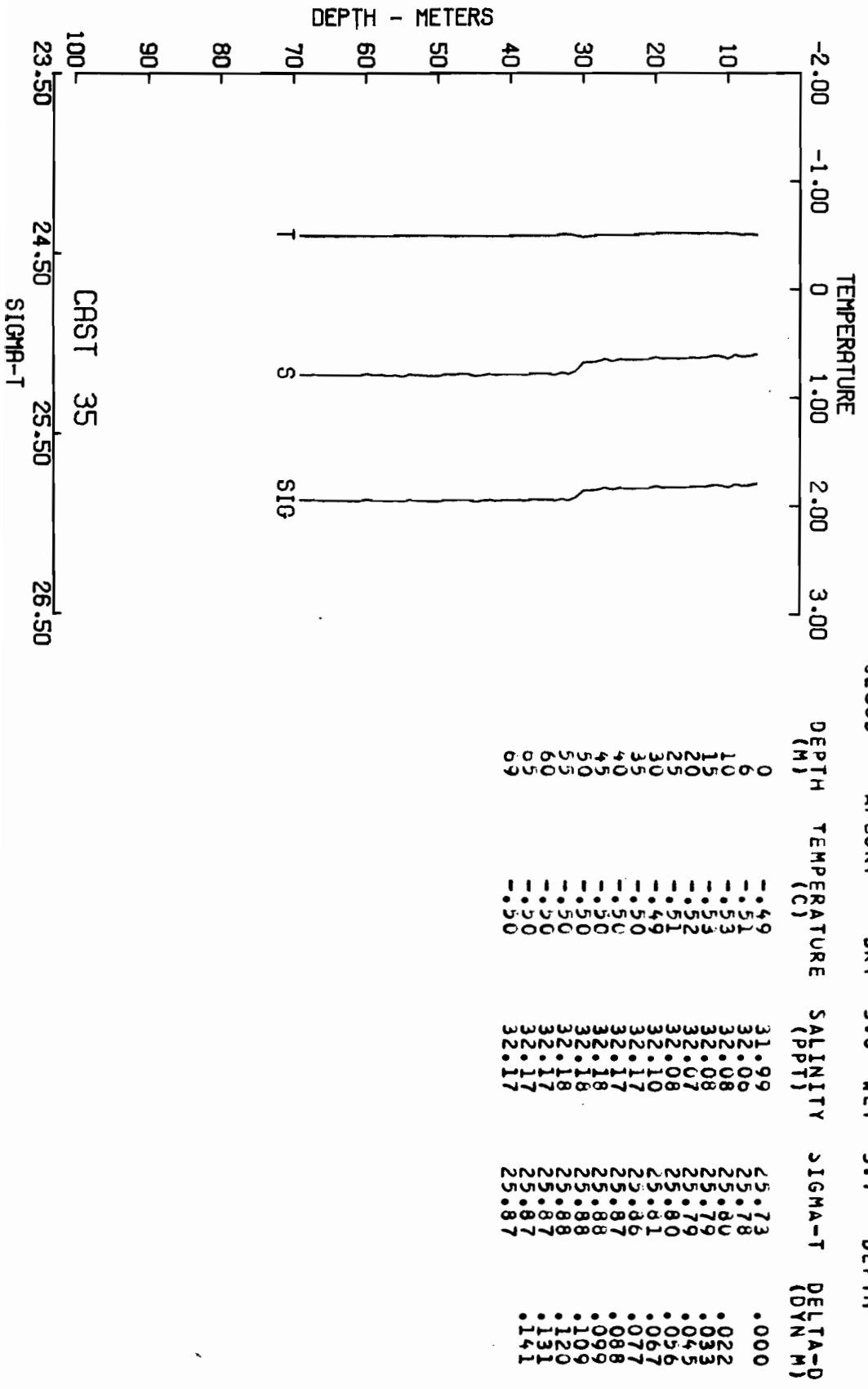


CAST R44-SU-79A-34 DATE 12 MAR 79 TIME 439 GMT  
 LAT 58 53.6N LONG 170 13.9W WEATHER SEA STATE 0  
 BAROMETER AMOUNT WIND DIR 328 T SPD 22 KT VISIBILITY 7  
 CLOUD DRY -3.2 WET -3.6 DEPTH M

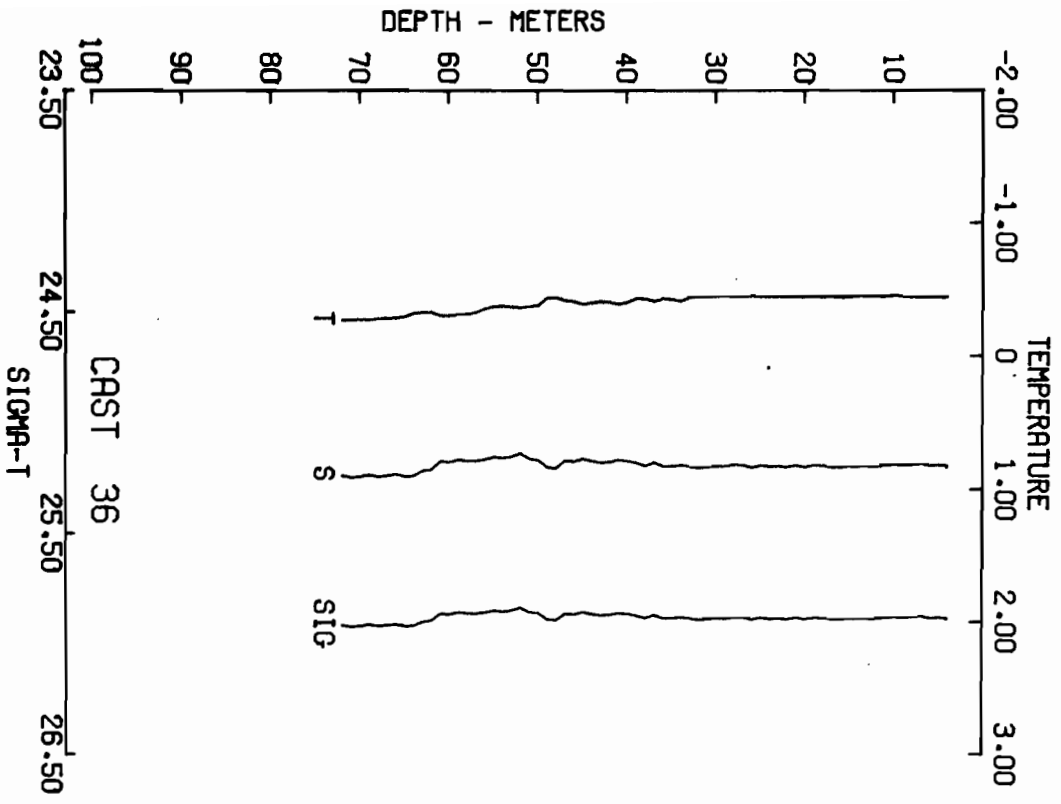
DEPTH (M)	TEMPERATURE (C)	SALINITY (PPT)	SIGMA-T	DELTA-D (DYN M)
0	-1.64	32.07	25.79	.000
5	-1.64	32.09	25.81	.022
10	-1.65	32.10	25.82	.033
15	-1.64	32.10	25.82	.044
20	-1.55	32.08	25.79	.055
25	-1.49	32.10	25.81	.066
30	-1.49	32.11	25.82	.077
35	-1.49	32.11	25.82	.088
40	-1.49	32.11	25.82	.099
45	-1.48	32.11	25.82	.110
50	-1.48	32.11	25.82	.121
55	-1.51	32.11	25.86	.132
60	-1.51	32.11	25.87	.142
65	-1.51	32.11	25.87	.142
67	-1.51	32.11	25.87	.142



CAST RP4-SU-79A-35 DATE 12 MAR 79 TIME 022 GMT  
 LAT 58 52.6N LONG 170 17.9W WEATHER SEA STATE 3  
 BAROMETER 818 WIND DIR 77 T SPD 23 MET VISIBILITY 6  
 CLOUD AMOUNT 8 DRY -3.0 MET -3.7

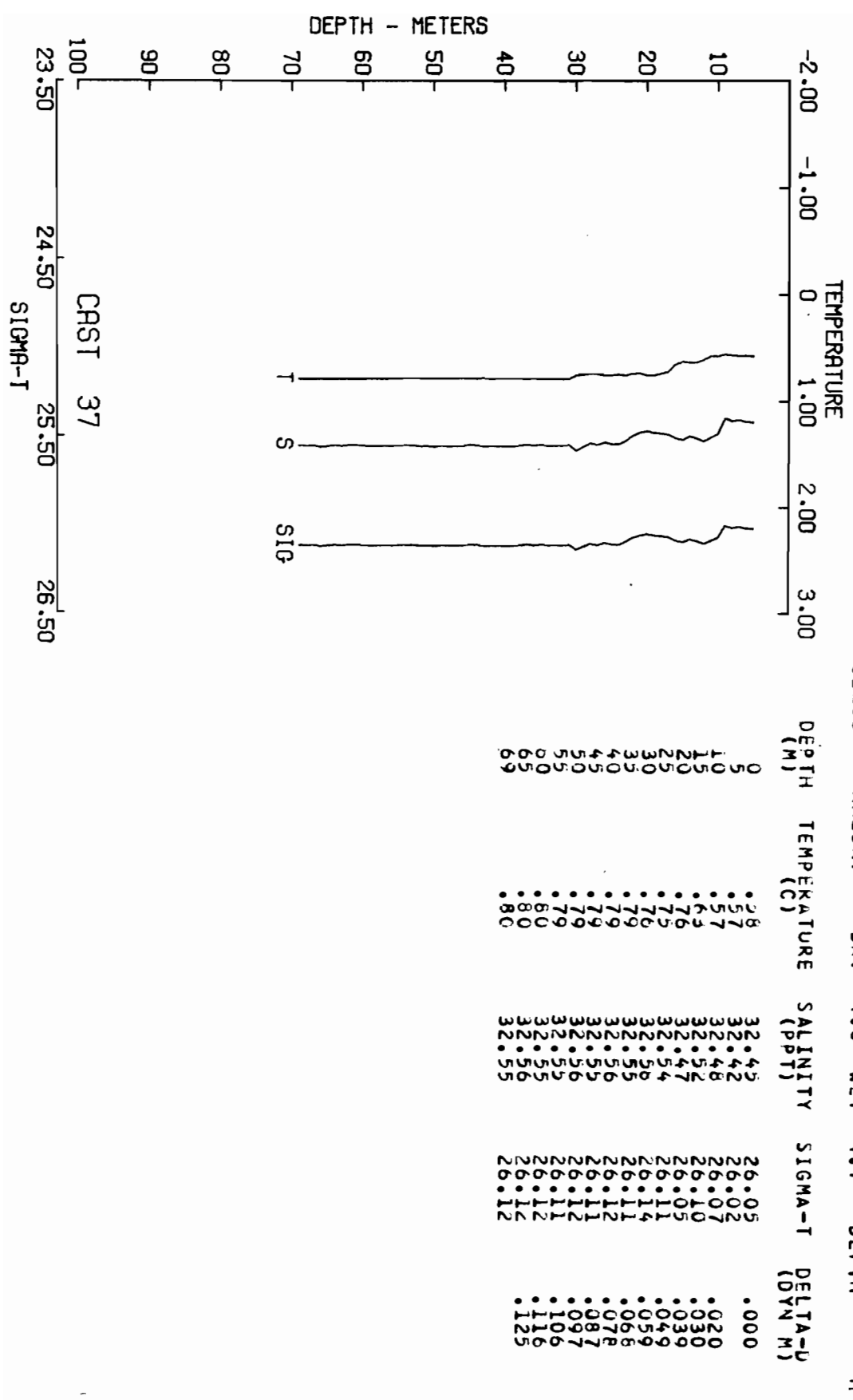


CAST RPT4-SU-79A-36 DATE 12 MAR 79 TIME 1636 GMT  
 LAT 58 46.9N LONG 170 25.3W WEATHER SEA STATE 0  
 BARUMETER 12 WIND DIR 10 T SPD 18 KT VISIB 7 M  
 CLOUD AMOUNT -4.9 WET -5.2 DEPTH

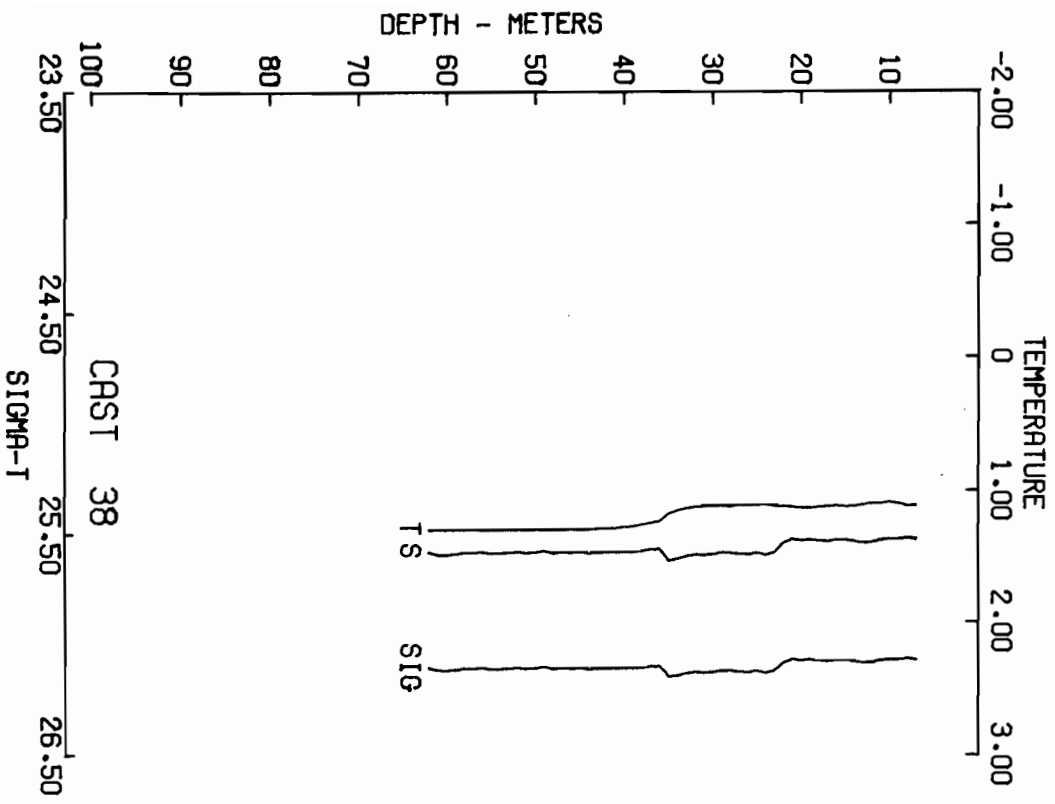


DEPTH (M)	TEMPERATURE (C)	SALINITY (PPT)	SIGMA-T	DELTA-D (DYN M)
0	4.5	32.21	25.90	.000
4	4.5	32.19	25.88	.011
5	4.5	32.19	25.88	.021
10	4.5	32.20	25.89	.032
15	4.5	32.20	25.89	.042
20	4.5	32.20	25.89	.053
25	4.3	32.19	25.88	.064
30	4.3	32.17	25.87	.074
35	4.1	32.16	25.86	.085
40	3.9	32.17	25.86	.096
45	3.7	32.18	25.87	.106
50	3.7	32.18	25.87	.117
55	3.0	32.24	25.92	.128
60	2.8	32.24	25.92	.138
65	2.7	32.24	25.92	.149
70	2.7	32.24	25.92	.149
72	2.7	32.24	25.92	.149

SRLINITY 30.50 31.50 32.50 33.50  
 CAST RP4-SU-79A-37 DATE 13 MAR 79 TIME 438 GMT  
 LAT 27 58.5N LONG 168 21.1W WEATHER SEA STATE Y 2  
 BAROMETER 11 WIND DIR 358 T SPD 41 KT VISIBILITY 7 M  
 CLUD AMOUNT -4.0 MET -4.7 DEPTH

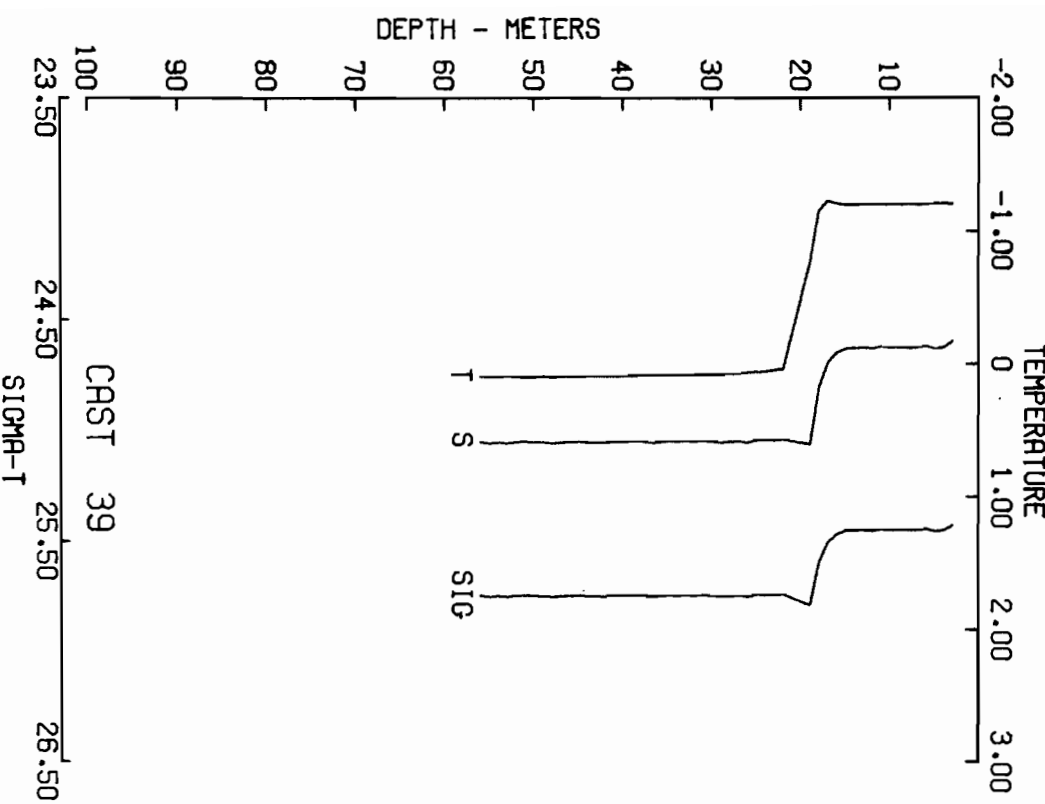


SALINITY 30.50 31.50 32.50 33.50  
 CAST R44-SU-79A-38 DATE 13 MAR 79 TIME 812 GMT  
 LAT 57 45.2N LONG 167 37.7W WEATHER VIS STATE 3  
 BAROMETER 10 WIND SPD 15 KT VISIBLITY 6  
 CLOUD DRY -4.0 WET -5.0 DEPTH 62 M



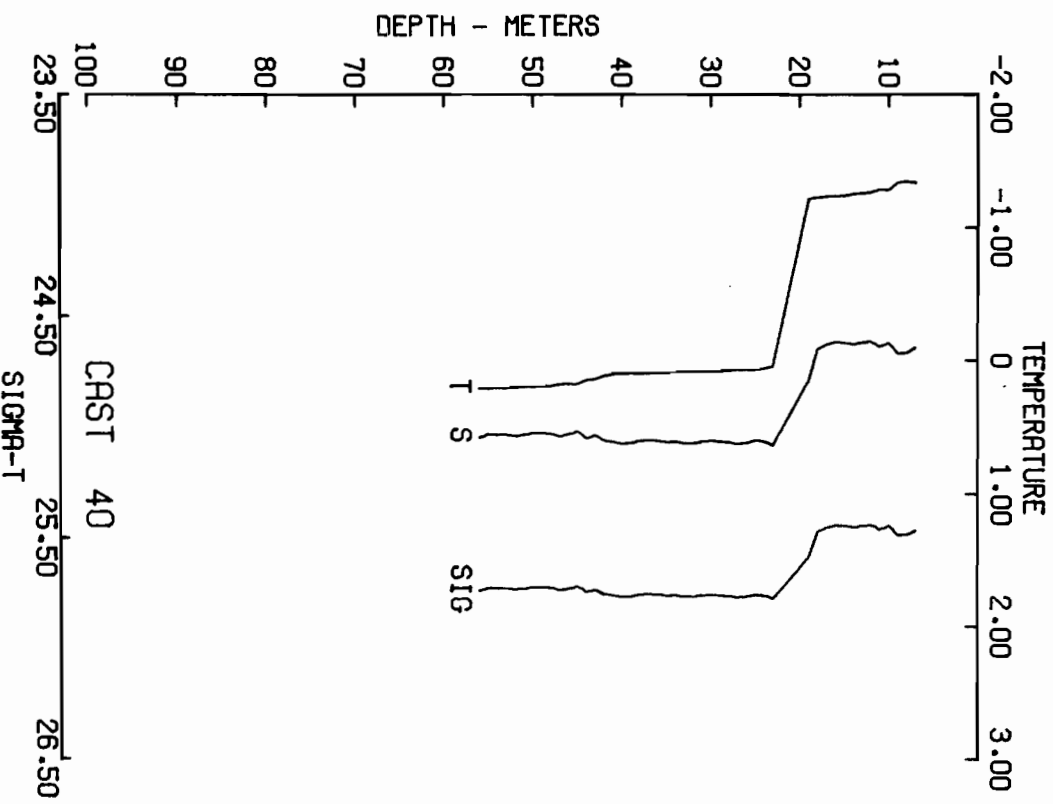
DEPTH (M)	TEMPERATURE (C)	SALINITY (PPT)	SIGMA-T	DELTA-D (DYN M)
7	1.09	32.52	26.07	.019
10	1.11	32.52	26.07	.029
15	1.12	32.53	26.07	.039
20	1.13	32.53	26.07	.048
25	1.11	32.58	26.12	.048
30	1.12	32.59	26.13	.058
35	1.18	32.62	26.15	.067
40	1.28	32.58	26.11	.077
45	1.30	32.58	26.11	.087
50	1.30	32.59	26.11	.096
55	1.30	32.60	26.11	.106
60	1.31	32.59	26.12	.106
62	1.31	32.59	26.11	.115

CAST RPP4-SU-79A-39 DATE 14 MAR 79 TIME 436 GMT  
 LAT 28 01.0N LONG 149 14.9W WEATHER SEA STATE 0  
 BAROMETER 999.9 WIND DIR 45 T SPU 4 KT VISIBILITY 7 M  
 CLOUD AMOUNT DRY -6.5 WET -7.5 DEPTH

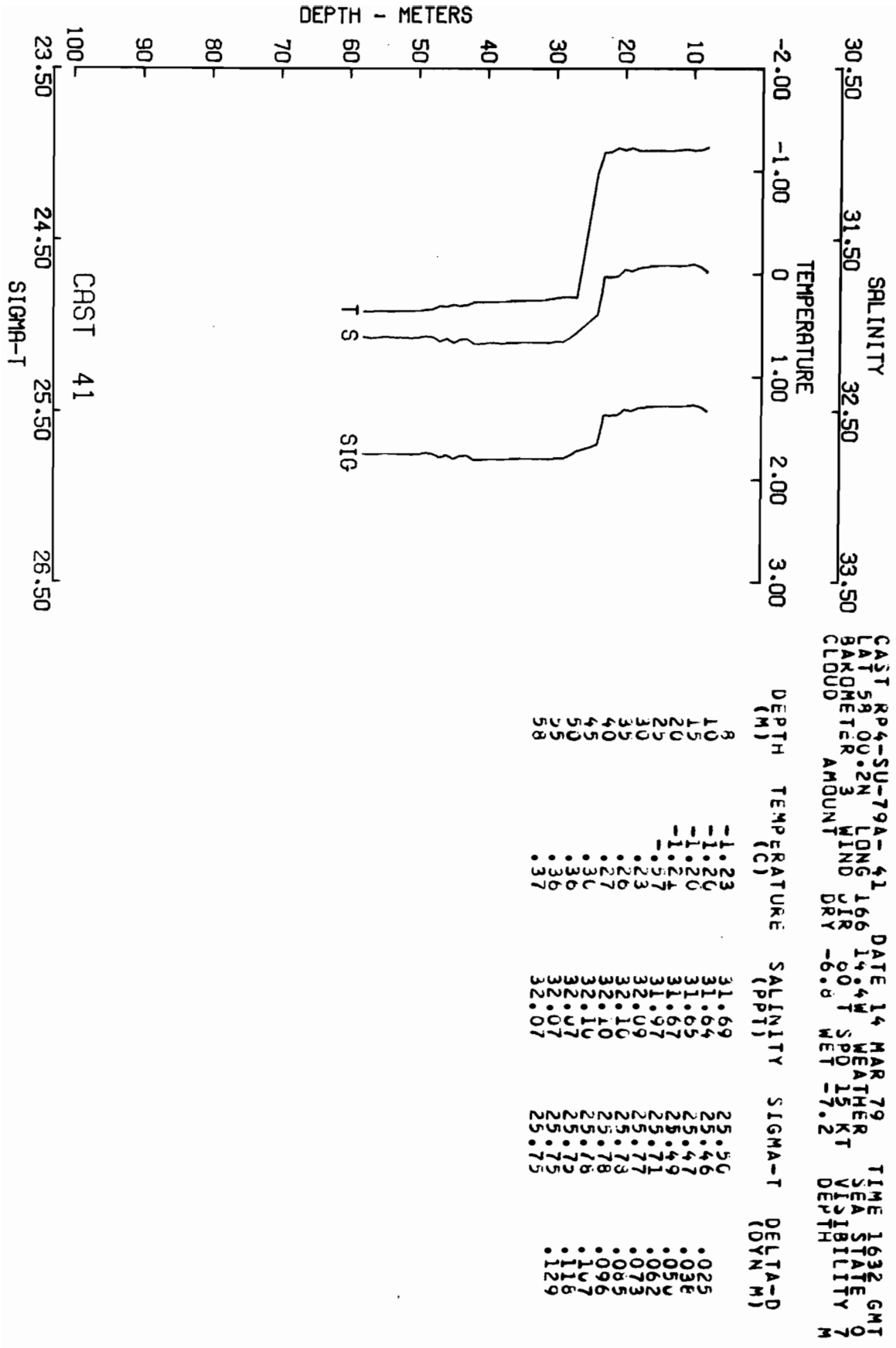


DEPTH (M)	TEMPERATURE (C)	SALINITY (PPT)	SIGMA-T	DELTA-D (DYN M)
0	1.0	31.5	25.4	.000
3	1.0	31.5	25.4	.013
5	1.0	31.5	25.4	.025
10	1.0	31.5	25.4	.036
15	1.0	31.5	25.4	.061
20	-1.0	31.0	25.0	.073
25	-1.0	31.0	25.0	.084
30	-1.0	31.0	25.0	.095
35	-1.0	31.0	25.0	.107
40	-1.0	31.0	25.0	.118
45	-1.0	31.0	25.0	.129
50	-1.0	31.0	25.0	.129
55	-1.0	31.0	25.0	.129
60	-1.0	31.0	25.0	.129
65	-1.0	31.0	25.0	.129
70	-1.0	31.0	25.0	.129
75	-1.0	31.0	25.0	.129
80	-1.0	31.0	25.0	.129
85	-1.0	31.0	25.0	.129
90	-1.0	31.0	25.0	.129
95	-1.0	31.0	25.0	.129
100	-1.0	31.0	25.0	.129

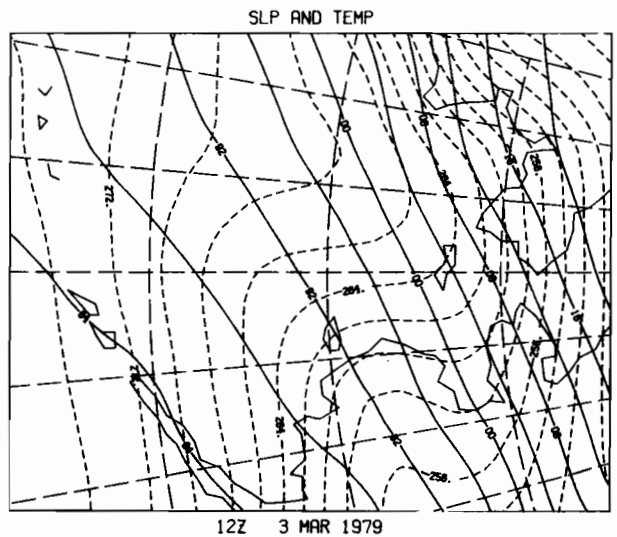
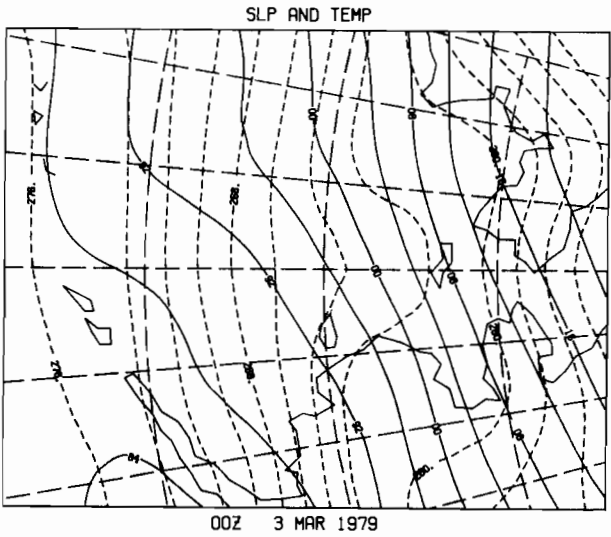
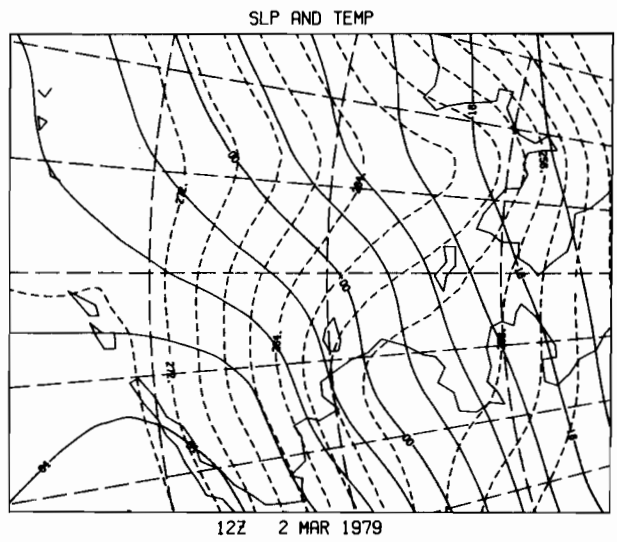
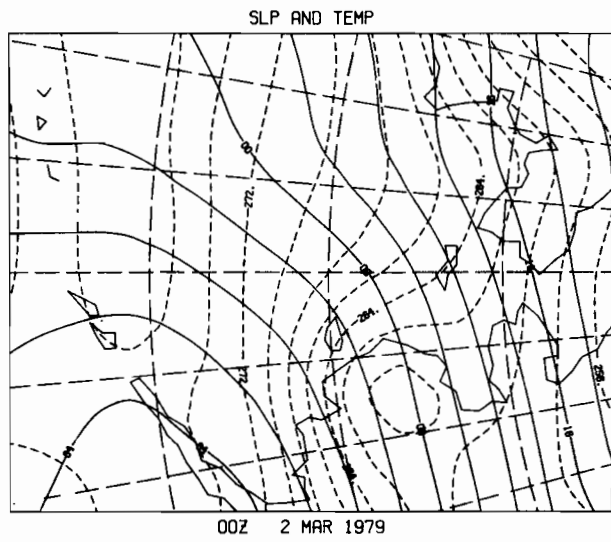
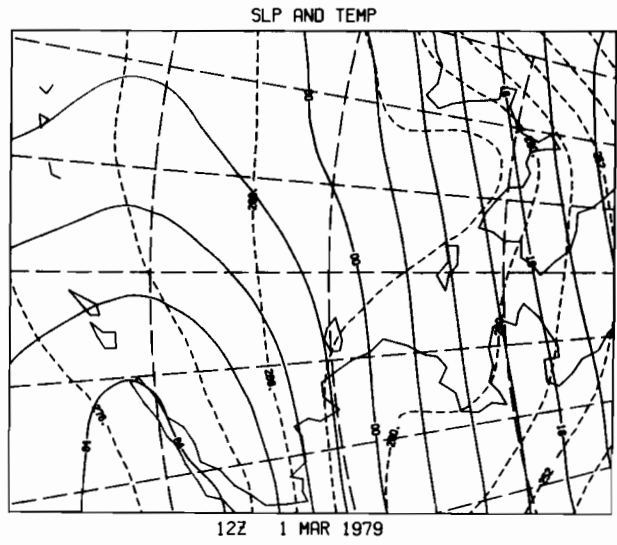
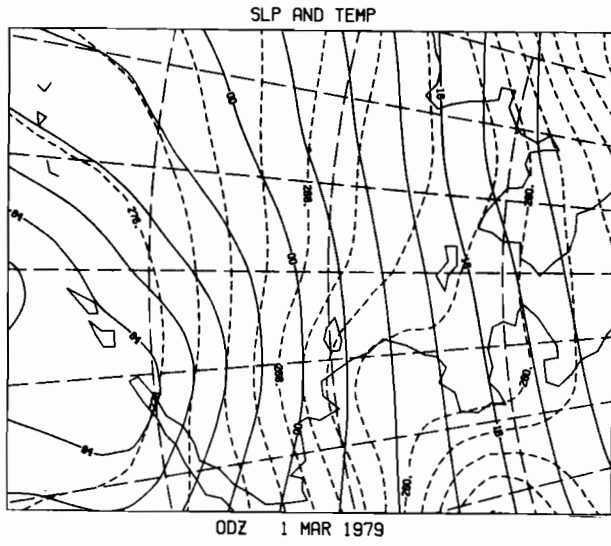
30.50 SALINITY 31.50 32.50 33.50  
 CAST RP4-SU-79A-40 DATE 14 MAR 79 TIME 809 GMT  
 LAT 28 00.5N LONG 166 14.7W WEATHER SEA STATE O  
 BAROMETER 8 WIND DIR 37 T SPD 8 KT VISIBILITY 7  
 CLOUD AMOUNT -5.5 WET -7.1 DEPTH M



DEPTH (M)	TEMPERATURE (C)	SALINITY (PPT)	SIGMA-T (DYNA-M)
7	-1.34	31.04	25.47
10	-1.29	31.04	25.45
15	-1.24	31.06	25.44
20	-0.90	31.86	25.63
25	.07	32.06	25.75
30	.08	32.06	25.75
35	.09	32.07	25.76
40	.10	32.07	25.77
45	.16	32.03	25.72
50	.20	32.03	25.72
55	.21	32.05	25.73
56	.21	32.05	25.74

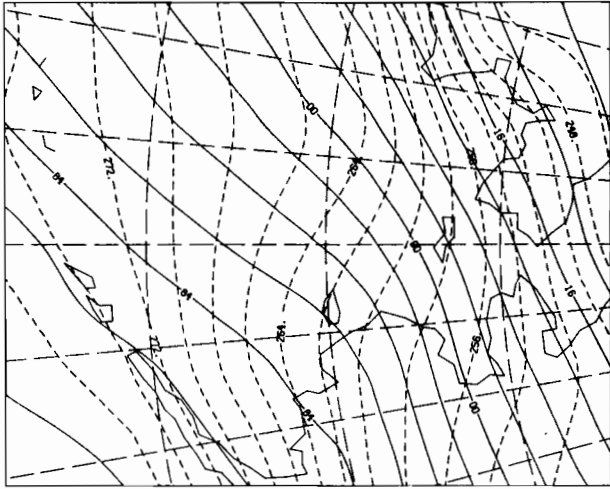


APPENDIX B: SURFACE AIR ISOTHERMS AT 00Z AND 12Z, FROM THE WSFO SURFACE ANALYSES. TEMPERATURES ARE DEGREES KELVIN.



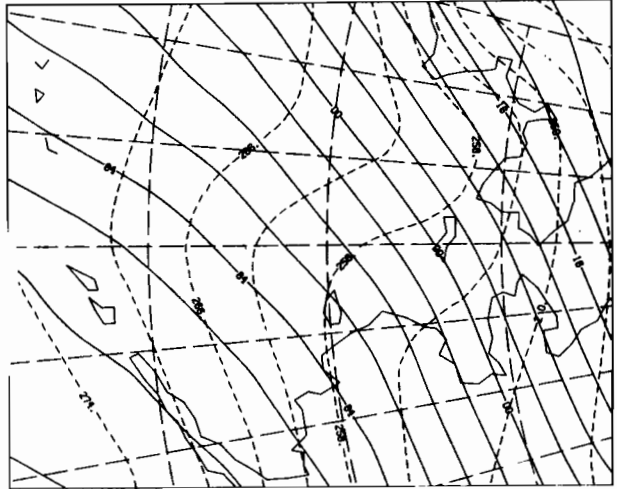


SLP AND TEMP



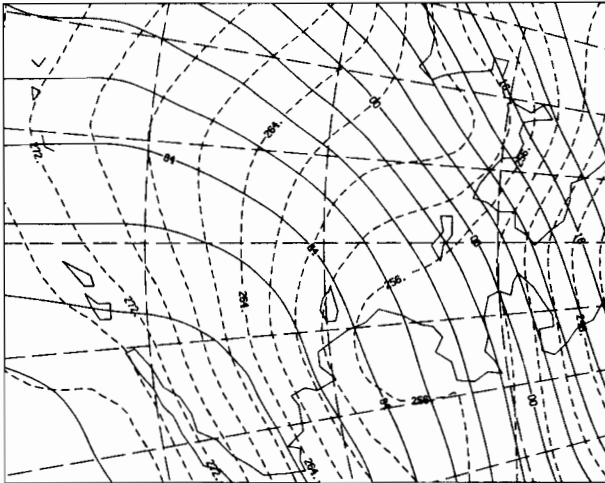
00Z 4 MAR 1979

SLP AND TEMP



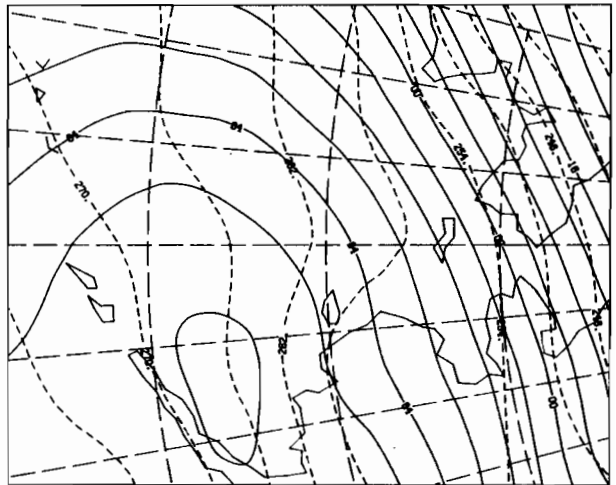
12Z 4 MAR 1979

SLP AND TEMP



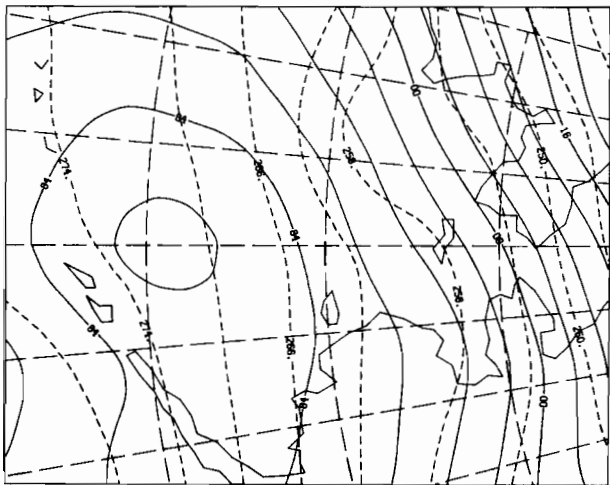
00Z 5 MAR 1979

SLP AND TEMP



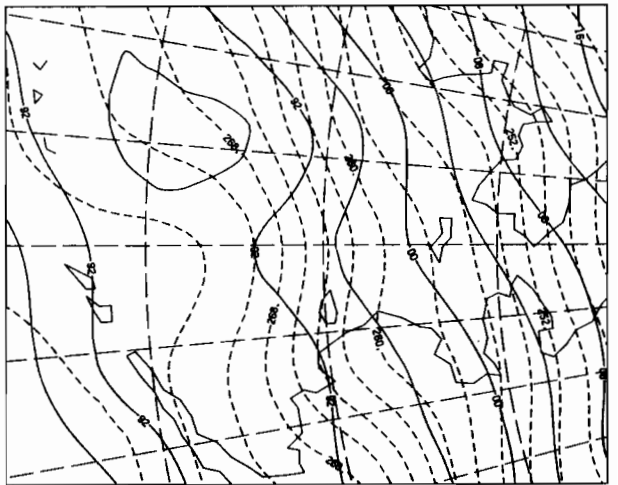
12Z 5 MAR 1979

SLP AND TEMP



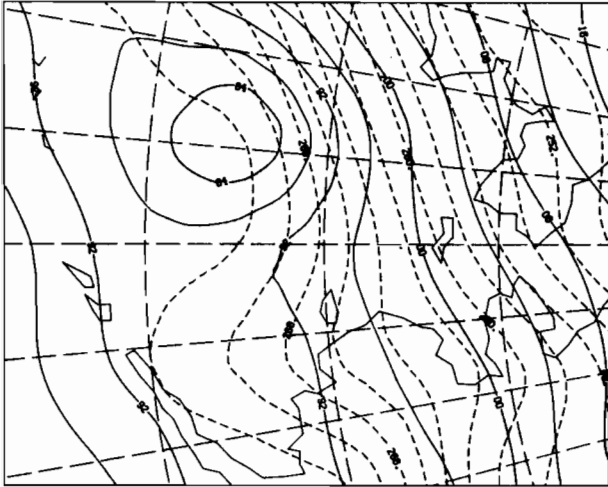
00Z 6 MAR 1979

SLP AND TEMP



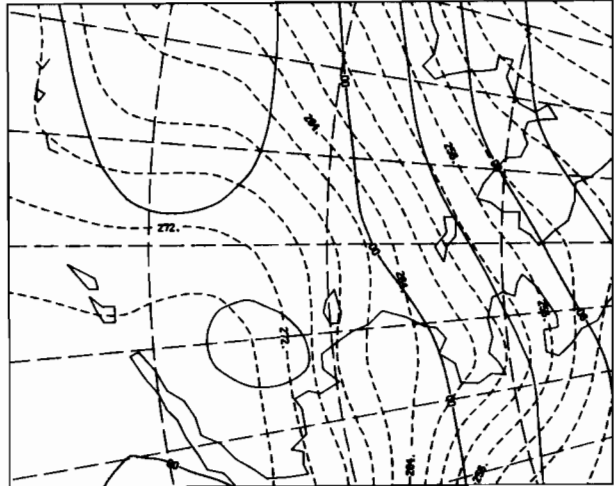
12Z 6 MAR 1979

SLP AND TEMP



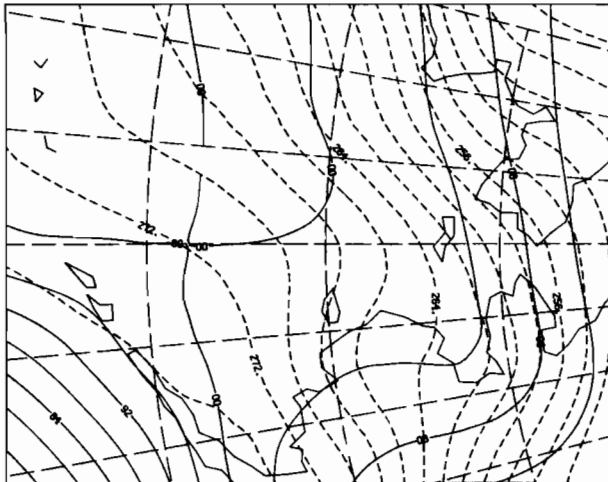
00Z 7 MAR 1979

SLP AND TEMP



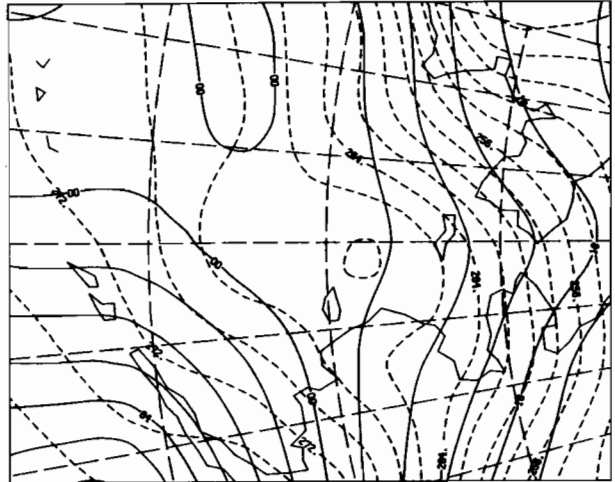
12Z 7 MAR 1979

SLP AND TEMP



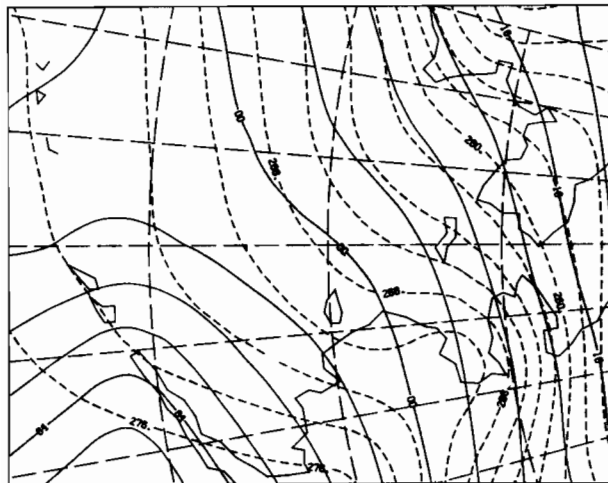
00Z 8 MAR 1979

SLP AND TEMP



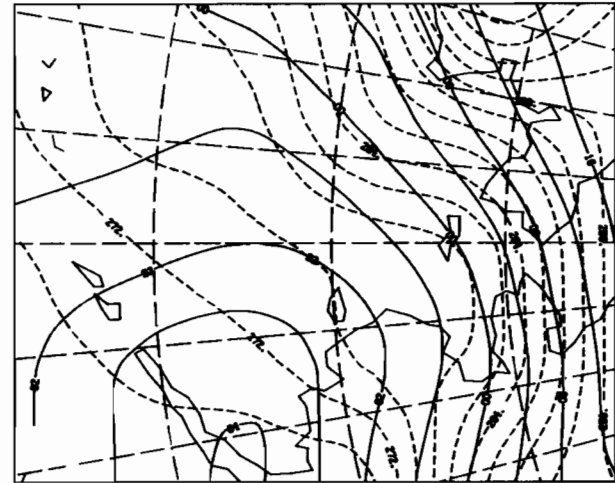
12Z 8 MAR 1979

SLP AND TEMP



00Z 9 MAR 1979

SLP AND TEMP



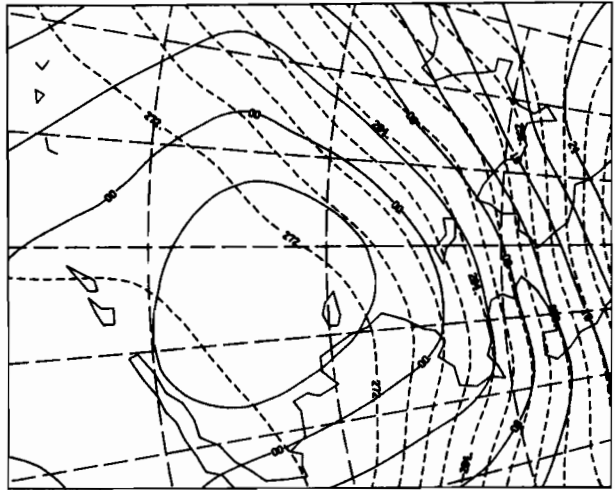
12Z 9 MAR 1979

SLP AND TEMP



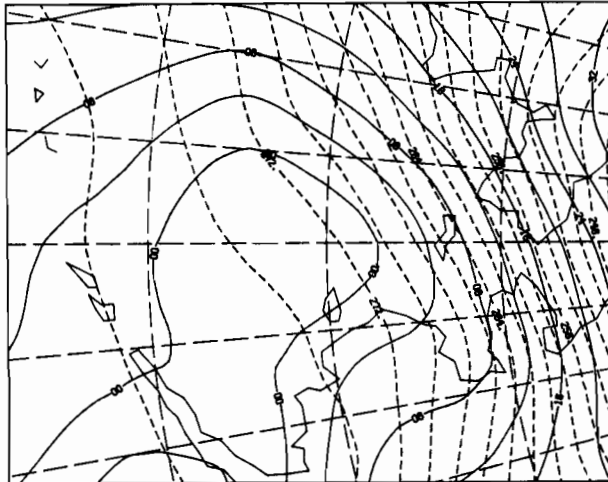
00Z 10 MAR 1979

SLP AND TEMP



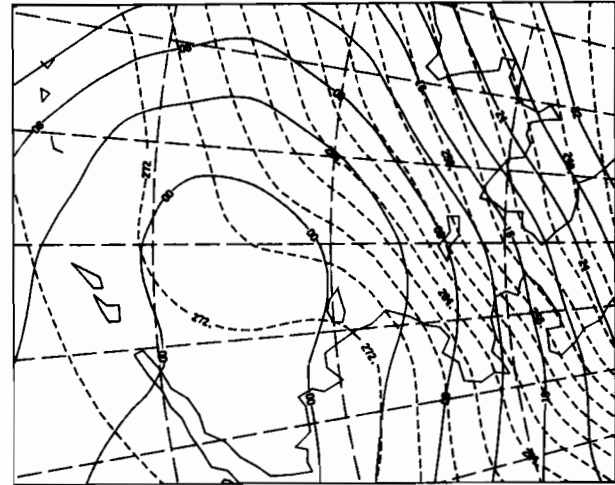
12Z 10 MAR 1979

SLP AND TEMP



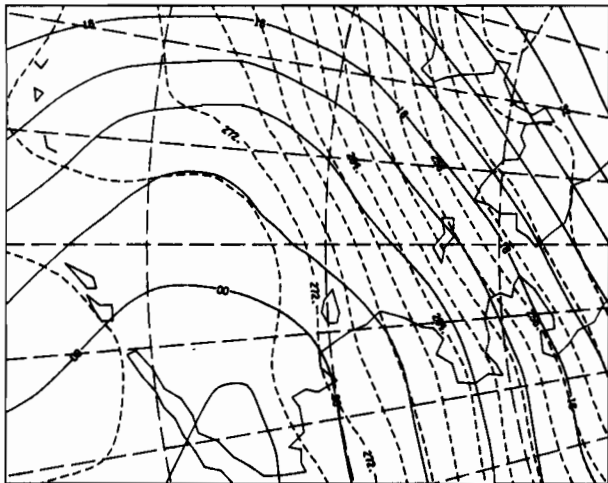
00Z 11 MAR 1979

SLP AND TEMP



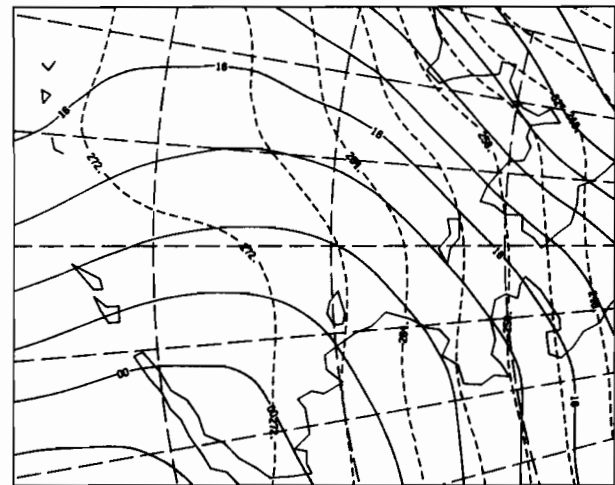
12Z 11 MAR 1979

SLP AND TEMP



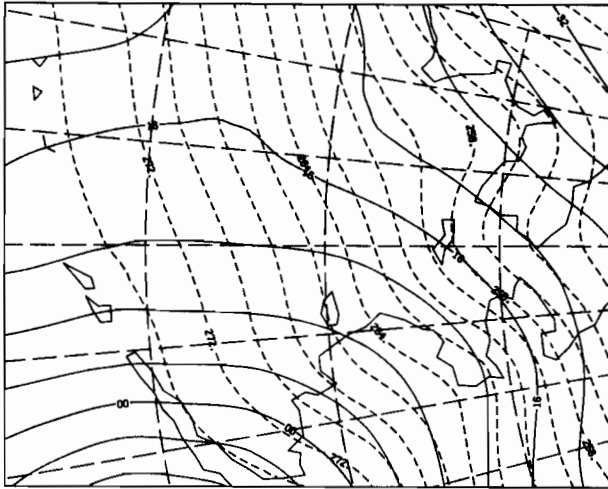
00Z 12 MAR 1979

SLP AND TEMP



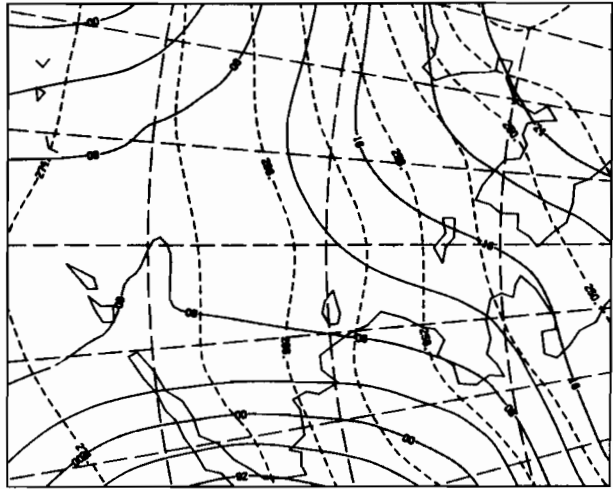
12Z 12 MAR 1979

SLP AND TEMP



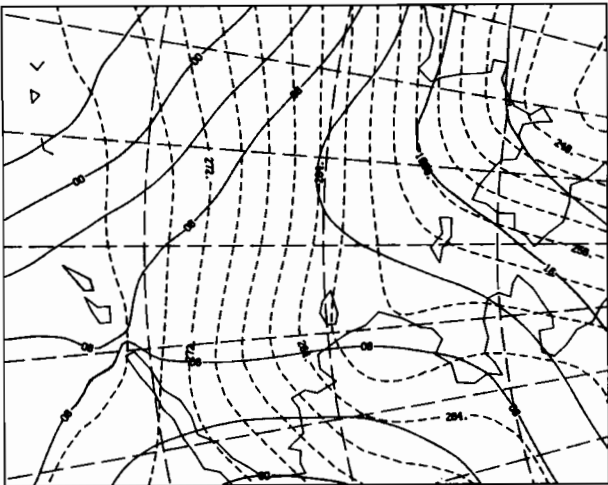
00Z 13 MAR 1979

SLP AND TEMP



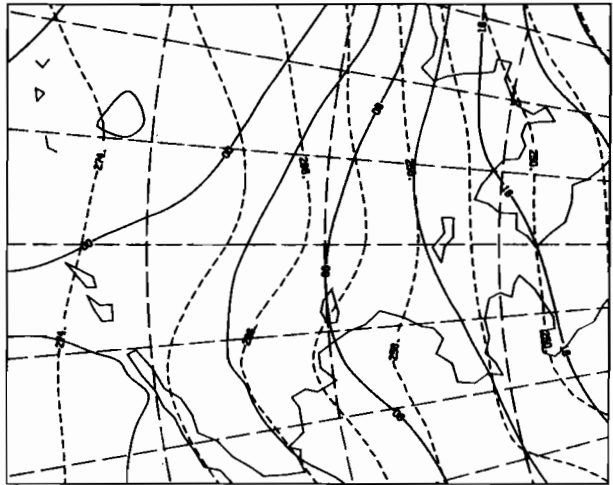
12Z 13 MAR 1979

SLP AND TEMP



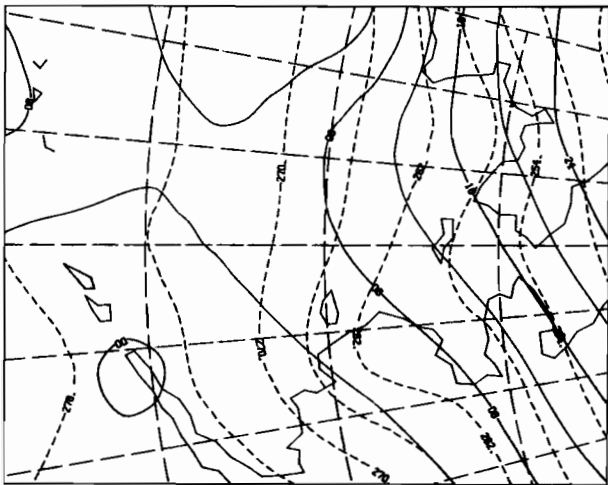
00Z 14 MAR 1979

SLP AND TEMP



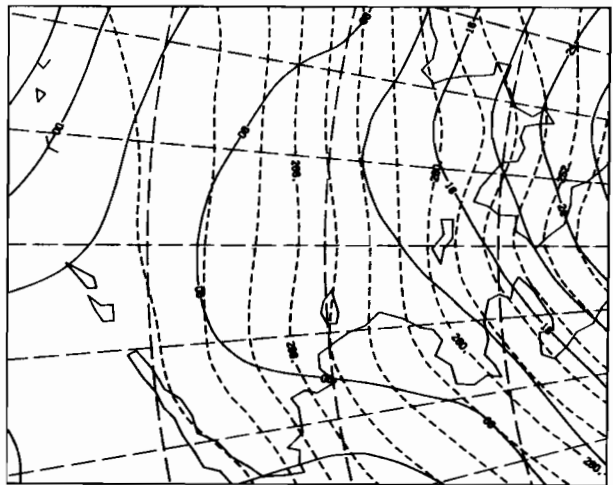
12Z 14 MAR 1979

SLP AND TEMP



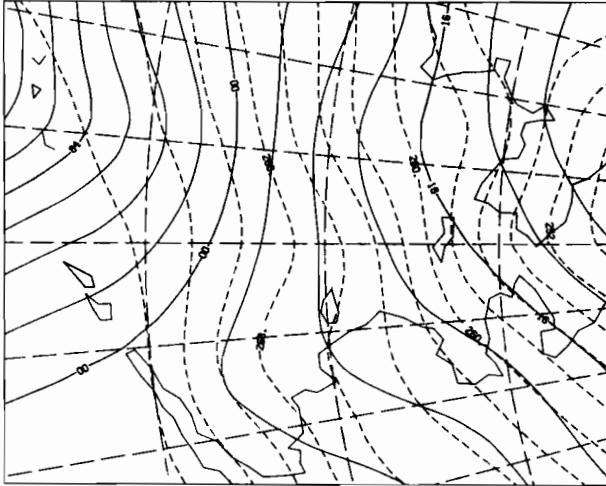
00Z 15 MAR 1979

SLP AND TEMP



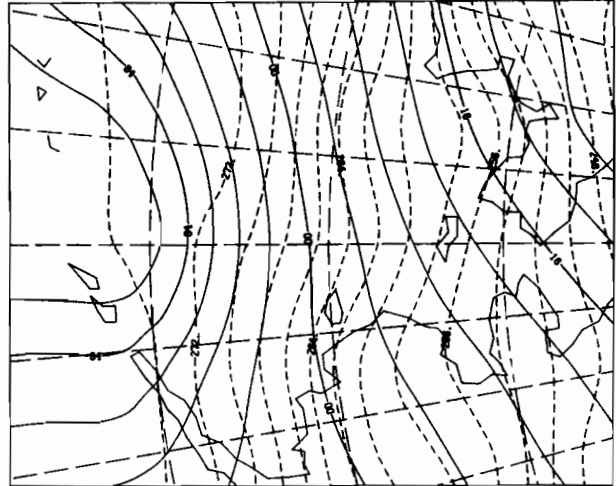
12Z 15 MAR 1979

SLP AND TEMP



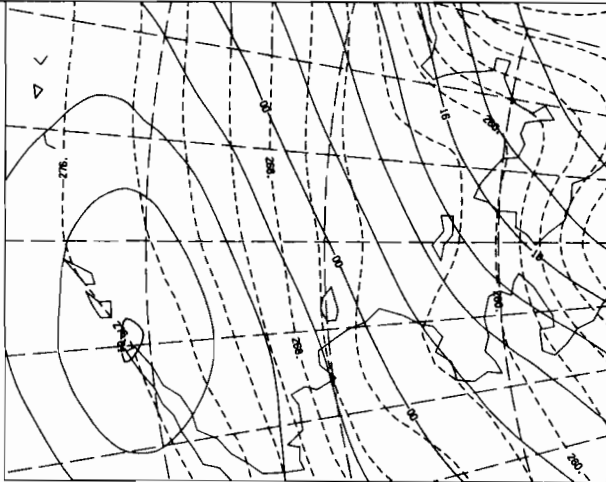
00Z 16 MAR 1979

SLP AND TEMP



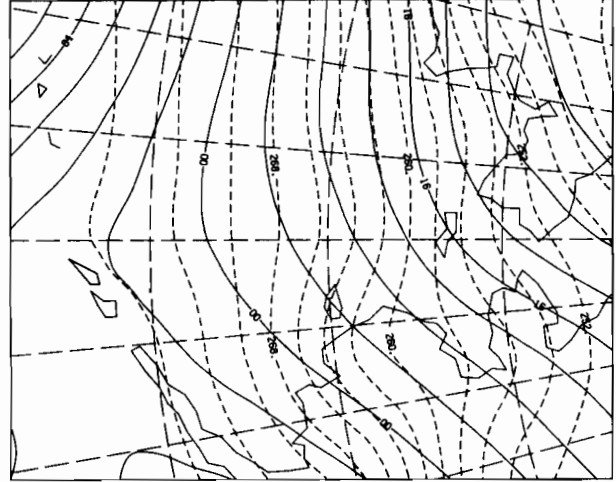
12Z 16 MAR 1979

SLP AND TEMP



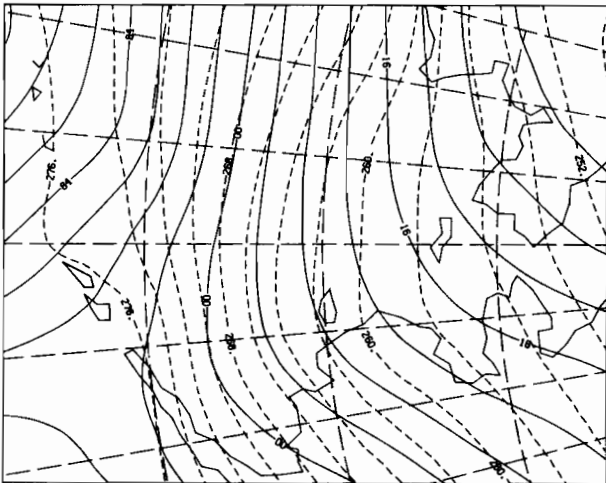
00Z 17 MAR 1979

SLP AND TEMP



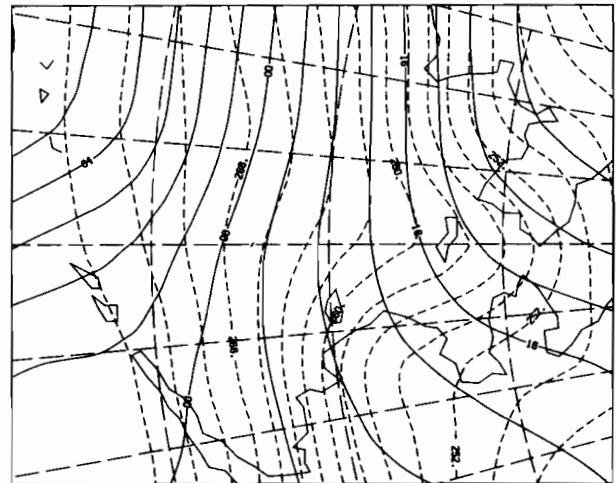
12Z 17 MAR 1979

SLP AND TEMP



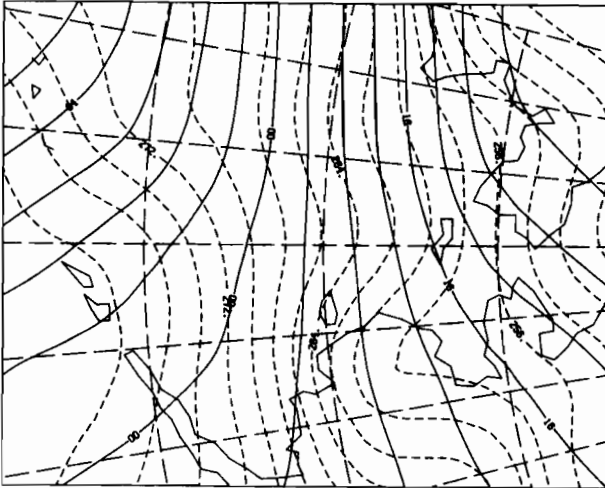
00Z 18 MAR 1979

SLP AND TEMP



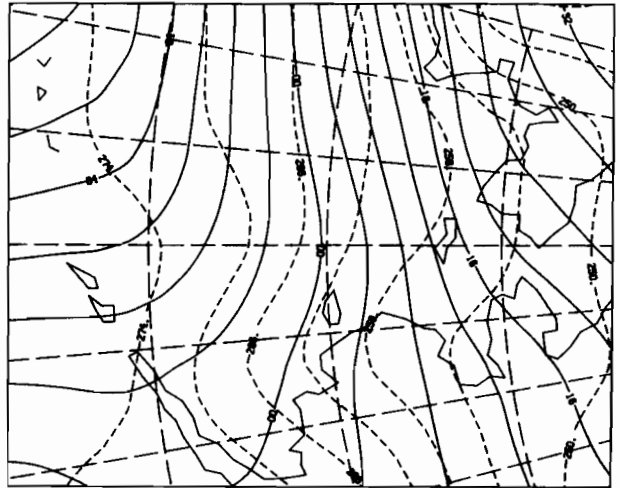
12Z 18 MAR 1979

SLP AND TEMP



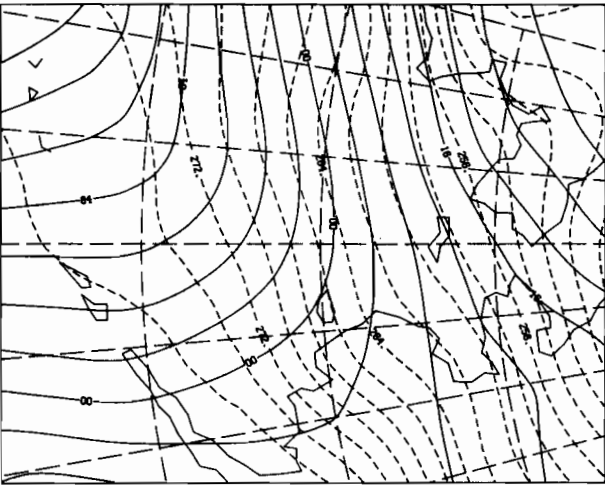
00Z 19 MAR 1979

SLP AND TEMP



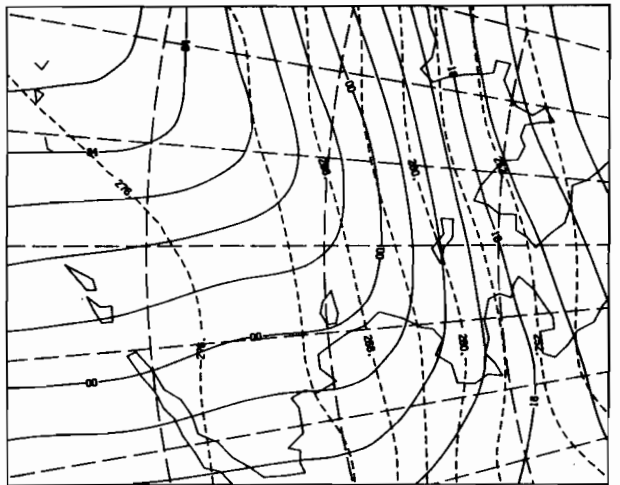
12Z 19 MAR 1979

SLP AND TEMP



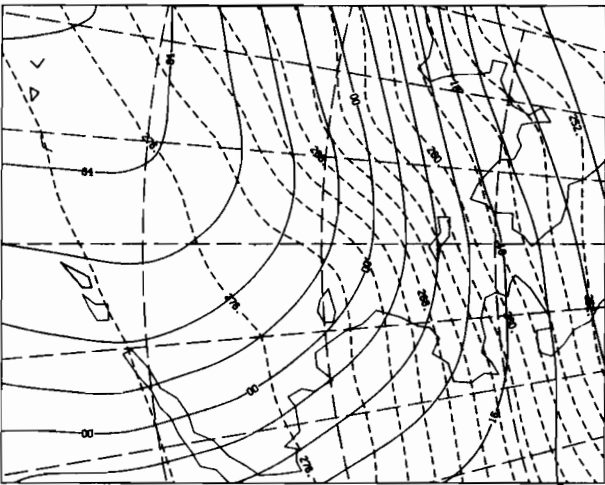
00Z 20 MAR 1979

SLP AND TEMP



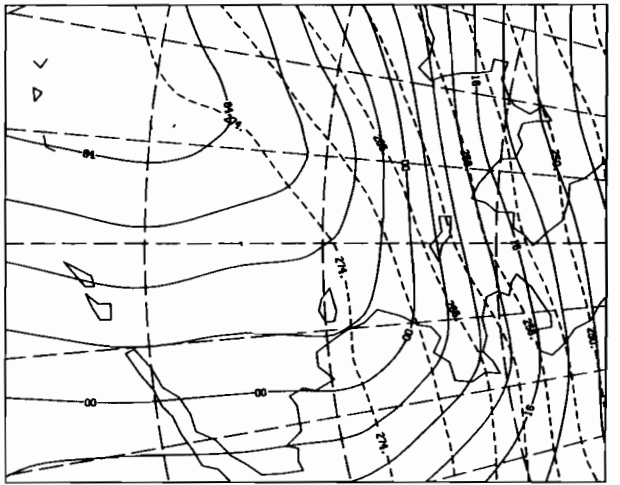
12Z 20 MAR 1979

SLP AND TEMP



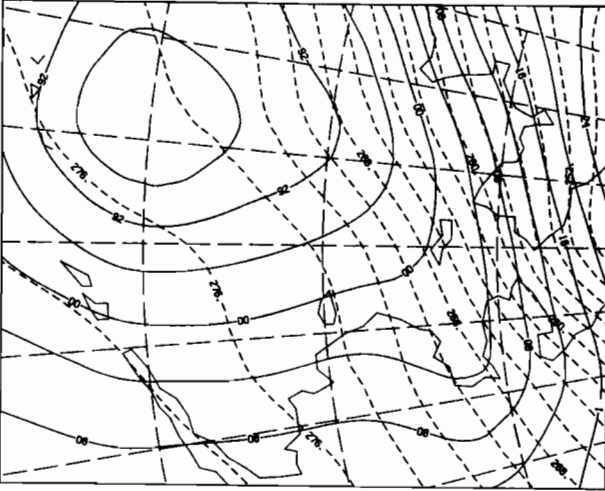
00Z 21 MAR 1979

SLP AND TEMP



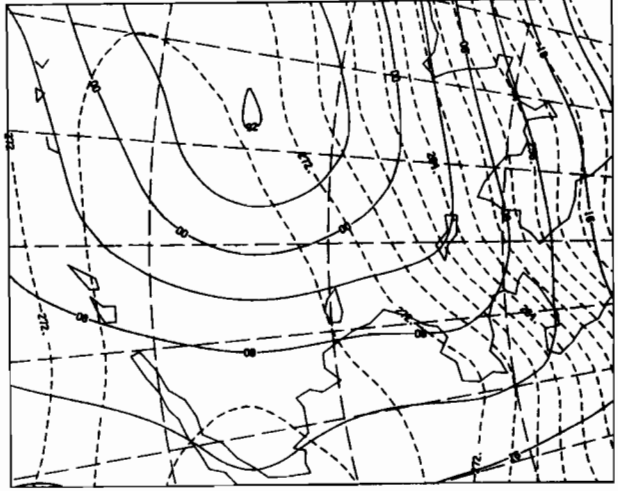
12Z 21 MAR 1979

SLP AND TEMP



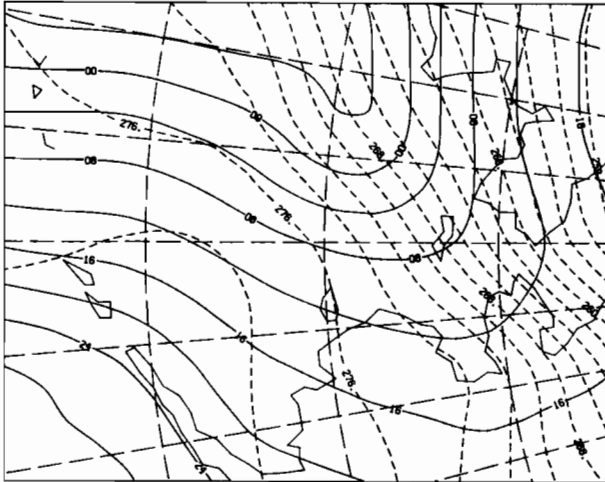
00Z 22 MAR 1979

SLP AND TEMP



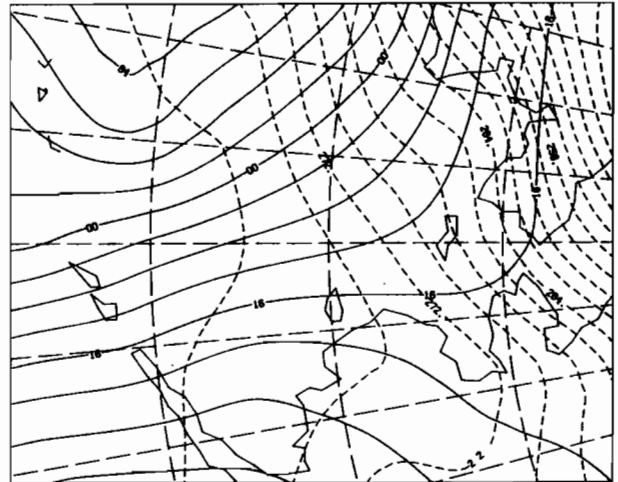
12Z 22 MAR 1979

SLP AND TEMP



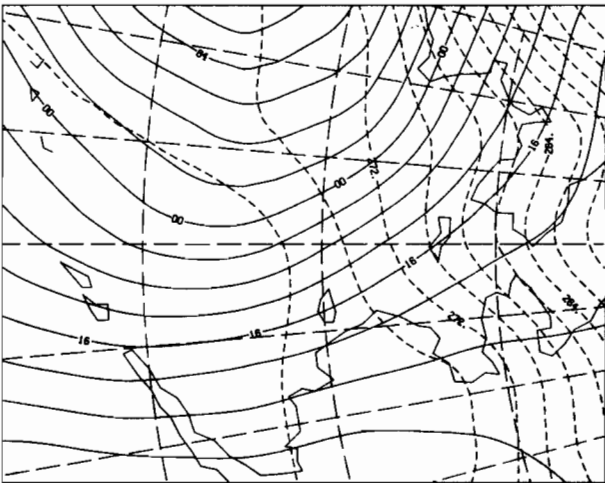
00Z 23 MAR 1979

SLP AND TEMP



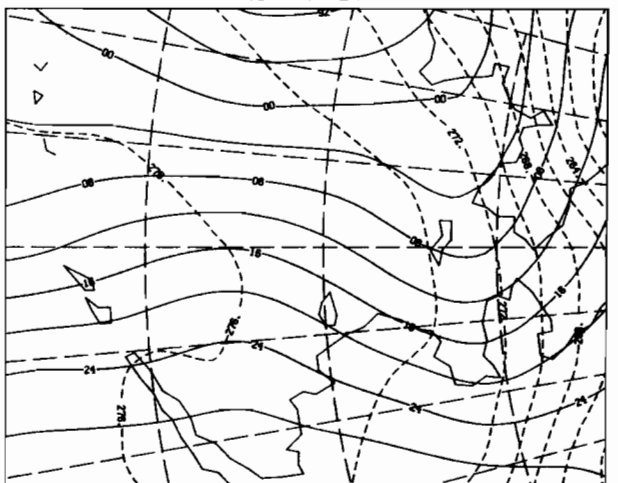
12Z 23 MAR 1979

SLP AND TEMP



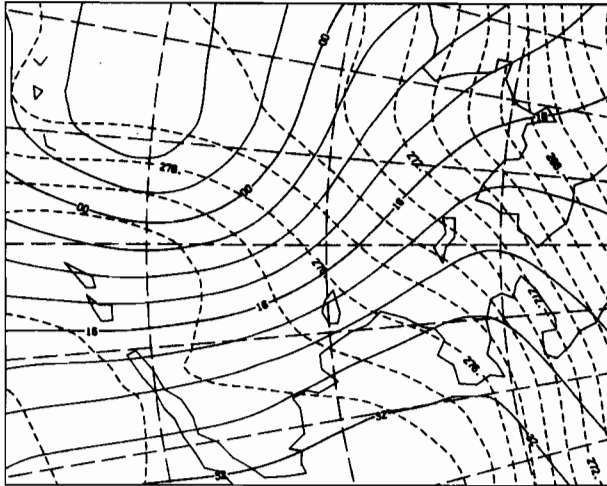
00Z 24 MAR 1979

SLP AND TEMP



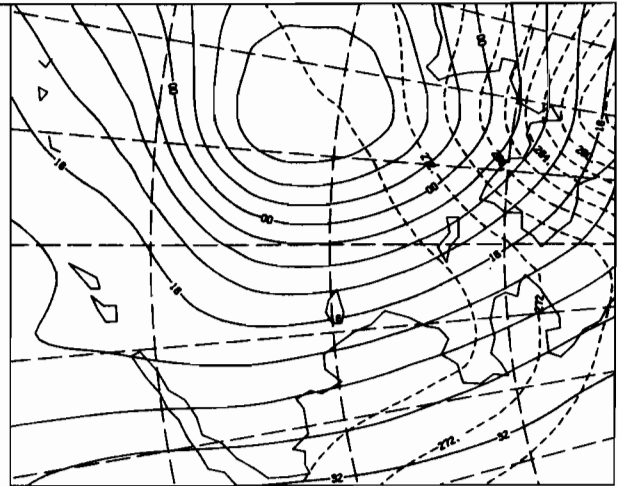
12Z 24 MAR 1979

SLP AND TEMP



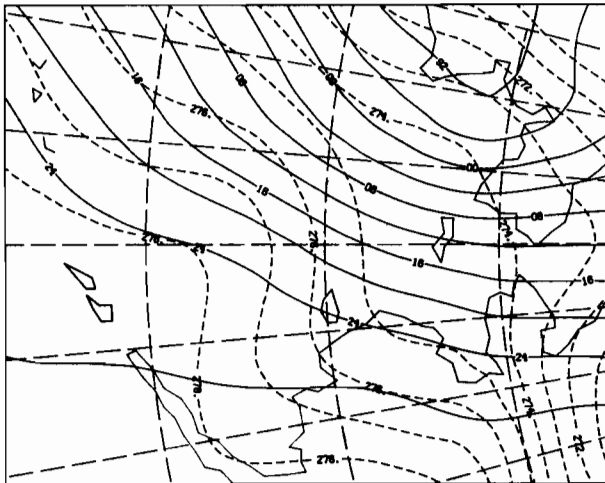
00Z 25 MAR .979

SLP AND TEMP



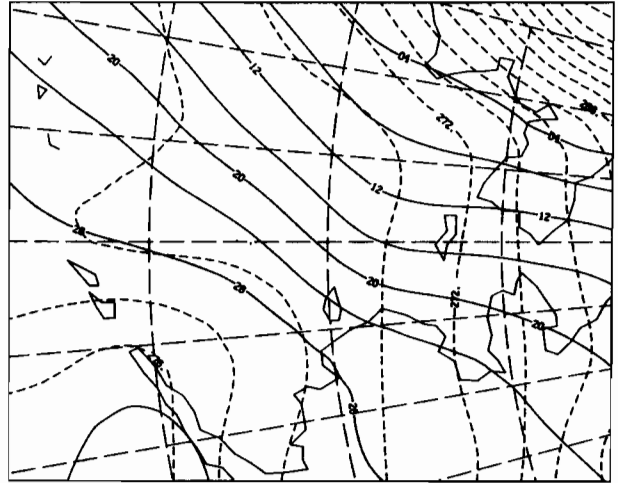
12Z 25 MAR 1979

SLP AND TEMP



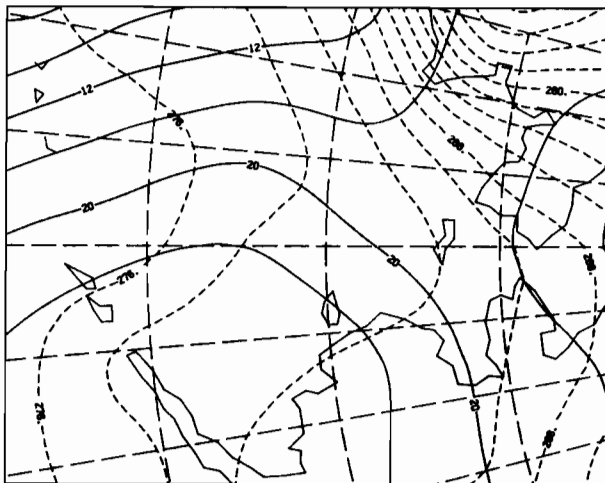
00Z 26 MAR 1979

SLP AND TEMP



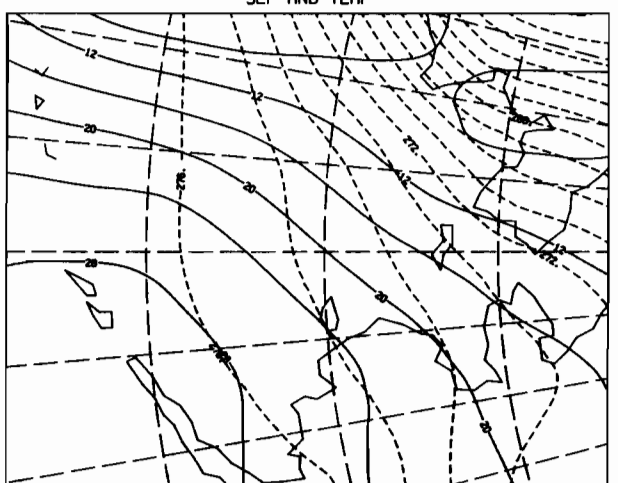
12Z 26 MAR 1979

SLP AND TEMP



12Z 27 MAR 1979

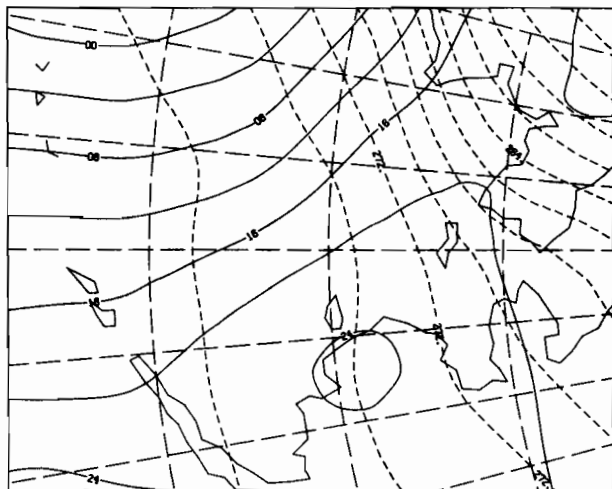
SLP AND TEMP



00Z 27 MAR 1979

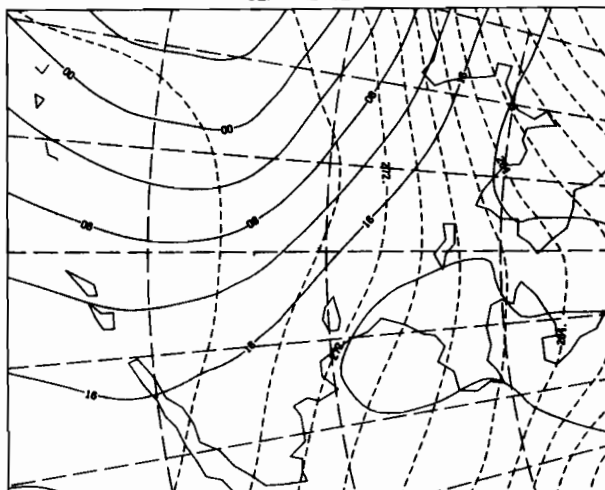


SLP AND TEMP



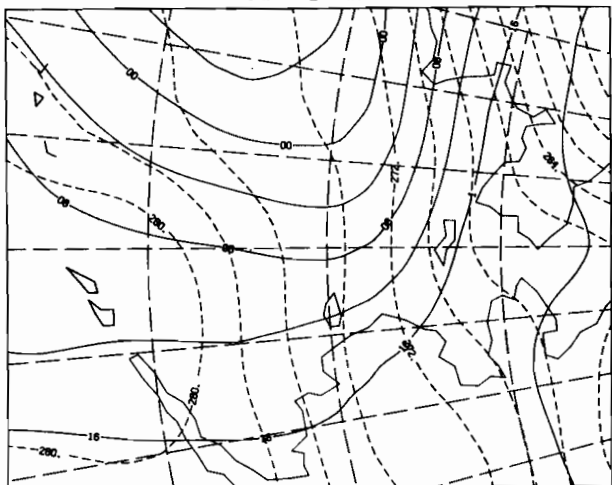
00Z 28 MAR 1979

SLP AND TEMP



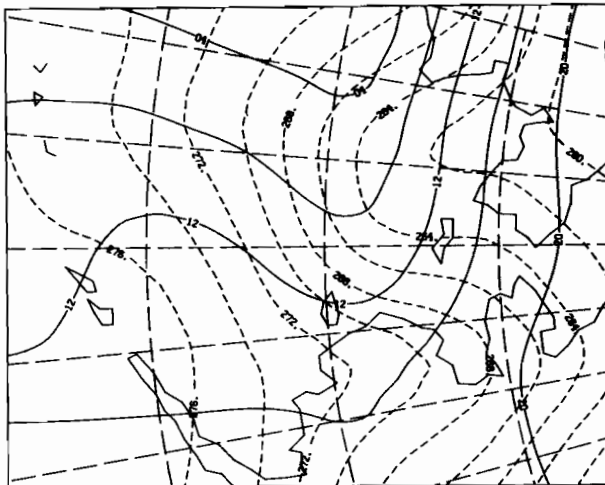
12Z 28 MAR 1979

SLP AND TEMP



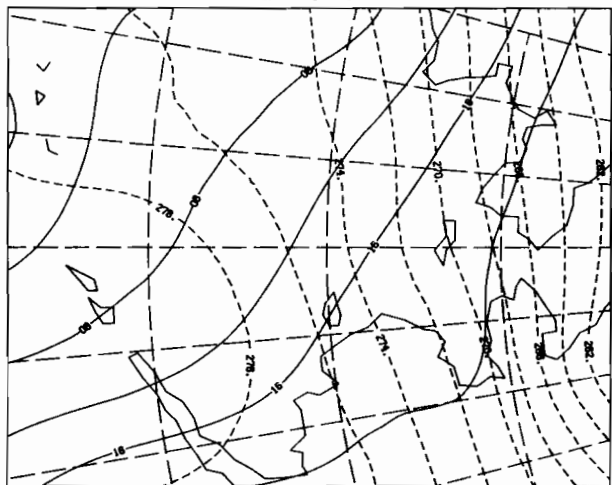
00Z 29 MAR 1979

SLP AND TEMP



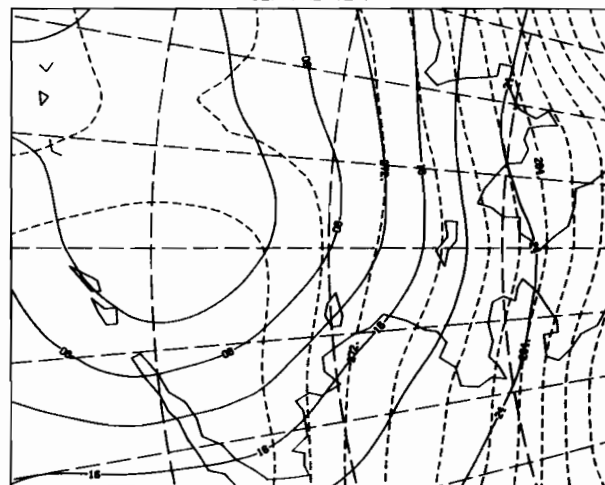
12Z 29 MAR 1979

SLP AND TEMP



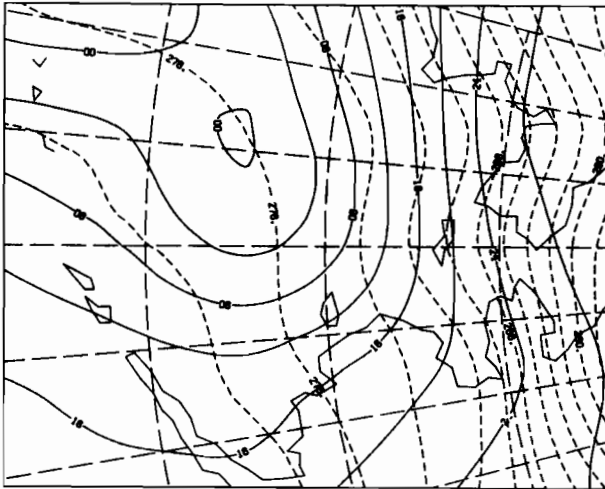
00Z 30 MAR 1979

SLP AND TEMP



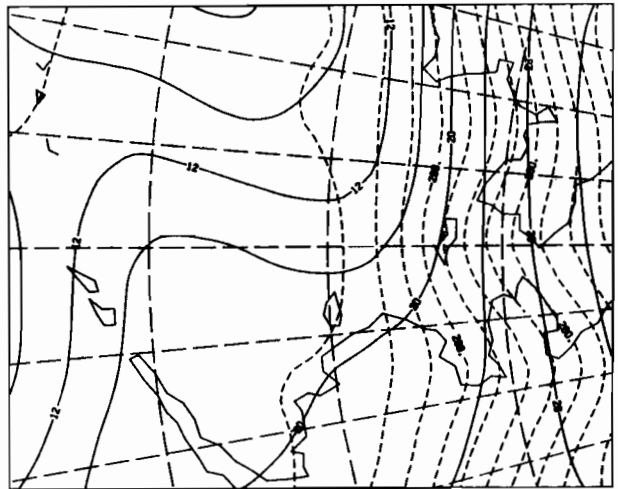
12Z 30 MAR 1979

SLP AND TEMP



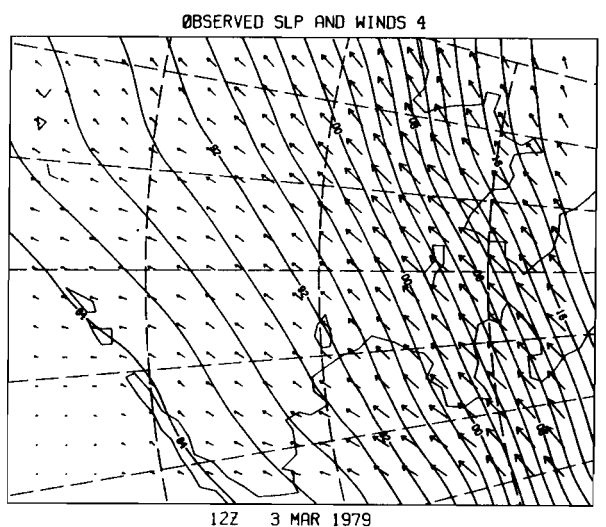
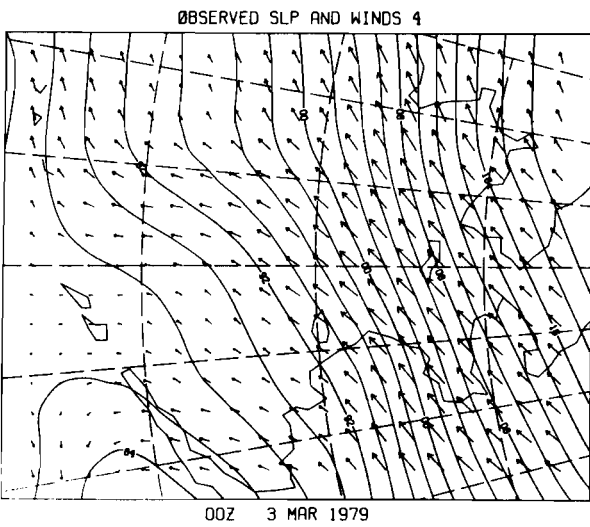
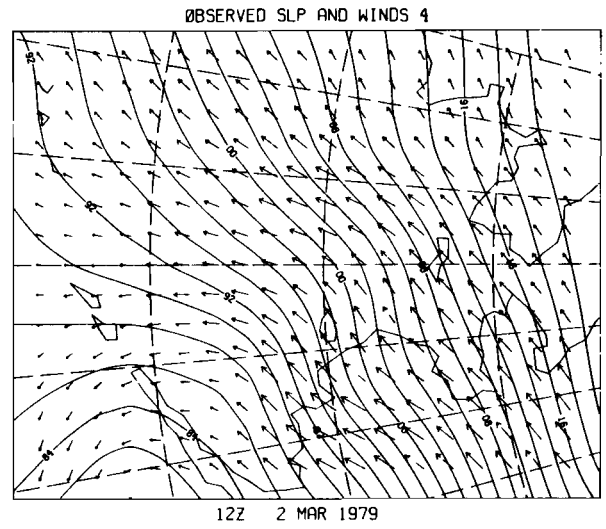
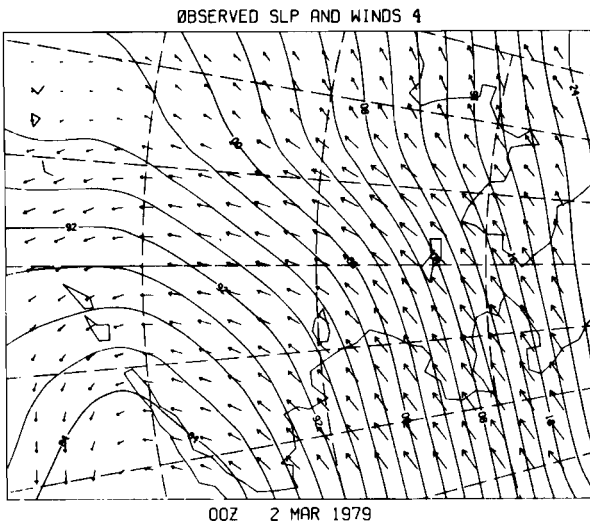
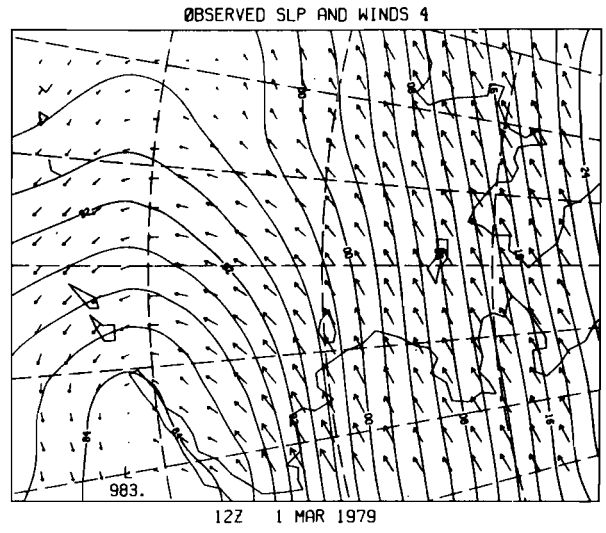
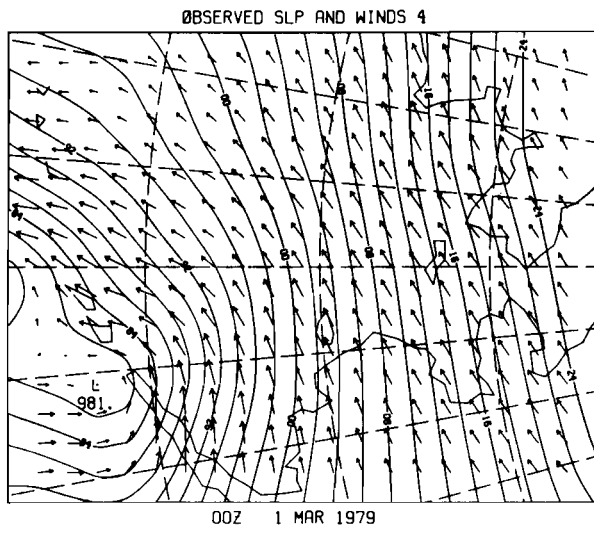
00Z 31 MAR 1979

SLP AND TEMP

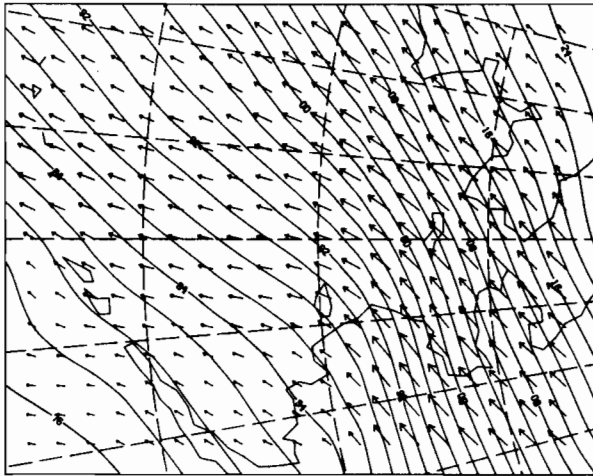


12Z 31 MAR 1979

APPENDIX C: SURFACE WINDS DERIVED FROM THE WSFO SURFACE ANALYSES.

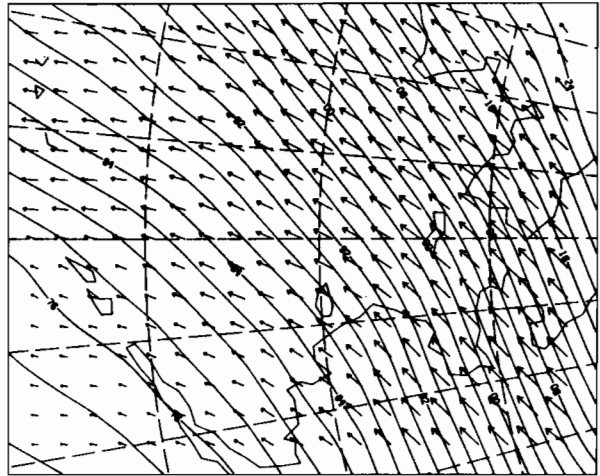


ØBSERVED SLP AND WINDS 4



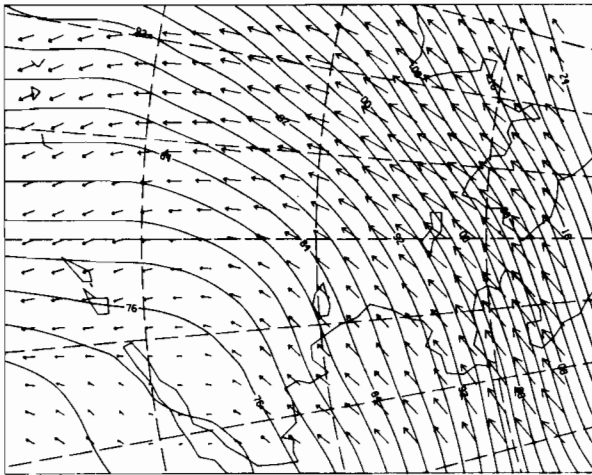
00Z 4 MAR 1979

ØBSERVED SLP AND WINDS 4



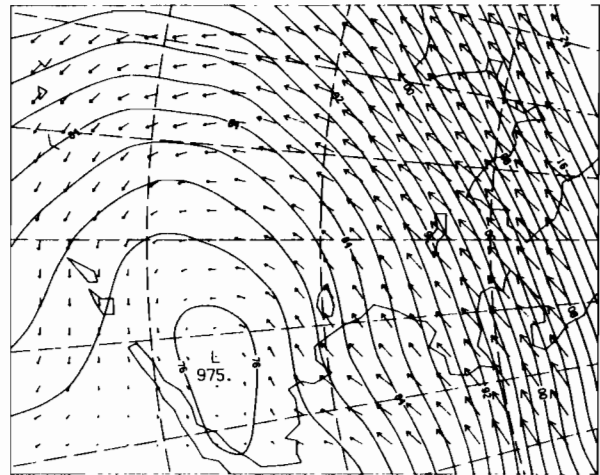
12Z 4 MAR 1979

ØBSERVED SLP AND WINDS 4



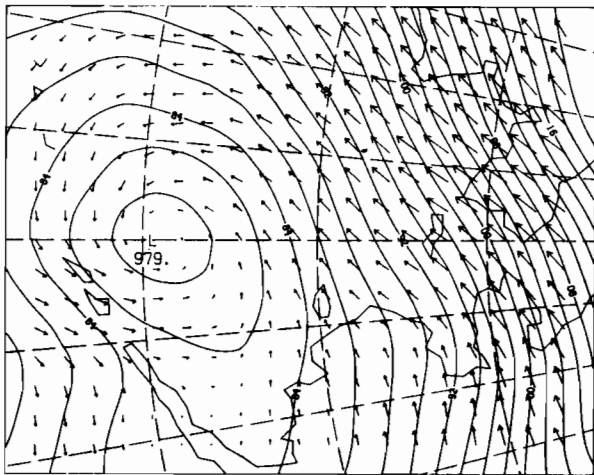
00Z 5 MAR 1979

ØBSERVED SLP AND WINDS 4



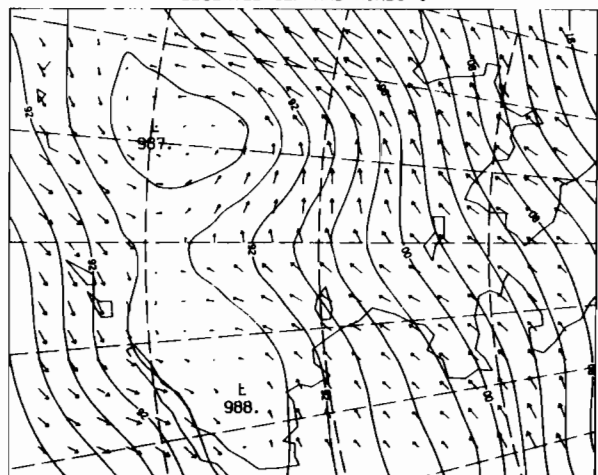
12Z 5 MAR 1979

ØBSERVED SLP AND WINDS 4



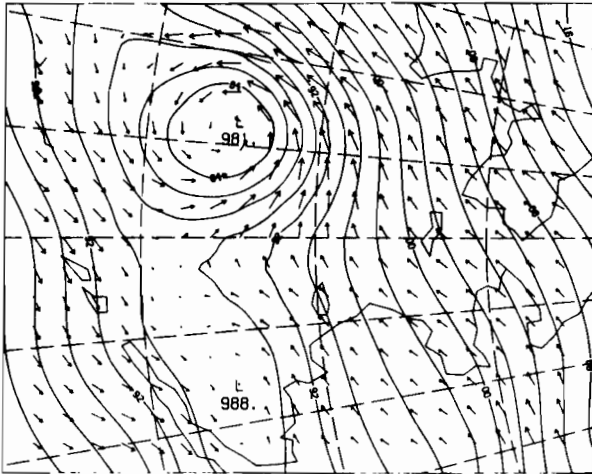
00Z 6 MAR 1979

ØBSERVED SLP AND WINDS 4



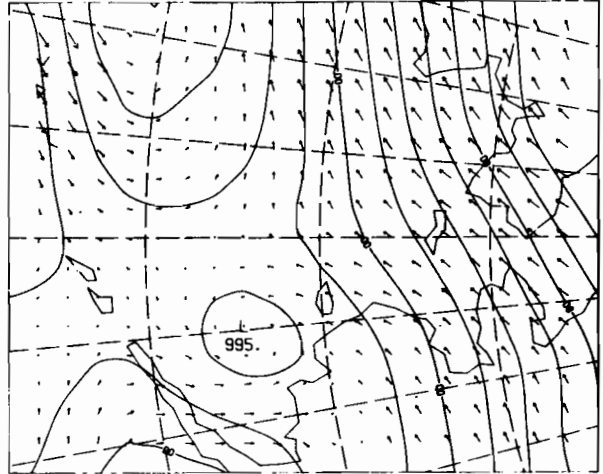
12Z 6 MAR 1979

ØBSERVED SLP AND WINDS 4



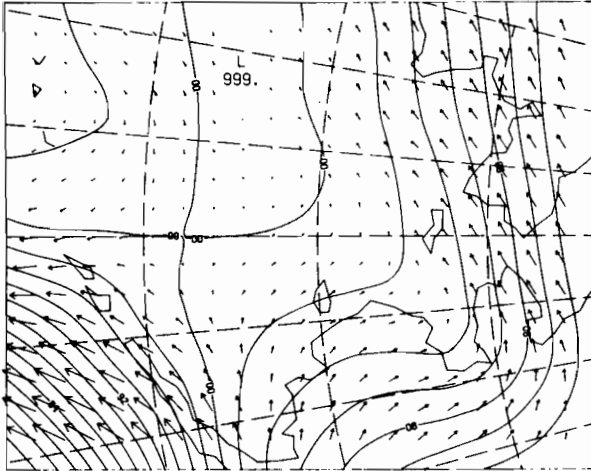
00Z 7 MAR 1979

ØBSERVED SLP AND WINDS 4



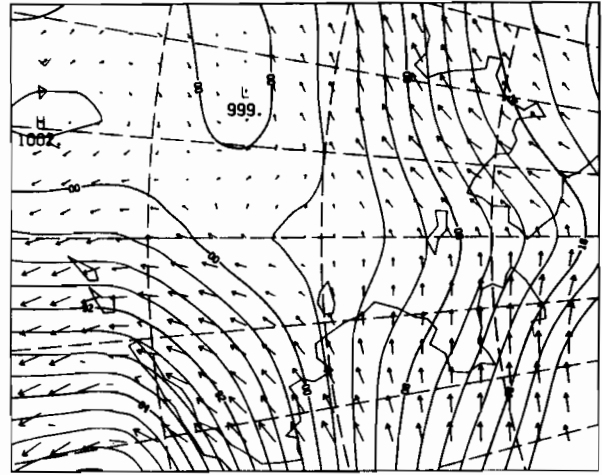
12Z 7 MAR 1979

ØBSERVED SLP AND WINDS 4



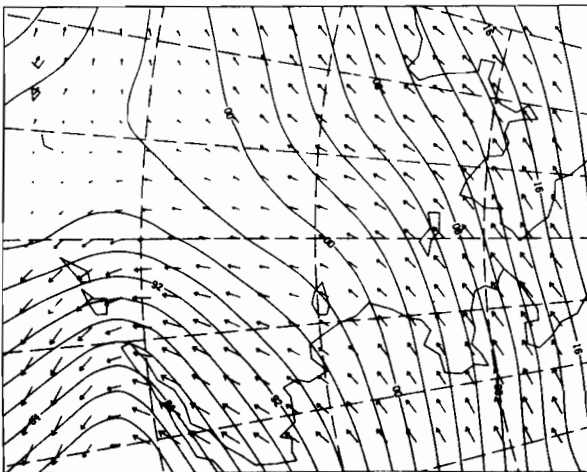
00Z 8 MAR 1979

ØBSERVED SLP AND WINDS 4



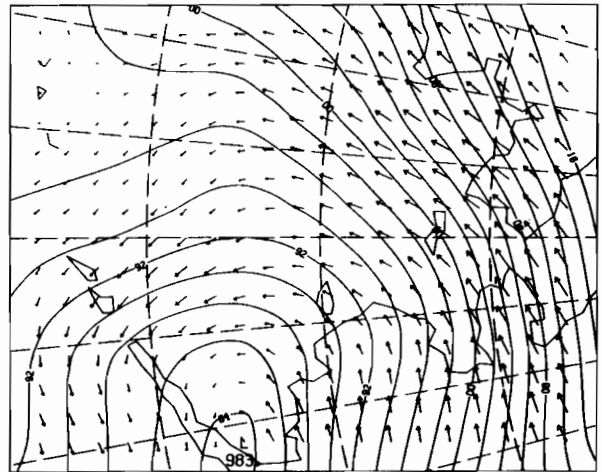
12Z 8 MAR 1979

ØBSERVED SLP AND WINDS 4



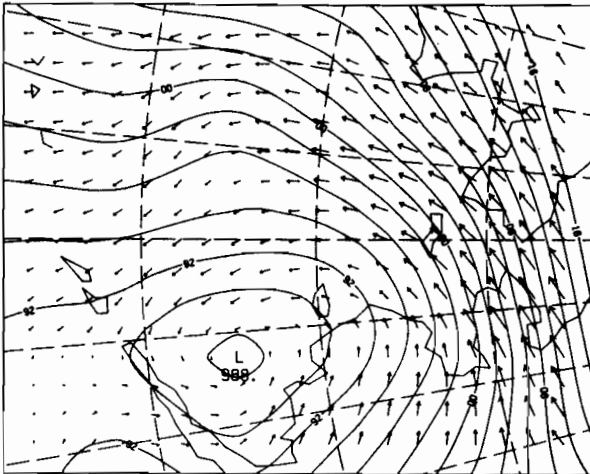
00Z 9 MAR 1979

ØBSERVED SLP AND WINDS 4



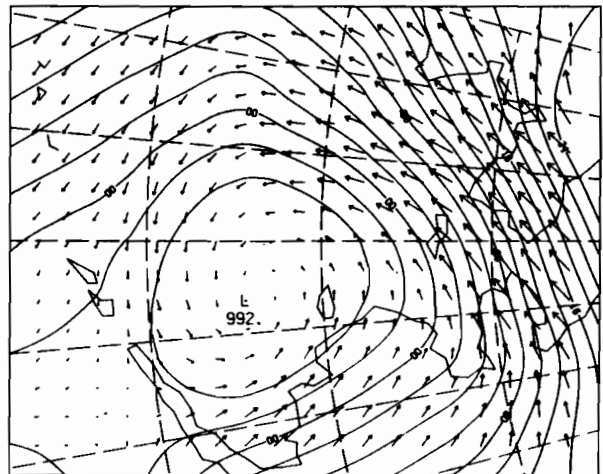
12Z 9 MAR 1979

ØBSERVED SLP AND WINDS 4



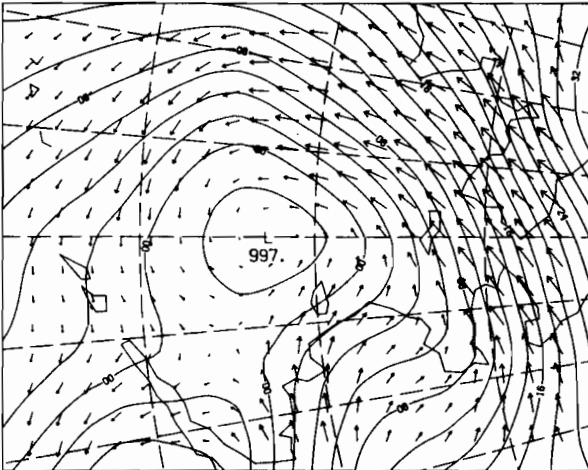
00Z 10 MAR 1979

ØBSERVED SLP AND WINDS 4



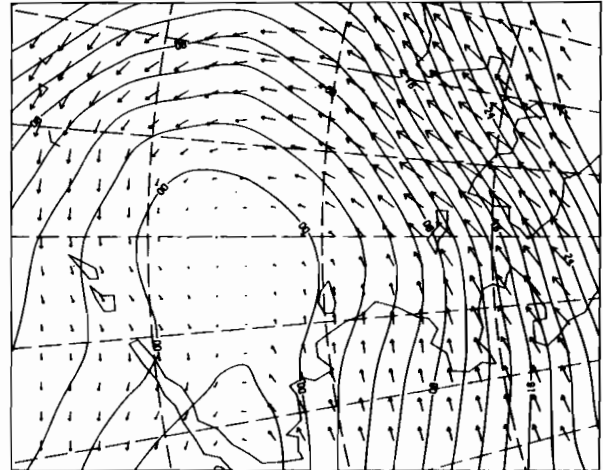
12Z 10 MAR 1979

ØBSERVED SLP AND WINDS 4



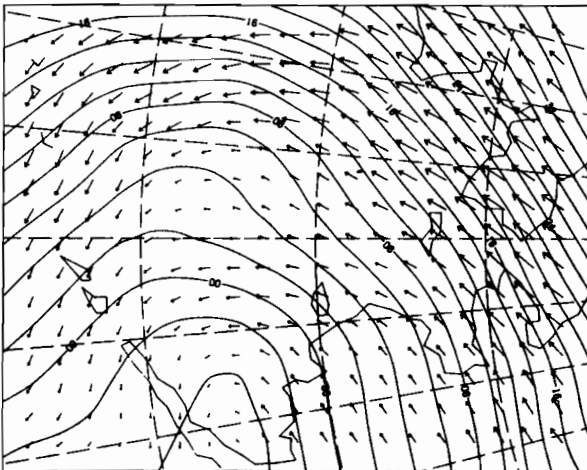
00Z 11 MAR 1979

ØBSERVED SLP AND WINDS 4



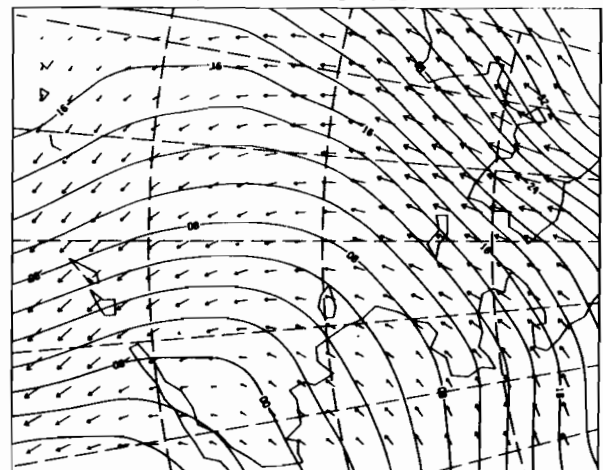
12Z 11 MAR 1979

ØBSERVED SLP AND WINDS 4



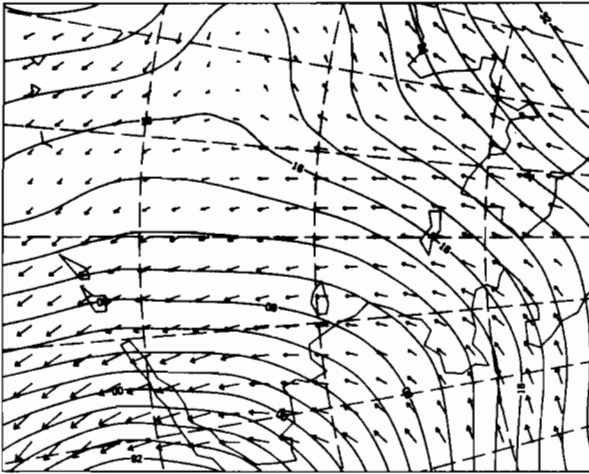
00Z 12 MAR 1979

ØBSERVED SLP AND WINDS 4



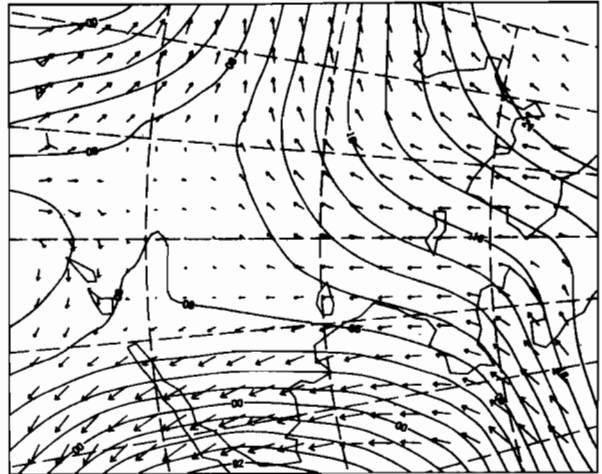
12Z 12 MAR 1979

ØBSERVED SLP AND WINDS 4



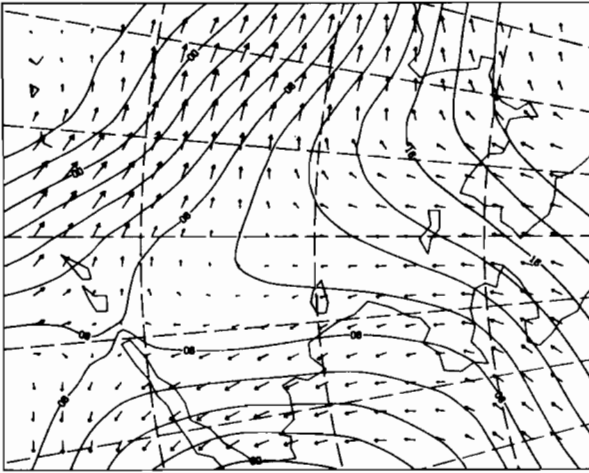
00Z 13 MAR 1979

ØBSERVED SLP AND WINDS 4



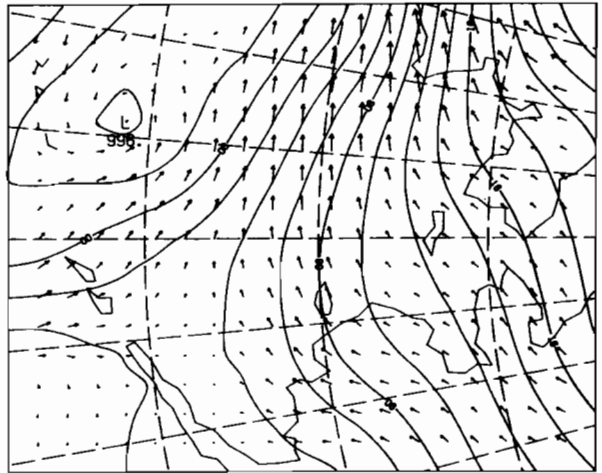
12Z 13 MAR 1979

ØBSERVED SLP AND WINDS 4



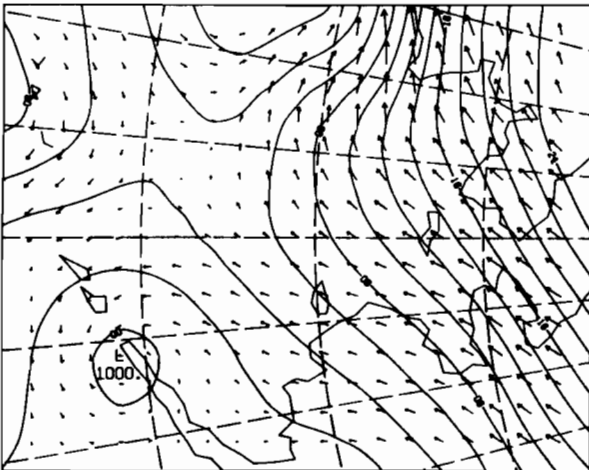
00Z 14 MAR 1979

ØBSERVED SLP AND WINDS 4



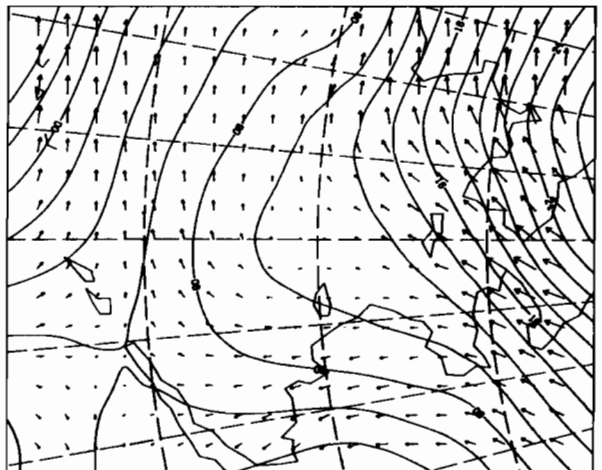
12Z 14 MAR 1979

ØBSERVED SLP AND WINDS 4



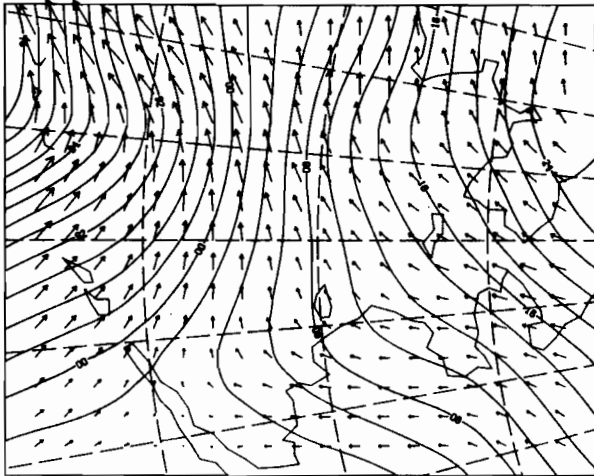
00Z 15 MAR 1979

ØBSERVED SLP AND WINDS 4



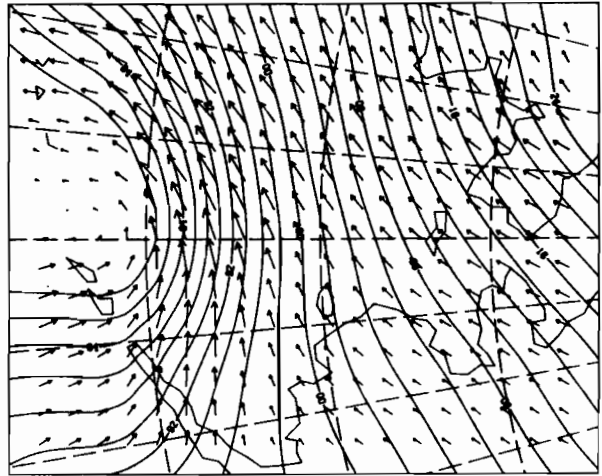
12Z 15 MAR 1979

OBSERVED SLP AND WINDS 4



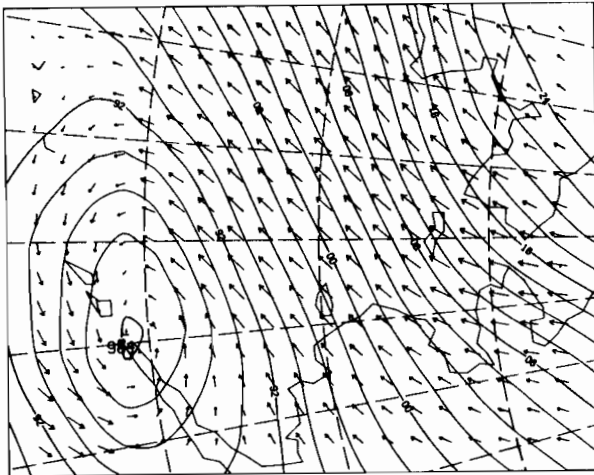
00Z 16 MAR 1979

OBSERVED SLP AND WINDS 4



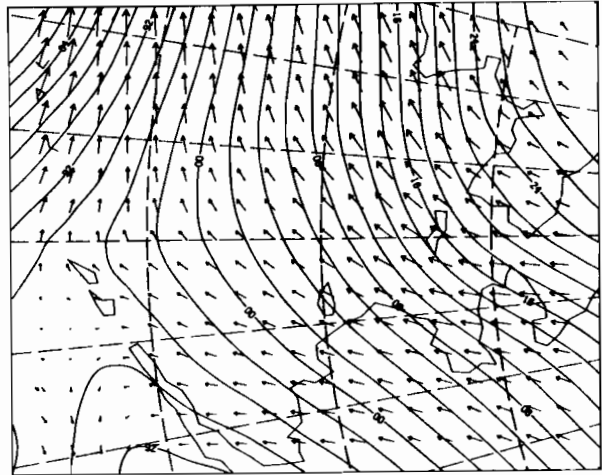
12Z 16 MAR 1979

OBSERVED SLP AND WINDS 4



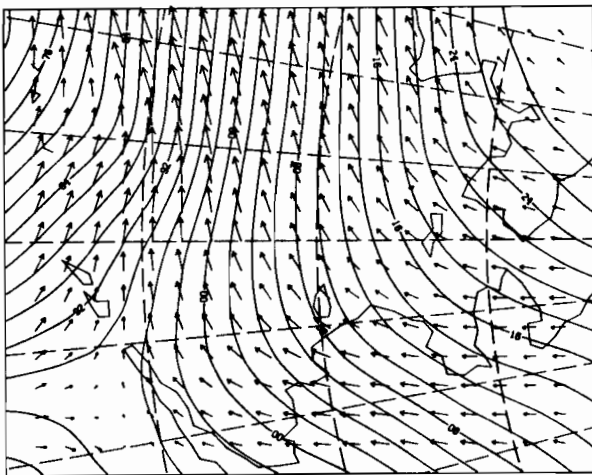
00Z 17 MAR 1979

OBSERVED SLP AND WINDS 4



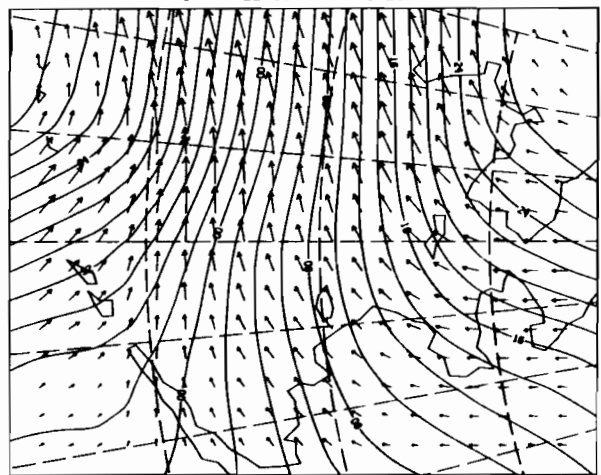
12Z 17 MAR 1979

OBSERVED SLP AND WINDS 4



00Z 18 MAR 1979

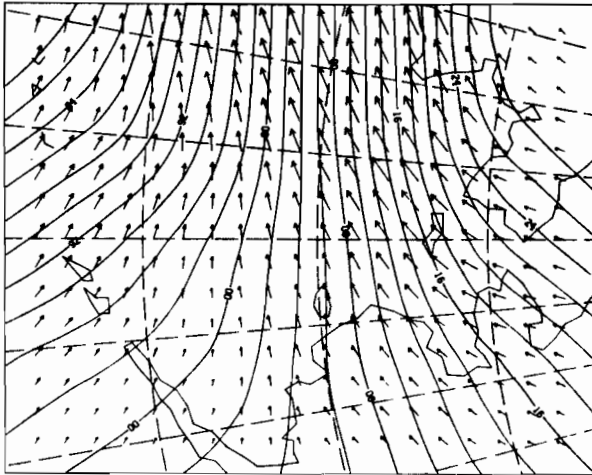
OBSERVED SLP AND WINDS 4



12Z 18 MAR 1979

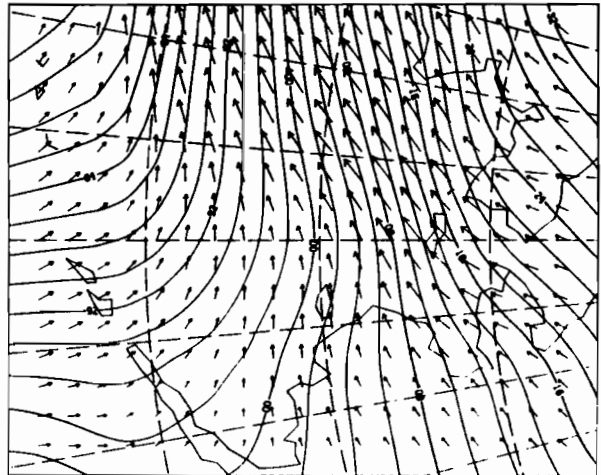


ØBSERVED SLP AND WINDS 4



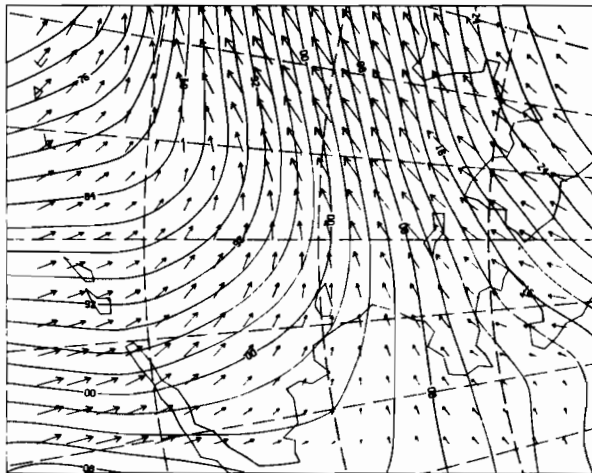
00Z 19 MAR 1979

ØBSERVED SLP AND WINDS 4



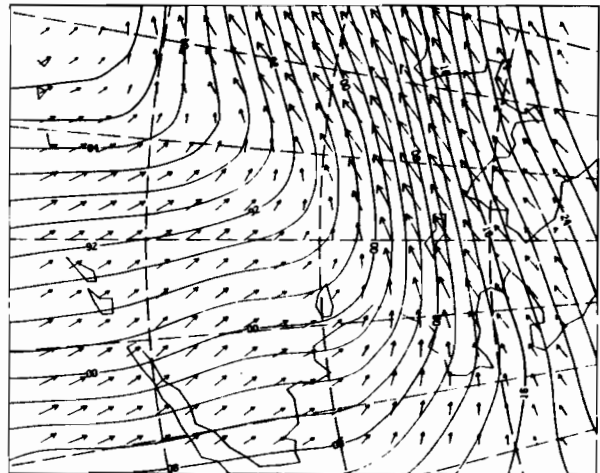
12Z 19 MAR 1979

ØBSERVED SLP AND WINDS 4



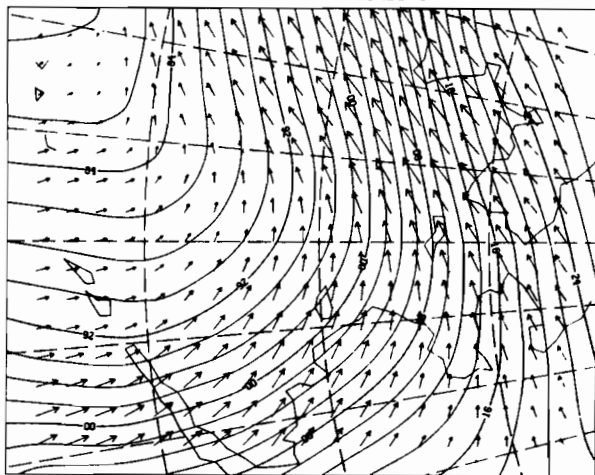
00Z 20 MAR 1979

ØBSERVED SLP AND WINDS 4



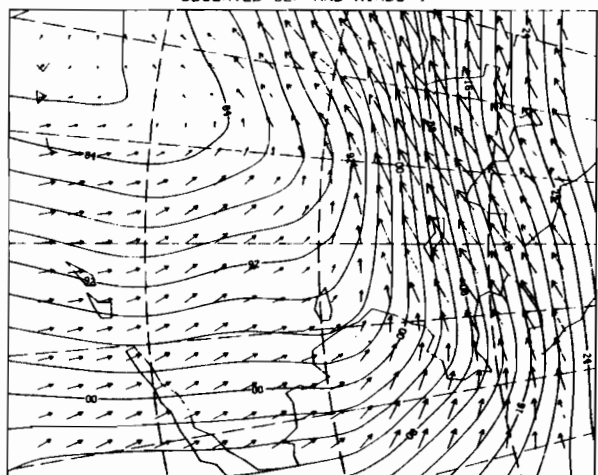
12Z 20 MAR 1979

ØBSERVED SLP AND WINDS 4



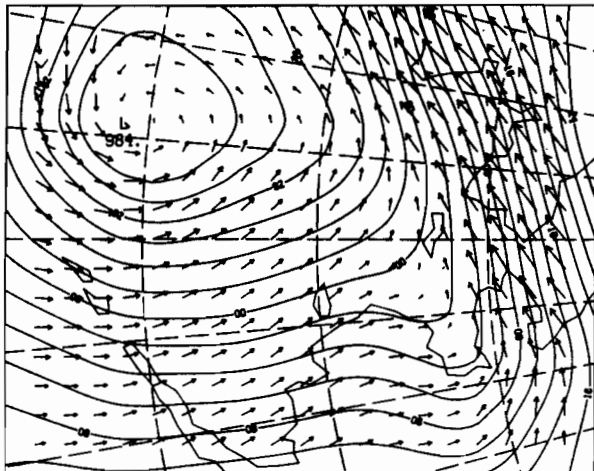
00Z 21 MAR 1979

ØBSERVED SLP AND WINDS 4



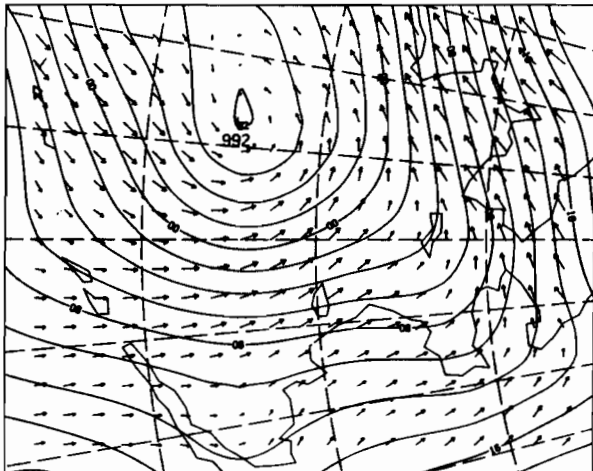
12Z 21 MAR 1979

OBSERVED SLP AND WINDS 4



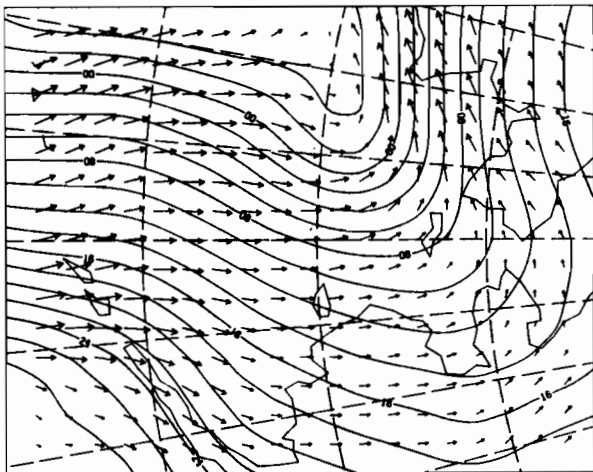
00Z 22 MAR 1979

OBSERVED SLP AND WINDS 4



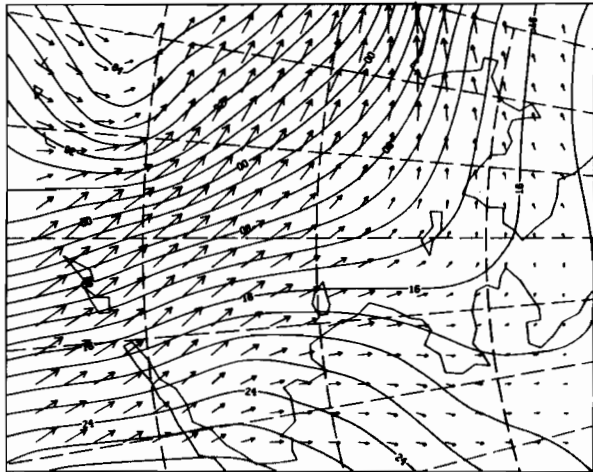
12Z 22 MAR 1979

OBSERVED SLP AND WINDS 4



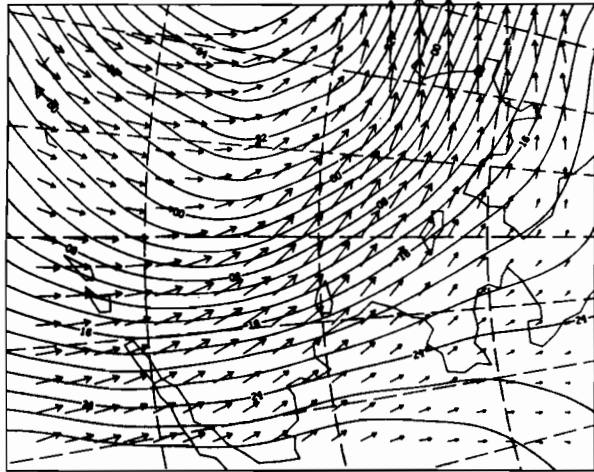
00Z 23 MAR 1979

OBSERVED SLP AND WINDS 4



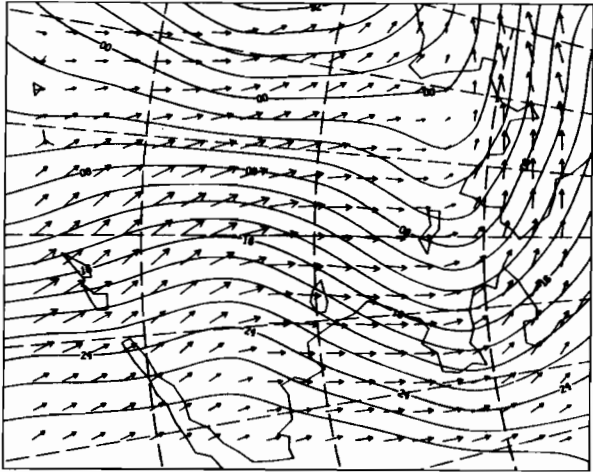
12Z 23 MAR 1979

OBSERVED SLP AND WINDS 4



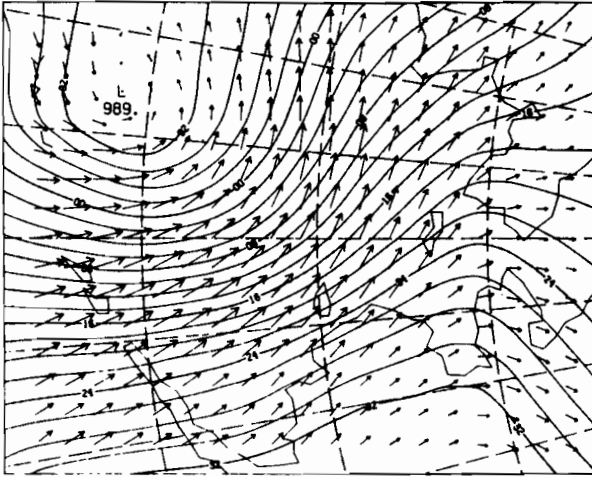
00Z 24 MAR 1979

OBSERVED SLP AND WINDS 4



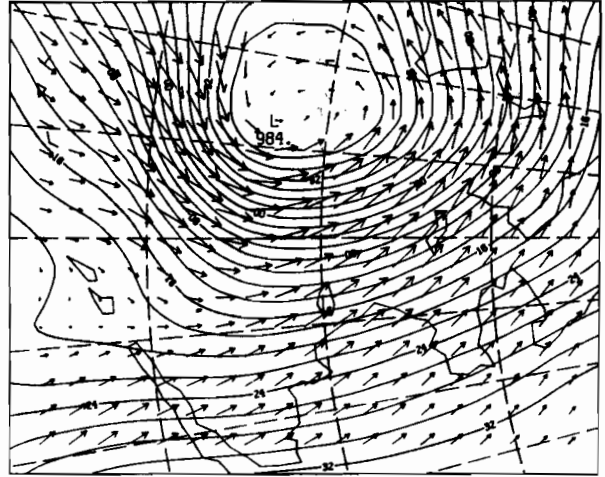
12Z 24 MAR 1979

ØBSERVED SLP AND WINDS 4



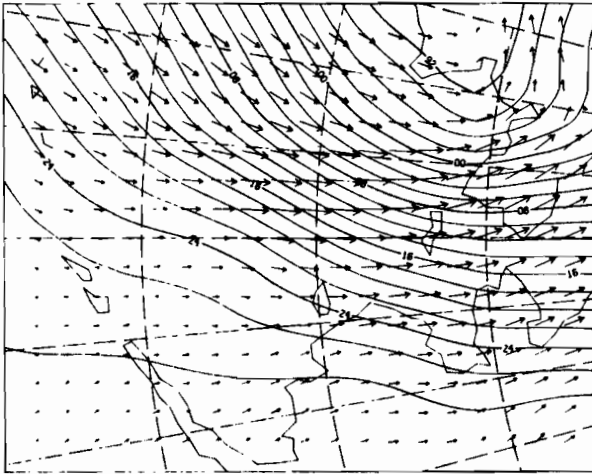
00Z 25 MAR 1979

ØBSERVED SLP AND WINDS 4



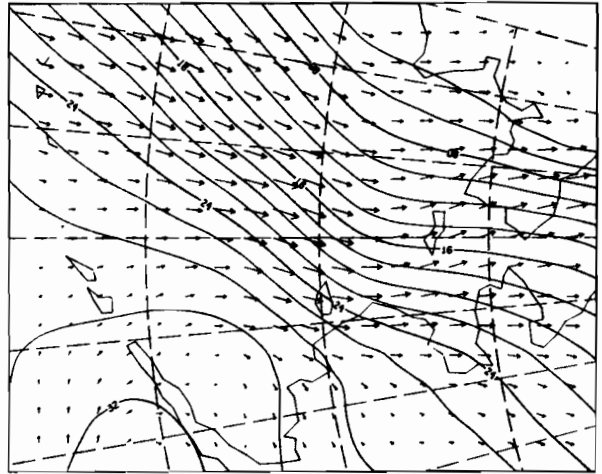
12Z 25 MAR 1979

ØBSERVED SLP AND WINDS 4



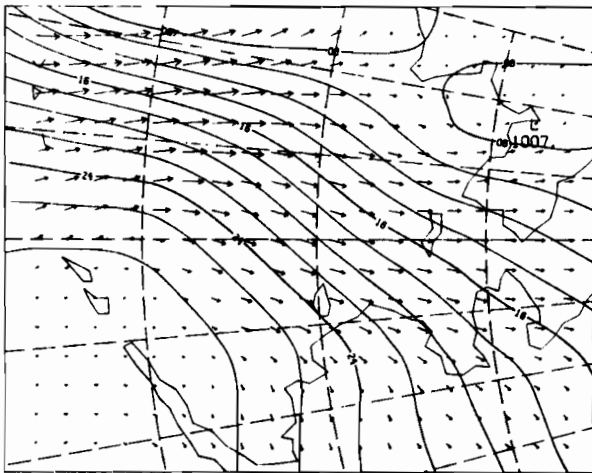
00Z 26 MAR 1979

ØBSERVED SLP AND WINDS 4



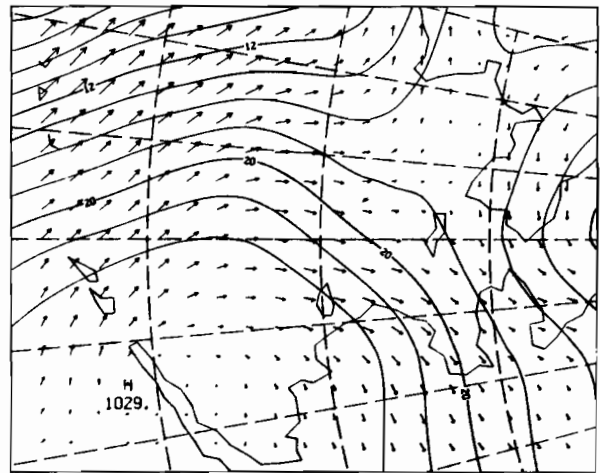
12Z 26 MAR 1979

ØBSERVED SLP AND WINDS 4



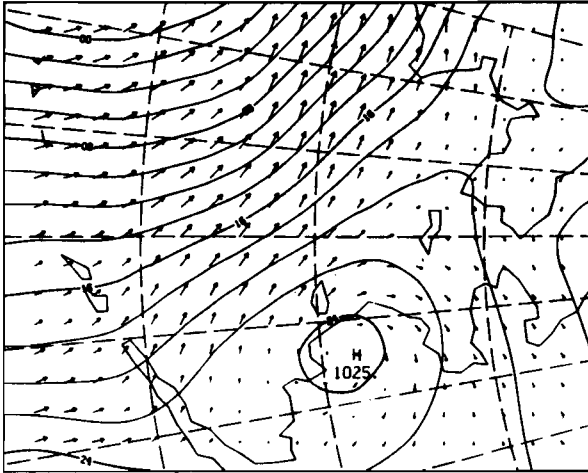
00Z 27 MAR 1979

ØBSERVED SLP AND WINDS 4



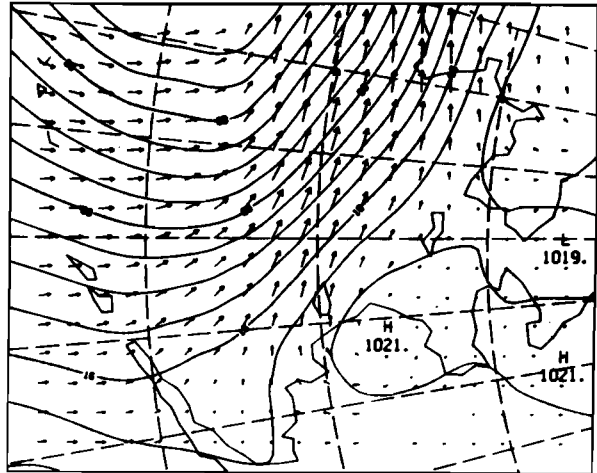
12Z 27 MAR 1979

OBSERVED SLP AND WINDS 4



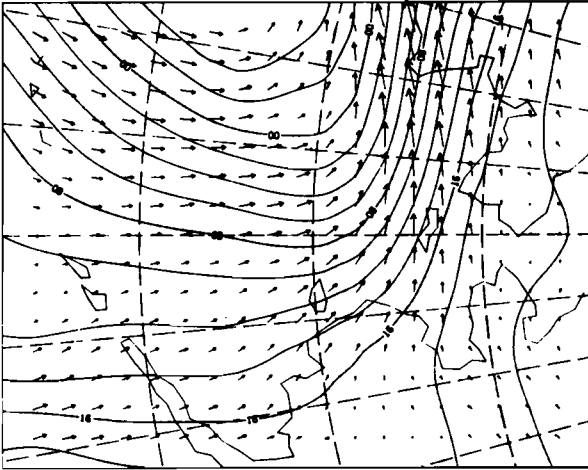
00Z 28 MAR 1979

OBSERVED SLP AND WINDS 4



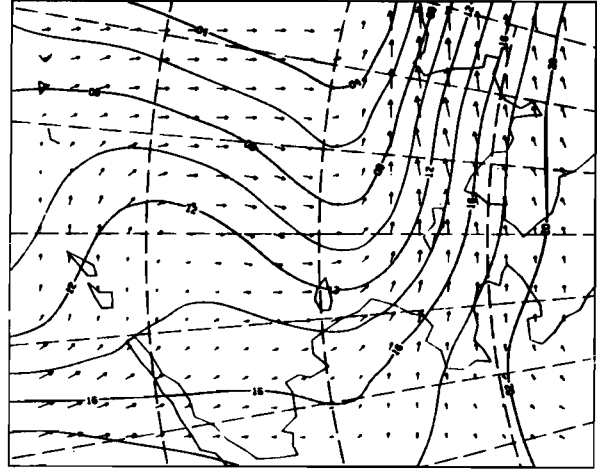
12Z 28 MAR 1979

OBSERVED SLP AND WINDS 4



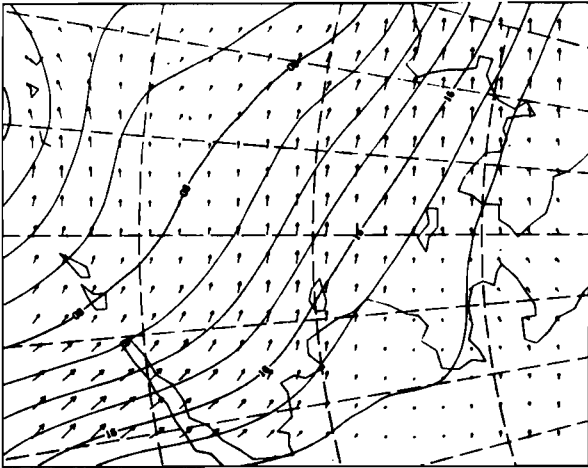
00Z 29 MAR 1979

OBSERVED SLP AND WINDS 4



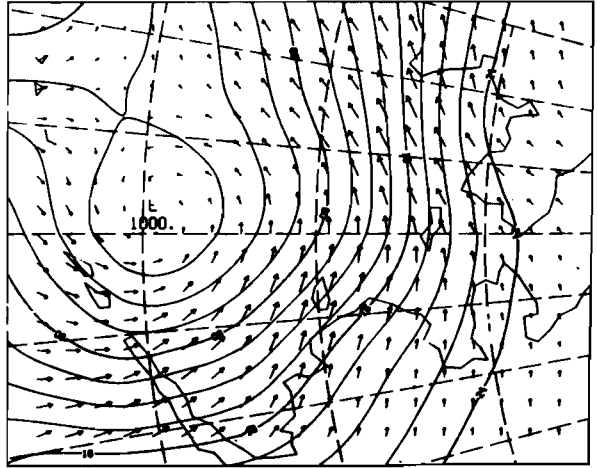
12Z 29 MAR 1979

OBSERVED SLP AND WINDS 4



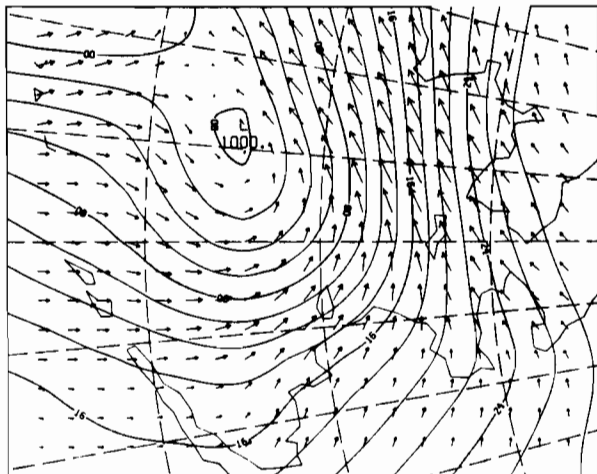
00Z 30 MAR 1979

OBSERVED SLP AND WINDS 4



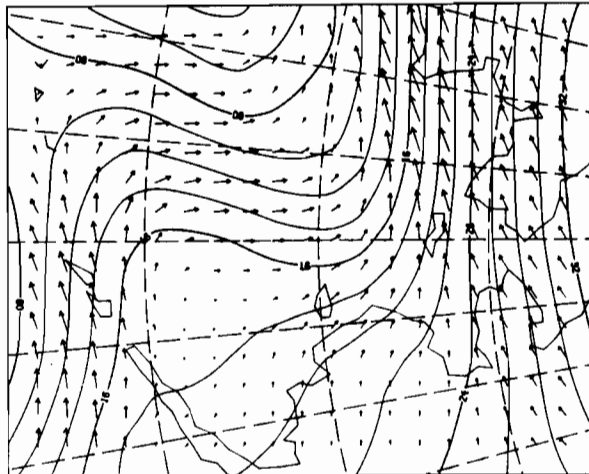
12Z 30 MAR 1979

OBSERVED SLP AND WINDS 4



00Z 31 MAR 1979

OBSERVED SLP AND WINDS 4



12Z 31 MAR 1979